THE DISSOLUTION AND TRANSPORT OF DENSE NON-AQUEOUS PHASE LIQUIDS IN SATURATED POROUS MEDIA

Michael Robert Anderson
B.S., Chemistry, University of Wisconsin-Madison, 1970
M.S., Chemistry, University of Wisconsin-Madison, 1972

A dissertation submitted to the faculty
of the Oregon Graduate Center
in partial fulfillment of the
requirements for the degree
Doctor of Philosophy
in
Environmental Science and Engineering

August 1988

The dissertation "The Dissolution and Transport of Dense Non-Aqueous Phase Liquids in Saturated Porous Media" by Michael R. Anderson has been examined and approved by the following examination committee:

James F. Pankow, Thesis Advisor
Professor

Richard L. Johnson
Assistant Professor

Carl D. Palmer
Assistant Professor

Jack H. Devletian
Professor

DEDICATION

This dissertation is dedicated to my wife, Kathy, whose undying love, encouragement and support have helped me reach this goal.

ACKNOWLEDGEMENTS

In the brief space allowed for these acknowledgements, it is difficult for me to express the true extent of my appreciation to all those who have helped me during my six years at OGC. What follows is, therefore, the "Readers' Digest" version. First of all, I would like to thank my advisor, James F. Pankow, for not only giving me the opportunity to work on an interesting project, but also for providing the financial support necessary to complete this work. I am also grateful for the funding for this project which came from USGS Grant Number 14-08-0001-A0510 and from the Waterloo/OGC University Consortium Research Program on Solvents in the Subsurface.

Many OGC Faculty and Staff members were instrumental in the success of this project and deserve a special note of thanks. James F. Pankow and Richard L. Johnson provided valuable guidance on both the design and the execution of the experiments. Carl D. Palmer persevered in his attempt to help me understand some of the concepts of groundwater modeling. Lorne Isabelle turned me on to Epoxy Putty, J-B Weld and other miracles of modern science which helped convert a sorry sand box into a lean, mean hydrological machine.

Doug Davis in the machine shop and Allan Ryall in the glass shop are to be thanked for their expertise and their interesting stories.

I will always be thankful for and amazed at the ability of Chris Lightcap to locate articles published in obscure petroleum journals. Dave Duncan deserves credit for tearing the lab down around me without once interrupting my experiments. I am grateful to Margaret Day for her laughter and free candy despite my late SPC forms. The patience and kindness of the departmental secretaries, Edie Taylor, Dorothy Malek, Nancy Christie and Judi Irvine, is also greatly appreciated.

I am indebted to my thesis committee, James F. Pankow, Richard L. Johnson, Carl D. Palmer and Jack H. Devletian, for their helpful comments not only about the content, but also about the organization and style of my dissertation. I am sure that the few brave souls who read this document will also appreciate my committee's efforts.

As in any job, the lasting joy is not the work, but the people. I am especially grateful for the friendship and support given to me by Mike Rosen and Ken Hart. They were always willing to commiserate over coffee or beer (especially beer). I also wish to thank Bill Asher, Rick DeCesar, Steve McDow, Barb Turpin, J. MacPherson, Bernie Bonn and Stewart Rounds for providing helpful comments about my research, new perspectives on life, and baked goods in the office. Needless to say, Steve Crawford, Bill Pengelly, Andy Grange and the other members of the OGC Softball team are to be thanked for their friendship and commended for their courage.

Finally, I want to extend my heartfelt thanks and appreciation to my father and the rest of my family both near and far for their support, both moral and financial, during the lean years.

TABLE OF CONTENTS

LIST OF FIGURES

LIST OF TABLES

ABSTRACT

The Dissolution and Transport of
Dense Non-Aqueous Phase Liquids
in Saturated Porous Media

Michael R. Anderson, Ph. D.
Oregon Graduate Center, 1988

Supervising Professor: James F. Pankow

In this study, experiments were undertaken to examine both the dissolution of residual dense non-aqueous phase liquids (DNAPLs) in saturated porous media and the transport of the immiscible phase which produces these residuals. Dissolution experiments were carried out in a 75x100x100 cm tank containing Ottawa sand. A zone of residual DNAPL was created in the center of the tank and water samples were taken from a grid of needles that penetrated the sand at the downgradient end of the tank. Experimental data were used to determine contaminant concentrations as a function of velocity, the effect of DNAPL residuals on the permeability of the porous medium, and the interaction of two DNAPLs in a zone of mixed residuals.

DNAPL flow was investigated by observing the movement of dye-containing DNAPLs in glass columns and in small sand tanks. Sands with different grain sizes and wetting histories were employed to determine the effect of these factors on the flow. The behavior of flow in the tanks was determined by excavating the sand and observing the distribution of the dye at different depths. In this manner, possible wall effects were avoided. Residual DNAPL saturations were also measured.

Results of the dissolution experiments showed that concentrations equal to the aqueous solubility of the compound were easily obtained for the velocities used in this study (10 - 100 cm/day). Modeling of the contaminant plume indicated that there may have been a slight narrowing in the streamlines resulting from reduced permeability in the residual zone. The interaction of two different DNAPL residuals produced lower concentrations but was accounted for by treating the DNAPLs as an ideal solution.

Observations made during the flow experiments indicated that a slight reduction in permeability can cause a DNAPL to flow laterally until it finds a more permeable spot through which to continue its downward progress. DNAPL residual saturations were found to be in the range of 15-40%. Model studies showed that the combined demands of relatively low concentrations and long source life found at field sites require sources that consist primarily of small horizontal pools rather than permeable zones of residual.

1. INTRODUCTION

1.1 Groundwater Contamination: The Extent of the Problem

Groundwater contamination is a matter of growing concern in the United States where approximately 50 percent of the population rely on groundwater for part or all of their drinking water (Council on Environmental Quality (CEQ), 1984). Although there has not yet been a systematic national survey to determine the full extent of the problem, it has been estimated that as much as two percent (by area) of the useable near-surface aquifers in the US have already been contaminated (Lehr, 1982). This value may be small, but it must be remembered that most reports of contaminated wells occur in regions with high population densities where clean water is in great demand. Therefore, the fraction of the population impacted by contaminated groundwater is significantly larger than two percent. For example, the nearly three million people in Nassau and Suffolk Counties on Long Island depend almost entirely on groundwater for their drinking water supply. So far, more than 36 of their community wells have been shut down due to contamination by a variety of synthetic volatile organic compounds including perchloroethylene (PCE, also known as tetrachloroethylene) and 1,1,1-trichloroethane (1,1,1-TCA) (CEQ, 1981). In 1980, 39 public wells in the San Gabriel Valley of California were closed

because of trichloroethylene (TCE) contamination. This closure affected the water supply of more than 400,000 people in thirteen cities (CEQ, 1981).

In an attempt to gauge the severity of the problem within their own boundaries, some states have begun to survey the quality of their groundwater supplies. Out of a total of 1174 community wells and 617 private wells that were screened in the state of Wisconsin, 65 community wells and 82 private wells were found to contain detectable levels of volatile organic compounds (Krill and Sonzogni, 1986). Although the most frequently detected compounds were TCE, PCE, 1,1,1-TCA and 1,1,2-TCA, the compounds that exceeded the recommended state health advisory levels most often were benzene and ethylbenzene. A survey of 3000 drinking water wells in California found that 18% were contaminated with organic compounds. The most common contaminants were PCE, TCE and dibromochloropropane (DBCP) (American Chemical Society, 1986).

In general, the sources of groundwater contamination can be divided into three categories: (1) natural pollution, (2) waste disposal practices and (3) non-disposal sources such as leaking underground storage tanks and other accidental spills (Pye et al., 1983). The research described in this dissertation deals with groundwater contamination resulting from the infiltration of organic liquids that originate from the latter two categories of sources. It focuses on the factors that control their dissolution and subsequent transport by groundwater.

To determine the types of contaminants that may enter the groundwater because of poor waste disposal practices, the Environmental Protection Agency surveyed 546 abandoned dump sites designated for its National Priority List. At these sites, the EPA found that with the exception of heavy metals, most of the materials leaching from the dumps consisted of chemicals that are liquids under ambient conditions (Abelson, 1985). Of the twenty-five components that accounted for more than two-thirds of the occurrences, eleven were chlorinated hydrocarbons (CHCs) and four were hydrocarbons (HCs). Because of the severity of the problem, the EPA has recently announced new rules which prohibit land disposal of twelve classes of hazardous waste including liquid and solid wastes containing CHCs (American Chemical Society, 1987a).

Under normal conditions, most HCs (petroleum products) and CHCs are liquids that are immiscible with water. Because of this, both HCs and CHCs are often referred to as non-aqueous phase liquids (NAPLs). Unlike most petroleum products, however, CHCs have densities greater than that of water and as such are sometimes referred to as dense non-aqueous phase liquids (DNAPLs). As will be discussed in Chapter 2, this density difference provides the potential for the CHCs to penetrate and contaminate an aquifer more deeply than is possible by HCs. The cleanup of CHC-contaminated sites may therefore be more difficult and expensive than HC-contaminated sites.

Table 1.1 lists several representative DNAPLs along with some of their chemical and physical properties. Although the solubility of

Table 1.1: Physical and chemical properties of representative DNAPLs and water.

Compound	Solubility[a] (mg/L)	Density[b] (20°C) (g/cm^3)	Viscosity (cp)	Interfacial Tension[c] (dyne/cm)	Vapor Pressure[a] (torr)
Carbon tetrachloride	785 (20°C)	1.59	0.969[b] (20°C)	45.0	90 (20°C)
Chlorobenzene	488 (25°C)	1.10	0.80[d] (20°C)	37.4	11.7 (20°C)
1,2-Dichloroethane	8690 (20°C)	1.26	0.89[d] (20°C)	-	61 (20°C)
Dichloromethane	20000 (20°C)	1.33	0.441[d] (20°C)	28.3	362.4 (20°C)
Tetrachloroethylene	200 (20°C)	1.62	0.876[d] (22°C)	47.5	14 (20°C)
1,1,1-Trichloroethane	720 (25°C)	1.34	1.2[b] (20°C)	-	123 (25°C)
Trichloroethylene	1100 (20°C)	1.47	0.57[d] (20°C)	-	58 (20°C)
Trichloromethane	8200 (20°C)	1.48	0.58[b] (20°C)	31.6	150.5 (20°C)
Water	-	1.00	1.00[b] (20°C)	-	17.5 (20°C)

[a]Mabey et al., 1982.

[b]Weast, 1970.

[c]Girifalco and Good, 1957; for water-organic interfaces at 20°C.

[d]Dean, 1973.

these compounds is generally low, many CHCs are known or suspected carcinogens and the standards set for drinking water are often several orders of magnitude lower than their respective solubilities. Table 1.2 compares the aqueous solubility (Mabey et al., 1982) to the maximum contaminant level (MCL) set by the EPA for the eight volatile organic chemicals most commonly found in drinking water (American Chemical Society, 1987b). Seven out of the eight compounds are CHCs. The solubilities of these eight compounds range from just over a thousand times to almost two million times their respective MCLs. Thus, even relatively small spills of these compounds could contaminate large volumes of water at unacceptably high levels. Considering that many common incidents of contamination such as leaking underground storage tanks, ruptured pipelines and accidental spills are sources of CHCs, it is easy to understand the importance of studying the transport and fate of these compounds in aquifers.

1.2 The Dissolution of NAPLs in Groundwater

When a NAPL spill occurs, contamination of a water supply may result from free product entering a well screened at the water table. This is a likely scenario in the case of wells located in the vicinity of gasoline spills. In most cases, however, contamination of a water supply results from the NAPL dissolving in the groundwater and being transported to a well at a concentration that exceeds safe drinking water standards. Although there is little data on subsurface dissolution rates of NAPLs, in most groundwater flow regimes mass

Table 1.2: A comparison of aqueous solubilities (Mabey et al., 1982) to maximum contaminant levels (MCLs) allowed by the EPA for the eight volatile organic compounds most commonly found in drinking water (American Chemical Society, 1987b).

COMPOUND	MCL (mg/L)	SOLUBILITY (mg/L)
Benzene	0.005	1780 (25 °C)
Carbon tetrachloride	0.005	785 (20 °C)
p-Dichlorobenzene	0.075	79 (25 °C)
1,2-Dichloroethane	0.005	8690 (25 °C)
1,1-Dichloroethylene	0.007	400 (20 °C)
1,1,1-Trichloroethane	0.2	720 (25 °C)
Trichloroethylene	0.005	1100 (20 °C)
Vinyl chloride	0.002	2700 (25 °C)

transfer is thought to be dependent upon the solubility of the compound rather than the flow rate of the water (Pfannkuch, 1984).

To study the transfer of mineral oil components to groundwater, van der Waarden et al. (1971) performed a series of laboratory experiments in columns that were packed with glass particles. Initially, the columns contained water at residual saturation. The NAPL used in their tests was a solution of either 2-isopropylphenol or o-xylene dissolved in an aromatic-free gas oil fraction. The NAPL was injected into the column and allowed to disperse until it became immobilized. Water was then trickled through the column and analyzed for contaminants. They found that the water soluble components of the mixtures leached out at concentrations that were equal to the expected equilibrium concentrations. Fried et al. (1979) performed similar experiments using toluene/iso-octane mixtures as the immobile NAPL in columns of sand that were otherwise saturated with water. They also found the solute concentrations in the drain water to be at equilibrium levels. By varying the length of the contaminated zone in their columns, they concluded that for normal aquifer velocities, a contact distance on the order of ten centimeters would be sufficient to produce equilibrium solute concentrations. Equilibrium values were also obtained for a CHC by Schwille (1984) who used sand columns to study the dissolution of PCE.

Since DNAPLs are common groundwater contaminants which appear to require little contact time to attain solubility-level concentrations in porous media, it seems likely that concentrations approaching these

high levels would be easy to find at contaminated sites. Observations in the field, however, show that maximum levels in the groundwater at such sites are at most a few percent of solubility values (Feenstra and Cherry, 1988). For example, in a summary of toxic organic chemicals found in drinking-water wells, Pye et al. (1983) list the maximum concentrations found for TCE, 1,1,1-TCA and PCE as 27.3, 5.44 and 1.50 ppm respectively. Although these concentrations greatly exceed the respective MCLs, they are, nonetheless, only 2.5%, 0.76% and 0.75% of their respective 20-25 ^{o}C solubilities. Most of the reported values are much lower than these.

Differences in the concentrations found in laboratory studies versus those found in field studies have led to questions about the true levels of contamination that result from NAPL spills. Some concern has been expressed about the validity of the results of column studies because typical laboratory hydraulic gradients in columns can be much larger than those commonly found in the field (Wilson and Conrad, 1984). This may lead to erroneously high solute concentrations due to mobilization of small droplets of NAPL. Also, in column studies water is forced to flow through the NAPL-containing medium. In an aquifer, the flow of water may be affected by local differences in permeabilities which result from the presence of the NAPL. This could result in a lower rate of mass transfer in the field compared to that found in column studies.

Certainly, one of the factors contributing to low levels of contaminants being measured in field samples is the inhomogeneity of

aquifers. This results in the mixing of clean and contaminated water during sampling (Feenstra and Cherry, 1988). Also, DNAPLs are relatively volatile solutes (see Table 1.1) and may be lost by improper or careless handling of the samples. However, the fact remains that there is little data to show that DNAPLs actually attain concentrations in groundwater approaching their solubilities under conditions that are more realistic than can be obtained in laboratory columns.

1.3 Experimental Objectives

This research was undertaken to determine if solubility level concentrations can be attained in a large tank under typical hydraulic gradients, and to examine two factors not amenable to study in columns that may influence the extent of groundwater contamination resulting from DNAPL spills. These factors are:

1. Formation of narrow "fingers" of DNAPL in the saturated zone.

   The movement of a DNAPL into a saturated porous medium is inherently unstable (Chouke et al., 1959). This can result in the formation of scattered "fingers" of DNAPL which penetrate the aquifer individually and create many small sources of contamination rather than one large source. Since this would result in narrow plumes of dissolved contaminants separated by clean water, it would increase the likelihood that samples collected in the field would be a

mixture of clean and contaminated water. This, of course, would decrease the likelihood of collecting samples with contaminant concentrations approaching their solubility values.

2. Reduced flow of water through the zone containing DNAPLs.

The presence of a second immiscible fluid in a porous medium will interfere with the normal flow of water in that region (Scheidegger, 1974). In laboratory column studies, water is forced to flow through the zone that contains the immiscible fluid. In an aquifer, however, the water may be partially deflected around that zone resulting in a contaminant plume that is narrower and lower in concentration than would be predicted from column studies.

Both of these factors will be discussed in more detail in later chapters. They are important because they directly affect the size, shape and strength of contaminant sources that result from the spill of DNAPLs into porous media. The nature of these sources will ultimately control both the level and distribution of contamination in an aquifer.

In order to study the importance of each of the factors mentioned above, two separate groups of experiments were carried out. The first group of experiments was concerned with dissolution of DNAPL in the saturated zone. The objectives here were to create a cylindrical "finger" of DNAPL in the saturated zone of a large (100x100x75 cm)

sand tank and, at mean water velocities of up to 1 meter per day, to observe: (1) the initial formation of the contaminant plume downgradient from the DNAPL zone, (2) the width of the plume when steady-state was attained to see if reduced permeability through the DNAPL affected the flow of water or the formation of the plume, and (3) the effects of velocity changes on the plume to identify the processes controlling mass transfer. Contaminant breakthrough from the tank was compared to breakthrough from a column experiment in order to investigate the possibility that the higher gradients found in column experiments lead to erroneously high solute concentrations. Flow was also stopped for eight days and then resumed in order to estimate the diffusion coefficient of the solute in the porous medium.

In the second group of experiments, DNAPL spills were conducted in both glass columns and rectangular tanks. The objectives were to: (1) observe the movement of an immiscible DNAPL phase as it entered a saturated porous medium, (2) look for the effects of water saturation on DNAPL flow by comparing spills in tanks containing a narrow imbibition capillary fringe with similar spills in tanks containing a thicker drainage capillary fringe, and (3) measure the percentage of the pore space occupied by the DNAPL.

2. MULTIPHASE FLUID FLOW IN POROUS MEDIA

2.1 Overview of a NAPL Spill

A NAPL spilled on or near the surface of the ground will enter the vadose zone as a separate phase and begin to move downwards under the influence of gravity. In this system, there are three fluid phases, air, water and NAPL, in contact with each other and with a solid porous medium. Depending on the size of the spill and the depth to groundwater, the NAPL may continue to flow downward until it reaches the fully water-saturated pores at the top of the capillary fringe. Subsequent migration of the NAPL will then be controlled primarily by its density. If the NAPL is less dense than water (such as a petroleum hydrocarbon), it will tend to spread out and float on the water table (Figure 2.1). Some lateral movement may also occur due to the slope of the water table. If the NAPL is more dense than water (i.e., a DNAPL, such as a chlorinated hydrocarbon), however, it will have the potential to penetrate the water table and make its way down through the aquifer (Figure 2.2). Further transport of the NAPL will involve a number of different pathways. Because of its volatility, some of the NAPL will evaporate into the soil gas and begin to diffuse through the vadose zone. Some of it will also dissolve in the pore water as well as sorb onto the grains of the

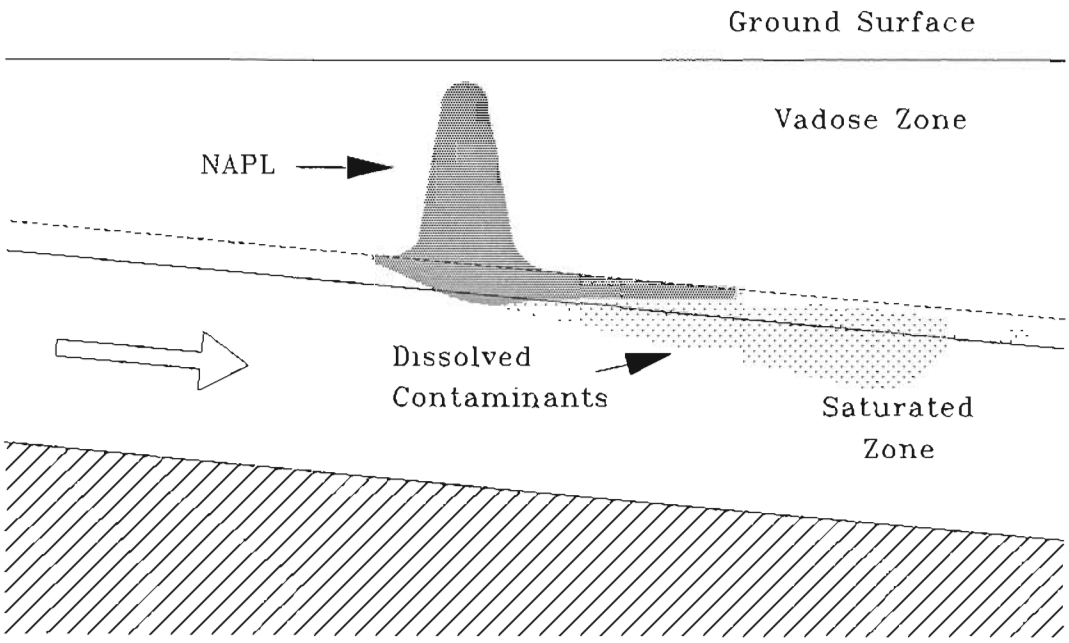

Figure 2.1: Idealized infiltration of a light non-aqueous phase liquid into a porous medium.

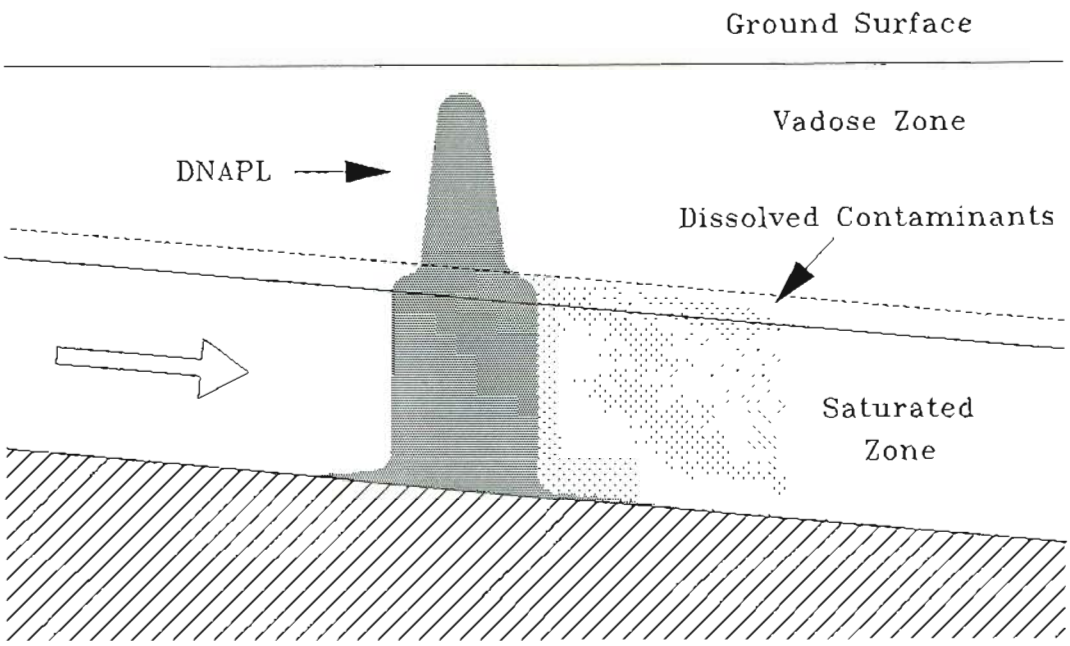

Figure 2.2: Idealized infiltration of a dense non-aqueous phase liquid into a porous medium.

porous medium. The situation is further complicated by the fact that a given pathway will probably involve a number of phase changes; vapor phase contaminant may subsequently be dissolved by infiltrating water, dissolved phase contaminant can volatilize into the soil gas and sorbed contaminant may desorb when clean water passes through the pores. Depending on the contaminant, biodegradation may also play a role in determining the fate.

It is obvious from the brief description given above that the problem concerning the fate of NAPL contaminants in the subsurface environment is a very complex one indeed. However, the initial transport for the bulk of the fluid, whether in the vadose zone or the saturated zone, results from the flow of fluid through a porous medium that already contains one or more additional immiscible fluids. This chapter will review some of the general properties of systems of multiphase fluids in porous media as well as discuss some aspects of DNAPL transport that differ from the transport of lower-density NAPLs.

2.2 Interfacial Tension and Capillary Pressure

When a liquid is in contact with a gas, a solid or a second immiscible liquid, the difference in the forces of attraction between the molecules within each phase and those at the surface will lead to the presence of interfacial energy (Adamson, 1982). If possible, the liquid surface will contract and the energy will manifest itself as interfacial tension. The effects of interfacial tension can be seen in the classic example of water rising in a glass capillary tube

(Figure 2.3). In this situation the magnitude of the interfacial tension (γ) is related to the height of the capillary rise (h_c) by the equation

$$\gamma_{wa} = \frac{\Delta\rho \; g \; h_c \; r}{2 \cos \theta} \qquad (2.1)$$

where $\Delta\rho$ is the density difference between the two fluids, g is the acceleration due to gravity, r is the radius of the tube and θ is the contact angle between the water and the capillary tube. The contact angle depends not only on the interfacial tension between the two fluids (γ_{wa}) but also on the interfacial tensions between each of the fluids and the solid (γ_{sw} and γ_{sa}) as shown in the Young equation (Adamson, 1982):

$$\cos \theta = (\gamma_{sa} - \gamma_{sw})/\gamma_{wa} \qquad (2.2)$$

Since the contact angle, by definition, is the angle that contains the fluid of interest, the contact angle for air in Figure 2.3 is simply the supplement of the contact angle for water.

In general, the terms "wetting" and "nonwetting" are used to describe the contact behavior between a liquid and a solid. For a wetting liquid, the contact angle is 0° (perfect wetting) or sufficiently close to 0° so that the liquid spreads out over the solid easily. For a nonwetting liquid, the contact angle is greater than 90° and the liquid will tend to form "beads" in order to reduce the area of contact between it and the solid surface. When two immiscible

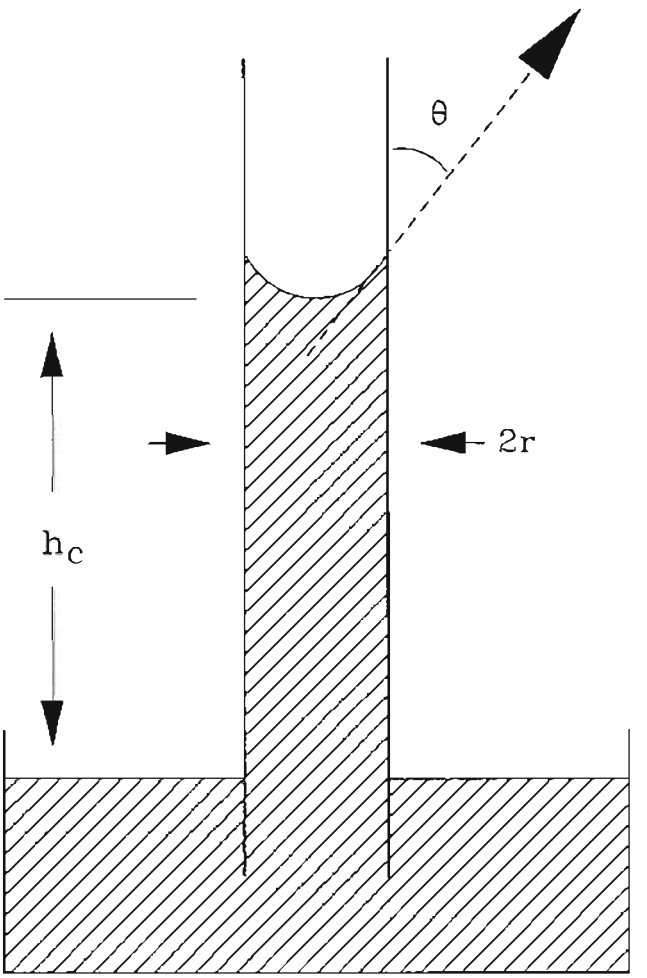

$$p_c = - \Delta\rho \; g \; h_c$$
$$= (-2 \; \gamma \cos \theta)/r$$

Figure 2.3: The relationship between interfacial tension, capillary pressure and the rise of water in a capillary tube.

fluids share the interstitial spaces of a porous medium, the wetting fluid will tend to coat the surface of the grains and occupy the smaller spaces (the pore throats). The non-wetting fluid will occupy the larger spaces (the pores) (Figure 2.4).

As the Young equation indicates, by itself, a specific compound cannot be given an a priori classification as a wetting or a nonwetting liquid. Its behavior will depend upon the nature of the other components of the system in which it is found. Thus, even though water is shown as a wetting fluid in Figure 2.3, it is obviously a nonwetting fluid when sitting on the fender of a freshly waxed car. Similarly, a NAPL will be a wetting fluid when it shares the pore spaces of a porous medium with air. However, when water is also present in the medium, the same NAPL will usually be a nonwetting fluid.

An important ramification of interfacial tension is the existence of a pressure difference across the interface between two immiscible fluids. The pressure will always be lower in the wetting fluid (p_w) than in the nonwetting fluid (p_{nw}). This pressure difference is referred to as the capillary pressure (p_c),

$$p_c = p_{nw} - p_w \tag{2.3}$$

and it is a measure of the tendency of a porous medium to suck in the wetting phase or to repel the nonwetting phase (Bear, 1972). Rearranging equation 2.1 shows the relationship between capillary pressure and other parameters of the system.

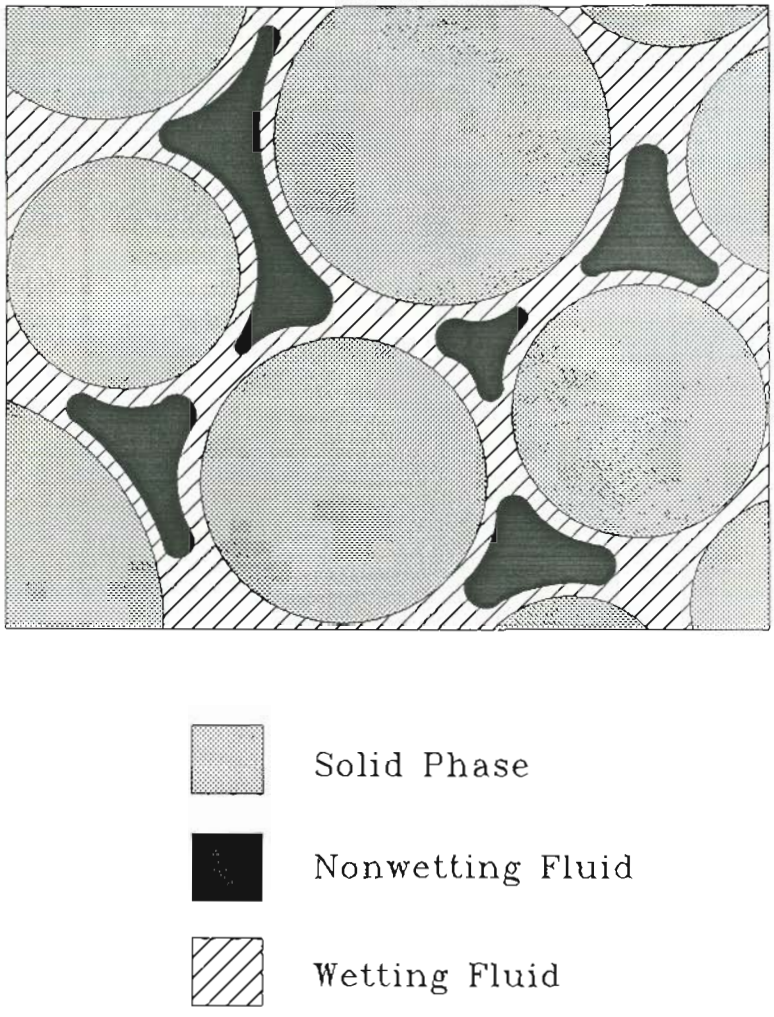

Figure 2.4: The distribution of wetting and nonwetting fluids in a porous medium.

$$p_c = \Delta\rho\ g\ h_c = (2\ \gamma\ \cos\ \theta)/r \qquad (2.4)$$

Although a porous medium is obviously more complex than a capillary tube, the same basic principles apply. In an aquifer, capillary pressure forces water to rise into the pore spaces above the water table. This results in the formation of the capillary fringe, sometimes referred to as the tension-saturated zone. Everything else being equal, a finer-grained porous medium will have narrower pore spaces (smaller r), higher capillary pressures and a larger capillary rise height than a coarser-grained porous medium.

2.3 Multiphase Fluid Flow

2.3.1 Darcy's Law

Single-phase fluid flow in a porous medium is described by Darcy's Law

$$q = -K\ \text{grad}\ h \qquad (2.5)$$

where q (L/T) is the specific discharge of the fluid, K (L/T) is the hydraulic conductivity and grad h (L/L) is the hydraulic gradient. The magnitude of K is a function of the properties of both the porous medium and the fluid. In order to emphasize the specific properties that affect fluid flow, K is often expressed in the form

$$K = k\rho g/\mu \qquad (2.6)$$

where k (L^2) is the permeability of the porous medium, ρ (M/L^3) and

μ (M/LT) are the density and viscosity of the fluid, and g (L/T^2) is the acceleration due to gravity. Likewise, the value for the head (h) in the gradient can be expressed as a sum of the pressure head and the elevation head.

$$h = p/\rho g + z \tag{2.7}$$

When these relationships are incorporated into Equation 2.5, a more explicit form of Darcy's Law results

$$q = -(k/\mu)(\text{grad } p - \rho g) \tag{2.8}$$

where g is now the gravitational acceleration vector.

2.3.2 Relative Permeability

When dealing with multiphase flow, the assumption is made that the flow of each of the individual fluids can still be described by Darcy's Law if it is modified to include a relative permeability term (k_r, a fraction of the total permeability) (Scheidegger, 1974). Thus, for water and DNAPL the equations are

$$q_w = -k_{rw}(k/\mu_w)(\text{grad } p_w - \rho_w g) \tag{2.9}$$

$$q_D = -k_{rD}(k/\mu_D)(\text{grad } p_D - \rho_D g) \tag{2.10}$$

The need for a relative permeability term arises from the fact that in multiphase flow, two or more fluids must share the pore spaces of the medium and therefore the flow of each fluid is only a fraction of what it would be if it were the only fluid present. Relative

permeability for a given fluid, then, is a function of the amount of that fluid present in the pore spaces. The amount is commonly expressed as the saturation (S); the percent of the pore space occupied by a given fluid.

$$S_i = \frac{\text{Volume of Fluid i}}{\text{Volume of Pore Space}} \times 100 \qquad (2.11)$$

By considering different areas within Figure 2.4, it can be seen that when examining a porous medium on a microscopic scale, the saturation of a given fluid can be found to vary over the complete range of 100% down to 0% depending upon which small area is being investigated. In order for percent saturation/relative permeability relationships to be meaningful, saturation must be taken as a mean property over a sufficiently large volume. This volume should contain enough pores so that no further changes occur in the saturation as the volume being considered is increased. The volume should be small enough, however, so that variations from one domain to the next can be considered continuous (de Marsily, 1986). This volume is referred to as a representative elementary volume (REV).

Relative permeability is not a linear function of saturation. It remains zero until a minimum saturation necessary for flow is reached and then curves upwards to a value of 1. Since the fluids interfere with each other, the sum of the relative permeabilities of all of the fluids in a given system is usually less than 1. The saturation/ relative permeability relationship is further complicated by the fact

that experimental permeability curves exhibit hysteresis depending upon whether the saturation for a given fluid is increasing or decreasing during the course of an experiment. In most cases, however, the effects of hysteresis are considered insignificant (de Marsily, 1986). Figures 2.5 and 2.6 are examples of relative permeability curves for both two-phase and three-phase flow.

2.3.3 Residual Saturation

When a DNAPL moves down through the vadose zone, some of it will break off and become immobilized as the remaining portion of fluid continues to move downward. The immobilized fluid may be trapped as individual droplets in the pores, or as a series of several droplets in adjacent pores connected via the pore throats (Conrad et al., 1987). These droplets will remain trapped in the larger pore spaces unless sufficient hydraulic pressure is applied to overcome capillary pressure and force the droplets through the narrow pore throats. The amount of fluid trapped in this manner is referred to as the "residual saturation", S_r. A number of factors influence the magnitude of the residual saturation, including the wettability of the grains, the ratio of the pore size to the throat size (the aspect ratio) and the heterogeneity of the medium. How these factors are inter-related can be quite complex, but in general there is a tendency for the value of the residual saturation of a NAPL to increase as the permeability of the porous medium decreases (Schwille, 1984).

Another way to express the trapping capability of a porous medium

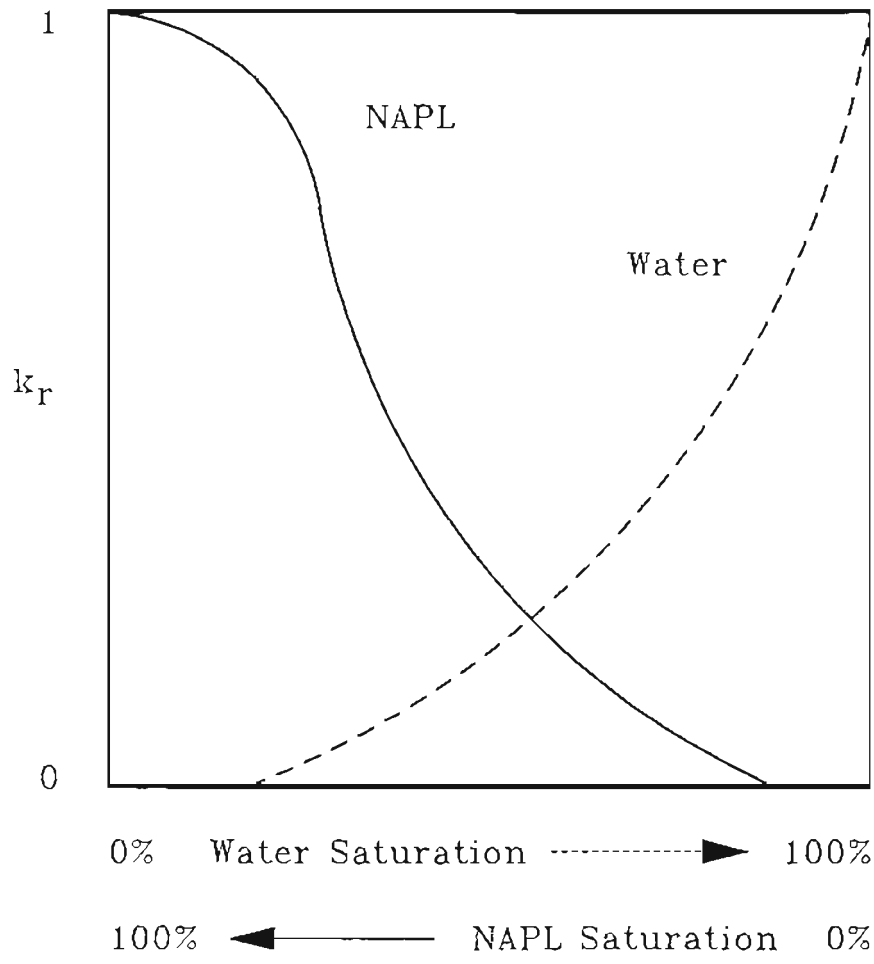

Figure 2.5: Relative permeability curves for two-phase flow (adapted from van Dam (1967)).

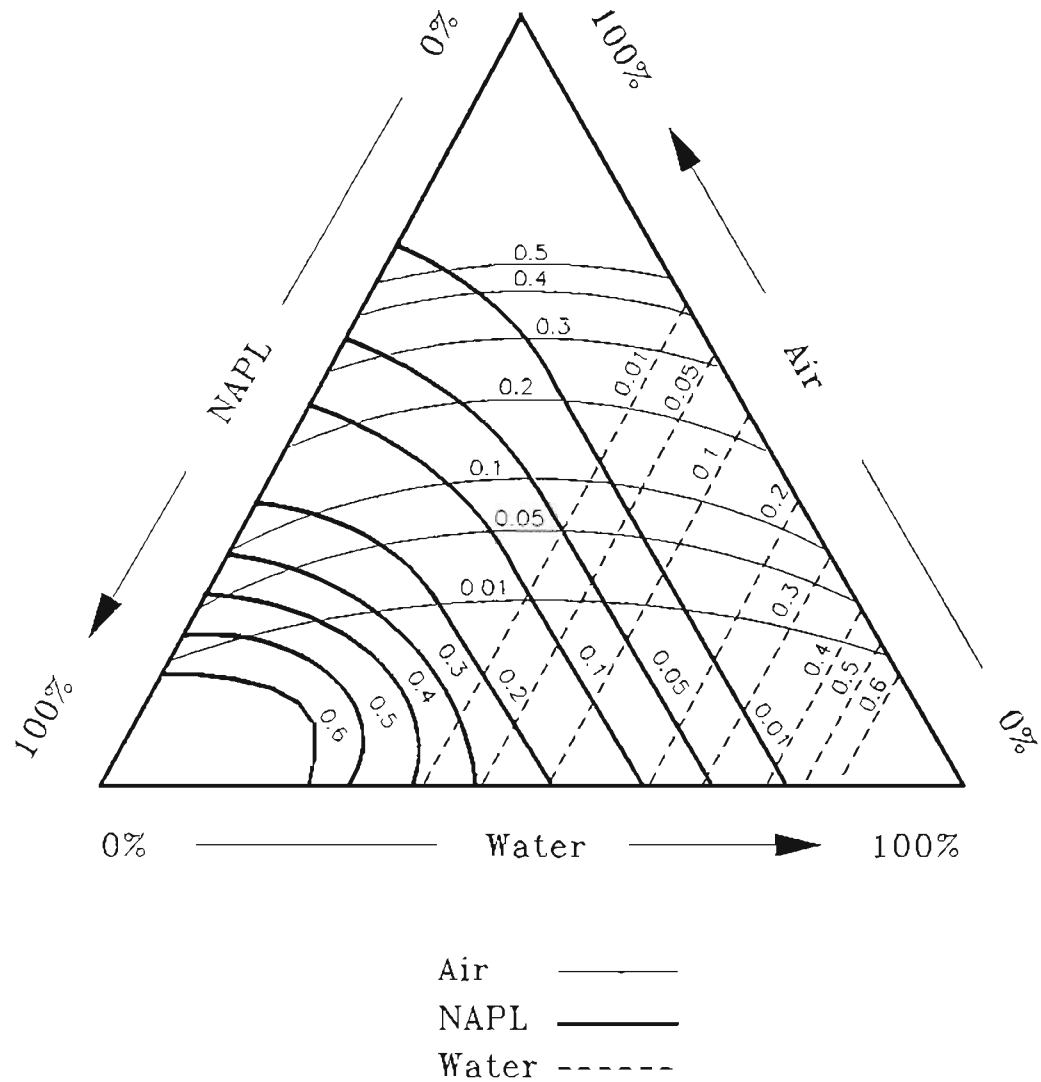

Figure 2.6: Relative permeability curves for three-phase flow (adapted from van Dam (1967)).

is to combine percent residual saturation with porosity (n) to produce retention capacity, R, in L/m^3.

$$R = (S_r)\ (n)\ (10) \qquad (2.12)$$

According to Schwille (1984), the retention capacity for oil in the vadose zone ranges from about 3-5 L/m^3 in highly permeable media to 30-50 L/m^3 in media with low permeability. He found that values for CHCs were similar. For a typical porosity of 0.40, these values correspond to residual saturations on the order of 1% in highly permeable media to 10% in media with low permeability. Although Schwille does not state whether these quantities are for dry or moist media, he does emphasize that the vadose zone retention capacity is strongly affected by both heterogeneities and moisture content.

Table 2.1 lists some values for NAPL residual saturations and retention capacities in the vadose zone. These were obtained by Wilson and Conrad (1984) using a hydrocarbon (Soltrol-130, a light isoparaffinic oil) in glass bead columns. These values fall within the range given by Schwille and clearly show the trend of increasing retention capacity with decreasing permeability. Hoag and Marley (1986) measured both dry and wet vadose zone residual saturations for gasoline and also found that grain size was of primary importance in determining the amount of residual. Their results ranged from 14-55% for coarse and fine sands that were initially dry. When the sands were initially water wet, however, the degree of residual gasoline saturation decreased. For medium sands, the saturation was only about

Table 2.1: Vadose zone and saturated zone residual saturations and retention capacities versus permeability for a hydrocarbon (Soltrol-130[a]) in glass bead columns (Wilson and Conrad, 1984).

		Vadose Zone[b]		Saturated Zone	
Mean Bead Diameter (mm)	Permeability (darcy)	S_r (%)	R (L/m^3)	S_r (%)	R (L/m^3)
0.655	147	3	11	14	57
0.327	85	5	19	14	57
0.167	22	8	30	14	57

[a]Relevant properties of Soltrol-130 at 23 °C are:
ρ = 0.7484 g/cm^3, γ = 23.19 dyne/cm and μ = 1.42 cp.

[b]The vadose zone was initially water-wet.

0.7-0.8 of what it had been for the comparable dry sands. The residual gasoline saturation in water wet fine sands was only about 0.4 of the comparable dry sand value.

Hoag and Marley's (1986) results are significantly higher than those of Wilson and Conrad (1984). Although the reason for this disagreement is not clear, two procedural differences may be partly responsible. First, Hoag and Marley used quartz sands rather than uniform sized glass beads. The irregular nature of the sand may have contributed to a higher retention capacity. Second, Hoag and Marley generated their residuals by saturating the sand with water, draining it freely in air, and then repeating the saturation/drainage cycle with gasoline. The results reported by Wilson and Conrad, however, were generated by saturating the glass beads with water, draining the water with the infiltrating hydrocarbon, and then draining the hydrocarbon in air. Therefore, the wetting/drainage histories of the two sets of samples differed.

As discussed above for the vadose zone, an immiscible fluid moving through the saturated zone will also leave behind a trail of residual droplets trapped in the pore spaces. In fact, experimental results indicate that residual saturations and retention volumes in this region are larger than those for the vadose zone. This is not too surprising considering that a much smaller fluid density difference exists in the saturated zone (NAPL versus water) than in the vadose zone (NAPL versus air). Therefore, gravity drainage in the saturated zone will be less efficient at removing the NAPL from the

pore spaces. Also, in the vadose zone, the NAPL will be a wetting fluid relative to air. As previously mentioned (Section 2.2), capillary pressure will cause a wetting fluid to be drawn into the narrower portions of the pore spaces. In the vadose zone, therefore, there will be a tendency for the NAPL to spread out into adjacent pore spaces, thus leaving lower residual amounts. In the saturated zone, however, the NAPL will usually be a nonwetting fluid and capillary pressures will tend to prohibit spreading into adjacent pores. Greater residual saturations will result as droplets of NAPL remain trapped in the larger pore spaces. The saturated zone retention volumes shown in Table 2.1 are about 2-5 times higher than the corresponding vadose zone volumes. Although they do not speculate on the reason, Wilson and Conrad (1984) also found that the saturated zone values did not seem to depend upon the particle size.

2.4 Penetration of the Water Table

Upon reaching the saturated capillary fringe, a DNAPL must be able to displace water from the pores in order to continue its downward migration. Although it would seem like an easy matter for a fluid moving under the influence of gravity to displace a second fluid having a lower density, it must be remembered that the small radii of the pores can lead to significant capillary pressures across the interface of the two immiscible fluids (see equation 2.4). Therefore, even though the pressure of the nonwetting fluid is greater than the pressure of the wetting fluid, penetration of the water table will not

occur unless the pressure head of the DNAPL can also overcome this capillary pressure barrier between the water and the DNAPL. Villaume et al. (1983) have shown how the critical height of DNAPL (z_c) required to generate a pressure head sufficient to overcome capillary pressure can be calculated using Hobson's equation,

$$z_c = \frac{2\gamma \cos \theta \, (1/r_t - 1/r_p)}{\Delta\rho \, g} \qquad (2.13)$$

where γ is the water-CHC interfacial tension, θ is the contact angle between the fluid boundary and the solid surface, r_t and r_p are the radii of the throat and the pore respectively, and g is the acceleration due to gravity. If one assumes spherical grains in a rhombohedral (most stable) packing, the pore radius will be 0.207D and the throat radius will be 0.077D where D is the grain diameter (Villaume et al., 1983). Critical height estimates are given in Table 2.2 for PCE in saturated porous media of varying grain sizes. Because of their small pores, saturated silts and clays can present a very significant barrier to the infiltration of a DNAPL spill. The large pores of the coarse sands and gravels found in many aquifers, however, may be easily infiltrated by these fluids.

After penetrating the water table, a DNAPL will continue its downward flow until it either encounters an impermeable zone or spreads out to the point where the pressure head is depleted and the DNAPL becomes totally immobilized as residual. While moving through the saturated zone, the downward progress of the immiscible fluid does

Table 2.2: Critical height that must be exceeded for a column of perchloroethylene to penetrate porous media saturated with water.

Porous Medium	D (mm)	z_c (cm)[a]
Course Sand	1.0	13
Fine Sand	0.1	130
Silt	0.01	1300
Clay	0.001	13000

[a]Values of z_c were calculated using $\Delta\rho = 0.62$ g/cm^3, $\gamma = 47.5$ dyne/cm, and $\cos\theta = 1$.

not appear to be affected by the local hydraulic gradient (Schwille, 1981). If sufficient fluid reaches an impermeable layer, however, it can move laterally and follow the slope of the barrier. Its direction of flow may therefore be totally counter to the direction of the flowing groundwater. The remaining DNAPL will then collect in depressions and remain as a contaminant source trapped on the bottom of the aquifer.

2.4.1 The Effects of Viscous Fingering

When a fluid saturating a porous medium is displaced by the pressure of another fluid, the interface between them may become unstable. This instability is manifested by "fingers" of the driving fluid penetrating the displaced fluid (Saffman and Taylor, 1958). This phenomenon, well-known in the petroleum industry, is generally referred to as "viscous fingering" because the viscosity difference between the two fluids is one of the key factors contributing to the instability (Homsy, 1987). Chouke *et al.* (1959) have derived an equation to predict the critical displacement rate, U_c, which, if exceeded, will result in instability:

$$U_c = \frac{-(\rho_2 - \rho_1)\, g \cos(zz')}{(\mu_2/k_2 - \mu_1/k_1)} \qquad (2.14)$$

In this equation, ρ, μ and k are density, viscosity and effective permeability; liquids 1 and 2 are the displacing and displaced fluids, respectively; cos (zz') is the direction cosine between the vertical

(positive upward) and the direction normal to the displaced interface (positive from liquid 1 to liquid 2); and g is the absolute value of the acceleration due to gravity. For a DNAPL moving down and displacing water, cos (zz') = -1. If we assume equal effective permeabilities,

$$U_c = gk\,(\rho_2 - \rho_1)/(\mu_2 - \mu_1) \qquad (2.15)$$

Besides being more dense than water, most DNAPLs are also less viscous than water (Table 1.1). Therefore, $(\rho_2 - \rho_1) < 0$ and $(\mu_2 - \mu_1) > 0$. This results in a negative critical displacement rate indicating that the downward displacement of water by a less viscous DNAPL is always unstable. This differs from the situation where a DNAPL is displacing air in the vadose zone. In that case, $(\mu_2 - \mu_1) < 0$ and the displacement will be stable except at relatively high velocities. Scheidegger (1960) points out that whether or not a displacement front is unstable does not depend at all on the properties of the porous medium. He maintains, however, that where a viscous finger starts and what its geometry will be are influenced by heterogeneities present in the medium which can lead to deformations in the displacement front. Chouke et al. (1959) further stipulate that even if the critical rate is exceeded, fingers will not form unless the Fourier decomposition of the deformation of the displacement front contains modes with wavelengths greater than a critical wavelength (λ_c). They warn that it is quite possible for λ_c to exceed the dimensions of a laboratory model thus leading to results that differ greatly from what may be

found in the field under similar conditions.

As a result of viscous finger formation, a DNAPL spill that occupies a given cross-sectional area in the vadose zone may, upon reaching the water table, split into a number of smaller fingers that push their way into the aquifer. This behavior could have two important effects on the subsequent contamination of the aquifer. First, if the infiltrating fingers now occupy a smaller total cross-sectional area, the DNAPL will be able to penetrate to a greater depth than one might estimate from retention volume considerations. This will increase both the difficulty and the cost of possible remediation schemes. Second, as discussed earlier, dissolved contaminants may then emanate from a number of narrow sources separated by regions of clean water. The resulting contaminant plume may therefore be more dilute than expected. Both of these factors can greatly complicate attempts to model immiscible fluid transport and contamination in the saturated zone.

2.4.2 The Effects of Reduced Permeability

When the flow of immiscible fluid from a DNAPL spill finally ceases, the fluid that penetrated the water table will remain trapped in the pore spaces of the aquifer at residual saturation. Because of the presence of the DNAPL, the permeability of this residual zone to water will be reduced. Reduced permeability means that there will be a smaller flux of water through the residual since the streamlines will be partially deflected around this region. Figure 2.7 shows

(a) $k_r = 0.60$

(b) $k_r = 0.30$

(c) $k_r = 0.10$

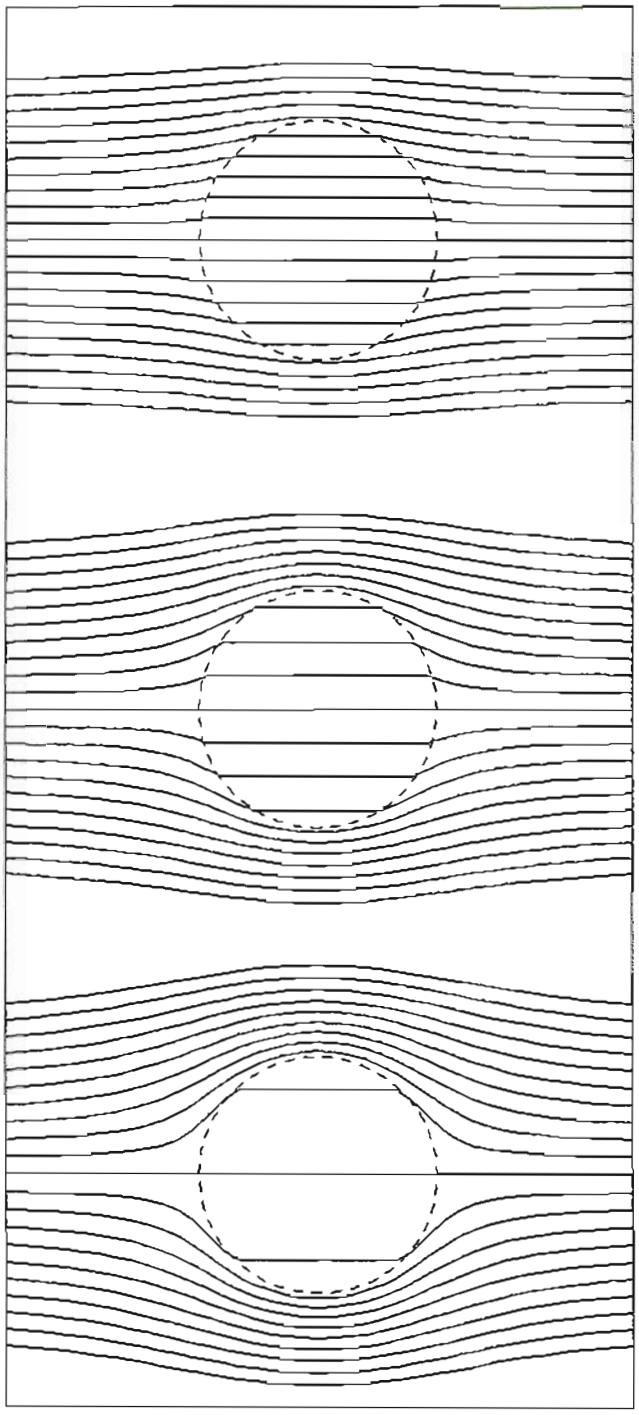

Figure 2.7: The effects of a circular zone of reduced permeability on streamlines.

streamlines calculated using the method of Wheatcraft and Winterberg (1985) for water passing through circular zones having relative permeabilities of 0.60, 0.30 and 0.10. The streamlines were calculated so that the region between any two adjacent lines (a streamtube) would have the same flux as that between any other pair of adjacent lines. When $k_r = 0.60$ there was only a slight distortion of the flow, whereas when $k_r = 0.10$ there was a rather significant distortion. Wheatcraft and Winterberg (1985) have shown that the fraction of the flow passing through a circular cross-section having a relative permeability of k_r compared to the flow passing through a comparable cross-section with $k_r = 1$ can be calculated from the relationship

$$F = 2 k_r / (1 + k_r) \qquad (2.16)$$

For the cases shown in Figure 2.7, the fractions of flow through the residual zone are 0.75, 0.46 and 0.18, respectively. Even if it was assumed that any water coming into contact with the residual DNAPL would emerge with saturation-level concentrations of dissolved contaminant, it can be seen from this figure that reduced permeability would contribute to a reduction in the flux of dissolved contaminant from the residual zone.

For a DNAPL spill, it should be possible to calculate how much the flow of water will be reduced through the residual-containing region. To accomplish this it will be necessary to know first, what the saturated zone residual saturation is for the given combination of

immiscible fluid and porous medium, and second, what the relative permeability of water is for this combination. Unfortunately, although these topics have been studied for years with respect to petroleum hydrocarbons, with the exception of a study by Lin et al. (1982) involving water and trichloroethylene, similar data for DNAPLs are virtually nonexistent. Nevertheless, a rough estimate might be made by assuming that DNAPL residuals will be in the range of 15-40% given by Wilson and Conrad (1984) for hydrocarbons. Using the relative permeability/saturation curves in Lin et al. (1982), these DNAPL saturations should produce k_{rw} values of approximately 0.1-0.6. These values correspond to those used to calculate the streamlines in Figure 2.7. In the worst case, then, reduced permeability may be responsible for a fivefold reduction in the rate at which water is advected through the zone of residual saturation. If the water leaving the zone is always saturated, there will also be a fivefold reduction in the mass removal rate. Any additional mass transport due to diffusion from the perimeter will depend on the groundwater velocity and will only enhance contaminant concentrations. Therefore, one cannot use this model alone to explain the fact that contaminant concentrations found in the field are orders of magnitude lower than the solubility-level concentrations found in laboratory experiments.

One possible problem with using relative permeability data from the literature is that most relative permeability versus saturation results are obtained by experimental methods in which both the wetting and the nonwetting fluid flow at measured rates under a given pressure

drop until equilibrium is reached (Scheidegger, 1974). It is not clear that this data can be applied to the situation of interest in this research project where the nonwetting fluid remains immobilized and only the wetting fluid is flowing. This being the case, the possible effects of reduced permeability on the formation of the dissolved contaminant plume is one of the factors that will be considered when analyzing the data from the planned experiments.

3. DNAPL DISSOLUTION: EXPERIMENTAL METHODS

3.1 Introduction

As mentioned in Chapter 1, the experiments that were designed and performed during the course of this research project can be divided into two distinct groups: (1) experiments to study the factors that control the rate of dissolution of residual DNAPLs in saturated porous media, and (2) experiments to examine the flow of DNAPLs and measure levels of residual saturation. After a description of the types of sand that were used in both groups of experiments, this chapter will detail the experimental methods used to study DNAPL dissolution. The flow experiments will be introduced and discussed in later chapters.

3.2 Sand Characterization

Four different sands were used in the various experiments that comprise this research project. One of the sands was collected at a field site located on Canadian Forces Base, Borden, situated approximately 80 km northwest of Toronto, Ontario. A description of this site can be found in MacFarlane et al. (1983). This sand was dried at 105 ^{o}C and sieved prior to use. The 35 to 80 mesh fraction was used for some of the preliminary experiments. Most of the experiments were performed using three silica sands marketed by the

Ottawa Industrial Sand Company (Ottawa, Illinois), and purchased in 50 or 100 pound bags from a local supplier. The three grades used were Flintshot 2.8 (-45 mesh), F-80 (-80 mesh), and No. 17 Silica (-50 mesh). Standard tests were run on each of the four sands to measure hydraulic conductivity (K), permeability (k), density (ρ_s), bulk density (ρ_b) and porosity (n). The methods used for the measurement and calculation of these quantities are described below. The results are summarized in Table 3.1. Product data information supplied by Ottawa Industrial Sand Company for the Flintshot, No. 17 Silica, and F-80 sands are included for reference in Appendix A.

3.2.1 Hydraulic Conductivity and Permeability

The hydraulic conductivity of a porous medium can be measured using either a constant-head permeameter or a falling-head permeameter (Freeze and Cherry, 1979). Klute (1965) recommends the use of a constant-head system for media having hydraulic conductivities greater than 0.01 cm/min and a falling-head system for media having hydraulic conductivities less than that. Since preliminary test results on the F-80 sand (which was the finest and therefore most likely to have the lowest conductivity) showed it to have a value greater than 0.01 cm/min, a constant-head permeameter was used for the measurement of all of the hydraulic conductivities.

The permeameter consisted of a 30-cm long, 4.66-cm i.d. glass cylinder connected with a short section of 1/4-inch tubing to a constant-head reservoir (Figure 3.1). A piece of 100 mesh wire screen

Table 3.1: A summary of the properties of the four sands used in the DNAPL flow and dissolution experiments.

	Sand Density (ρ_s) (g/cm^3)	Bulk Density (ρ_b) (g/cm^3)	Porosity (n)	Hydraulic Conductivity (K) (cm/s)	Permeability[a] (k) (cm^2)
Borden 35/80	2.59	1.58	0.39	0.0244	2.56×10^{-7}
Flintshot 2.8	2.62	1.72	0.34	0.0860	9.03×10^{-7}
No. 17 Silica	2.62	1.72	0.34	0.0377	3.96×10^{-7}
F-80	2.62	1.71	0.35	0.0172	1.81×10^{-7}

[a]Calculated from the corresponding value of hydraulic conductivity using Equation 3.1 and the following properties of water at T = 19 °C: μ = 0.01027 g/cm s and ρ = 0.998 g/cm^3.

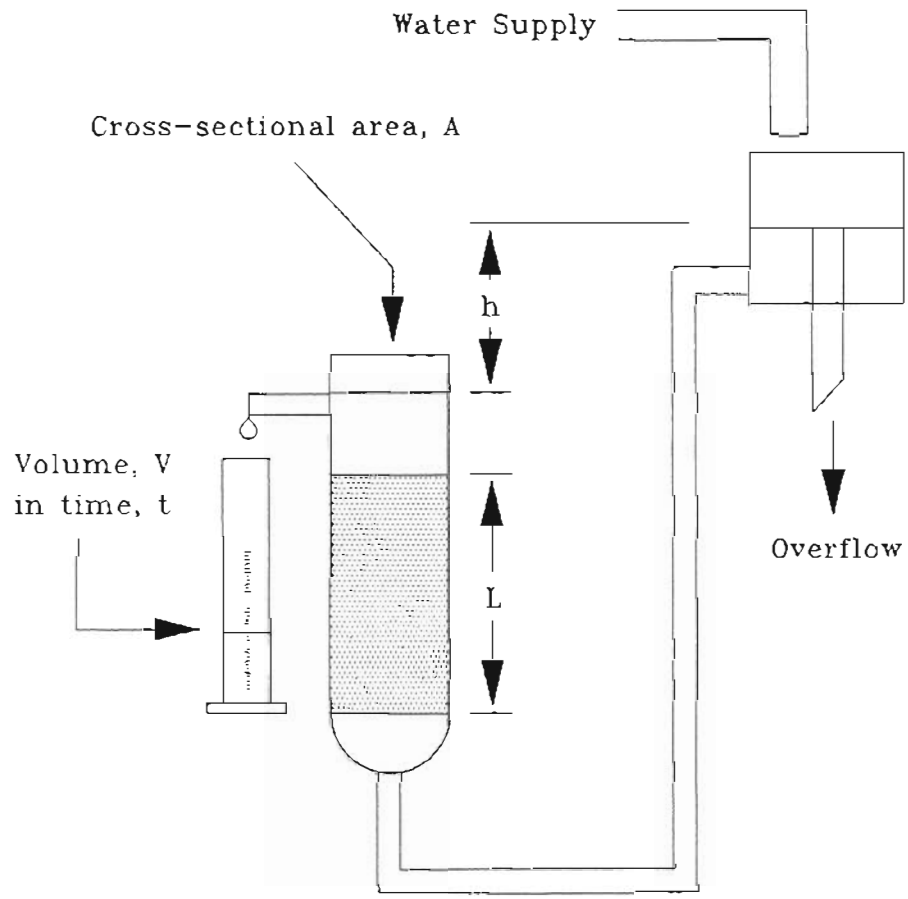

Figure 3.1: Constant-head permeameter.

over a 1/4-inch thick teflon grid was used to support the sand in the cylinder. After adding the sand, the column was filled from the bottom and flushed with deaerated water to remove residual air. The deaerated water was produced by sparging 20 ^{o}C tap water with helium. The removal of the air from the sand could be monitored both visually from the slow disappearance of tiny bubbles at the sand-glass interface and also experimentally from the gradual leveling off of an initially increasing hydraulic conductivity. The finest sand had to be flushed overnight to remove all of the air. The coarsest sand, however, was fully saturated as soon as the column was filled.

After the air was removed from the sand, the hydraulic conductivity was measured by collecting a volume of water (V) in time (t) and using the equation

$$K = VL/tAh \qquad (3.1)$$

where A is the cross-sectional area of the column, L is the length of the sand pack and h is the head (Freeze and Cherry, 1979). Since V/tA is the specific discharge from the permeameter and h/L is the hydraulic gradient, Equation 3.1 is just a direct application of Darcy's Law. Permeability was then calculated from the hydraulic conductivity using Equation 2.6 and known fluid parameters.

3.2.2 Density, Bulk Density and Porosity

The density, bulk density and porosity of each of the sands were readily measured by slowly pouring a preweighed mass of sand (M_s) into

a graduated cylinder containing a known volume of water (V_w). After tapping the cylinder firmly on the bench top several times to make sure that the sand was settled, the total volume of the sand and water (V_T) as well as the bulk volume of the sand (V_b) were read from the cylinder. The three properties were then calculated from the following equations:

$$\rho_s = M_s/(V_T - V_w) \quad (3.2)$$

$$\rho_b = M_s/V_b \quad (3.3)$$

$$n = 1 - (\rho_b/\rho_s) \quad (3.4)$$

3.3 Large Tank Experiments

The goal of these experiments was to study the dissolution of residual DNAPL under conditions where water flowing with typical hydraulic gradients would be allowed to pass around and/or through the residual zone as dictated by relative permeabilities. To accomplish this, a model aquifer was required that would be large enough to contain the residual zone while providing ample room on each side of the residual for the free flow of water. A tank that was 1 m high by 1 m long by 0.75 m wide was designed for this purpose. Two long-term dissolution experiments were carried out in this tank. In the first (DE-1), PCE was the only DNAPL added to the system. In the second (DE-2), both PCE and chlorobenzene (CB) were used. Preparations and procedures for the first experiment are discussed below in detail. Modifications made for the second experiment are also described.

3.3.1 The Design of the Tank

The frame of the tank was constructed from 1-1/2" x 1-1/2" x 3/16" angle iron (Figure 3.2). It was mounted on 12" legs made of 4" box iron. The legs were added to provide access for viewing the bottom and also to facilitate drainage. Extra supports made from 1/2" pipe nipples mounted in pipe flanges were positioned under the midpoint of each side and directly under the center of the tank to prevent it from sagging under the weight of the 3000 pounds of sand and water that would be required to fill it.

The bottom and sides of the tank were made out of 1/2" thick tempered glass and the two ends were made of 1/2" thick Lucite LM (Du Pont, Wilmington, DE). The Lucite was chosen for the two ends so that holes could easily be drilled for the installation of influent and effluent lines and sampling ports. All of the required drilling was done before the tank was assembled. The location and installation of the lines and sampling ports will be discussed later.

Since the welded angle iron frame was neither smooth nor perfectly straight, each sheet of glass and Lucite was laid into the frame on a rope of Pro-poxy Epoxy Sealing Putty (Hercules Chemical Co., New York). This putty was initially soft enough to spread out and provide a smooth even contact surface for the glass and Lucite sheets. Upon hardening, however, the putty easily supported the bottom and sides of the tank without further flowing or cracking. To prevent leaking, all of the joints were caulked with 3M Polyurethane

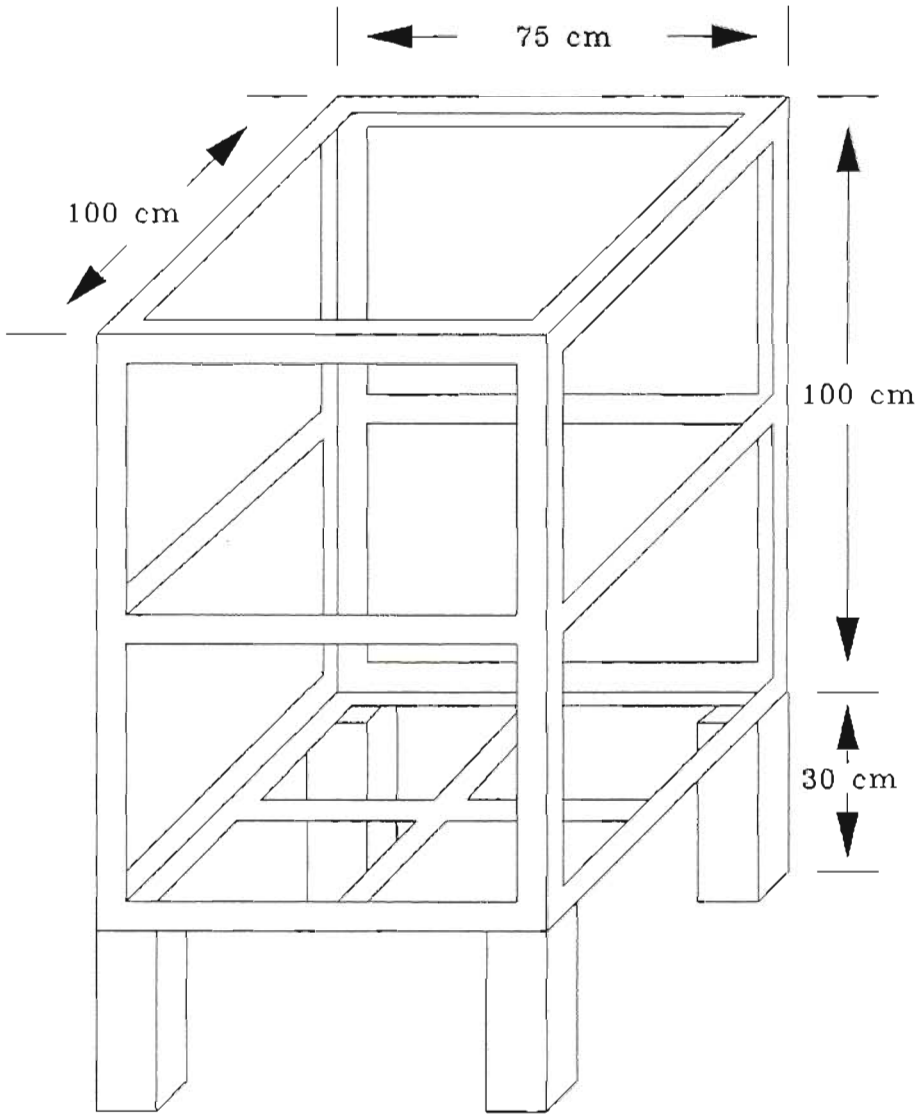

Figure 3.2: Design of the tank frame.

Marine Sealant 5200 (3M Co., St. Paul, MN). Besides caulking all of the interior joints, a bead of caulk was also injected between the angle iron frame and the walls on the outside of the tank. This was done to provide for secondary containment in case the joints had begun to leak.

Reservoirs were constructed on each end of the tank to provide for horizontal flow of water through the sand. This was accomplished by installing screens inside the tank 1/2" from each end. Each screen consisted of 80 mesh type 304 stainless steel wire cloth which, for support, was riveted to a sheet of 20 gauge type 304 stainless steel perforated metal. The metal sheets contained 1/8" perforations on 3/16" staggered centers. An array of 1/2" plexiglas spacers was glued on the inside of each end of the tank to keep the screens from bending when the tank was filled with sand. The edges of the screens were caulked to the sides and bottom of the tank to prevent sand from spilling into the reservoirs.

To control the concentration of fumes in the laboratory, the tank was positioned under a 1-m square ceiling-mounted hood. Clear plastic curtains were attached to the sides of the hood and draped around the tank whenever organic solvents were present. A plexiglas cover was also placed on top of the tank. These precautions were sufficient to ensure that organic vapors were not noticeable in the laboratory except for those times when the DNAPLs were being added to the tank or during excavation of the tank. An organic vapor respirator (Lab Safety Supply, Janesville, WI) was worn on those occasions.

3.3.2 The DNAPL-Containment Cylinder

In the case of an actual spill, dissolution of the contaminant would begin as soon as the DNAPL encountered water. As the DNAPL moved down through the aquifer, the size of the contaminant source would continually change. To simplify the initial conditions in the model, however, it was necessary to create a residual zone of known dimensions that would remain isolated from the aquifer prior to the start of the dissolution experiment. This residual zone also had to meet three criteria: (1) it had to contain sufficient DNAPL so that the contaminant source would remain essentially constant during the course of the experiment, (2) it had to be wide enough to generate a plume that could easily be sampled at a number of locations across its width, and (3) it had to be situated so that the transport of the contaminant plume would not be affected by the walls of the tank.

To create a source of residual PCE for DE-1 that would meet the requirements specified above, a 9" x 14" x 2" glass pan was placed in the center of the tank. A 10 micron slip-on mobile phase HPLC filter (Alltech Associates Inc., Deerfield, IL) was caulked to the bottom of the glass pan and a 3-meter length of 1/8" nylon tubing was slipped onto the filter. A 1-meter length of 15.2 cm diameter sheet metal tubing was then placed in the glass pan over the nylon tubing and filter (Figure 3.3). The seam in the sheet metal tubing was sealed with J-B Weld (J-B Weld Co., Sulphur Springs, TX). Silicone caulk was used to seal the bottom of the sheet metal cylinder to the glass pan.

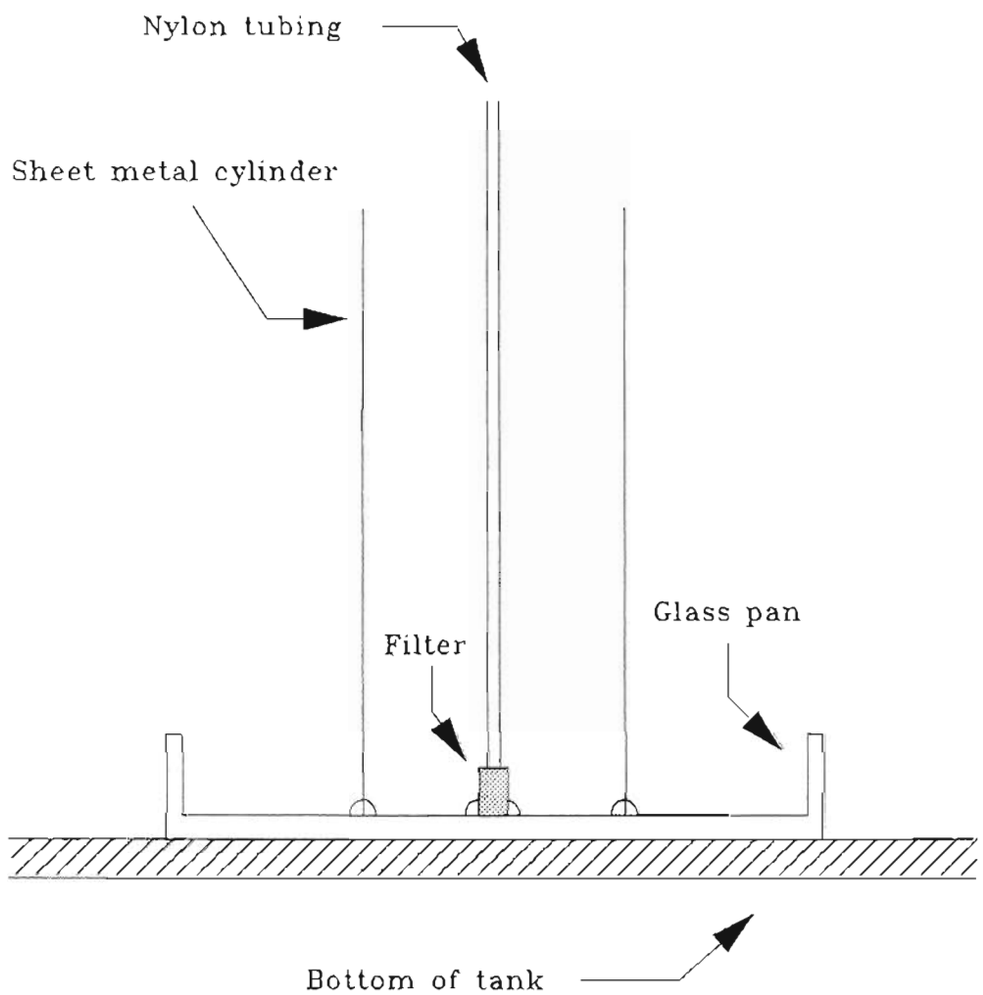

Figure 3.3: Cross-sectional view showing the installation of the DNAPL-containment cylinder in the center of the tank.

The distance from the downgradient end of the cylinder to the nearest sampling point was 40 cm. The nylon tubing and filter were used later to add water and DNAPL to the sand in the cylinder. The cylinder was sealed into the glass pan rather than directly to the bottom of the tank to prevent any DNAPL that might accidentally leak out of the cylinder from flowing along the bottom of the tank and reaching the edges where it might be able to attack the caulk and cause a leak.

In order to create a source consisting of two initially separated DNAPLs in DE-2, two concentric sheet metal cylinders with diameters of 5 cm and 15.2 cm were used. Each cylinder was caulked to the glass pan and contained a piece of tubing connected to a 10 micron filter as described above. The distance from the downgradient edge of the outer cylinder to the nearest sampling point was 20 cm. The inner cylinder was used to contain a residual zone of CB and the annular region was used for a residual zone of PCE.

The tank and cylinder(s) were filled to a depth of 92 cm with Flintshot 2.8 sand. The sand was added to the tank about 35 pounds at a time. After each addition, a plastic trowel was used to spread out the sand as evenly as possible and gently tamp it down. This resulted in a sand pack that consisted of many thin horizontal layers. Because of its narrow size, the cylinder could not be filled in a similar fashion. It was filled by simply pouring the sand in through a large funnel. Care was taken to keep the nylon tube straight and positioned in the center of the cylinder. A total of 2300 pounds of sand were required to fill the tank and cylinder(s).

3.3.3 The Sampling Ports

A series of sampling ports was installed in the downgradient end of the tank. Three horizontal rows and one vertical column of holes were drilled in the Lucite with a #56 (0.0465 inch) drill. The rows were located approximately 20, 40 and 60 cm from the bottom of the tank. The column was placed equidistant from the two sides. For reference, the rows were labeled R1 to R3 (top to bottom) and the needles in each row were numbered from 1 to 23 (left to right). The needles in the column were labeled C1 to C12 (top to bottom) (Figure 3.4). The distance between adjacent holes in each row was 2.8 cm; in the column, 3.3 cm. Two factors influenced the choice of these distances. First, although it was desired to have as many sampling points as possible across the contaminant plume, each point had to be sufficiently far from its neighbors so that the sample volumes from two adjacent points would not overlap. A planned maximum sample volume of 2 mL and a porosity of 0.35 required that this distance be greater than 2.2 cm. Second, the holes in the Lucite had to line up with the holes in the perforated metal sheet so that the samplers could penetrate the screen and enter the sand pack. The chosen distances satisfied both of these requirements.

A series of two-inch long 20 gauge stainless steel hypodermic needles (Popper and Sons, Inc., New York) were inserted into the holes in the Lucite and pushed through the screen into the sand. Cleaning wires were kept in place during the insertion so that sand would not

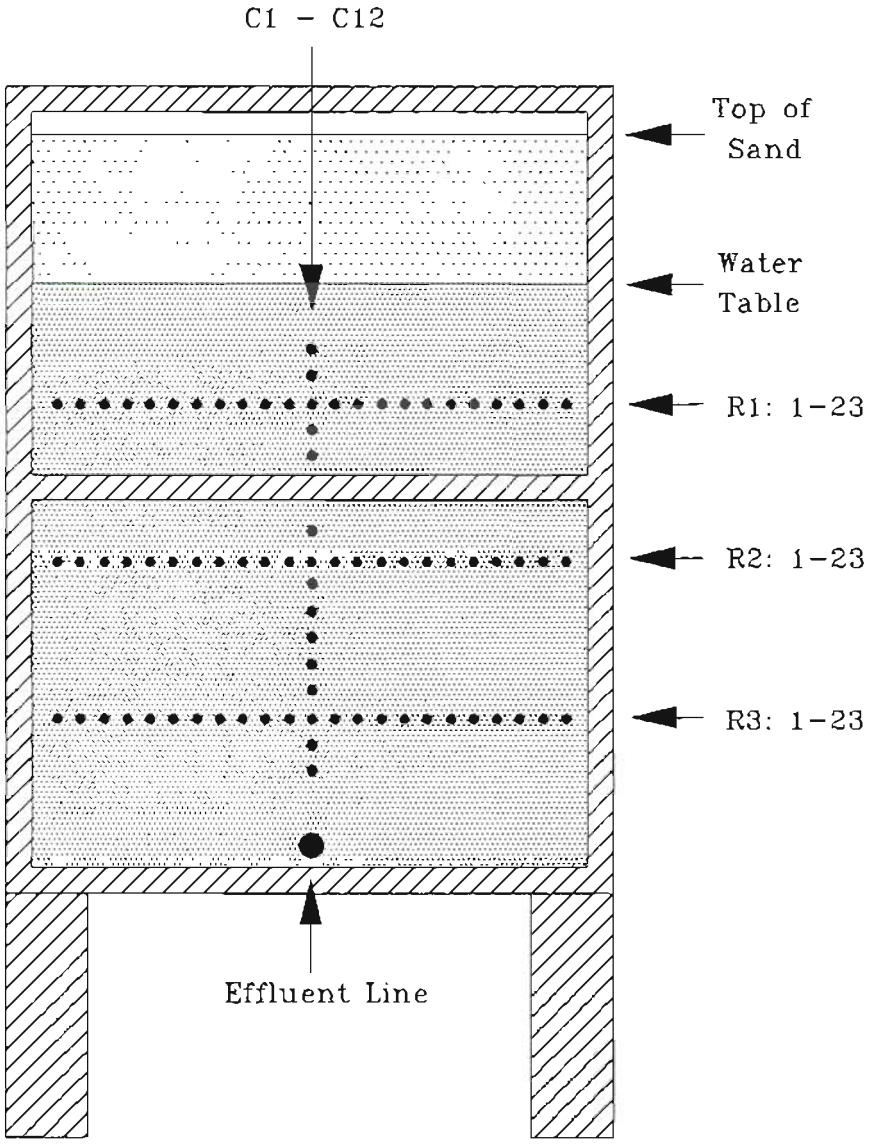

Figure 3.4: Location of the sampling ports in the downgradient end of the tank.

get into and clog the needles. Since both the Lucite and the reservoir were 1/2" thick, the point of each needle ended up 1" from the screen. This distance was more than sufficient to prevent the water in the reservoir from being pulled into the needles when samples were being taken. Silicone caulk was used to seal the needles in the Lucite. The Luer hubs of the needles were then sealed with removable plugs fashioned from teflon. A total of 81 sampling ports were installed in this manner.

3.3.4 The Water Supply

A 1/2" hole was drilled into each Lucite sheet about 2" from the bottom of the tank. Plastic tubing connectors were glued and caulked into the holes and used to connect 3/8" o.d.-1/4" i.d. Tygon tubing (Norton Performance Plastics, Akron, OH) influent and effluent lines to the tank. During the course of the experiments, it was necessary to have a sufficient quantity of deaerated water available to provide for continuous flow through the sand tank at mean velocities of up to 100 cm/day. Two 35-gallon plastic containers were used to store the water. A 1/4" Swagelok bulkhead union (Crawford Fitting Co., Solon, OH) was installed near the bottom of each water container. This was used to connect each of the water supply tanks via a common 1/4" Swagelok union tee to a pump (Figure 3.5). A separate shut-off valve on each water tank allowed one tank to remain on line for supply while the other was off for refilling and sparging. The tanks were filled with 20 ^{o}C tap water and sparged with helium prior to use.

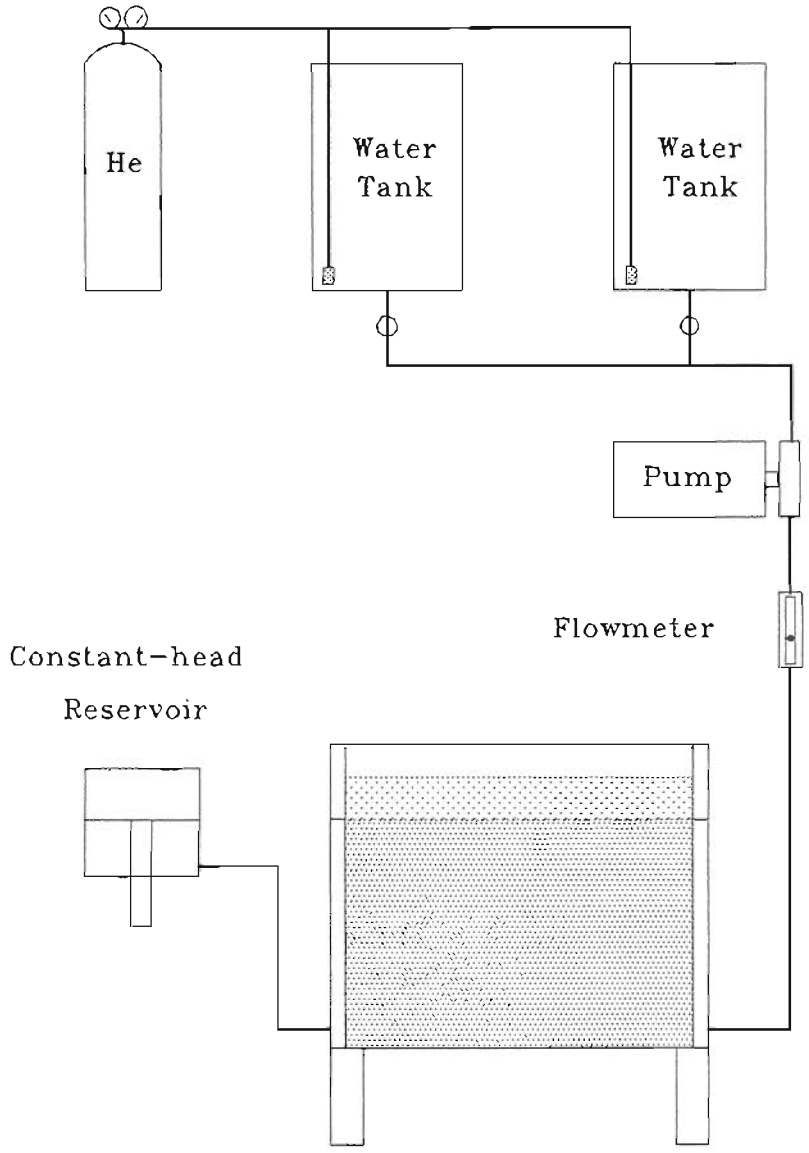

Figure 3.5: General laboratory set-up for the large tank dissolution experiments.

The flow of water into the upgradient end of the model aquifer was maintained with a Masterflex tubing pump system (Cole-Parmer Co., Chicago, IL). This system consisted of a 6-600 RPM variable speed drive fitted with a size 15 standard pump head and controlled by means of a Masterflex solid-state speed controller. This combination of drive and pump head produced flow rates ranging from 10-1000 mL/min; more than ample for the planned range of velocities. The pump head was fitted with C-flex pump tubing (Cole-Parmer Co.) which in turn was connected to the Tygon tubing used to deliver the water to the upgradient end of the tank. A 150-mm flowtube valveless flowmeter (flow range = 9-540 mL/min; Cole-Parmer) was installed in the delivery line to monitor the pump output.

The tank effluent line was connected to a constant-head reservoir which was used to help control the water level in the model aquifer. Since the water flowing through the effluent line experienced a pressure drop, the water level in the aquifer was not the same as that found in the constant-head reservoir. Therefore, the height of the water table was actually controlled by a combination of the pumping rate and the height of the constant-head reservoir. Preliminary tests were performed to ensure that when the pumping rate was changed during the course of the experiment, the constant-head reservoir could be adjusted accordingly to maintain the desired water table in the model aquifer.

A sampling port was installed in the effluent line by placing a Swagelok union tee in the line and using a teflon ferrule to seal a

shortened syringe needle into the tee. This port was used to monitor the total flow of contaminant mass from the tank during the course of the experiment.

3.3.5 Filling the Tank

Since carbon dioxide is significantly more soluble in water than air is in water, the tank was flushed with CO_2 to hasten the removal of residual bubbles of gas when the tank was subsequently flushed with water. Before starting to fill the tank with water, a plexiglas cover was placed on top of it. A piece of nylon tubing was pushed through a hole in the cover down to the bottom of one of the reservoirs. This tube was used to flush the tank with carbon dioxide at a flow rate that provided about three tank volumes of gas to the system in 24 hours. The water pump was then turned on and the tank was slowly filled with deaerated water. While the tank was filling, the flow of carbon dioxide was continued but the tube was pulled up to keep it above the rising surface of the water. When the water level reached the top of the sand, the CO_2 line and cover were removed from the tank.

The rate of water flowing through the tank was set at 150 mL/min and the elevation of the constant-head reservoir adjusted to maintain the water level even with the top of the sand. The water flowing from the tank was cloudy for most of the first day as very fine material was washed from the sand. Effluent conductivity was monitored and initially found to be 1100 μmhos. After two days, the conductivity

dropped to 100 μmhos, equal to that of the influent. Despite flushing the tank with CO_2, small bubbles of gas were still visible on the sides of the tank. Continued flushing with sparged water slowly removed these bubbles in about two to three weeks. When the sand appeared to be fully saturated, the constant-head reservoir was lowered and the water table was adjusted to an elevation of 74 cm above the bottom of the tank. As the water level dropped, a 5-6 cm unsaturated zone and a 12-13 cm saturated capillary fringe remained above the water table. The flow rate was then reduced to about 42 mL/min. This corresponded to a mean velocity of approximately 30 cm/day; the initial velocity planned for these experiments.

3.3.6 Producing the Residual Zones

Since the cylinder was caulked to the glass pan at the bottom of the tank, the sand inside of the cylinder remained dry during the entire tank-filling process. In creating the residual zone, it was not desirable to pour the DNAPL into totally dry sand since, unlike conditions in the field, the DNAPL would then be a wetting fluid rather than a nonwetting fluid. On the other hand, as previously discussed, pouring the DNAPL into a fully water-saturated column of sand is an inherently unstable situation which would lead to a very unpredictable distribution of nonwetting fluid. As a compromise, the procedure described below was used to create the residual zones inside of the cylinders for the two large tank dissolution experiments.

The nylon tube from the filter at the bottom of the cylinder was

connected to a container used to measure the volume of liquid being added to the sand. A 500 mL graduated cylinder modified by the addition of a piece of glass tubing near the bottom was used for this purpose. A snap valve was installed in the line to halt the flow when necessary. First, deaerated water was gravity fed through the nylon tubing into the DNAPL-containment cylinder until the water level reached the top of the sand. The excess water was siphoned from the cylinder leaving water-wet sand. DNAPL was then added to the cylinder. It was not, however, allowed to reach the surface of the sand. Rather, the volume added was calculated to fill only that portion of the cylinder which was below the water table. This was done to reduce volatilization losses and maintain better air quality in the laboratory. The excess DNAPL was also siphoned off so that only residual nonwetting fluid remained in the wet sand. Finally, water was again added to produce a core of sand which contained residual DNAPL in an otherwise water-saturated region. The nylon tubing was then pulled out, leaving the filter at the bottom of the tank. The measured volumes of water and DNAPL added to the cylinder were used to calculate the porosity of the sand and the residual saturation of the DNAPL.

3.3.7 Dissolution Experiment #1

The DNAPL used for the residual zone in DE-1 was a solution of PCE containing 1 g/L of Oil Red EGN dye (Aldrich Chemical Co., Milwaukee, WI). The dye was added to the PCE so that visual

inspection during excavation of the tank would reveal whether or not the residual zone was evenly distributed throughout the volume of the cylinder. The red dye also made it easy to see if any PCE had escaped through the bottom of the cylinder into the glass pan. Preliminary tests showed the dye to be very hydrophobic, producing a dark red color in the organic phase but not dissolving sufficiently in water to provide any visible color. Therefore, the presence of red color could always be interpreted to mean the presence of DNAPL.

During the first step in the formation of the residual zone, 6400 mL of water were required to fill the cylinder to the top of the sand. Subsequent drainage removed 80% of the water that had been added. In earlier experiments it had been determined that Flintshot 2.8 was sufficiently coarse so that the slow addition of deaerated water to the bottom of a column of this sand was capable of displacing all visible signs of air. Assuming that this was the case inside of the metal cylinder, the volume of added water corresponded to a porosity of 0.38. This was higher than the previously measured value of 0.34 (see Table 3.1). The difference was probably due to the fact that it was not possible to firmly pack the sand while filling the cylinder.

The addition of the PCE to the water-wet sand was a slow process. This was not only because the presence of the water reduced the permeability, but also because capillary pressure tended to repel the nonwetting phase from the pores (see Section 2.2). Approximately 20 hours were required to add sufficient PCE to fill the cylinder to a depth of 76 cm. During this time, a small amount of the immiscible

fluid seeped through the seal at the bottom of the cylinder into the glass pan. Since the leak was very narrow and did not move more than two to three centimeters during the course of the experiment, it was not expected to interfere with the subsequent analyses. Excess DNAPL was drained from the cylinder over a period of about seven hours. Assuming a porosity of 0.38 and an even distribution of immiscible fluid throughout the bottom 76 cm of the cylinder, the volume of DNAPL remaining in the sand corresponded to a residual saturation of 13%. Table 3.2 lists the volumes of fluids used during each step in the preparation of this residual zone.

With the water flowing at a mean velocity of approximately 30 cm/day, a block and tackle was used to pull the cylinder from the tank. Removal of the cylinder caused the central core of sand to settle about 3 cm. Water samples were collected and analyzed at two-hour intervals from several centrally located sampling ports. After PCE began to show up in the samples, sampling was done at a sufficient number of positions across the middle row of sampling ports to monitor the full width of the growing contaminant plume. Sampling was restricted to one row during this stage of the experiment because it was not possible to both collect samples from a large number of positions and have repeat sampling events at short time intervals. Since the concentrations were rapidly changing, frequent sampling from a restricted number of locations provided more valuable information about the breakthrough of the contaminant plume. Samples from the effluent line were also collected at regular intervals. When the

Table 3.2: The volumes of water and PCE used to create the zone of residual DNAPL which was the contaminant source in DE-1.

Bulk volume of sand in cylinder = 1.67×10^4 cm^3 (depth = 92 cm)

Initial Vol. of Water In	6400 cm^3
Volume of Water Out	5110
Volume of Residual Water	1290
Saturation of wet sand	20%
Volume of PCE In (depth = 76 cm)	4180 cm^3
Volume of PCE Out	3475
Volume of Residual PCE	705
Residual saturation	13%
Final Vol. of Water In	3875 cm^3

contaminant plume appeared to have reached a steady-state, samples were taken across the width of the plume from all three rows of sampling ports. Samples were also collected from all of the column sampling ports. At any given point in time, about 50 samples were required to delineate the entire plume.

After the initial steady-state was reached, the mean velocity of the water in the tank was increased to 60 cm/day. Once again the plume was checked periodically until it appeared to have reached a new steady-state. Another complete series of samples was then collected and analyzed. This procedure was repeated at mean velocities of 100 cm/day and 10 cm/day. Flow through the tank was then halted for eight days to investigate the extent to which the plume would spread out due to the effects of molecular diffusion. Upon resuming flow at 100 cm/day, contaminant concentrations were measured at regular intervals across the diffusion-broadened plume. This was continued until the plume narrowed and concentrations returned to the levels observed before the flow had been stopped.

As a check, steady-state plumes were re-established and concentrations again measured at each of the four velocities (10, 30, 60 and 100 cm/day). Samples were only collected from R2 at this time. In all cases, the time between the initial steady-state and the repeat experiment was approximately three to four weeks. The total time elapsed between pulling out the cylinder and collecting the final samples was 46 days. Table 3.3 provides a summary and timeline of the procedures just described.

Table 3.3: A summary of events during DE-1.

DAY	TIME	EVENT
1	10 am	Cylinder pulled out of tank Velocity = 30 cm/day
2	8 pm	First signs of PCE in samples Analyzed breakthrough of contaminant plume
		[The first set of steady-state plumes (SSP)]
3	>6 pm	Analyzed 30 cm/day SSP (30-1)
4	1 pm	Velocity increased to 60 cm/day
6	>10 am	Analyzed 60 cm/day SSP (60-1)
	Midnight	Velocity increased to 100 cm/day
8	>3 pm	Analyzed 100 cm/day SSP (100-1)
	8 pm	Velocity reduced to 10 cm/day
15	>9 am	Analyzed 10 cm/day SSP (10-1)
19	9 am	Velocity increased to 100 cm/day
24	9 am	Flow halted
32	9 am	Flow resumed; Velocity = 100 cm/day Analyzed diffusion-broadened plume
		[The second set of steady-state plumes]
33	10 am	Analyzed Row 2 of 100 cm/day SSP (100-2)
	Noon	Flow reduced to 60 cm/day
35	10 am	Analyzed Row 2 of 60 cm/day SSP (60-2)
	11 am	Flow reduced to 30 cm/day
38	6 pm	Analyzed Row 2 of 30 cm/day SSP (30-2)
	7 pm	Flow reduced to 10 cm/day
46	3 pm	Analyzed Row 2 of 10 cm/day SSP (10-2)

3.3.8 Dissolution Experiment #2

The DNAPLs used for the residual zone in DE-2 were PCE and CB. As in DE-1, dyes were added to these DNAPLs. The CB contained 1 g/L of Oil Blue N dye (Aldrich Chemical Co., Milwaukee, WI) and the PCE contained 1 g/L of Oil Red EGN. Residual CB was generated inside the 5 cm cylinder and residual PCE was generated in the annular region between the concentric 5 cm and 15.2 cm cylinders. Table 3.4 lists the volumes of fluids used during each step in the preparation of these residuals.

The CB residual in the inner cylinder was prepared first. The volume of CB residual in this cylinder corresponded to a saturation of 14%. No problems were encountered during this procedure. However, while the PCE was being added to the sand in the annular region, some of it began to leak through the caulk seal into the glass pan at the bottom of the tank. This started when less than one-half of the necessary amount of PCE had been added. The leak continued to get worse and before two-thirds of the PCE had been added, it was decided that the procedure for the addition of PCE had to be changed before PCE escaped from the pan. Inspection of the residual zones through the bottom of the tank indicated that there was no exchange of fluids between the PCE in the annulus and the CB in the inner cylinder.

Siphoning the mobile PCE from the cylinder halted the advance of this fluid across the bottom of the pan. In fact, PCE could be seen flowing from the pan back into the cylinder during this step. When

Table 3.4: The volumes of water, PCE, and CB used to create the zones of residual DNAPL which were the contaminant sources in DE-2.

	Inner Cylinder (CB)	Annular Region (PER)
Initial Vol. of Water In	595 cm^3	4390 cm^3
Volume of Water Out	500	3725
Volume of Residual Water	95	665
Saturation of wet sand	16%	15%
Volume of CHC In	470 cm^3	[a]2500 cm^3
Volume of CHC Out	387	2025
Volume of Residual CHC	83	475
Residual saturation	14%	11%
Final Vol. of Water In	355 cm^3	--

[a]See text concerning problems encountered during this step.

the last of the mobile PCE had been removed, water began to flow into the cylinder. It was necessary to continue siphoning this water to prevent the cylinder from flooding before the final addition of PCE was made. In order to continue the addition of PCE, a piece of 1/4" stainless steel tubing was inserted into the sand in the annulus. The bottom of the tube was at an elevation about equivalent to R1. This meant that the PCE would probably not reach its originally planned elevation (the water table). However, this was done in order to increase the chances of having an evenly distributed residual zone throughout the middle of the cylinder where most of the sample collection would take place. A 1/4"-1/16" Swagelok reducing union (Crawford Fitting Co., Solon, OH) was used to attach a 16-gauge syringe needle to the tube. A syringe was then used to inject 100 mL of PCE into the tube. The tube was then moved and another injection was made. A total of eight injections were made at regularly spaced locations around the annulus. It was hoped that this fluid would flow through the wet, unsaturated sand and complete the formation of the PCE residual zone.

As the excess PCE from the injections made its way to the bottom of the cylinder, it was removed in the siphon tube. Eighteen hours after the final addition, PCE was no longer showing up in the siphon tube. Siphoning was then halted and water was allowed to flow into the cylinder. Because of the problems encountered, it was difficult to estimate the residual saturation of PCE. Since some of the PCE had escaped from the cylinder, the real saturation would be less than that

calculated from the volume of unrecovered PCE divided by the pore volume in the annulus. However, the final depth of the PCE residual zone was not well-known, but due to the changes discussed above, it was less than originally planned. This would tend to make the real saturation greater than the calculated saturation. Since it was impossible to know the relative size of these counteracting errors, a residual saturation of 11% was calculated by assuming that they cancelled each other out.

With the water flowing at a mean velocity of 30 cm/day, the two cylinders were pulled from the tank. The inner cylinder was pulled out first so that the water would have access to both residual zones as soon as the outer cylinder was withdrawn. When the outer cylinder came out of the tank, a small amount of sand was pulled out with it. Inspection of this sand revealed it to be clean, water-damp sand apparently from the vadose zone. The residual-containing sand, therefore, was probably not unduly disturbed during this step. The mean velocity of the water was maintained at 30 cm/day for the entire experiment. Samples were regularly collected across the contaminant plume and analyzed for both CB and PCE. The plume was monitored until the CB concentrations no longer appeared to be increasing. The elapsed time for this experiment was 104 days.

The configuration of the residual zones in DE-2 meant that water flowing down the center of the tank would first pass through 5 cm of residual PCE, then through 5 cm of residual CB, and finally through another 5 cm of residual PCE. Under these conditions, the

breakthrough of CB would be affected by: (1) a reduction in the velocity of water through this zone due to a reduction in the permeability caused by the presence of the residual, and (2) the partitioning of the dissolved contaminant into the droplets of residual PCE that are encountered downgradient. Unlike the situation just described for DE-2, water being forced through a column cannot slow down as it passes through a residual zone. Therefore, by comparing the CB breakthrough from DE-2 to what is observed from a column with a similar pattern of residuals, it should be possible to determine what effect, if any, reduced permeability in the residual zone has on the transport of dissolved contaminants from that zone. To this end, a column dissolution experiment (DE-3) was also carried out. The details of this experiment are given in Section 3.4.

3.3.9 Preparation of Standards

Standards were prepared by injecting a concentrated DNAPL-methanol stock solution into vials of water. Several factors had to be taken into account when making up both the stock solution and the standards. First of all, standards were required which would span the full range of concentrations being analyzed. In these experiments, sample concentrations ranging up to the solubility limit were considered possible. The range of concentrations being analyzed, however, was reduced by diluting the more concentrated samples (see Section 3.3.10). Second, Munz and Roberts (1986) have shown that the presence of a cosolvent such as methanol will affect the activity of

an organic solute in water if the mole fraction of methanol exceeds $5x10^{-3}$. Therefore, the concentration of PCE or CB in the stock solution had to be high enough so that the amount of stock solution required for the standards would not result in a mole fraction of methanol that exceeded this amount. The concentration of the stock solution could not be too high, however, or the amount required for the standards would be so small that it would not be possible to weigh out the required amount with reasonable accuracy. With these constraints in mind, a stock solution was prepared for DE-1 which contained approximately 0.5 weight percent PCE in methanol. Two stock solutions were prepared for DE-2. The first contained approximately 0.5% PCE and 0.3% CB in methanol and was used for the early stages of CB breakthrough. The second had the amount of CB increased to about 1.4% and was used in the later stages of the experiment.

A set of three standards were made from each stock solution. The standards were prepared in 40 mL glass vials fitted with Mininert Valve screw caps (Supelco, Inc., Bellefonte, PA). The actual volume of each of the vials was measured prior to its use. The vials were then tared, a volume of water equal to 2/5 of the vial volume was added to each, and the mass of added water determined. A 100 μL Gastight Fixed Needle syringe (Hamilton Co., Reno, NV) was used to transfer approximately 20, 60 and 100 μL of stock solution, respectively, into the vials through the Mininert valves. The mass of added stock solution was measured. The standards were shaken and placed in a 20 ^{o}C water bath for equilibration prior to analysis.

The initial aqueous-phase concentration of CHC in each standard was calculated using the equation

$$\text{ppm CHC} = \frac{(\text{Wt. \% CHC in Stock})(\text{Mass of Stock})}{(\text{Total mass of solution})} \times 10^4 \qquad (3.5)$$

The PCE concentrations in the DE-1 and DE-2 standards were about 5, 15, and 25 ppm. The CB concentrations in the DE-2 standards were about 3, 8, and 14 ppm in the lower level standards and 13, 39 and 65 ppm in the higher level standards. Since the most concentrated samples were diluted 8-fold (0.25 mL to 2.0 mL) before analysis, these standards were useful for samples containing PCE and CB concentrations up to their respective solubility limits of 200 and 488 ppm.

3.3.10 Sample Collection and Analysis

Water samples were extracted from the syringe-needle sampling ports on the tank using Hamilton Gastight Teflon Luer Lock syringes (Hamilton Co., Reno, NV). The teflon plug was first removed from the Luer hub of one of the needles and several drops of water were allowed to flow out in order to flush and fill the needle with fresh sample. The syringe was then attached to the needle and used to withdraw the desired sample volume. For low concentrations, a 2.5 mL syringe was used to collect a 2.0 mL sample. For higher concentrations, a 1.0 mL syringe was used to collect samples with volumes ranging down to 0.25 mL. Each sample was placed in a 3.5 mL amber screw cap septum vial (Pierce Chemical Co., Rockford, IL; actual volume = 5.0 mL) and sealed

with a cap containing a teflon-lined butyl rubber septum. Samples with volumes smaller than 2.0 mL were placed in vials containing sufficient water so that the total volume equalled 2.0 mL.

The sample vials were shaken vigorously and placed in a 20 ^{o}C water bath. During the first half hour after collection, the vials were shaken every ten minutes. Test results indicated that this was sufficient for volatile CHCs in samples of this size to achieve gas/liquid-phase partitioning equilibrium. This equilibration step was necessary since the aqueous phase CHC concentrations were determined by headspace analysis. Most samples were analyzed within one hour of collection. None of the samples were in the water bath longer than two hours before analysis.

All of the analyses were made on a Hewlett-Packard HP 5890 Gas Chromatograph (Hewlett-Packard Co., Avondale, PA) equipped with a flame ionization detector. The column was a 30 m x 0.75 mm i.d. Supelco Wide-Bore Glass Capillary (Supelco, Inc., Bellefonte, PA) with a 1.0 μm SPB-1 coating. A column head pressure of 32 kPa maintained a helium carrier gas flow rate of 6 mL/min. The N_2 makeup gas flow rate was 35 mL/min.

A 1 mL Hamilton Gastight syringe was used to withdraw 0.4 mL of headspace gas from each sample or standard vial. Because of the small total volume of headspace gas in the sample vials (3 mL), extracting 0.4 mL with a syringe causes a significant reduction in the pressure in the vial. The following procedure was used to prevent the dilution to the sample that would have occurred if the syringe had been

withdrawn from the vials while the gas was at reduced pressure. First, the syringe needle was inserted through the septum into the sample vial and the tip was positioned above the surface of the liquid. The plunger of the syringe was raised and lowered several times to flush the needle and the sample was drawn into the syringe. Then, a second syringe needle (without syringe) was pushed through the septum. As soon as the second needle penetrated the septum, the syringe was quickly pulled out of the sample vial and its contents injected into a gas sampling valve attached to the inlet of the GC. The insertion of the second needle caused the pressure in the vial to quickly increase to ambient pressure and sweep more sample into the syringe. Because the needle restricted the mixing of the gases, rapid removal of the syringe prevented the sample already in the syringe from being diluted significantly by the air entering the vial.

Upon initiating a GC run, 0.1 mL of the sample was automatically flushed onto the column by carrier gas. Samples from DE-1 were analyzed isothermally at 130 ^{o}C for 3.5 minutes. Samples from DE-2 were analyzed at 100 ^{o}C for 4 minutes. The conditions were changed for the DE-2 samples to enhance separation of the PCE and CB peaks. Data was collected, stored and analyzed on a PC-compatible computer by means of a Nelson Analytical 3000 Series Chromatography Data System with Version 3.5 software (Nelson Analytical, Inc., Cupertino, CA). Sample concentrations were calculated by the software using an external standard calibration curve. The calibration curve was produced by linear regression of the data from the three standards.

Since both the standards and the samples had the same headspace-to-liquid volume ratio, it was not necessary to use the Henry's constants for PCE and CB to determine the actual vapor-phase concentration. Therefore, the calibration curve was prepared using the initial aqueous-phase concentrations calculated from Equation 3.5.

Fresh standards were prepared and analyzed, and a new calibration curve was generated prior to each sampling session. The standards were reanalyzed during the course of the day to correct for any response changes or baseline drift that may have occurred. The response of the HP 5890 proved to very stable, not only during the course of a day, but indeed from day to day. An analysis of the regression lines for 24 standard curves prepared over a period of 17 days showed that the coefficient of variation (CV) of the slope (the response factor) was less than 3%. Certainly, part (if not most) of this variation can be attributed to the uncertainty inherent in the preparation of a large number of replicate standards. The mean value for the intercept of the 24 curves was not significantly different from zero. The standard deviation for the intercept was 0.2 ppm.

To estimate the precision of the analytical procedure, replicate samples were collected and analyzed on a number of occasions. This was accomplished by withdrawing a larger than normal volume into the syringe and injecting equal fractions of it into three or four vials. After equilibration and analysis using the procedure discussed above, a CV was calculated for the data. The CVs calculated from these groups of replicate data ranged from 1.1% to 3.2%.

3.3.11 Excavation of the Tank

After the final samples were collected in DE-1, the flow of water through the tank was stopped. The tank was then excavated by scraping off layers of the sand a few centimeters at a time. The distribution of the red dye was observed in order to determine if the PCE had spread evenly throughout the cylinder during the formation of the residual zone. Observation of the dye distribution also indicated whether or not the PCE had remained within the original boundaries of the cylinder during the experiment. Water was pumped from the tank during this procedure to keep the water table below the layer that was being excavated. The tank was not excavated following DE-2, but was maintained for further experiments.

3.4 Dissolution Experiment #3 (Column Experiment)

The column used for DE-3 was a 30-cm long, 5.0-cm i.d. glass chromatographic column with an internally threaded end (Ace Glass Inc., Vineland, NJ). The column was modified by attaching a drip tip with a teflon stopcock to the bottom to control the flow rate. Glass wool was placed on the bottom to prevent sand from getting into the stopcock. First, dry sand (Flintshot 2.8) was poured into the cylinder to a depth of about 5 cm. Then, a second 5 cm depth of sand containing 15% water saturation and 10% PCE saturation was added. This was followed by 5 cm of sand containing 15% water and 10% CB saturations, a second 5 cm of sand containing water and PCE and

finally, another 5 cm of dry sand (Figure 3.6). A piece of nylon rod stock was used after each addition to pack down the sand. The DNAPL-containing portions of sand were prepared just prior to their addition to the column by thoroughly mixing 175 g of sand with 5.1 g of water and then adding either 5.5 g of PCE/red dye solution or 3.7 g of CB/blue dye solution and again mixing thoroughly. It was initially intended to have a 15% CB residual in the center of the column to better mimic the conditions in the tank. However, this high of a CB saturation was found to be mobilized by the flowing water in a preliminary test. Therefore, to make sure that the DNAPLs would remain immobile, the CB saturation had to be reduced to about 10%.

A piece of plastic tubing was slipped onto the drip tip and used to slowly add deaerated water to the bottom of the column. Air did not appear to remain trapped in the sand during this step. The addition of water was continued in this manner until it reached the top of the sand. The remaining portion of the column was filled with water added through the top. A teflon adapter was used to join the top of the column via a Swagelok connection to a piece of 1/8" nylon tubing. This tubing delivered deaerated water to the column during the dissolution experiment. The stopcock was opened and the water flowing from the column was collected and its volume measured. The flow rate was adjusted to obtain a mean linear velocity of about 30 cm/day; the same as maintained in the tank during DE-2. Since it was difficult maintaining a steady flow rate, the volume of effluent was continuously measured and the progress of the plume was monitored on

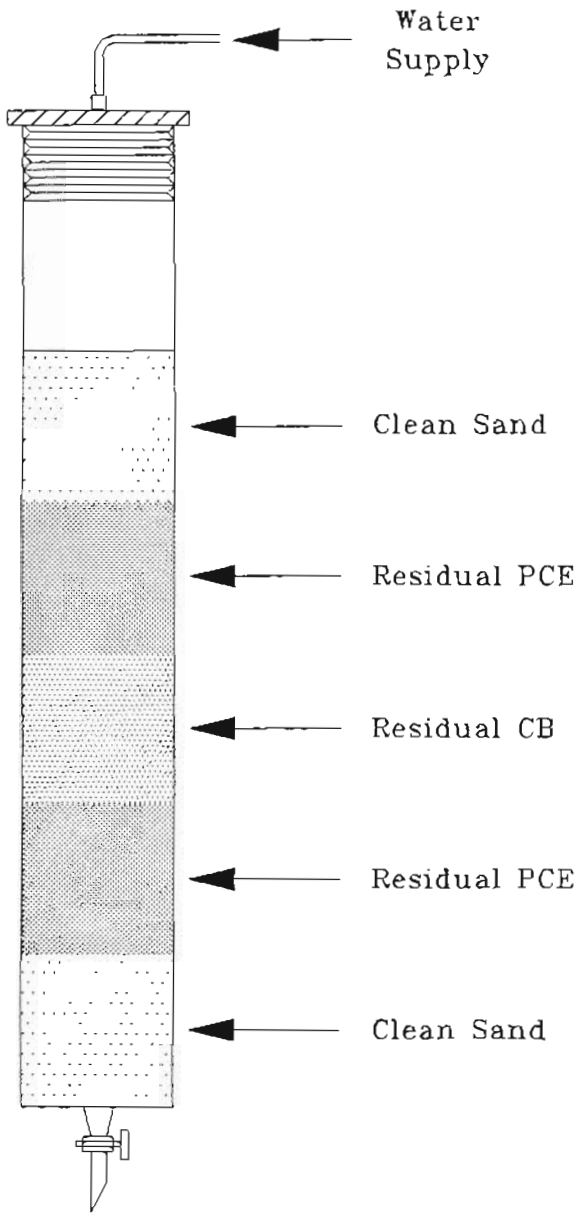

Figure 3.6: The column used to generate PCE and CB breakthrough data in DE-3.

the basis of bed volumes rather than time. In this case, one bed volume was considered to be the pore volume of the CB-containing section rather than the volume of the entire bed.

Samples were collected periodically in 5-mL screw-top septum vials. This was done by placing a vial containing 1.75 mL of clean water under the drip tip, catching 5 drops of the column effluent, and then quickly sealing the vial with a septum-containing screw top. To reduce volatilization losses, the mouth of the vial was held up around the drip tip so that the drops of effluent only had to travel a short distance through the vial before entering the water. Although 5 drops was usually close to 0.25 mL, a more precise volume and dilution factor were obtained by weighing the vial before and after collecting the sample. All samples were then shaken and allowed to equilibrate in a 20 ^{o}C water bath before analysis. The method of analysis was the same as that used for the samples collected from the tank (see Section 3.3.10). On the 75th day of the experiment, the column developed a crack and a large, unknown volume of water was lost before the leak could be halted. However, sufficient data had been collected by this time for comparison to the results of DE-2.

4. DISSOLUTION EXPERIMENT #1: RESULTS AND DISCUSSION

4.1 Breakthrough

4.1.1 Observations

The first measurable PCE concentrations were found in samples taken from the centers of Rows 1 and 2 (Ports R1-12 and R2-12) at a time of 34 hours after the cylinder was pulled from the tank. During the next 22 hours, the concentrations measured in the center of the tank rose rapidly from less than 1 ppm to over 190 ppm. The contaminant plume also broadened significantly during this time. The initial breakthrough of PCE as measured at Port R2-12 is shown in Figure 4.1. The evolution of the plume as measured across R2 is shown in Figure 4.2. The dashed vertical lines in Figure 4.2 represent the diameter of the cylindrical source. In this and all subsequent figures showing the concentrations across a row of sampling ports, the location of the Y = 0 point corresponds to the position in the sampling grid that was directly downgradient from the center of the residual zone. Although it was originally intended to have the central sampling ports exactly in this location, this was not the case. Either a minor error in the positioning of the cylinder or movement of the cylinder/glass pan assembly (which was not attached to

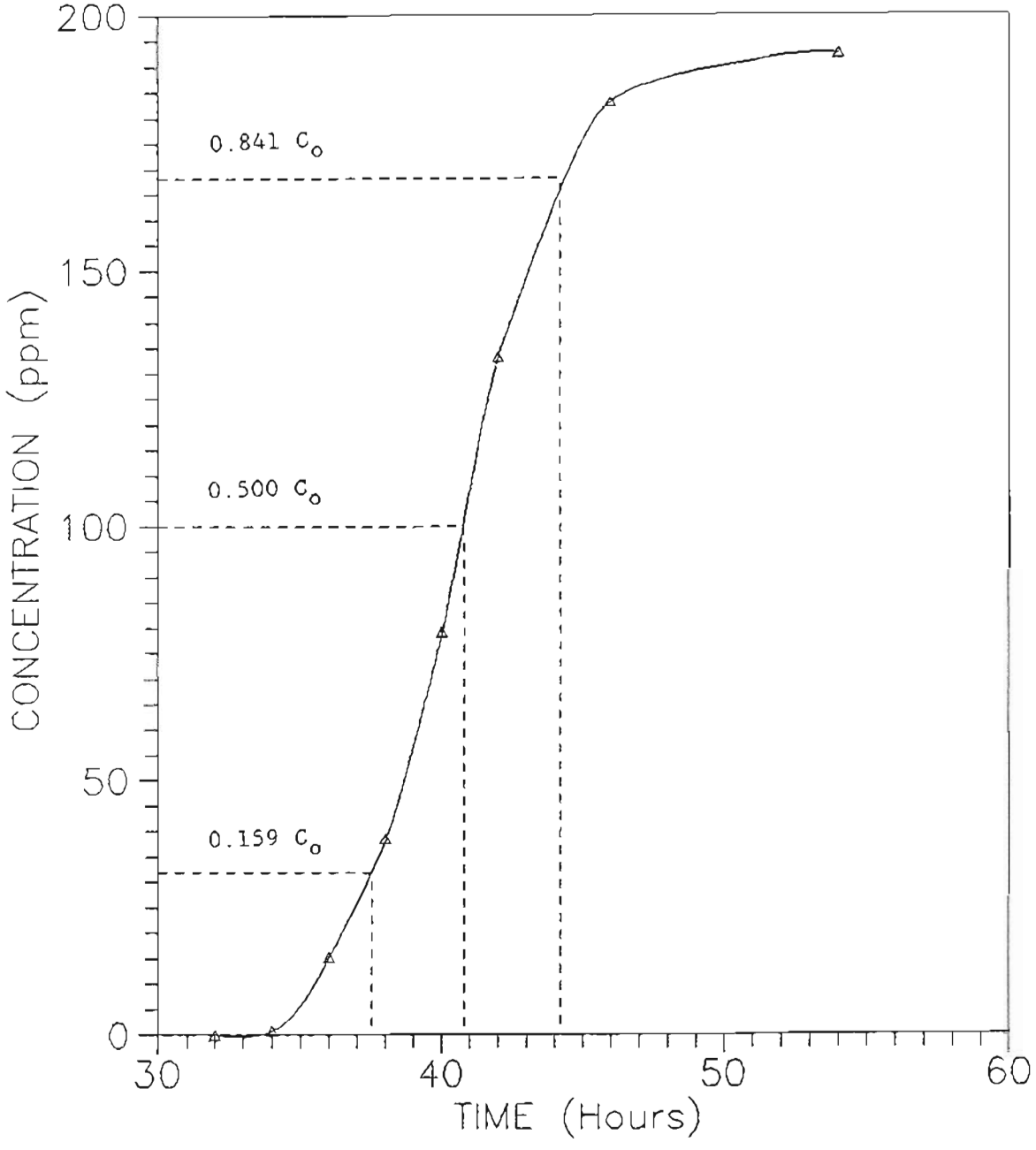

Figure 4.1: The breakthrough of PCE in dissolution experiment #1 as measured at sampling port R2-12.

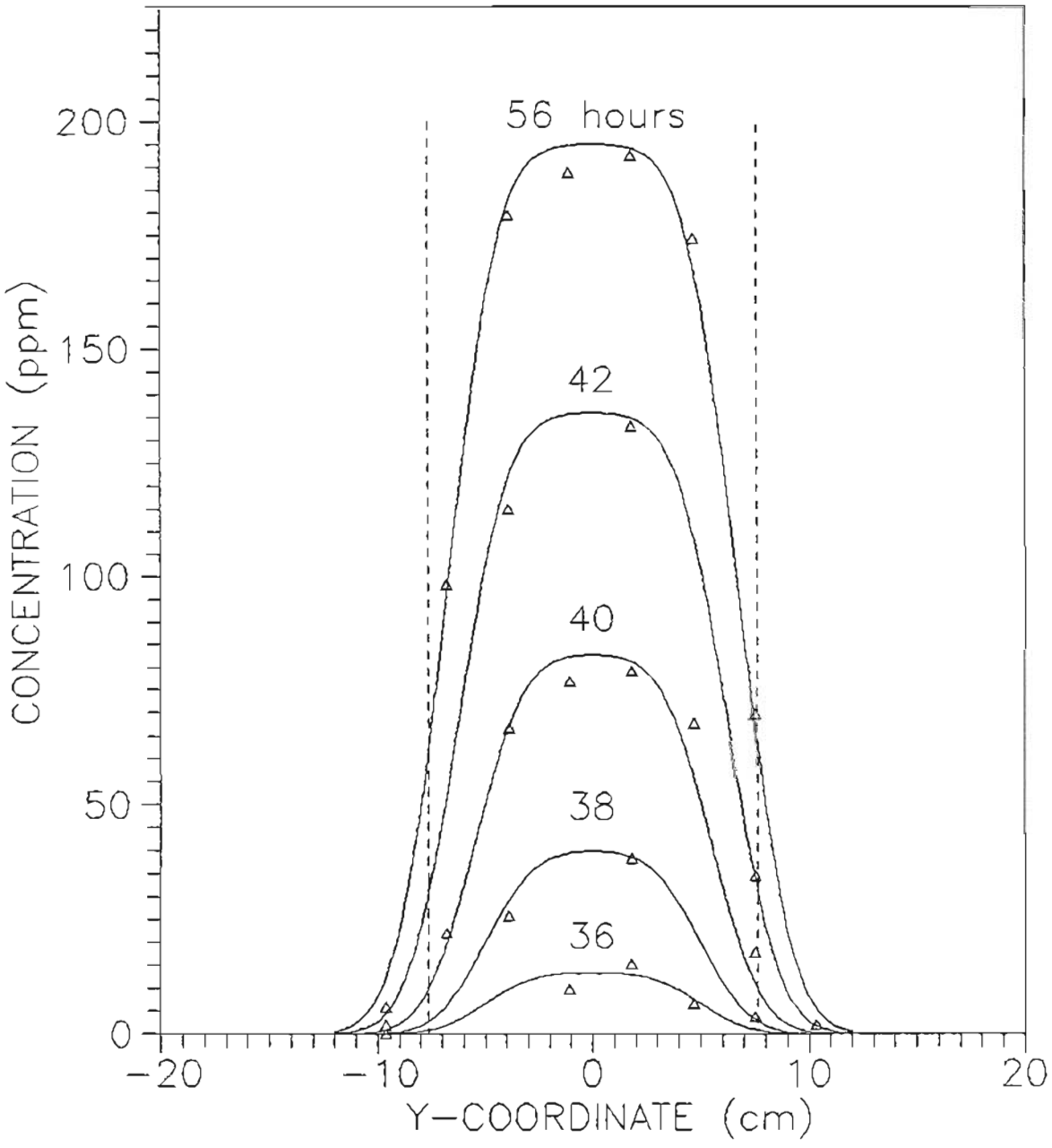

Figure 4.2: The evolution of the PCE contaminant plume as measured across the middle row of sampling ports.

the bottom of the tank) during the initial stages of filling the tank with sand resulted in the center of the cylinder being located about 1.8 cm from the centerline of the tank. This shift meant that the central column of sampling ports was not located exactly in the center of the plume. Because of the width of the plume, however, samples collected from these ports were still in that portion of the plume where the concentrations were the highest. The coordinates of each sampling port are given in Appendix B.

4.1.2 Models

Assuming that the dissolved PCE in the model aquifer was not subject to biodegradation, sorption or volatilization, then its transport was controlled entirely by advection and hydrodynamic dispersion. Advection is the transport of the solute by the bulk motion of the flowing groundwater. Hydrodynamic dispersion is the spreading out of the solute as a result of both molecular diffusion and mechanical mixing (Freeze and Cherry, 1979). Spreading in the same direction as the bulk flow is known as longitudinal dispersion. Spreading in a direction perpendicular to the bulk flow is called transverse dispersion. Under conditions of steady-state, uniform flow in a saturated, homogeneous, isotropic medium, this type of solute transport is described by the advection-dispersion equation

$$\frac{\partial C}{\partial t} = D_L \frac{\partial^2 C}{\partial x^2} + D_T \frac{\partial^2 C}{\partial y^2} - \bar{v}_x \frac{\partial C}{\partial x} \qquad (4.1)$$

In the two-dimensional form of the equation shown above, C is the solute concentration, $\bar{v}$ is the mean water velocity, and D_L and D_T are the coefficients of longitudinal and transverse dispersion, respectively.

The relationship between the mechanical and diffusive components of dispersion is given in the equations for the dispersion coefficients,

$$D_L = \alpha_L \bar{v} + D^* \tag{4.2}$$

$$D_T = \alpha_T \bar{v} + D^* \tag{4.3}$$

where α is a constant with units of length and is usually referred to as the dispersivity. The $\alpha_L\bar{v}$ and $\alpha_T\bar{v}$ terms in these equations represent the contribution of mechanical dispersion to the total dispersion. In laboratory column studies, α_L has been found to range from 0.01 to 1 cm (Anderson, 1978). In the field, however, it can range from 1 to 100 m depending on the heterogeneity of the aquifer. The magnitude of α_T is normally only about 0.2-0.01 that of α_L (de Marsily, 1986).

The relative importance of the two components of dispersion can be determined from a calculation of the Peclet Number, Pe, which is the ratio of advective to diffusive mass transfer.

$$Pe = \bar{v}\, d/D^* \tag{4.4}$$

In this equation, d is the average particle diameter, and D^* is the coefficient of molecular diffusion in the porous medium (Freeze and

Cherry, 1979). When $\bar{v}$ is very small, the Peclet number will be small and the magnitude of the dispersion coefficients will be controlled by the magnitude of D^*. As the mean water velocity is increased, both the Peclet number and the dispersion coefficients will increase. Eventually, the mechanical dispersion term will dominate. Studies have shown that for systems in which the Peclet number is less than 0.1, dispersion is controlled primarily by molecular diffusion, whereas for those in which the Peclet number is greater than 10, dispersion is controlled primarily by mechanical mixing (de Marsily, 1986). The range from 0.1-10 represents a transitional region where both components play a role. This is illustrated in Figures 4.3(a) and (b).

The steep slopes of the curves shown in both Figures 4.1 and 4.2 indicate that there was very little spreading of the contaminant plume in this experiment. Thus, both longitudinal and transverse dispersion must have been relatively small in this system. For the data shown in these figures, $\bar{v} = 3.5 \times 10^{-4}$ cm/s and $d = 0.036$ cm. Using a typical value for D^* of 5×10^{-6} cm^2/s (Freeze and Cherry, 1979) results in a Peclet number of 2.5. This is in the range where mechanical dispersion and diffusion are comparable. Since preliminary calculations showed that diffusion is minimal in the short transport time from source to sampling ports in this experiment (< 30 hours), it was not surprising that the observed dispersion was small. The use of a fairly uniform sand in these experiments probably also helped to keep dispersion to a minimum (Klotz et al., 1980).

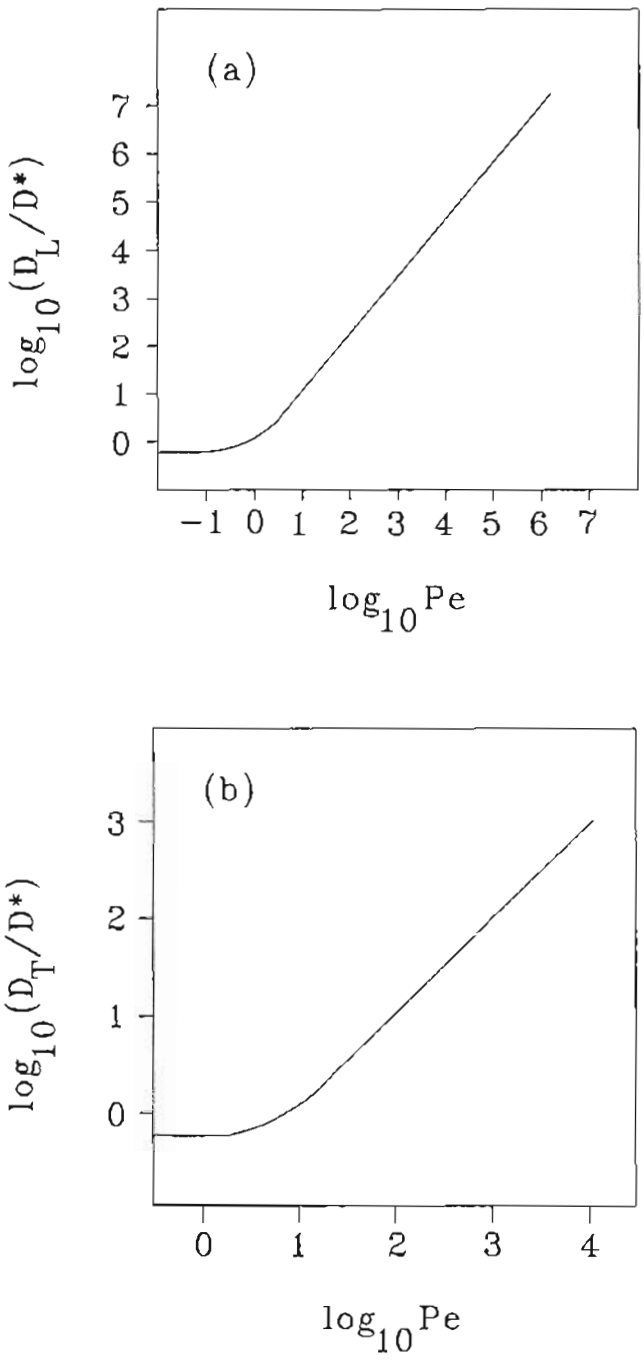

Figure 4.3: The coefficients of (a) longitudinal dispersion (D_L) and (b) transverse dispersion (D_T) as a function of the Peclet number (Pe) (adapted from the experimental results of Pfankuch (1963) as presented in de Marsily (1986)).

The breakthrough data collected from 32 to 56 hours after the start of DE-1 were used to calculate the value of D_L. Because of the design of the aquifer and geometry of the source, contaminant concentrations measured in a given row of sampling ports are probably best simulated with a two-dimensional mathematical model. However, since dispersion appeared to have been small in this system, and since the breakthrough data being modeled came from the center of a relatively wide source where lateral dispersion should have been at a minimum, the data was initially treated by assuming that the source behaved like a step-function and that the contaminant transport was one-dimensional. The validity of using a one-dimensional model to estimate D_L in this system will be further discussed later in this chapter.

Under the conditions stated above, the solution to the advection-dispersion equation is (Ogata and Banks, 1961)

$$C = (C_o/2)\left[\operatorname{erfc}\left(\frac{x - \bar{v}t}{2\sqrt{D_L t}}\right) + \exp\left(\frac{x\bar{v}}{D_L}\right) \operatorname{erfc}\left(\frac{x + \bar{v}t}{2\sqrt{D_L t}}\right)\right] \quad (4.5)$$

where C_o is the concentration of the source, x is the distance from the source at which the concentration is being calculated, and erfc represents the complimentary error function. Ogata and Banks (1961) have shown that when $(D_L/\bar{v}x)$ is less than 0.0075, this equation can be simplified to

$$C = (C_o/2) \operatorname{erfc}\left(\frac{x - \bar{v}t}{2\sqrt{D_L t}}\right) \quad (4.6)$$

with less than a 5% error. This was the case for the breakthrough portion of DE-1. An advantage of using Equation 4.6 to calculate D_L is that it is related to the cumulative normal distribution of $[-(x - \bar{v}t)/\sqrt{2\ D_L\ t}]$ with a mean,

$$t_m = x/\bar{v} \tag{4.7}$$

and a standard deviation,

$$\sigma = (\sqrt{2\ D_L\ t_m})/\bar{v} = (\sqrt{2\ D_L\ t_m})/(x/t_m) \tag{4.8}$$

Because of the properties of the normal distribution, an equation for D_L can be derived as shown below (Bear, 1979).

$$2\ \sigma = (t_{0.841} - t_{0.159}) \tag{4.9}$$

$$2\ (\sqrt{2\ D_L\ t_m})/(x/t_m) = (t_{0.841} - t_{0.159}) \tag{4.10}$$

$$D_L = (x^2/8\ t_m)[(t_{0.841} - t_{0.159})/t_m]^2 \tag{4.11}$$

In these equations, $t_{0.159}$, t_m, and $t_{0.841}$ are the times at which the effluent concentration is equal to 15.9%, 50%, and 84.1% of the source concentration, respectively.

The times, $t_{0.159}$ = 37.5 hr, t_m = 40.8 hr, and $t_{0.841}$ = 44.2 hr, are marked with dashed lines in Figure 4.1. Using these values along with x = 40.0 cm, the distance from the downgradient edge of the cylinder to the tip of syringe needle R2-12, results in an estimate of $D_L = 3.7 \times 10^{-5}$ cm^2/s. Direct comparison of this result to values of D_L obtained by other researchers is difficult due to the fact that

many longitudinal dispersion experiments are carried out in columns using higher water velocities and coarser sands than were used in DE-1 (see, for example, Harleman and Rumer (1963) and Rose and Passioura (1971)). However, from empirically determined parameters obtained for slightly coarser sands by Klotz et al. (1980), values of D_L at this velocity were found to be 5.3×10^{-5} cm^2/s for a sand with median grain diameter (d_{50}) = 0.061 cm and n = 0.31, and 1.9×10^{-5} cm^2/s for a sand with d_{50} = 0.08 cm and n = 0.34.

4.2 Mean Velocities in the Model Aquifer

During the breakthrough stage of DE-1, the mean water velocity was estimated to be 30 cm/day. This velocity, as well as each of the other three velocities used in DE-1, was calculated from the flow rate (Q), the cross-sectional area (A) of the sand below the water table, and the porosity (n).

$$\bar{v} = Q/(A\ n) \tag{4.12}$$

The volumetric flow of the water was checked repeatedly both with an inline flowmeter and by occasionally measuring the volume of effluent collected in a known period of time. The mean contaminant velocity for the breakthrough experiment, estimated from the distance traveled and the time at which $C = C_o/2$, was found to be 23.5 cm/day; 20% lower than the mean water velocity. Since this estimate was based on one-dimensional transport, any reduction in the plume concentration due to lateral spreading of the dissolved PCE would delay the arrival of the

$C = C_o/2$ point and contribute to a low estimate for the plume velocity. Also, if the residual zone was indeed a region of reduced permeability, a decrease in the local velocity downgradient from this region may have delayed the breakthrough of the contaminant. Sorption is not thought to have been a factor due to a lack of organic carbon in the silica sand.

Although the retarded contaminant velocity may have been real, there was some concern that the solute/water velocity difference was actually the result of an erroneous mean water velocity. It was already pointed out that the sand inside of the cylinder was found to have a porosity of about 0.38 rather than 0.34. Since a higher porosity would result in a lower velocity, this source of error was considered. However, because an attempt had been made to pack the sand firmly inside the tank, a procedure which was not possible inside of the cylinder, the porosity of the sand in the tank was probably somewhere between 0.34 and 0.38. Since a value of 0.42 is necessary for a 20% error, it is doubtful that an inaccurate porosity was the source of most of the observed velocity difference.

Further investigation into the reason for the low velocity led to the conclusion that it was due to the water in the capillary fringe. Driscoll (1986) points out that water in the saturated capillary fringe is subject to the same physical forces as is water below the water table. Therefore, hydraulic gradients in the saturated fringe will result in the flow of water even though this water is above the water table. In a study of this effect, Mixon

(1988) has recently demonstrated that capillarity can significantly increase the net flow of groundwater into an excavation. He found typical values 10-20% higher than what would be predicted without the effects of capillarity. The increase in flow was roughly proportional to the height of the capillary rise. Since the conditions for flow into the downgradient reservoir of the model aquifer were nearly identical to those given by Mixon for flow into an excavation, it is reasonable to assume that the flow was affected in the same way. If the mean water velocities in the model aquifer are recalculated by adding the 12-13 cm capillary fringe to the cross-sectional area, the results are 14-15% lower than those originally obtained. The remaining 5% could easily be attributed to one or more of the other factors discussed above. For convenience, the various stages of DE-1 will still be referred to by the original nominal velocities of 10, 30, 60 and 100 cm/day. However, the values used in the modeling results discussed in the rest of this chapter will only be 80% of these velocities.

4.3 Steady-State Plume

4.3.1 Observations

After 56 hours at the initial velocity of 30 cm/day, the concentrations in R2 no longer appeared to be changing. Samples were then collected from all of the sampling ports that were in the path of the contaminant plume. The concentrations across each of the three rows of samples are plotted in Figure 4.4. (The data used for this

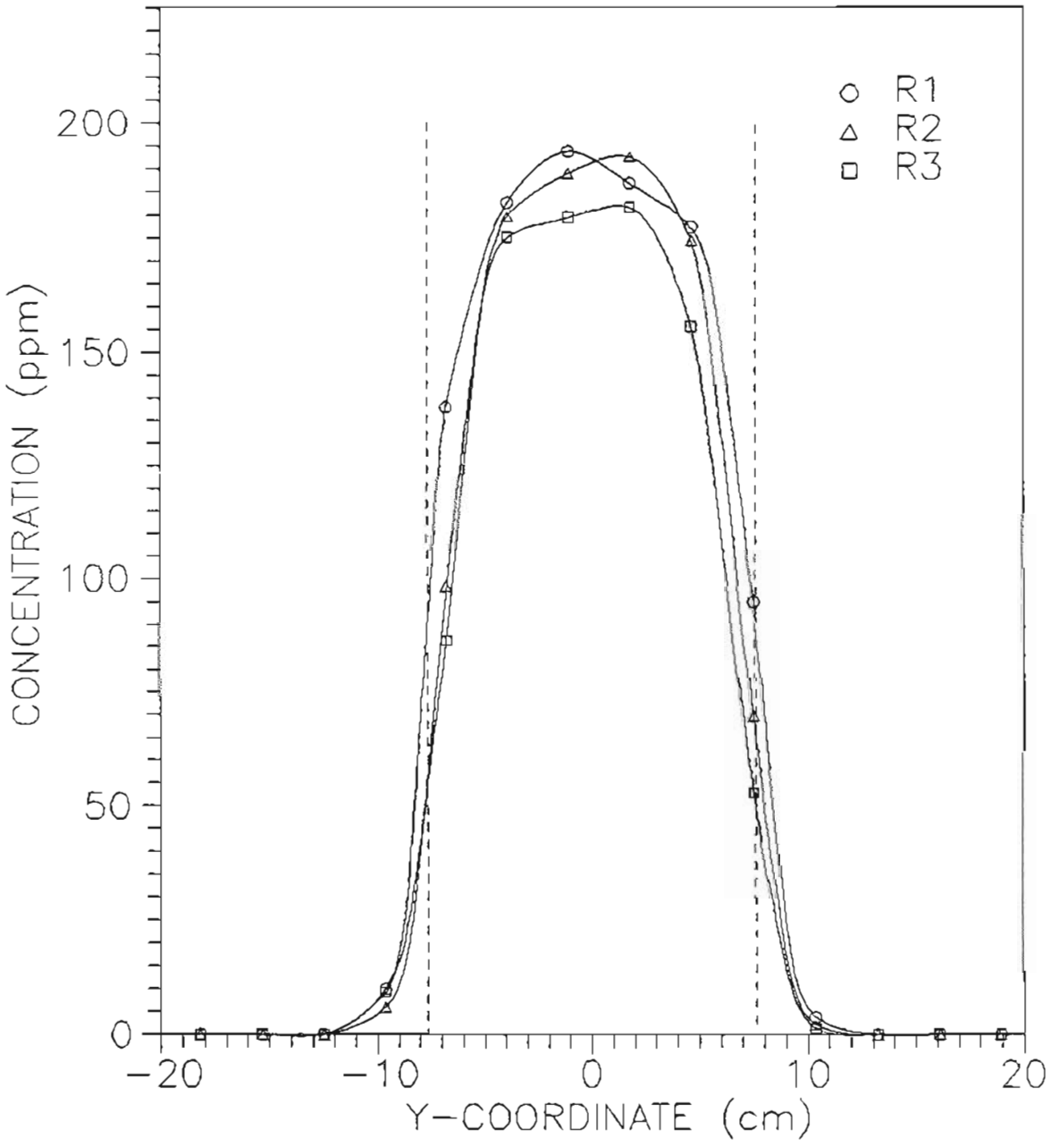

Figure 4.4: The steady-state concentrations of PCE across all 3 rows of sampling ports measured at a mean water velocity of 30 cm/day.

figure are listed in Appendix C along with the other data from both DE-1 and DE-2 used for the figures in Chapters 4 and 5.) The concentrations in R1 and R2 were quite comparable. Although the temperature in the laboratory did not remain constant at 20 ^{o}C, it did not deviate more than 1-2 degrees from this value. Therefore, maximum possible PCE concentrations were expected to have been close to 200 ppm, the reported 20 ^{o}C solubility limit for this compound. Although none of the samples were found to contain 200 ppm of PCE, the highest levels in R1 and R2, 193.7 and 192.5 ppm respectively, were within 4% of this value.

Contaminant levels measured in R3 were less than those measured at the same time in the other two rows. The highest concentration here was 181.4 ppm, almost 10% less than the expected solubility. A possible explanation for this is that this portion of the plume had not yet reached steady state when these samples were collected. This may have been caused by the sand at the bottom of the tank being more tightly packed due to the pressure of the overlying sand. A lower permeability produced by the tighter packing would have resulted in a lower mean water velocity. This would have delayed the breakthrough of contaminants in R3.

After increasing the mean water velocity from 30 to 60 cm/day, the concentrations in R2 were regularly monitored for signs of change. From the data collected during the first 24 hours after the velocity was increased, it was not possible to tell if the contaminant levels were remaining constant or if there were slight changes that were

masked by the normal scatter of the data. After 48 hours, however, it became clear that the concentrations had undergone small but definite changes. Table 4.1 lists the PCE concentrations measured in Ports R2-8 through R2-15 during this 48 hour interval. The significance of these changes were checked by performing a linear regression on the data from each sampling port as a function of time. The F-test was then applied to the ratio of the resulting mean square values (Davies and Goldsmith, 1972). The F-value obtained for each group of data as well as the relevant significance values for the appropriate degrees of freedom are also given in Table 4.1. The concentration changes were found to be highly significant (1%) in three of the ports, significant (5%) in three other ports and moderately significant (10%) in only two of the ports. From this data it can be seen that the concentrations on the edges of the plume had decreased while those in the middle had increased. Since the transverse dispersivity (α_T) is assumed to be a constant (see Section 4.1.2), this result is consistent with the decreasing influence of molecular diffusion that accompanies an increase in the mean water velocity.

When steady-state had been reached at 60 cm/day, concentrations were again measured throughout the entire plume. This data is plotted in Figure 4.5. The concentrations in R1 and R3 were comparable at this velocity. This confirmed the earlier suspicion that the values in R3 at 30 cm/day were low simply because the plume at this depth had not yet reached steady-state. The only noticeable difference in the three curves shown in Figure 4.5 is the higher concentration in the

Table 4.1: PCE concentrations measured in R2 after increasing the mean water velocity from 30 to 60 cm/day. Concentrations are expressed in ppm. See text for an explanation of the F-value.

Port	Hours After Increasing Velocity					[a]F-value
	0	24	32	40	48	
8	5.89	3.46	2.47	1.61	1.46	154.2
9	98.3	89.0	87.5	87.7	82.4	49.1
10	179.4	187.8	189.3	188.6	200.1	13.8
11	188.8	193.4	197.0	195.8	198.6	38.7
12	192.5	196.4	199.3	195.8	204.9	5.75
13	174.3	176.8	184.1	183.0	194.2	9.83
14	69.8	64.6	65.5	61.1	63.2	12.0
15	2.08	1.74	0.90	0.70	0.54	24.4

[a]The significance levels for these F-values are (Davies and Goldsmith (1972)):

1% = 34.1
5% = 10.1
10% = 5.54

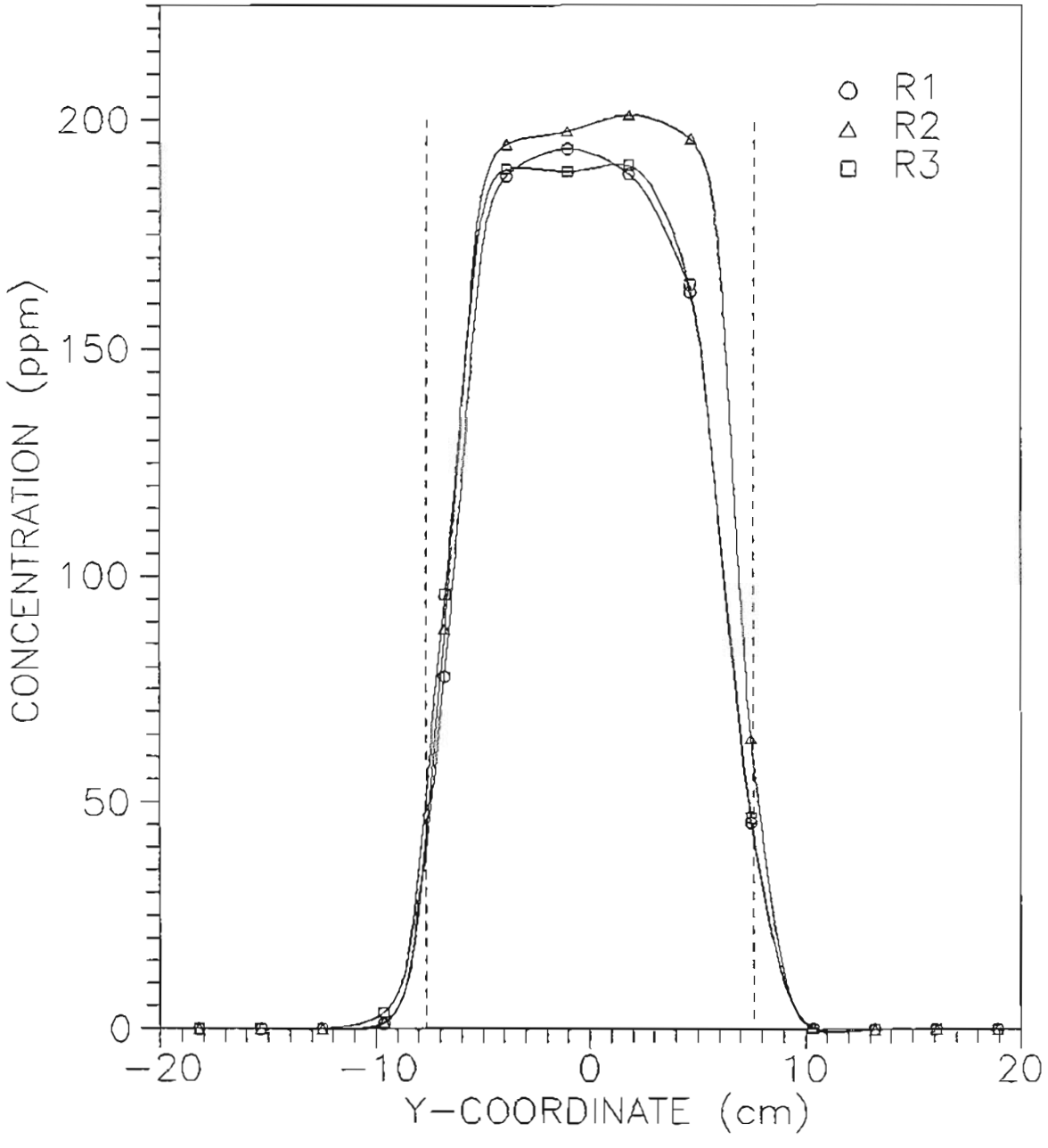

Figure 4.5: The steady-state concentrations of PCE across all 3 rows of sampling ports measured at a mean water velocity of 60 cm/day.

right half of the plume in R2. The reason for this is not known.

Increasing the mean water velocity to 100 cm/day did not appear to have any further effect on the width of the plume. Concentrations measured after two days at this velocity are shown in Figure 4.6. The slight drop that was observed in values measured in the center of the 100 cm/day plume was surprising. Considering the fact that at this point in the experiment less than 2% of the PCE had been dissolved, it would not be reasonable to expect to observe a decrease due to a depletion in the source. The low values may have simply been due to random sampling and/or analytical errors.

As mentioned above, the narrowing that was observed in the contaminant plume when the velocity was increased from 30 to 60 cm/day was thought to have been due to the decreasing influence of diffusion at the higher velocity. If this were true, then reducing the velocity below 30 cm/day should have caused the plume to broaden. To test this, the velocity was reduced to 10 cm/day. After seven days at this velocity, the concentrations were again measured across the entire plume. These results are shown in Figure 4.7. Comparison of this figure with the three previous figures shows two readily noticeable differences. First, the plume had broadened as expected. The effects of molecular diffusion on the contaminant plume were more predominant at this velocity. Since the Peclet number for this system at a mean velocity of 10 cm/day is 0.8, this observation is consistent with the empirical trends discussed earlier. Second, the PCE concentrations measured in the samples taken from R1 decreased significantly. This

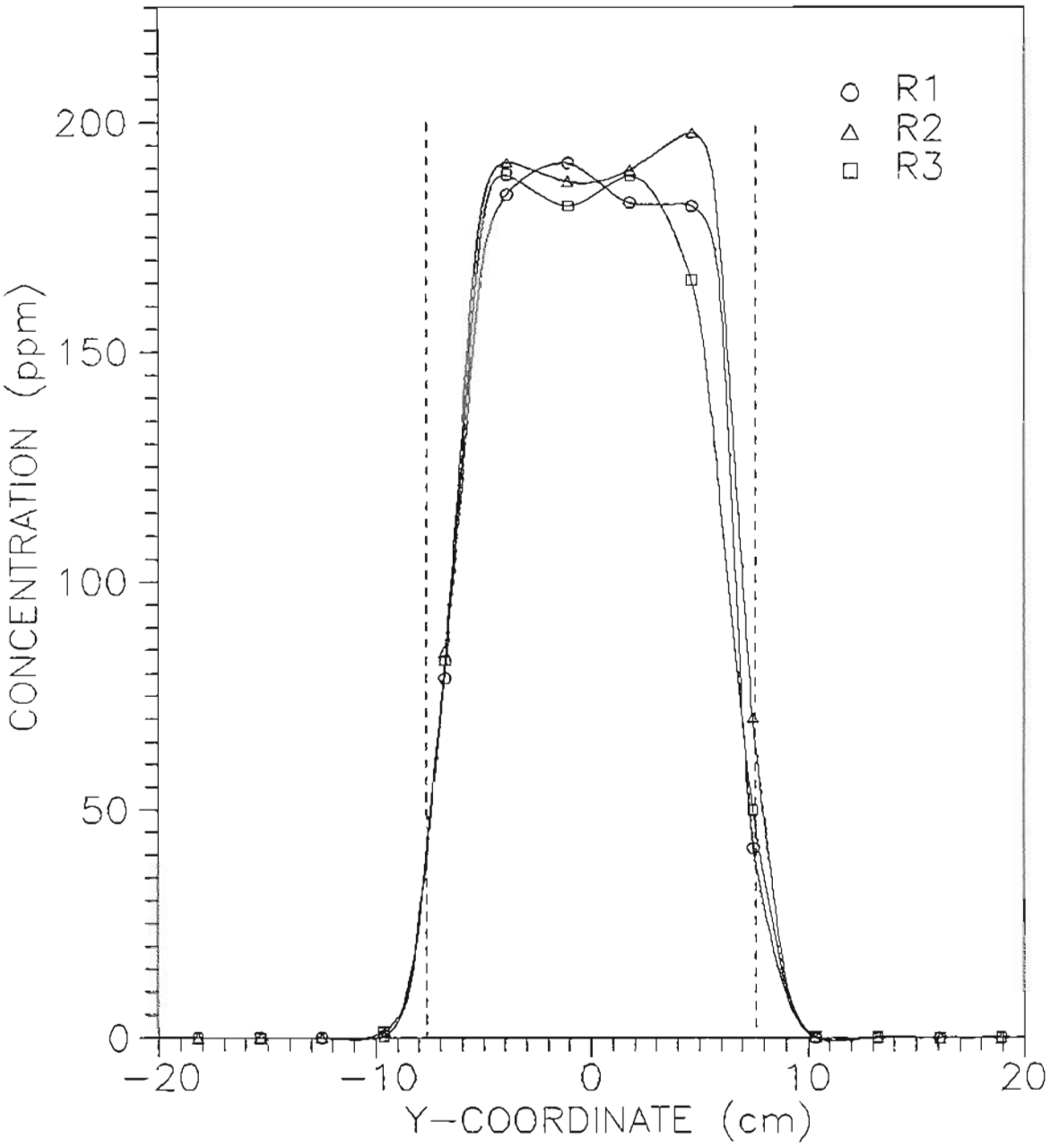

Figure 4.6: The steady-state concentrations of PCE across all 3 rows of sampling ports measured at a mean water velocity of 100 cm/day.

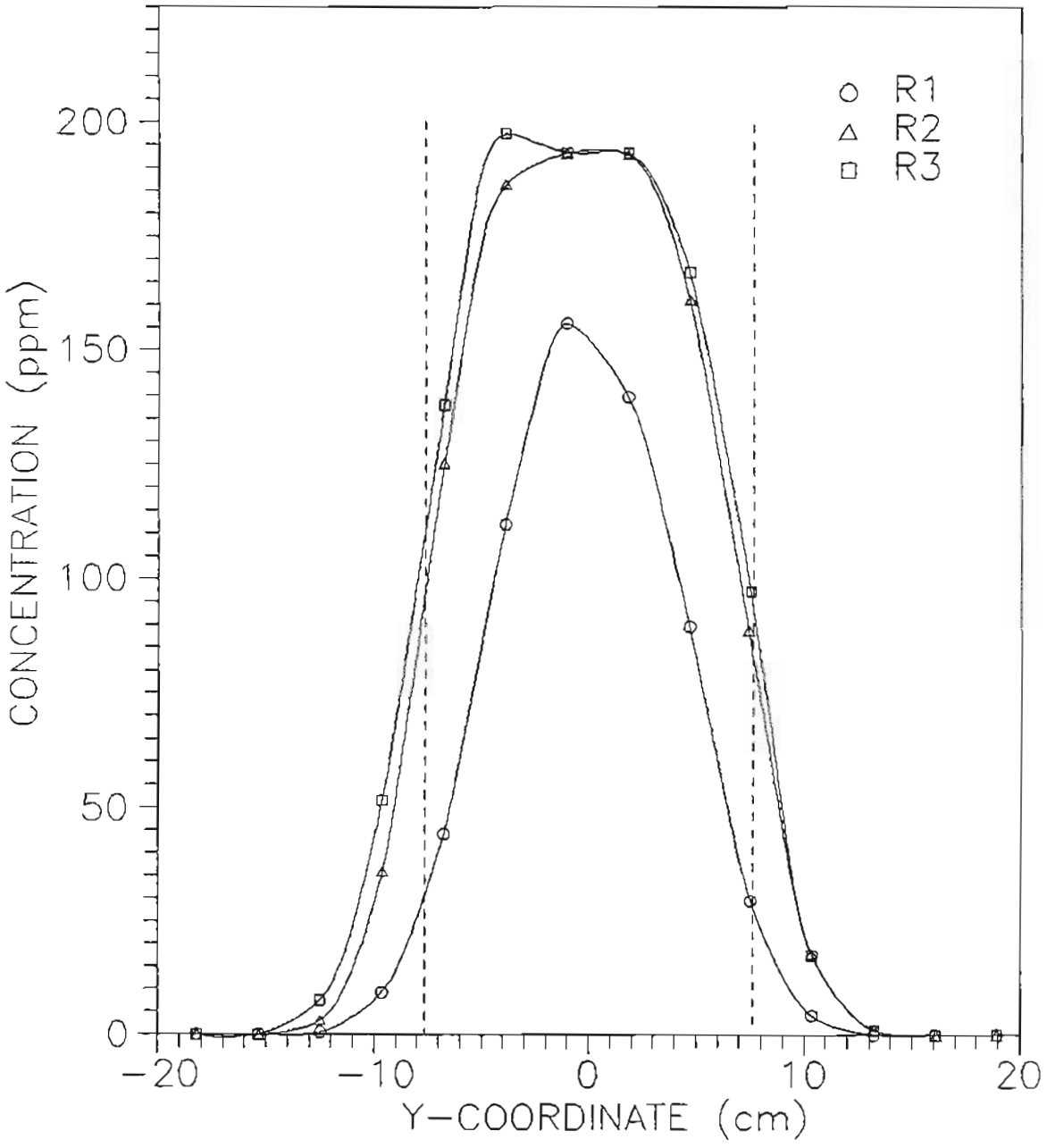

Figure 4.7: The steady-state concentrations of PCE across all 3 rows of sampling ports measured at a mean water velocity of 10 cm/day.

change had not been anticipated. Since the needles in R1 were the closest to the water table (approximately 15 cm below), and since the source only extended to the water table, dispersion into the capillary fringe aided by diffusion into the vadose zone may have been responsible in part for the lower concentrations. Although the decrease in concentration seems rather large to be attributed entirely to dispersion and diffusion, it is not known what else may have had an effect on the plume.

After the initial series of experiments were completed, the constant-concentration plumes were again established at each of the four velocities. Samples were collected from R2 and analyzed for comparison with previously measured data. The time between each pair of experiments at a given velocity was between three and four weeks. The results of these analyses are shown in Figure 4.8. The solid lines are the original R2 data taken from Figures 4.4-4.7. The dashed lines are the new data. The highest concentrations observed at this time were all slightly higher than those previously obtained. The new peak values were around the fully-saturated value of 200 ppm. The greatest change was in the 30 cm/day plume. Although this contaminant plume was thought to have been at a steady-state when the first set of analyses were made, subsequent results seem to indicate that peak concentrations continued to slowly increase until the solubility limit was reached. Silliman and Simpson (1987) have observed a similar pattern of breakthrough for a sodium chloride tracer in a heterogeneous sand pack. They found that concentrations

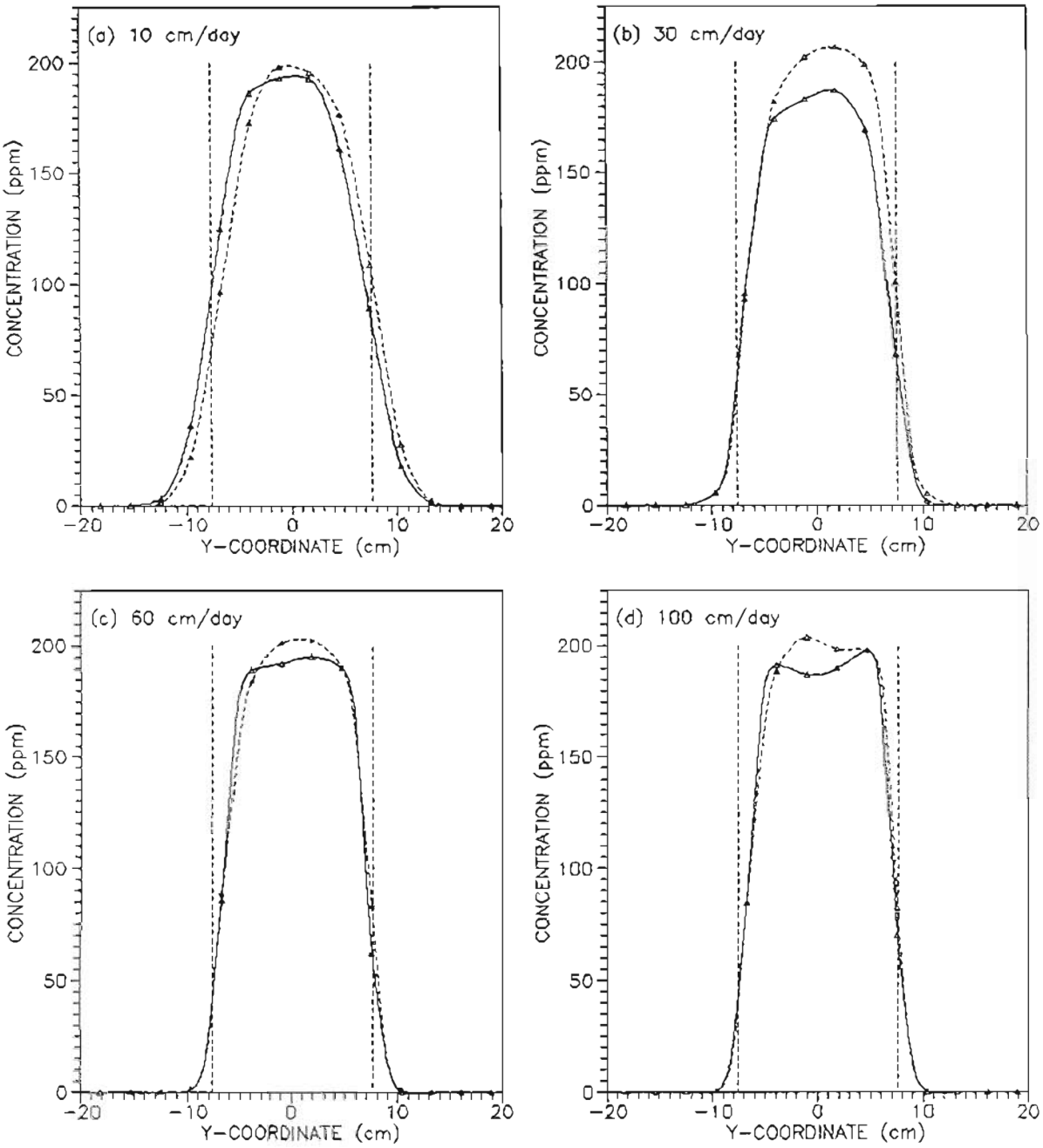

Figure 4.8: A comparison of duplicate steady-state concentration plumes at each of the four velocities studied in DE-1.

leveled off at 95-97% of their source concentration and that the subsequent rise to 100% was significantly delayed. These "late-time tails" were attributed to the relatively slower breakthrough that occurred in the less permeable layers. As pointed out in Chapter 3, although it was desired to construct a homogeneous model aquifer, the best that could be achieved was a system of thin horizontal layers. The layering, therefore, may have been responsible for the delay in the breakthrough of solubility level concentrations of PCE. A slight shift was observed in the 10 cm/day plume, but it is not known what might have caused this. In general, though, the shape and size of the plumes remained essentially unchanged. Changes due to depletion of the residual were not expected since only about 6.5% of the initial PCE mass had been dissolved and flushed from the tank by this time.

4.3.2 Models

It has been shown that when a contaminant plume has reached steady-state, it is possible to neglect longitudinal dispersion and attribute the spreading solely to transverse dispersion (Harleman and Rumer, 1963). If a cross-section of the contaminant plume at the downgradient edge of the residual zone is treated as a slug of finite width moving through the porous medium with the average flow velocity, the concentration profile can be modeled using the equation (Crank, 1975)

$$C = 0.5\, C_o \left(\mathrm{erf} \frac{h - y}{2\sqrt{D_T\, t}} + \mathrm{erf} \frac{h + y}{2\sqrt{D_T\, t}} \right) \qquad (4.13)$$

where h is the half-width of the source, y is the lateral distance from the center of the plume, and erf represents the error function. This is similar to the procedure used by Yule and Gardner (1978) to obtain transverse dispersion coefficients for unsaturated sands.

The concentrations measured in R2 for each of the eight steady-state plumes were fit to Equation 4.13 using the Levenberg-Marquardt method of nonlinear least-squares fitting (Press et al., 1986). Although the half-width of the residual zone was known, the plume of dissolved contaminant may have been narrowed due to the effects of reduced permeability (see Section 2.4.2). Therefore, this routine was used to simultaneously fit both D_T and h to the data. The best-fit results for these two parameters for each of the eight plumes are given in Table 4.2. The values of t used in the fitting routine are also listed in this table. They were calculated by dividing the distance between the downgradient end of the source and the sampling needles (40.0 cm) by the velocities of the plumes. As mentioned in Section 4.2, these velocities were only about 80% of the initially stated mean water velocities. Representative steady-state plume cross-sections generated by using the best-fit parameters in Equation 4.13 are plotted in Figure 4.9 along with the corresponding experimental data.

Values obtained for D_T are within the range usually observed in laboratory experiments (Anderson, 1979) and comparable to those obtained at similar pore velocities by Grane and Gardner (1961) for

Table 4.2: Values of h and D_T generated from the experimental results for each of eight steady-state plumes by a nonlinear least squares fit of the data to Equation 4.13.

Steady-state plume[a]	Time (hrs)	h (cm)	D_T (cm^2/s)
10-1	114.3	7.24	0.78×10^{-5}
10-2	114.3	7.18	0.79×10^{-5}
30-1	40.8	6.58	1.44×10^{-5}
30-2	40.8	7.07	1.03×10^{-5}
60-1	20.9	6.65	1.41×10^{-5}
60-2	20.9	6.82	1.87×10^{-5}
100-1	12.1	6.74	2.28×10^{-5}
100-2	12.1	6.82	2.68×10^{-5}

[a]The plume number indicates the nominal mean water velocity in cm/day and specifies whether it was the first steady-state at that velocity (1) or the second (2). Refer to Table 3.3 for the actual order in which the experiments were carried out.

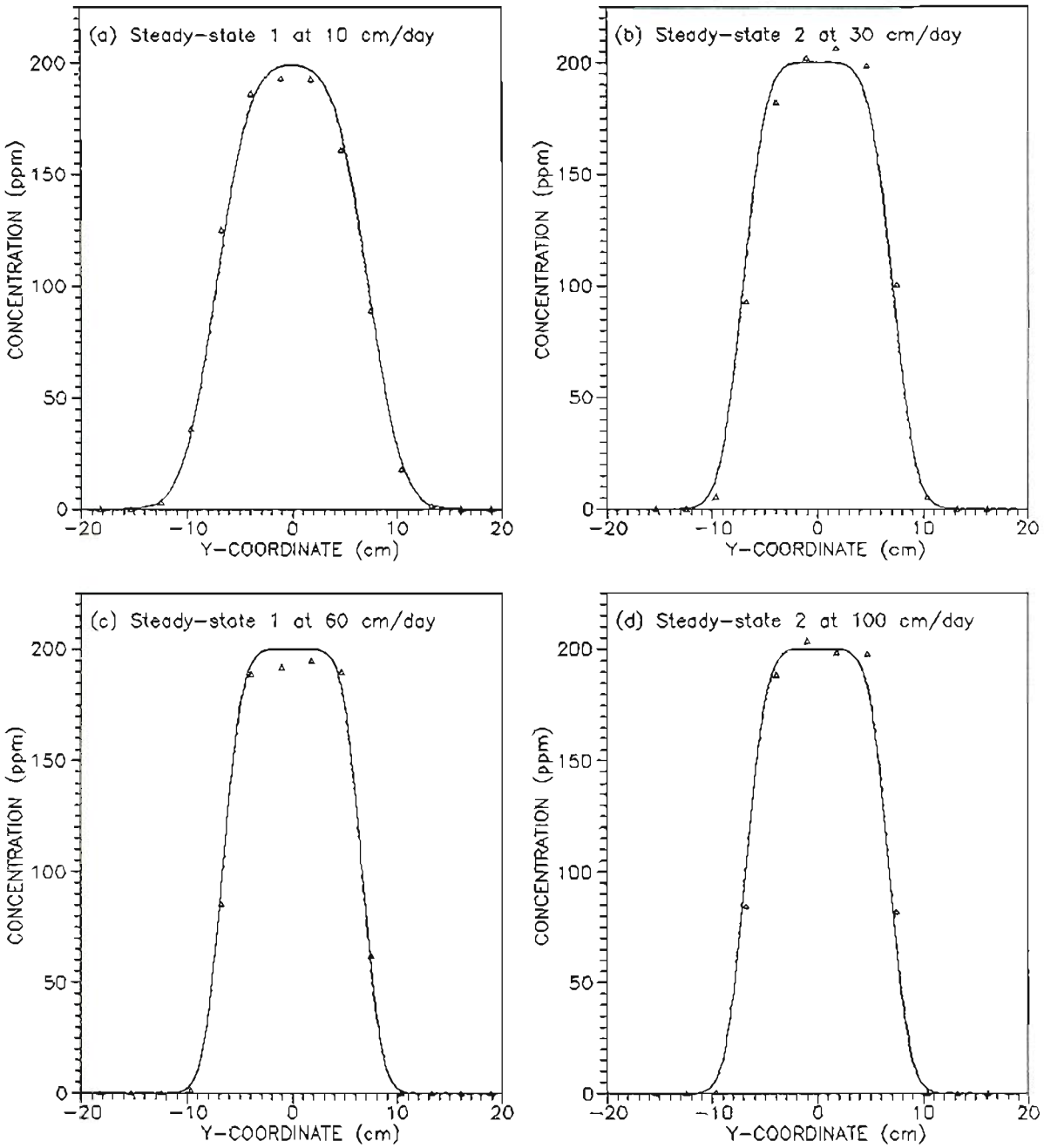

Figure 4.9: Modeled steady-state plumes (lines) versus experimental results (triangles) for representative data from DE-1.

1-iodopentane in Soltrol-C flowing through 0.025 cm glass beads. Analysis of the data by means of an F-test shows the increase in the value of D_T with increasing velocity to be highly significant. Considering the relationship given in Equation 4.3, this was certainly expected. The fact that a ten-fold increase in the velocity only resulted in about a three-fold increase in the value of D_T, confirms that the conditions in the model aquifer were such that dispersive transport in DE-1 was controlled by both mechanical dispersion and molecular diffusion. Consequently, a value for the molecular diffusion of PCE in this system is required before dispersivities can be calculated for the model aquifer.

Examination of the best-fit values of source half-width listed in Table 4.2 indicates that there appears to be a slight decrease in h with increasing mean water velocity. However, this trend was not found to be statistically significant. The mean value for h was 6.89 cm. The fact that the source width required by the model was 90% of the width of the experimental residual zone could be an indication that the streamlines were narrowing due to reduced permeability in the residual zone. Application of Equation 2.16 with F = 0.90 indicates that a relative permeability of 0.82 would be required to narrow the streamlines to this extent. It seems likely that a lower relative permeability and a narrower apparent source width would have been seen if the residual saturation of the DNAPL were greater than 13%. Under the conditions of DE-1, however, reduced permeability in the residual zone did not have a major impact on the rate at which contaminant mass

was being released from the source.

In Section 4.1.2, a one-dimensional model was used to estimate D_L from the breakthrough data. Using mean values for D_T and h obtained from the 30 cm/day steady-state data in this section, a two-dimensional model was used to test the validity of the earlier estimate of D_L. The model chosen was an analytical solution by Bruch and Street (1967) for contaminant transport from a source of finite width resulting from steady flow through a homogeneous, isotropic, saturated porous medium. A sketch of the model along with its initial and boundary conditions are given in Figure 4.10. The solution is given below.

$$C(x,y,t) = (hC_o/2w)\ \mathrm{erfc}\left(\frac{x - \bar{v}t}{2\sqrt{D_L t}}\right) +$$

$$(hC_o/2w)\ \exp\left(\frac{x\bar{v}}{D_L}\right)\ \mathrm{erfc}\left(\frac{x + \bar{v}t}{2\sqrt{D_L t}}\right) +$$

$$(1/2)\sum_{n=1}^{\infty} F_n \cos(n\pi y/w)\ \exp\{[x/2][(\bar{v}/D_L) - J_n]\}\ \mathrm{erfc}\left(\frac{x - J_n D_L t}{2\sqrt{D_L t}}\right) +$$

$$(1/2)\sum_{n=1}^{\infty} F_n \cos(n\pi y/w)\ \exp\{[x/2][(\bar{v}/D_L) + J_n]\}\ \mathrm{erfc}\left(\frac{x + J_n D_L t}{2\sqrt{D_L t}}\right)$$

where: $F_n = (2C_o/\pi n)\sin(n\pi h/w)$ and

$$J_n = [(\bar{v}/D_L)^2 + (4n^2\pi^2/w^2)(D_T/D_L)]^{1/2}$$

for $n = 1, 2, 3, \ldots$ (4.14)

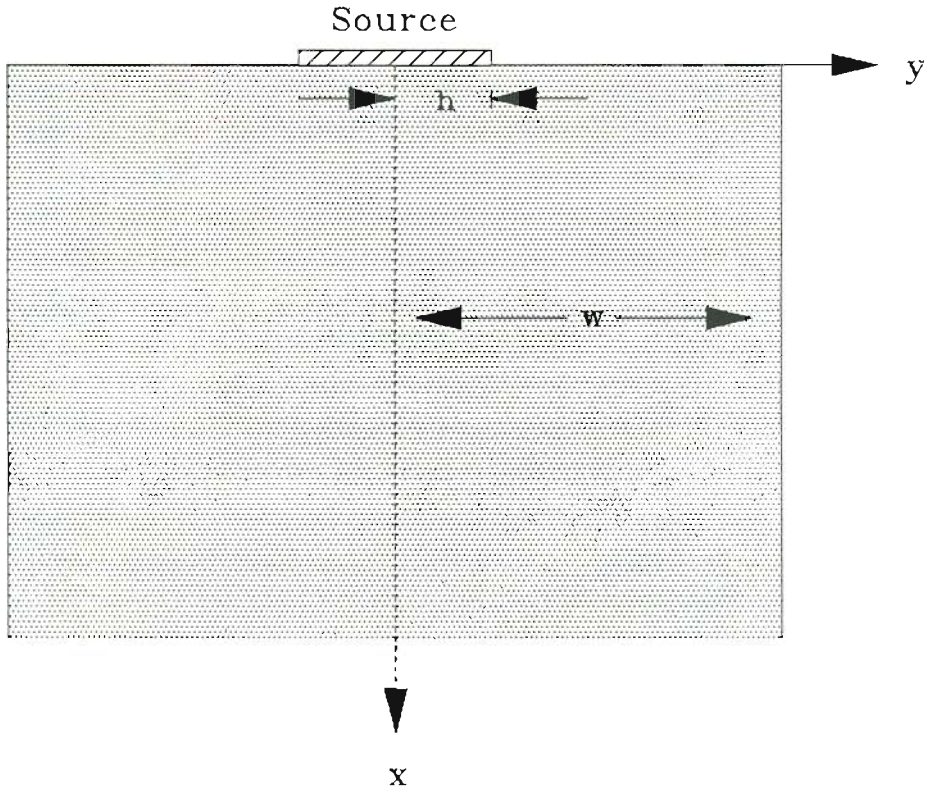

$$C(x,y,0) = 0 \qquad x > 0,\ 0 \le |y| < w$$

$$C(0,y,t) = C_o \qquad 0 \le |y| \le h$$

$$= 0 \qquad h < |y| < w$$

$$\frac{\partial C}{\partial y}(x,0,t) = 0 \qquad t > 0$$

$$\frac{\partial C}{\partial y}(x,w,t) = 0$$

$C(\infty,y,t)$ is bounded

Figure 4.10: Configuration and boundary conditions for the analytical solution to the two-dimensional advection-dispersion equation by Bruch and Street (1967).

Figure 4.11(a) compares the results of this model to both the 1-D model and the experimental breakthrough data. Both models give almost identical results and, with the exception of the last data point, fit the data quite well. The use of the 1-D model to calculate D_L for this system seems reasonable.

One of the rationalizations for using a 1-D model for the breakthrough results was that the data being simulated was from the center of a relatively wide source where transverse dispersion would be minimal. To test the sensitivity of the results to the width of the source, the 2-D model was used to simulate breakthrough from narrower sources. These results are shown in Figure 4.11(b). A decrease in the source half-width from 6.89 to 5.0 cm resulted in very little change in the data. A further decrease to 4.0 cm was necessary before the concentrations changed by more than 2%. By the time the half-width was reduced to 2.0 cm, the maximum concentration (C_{max}) had dropped to about 75% of the initial concentration (C_o).

A drop in C_{max} will also result from an increase in the distance from the source and/or from an increase in the magnitude of the dispersion coefficients. For example, using the dispersion coefficients calculated for the 30 cm/day data from DE-1 (D_L = 3.7×10^{-5} cm^2/s and $D_T = 1.2 \times 10^{-5}$ cm^2/s), the 2-D model shows that C_{max} at a distance of 100 cm downgradient from a 5-cm wide source will be 62% of C_o. At a distance of 100 m, C_{max} will be less than 7% of C_o. If the dispersion coefficients are increased by a factor of 10, C_{max} at 100 m will be reduced to about 2% of C_o. Another 10-fold

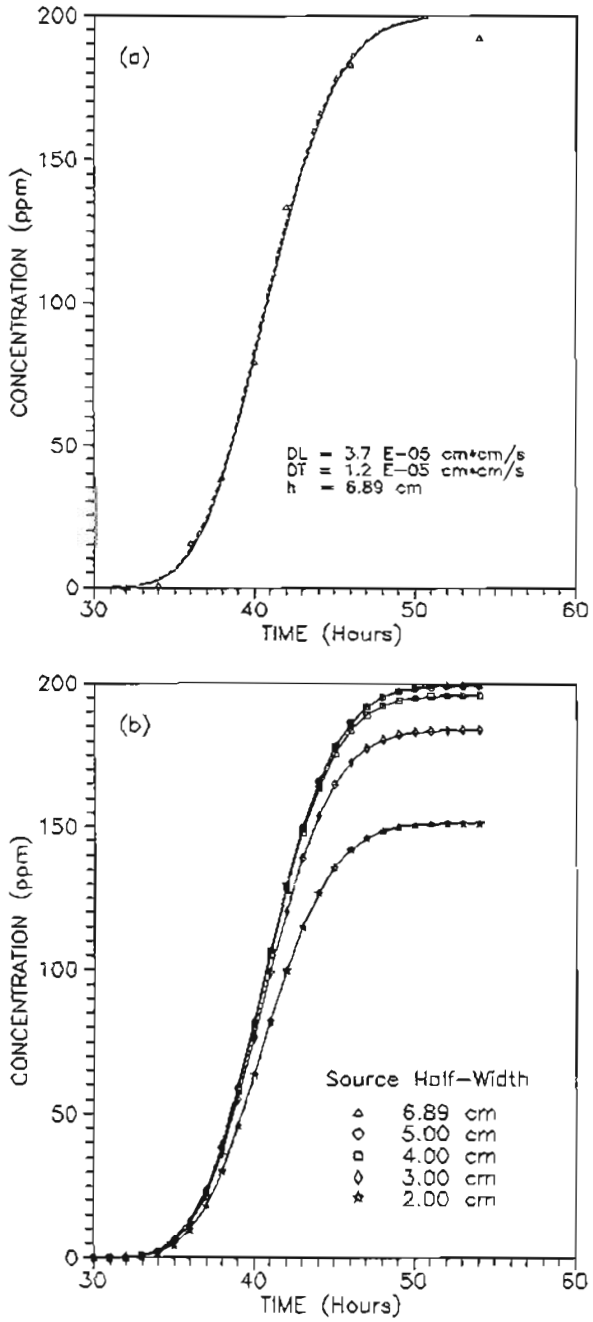

Figure 4.11: (a) Breakthrough data (triangles) as modeled by both a one-dimensional solution (solid line) and a two-dimensional solution (dashed line) to the advection-dispersion equation. (b) The effect of source half-width on breakthrough concentrations.

increase in the dispersion coefficients further reduces C_{max} to less than 1%. The concentrations will be even lower, of course, when measured at a distance from the center of the plume. Continuing the above example, 5 m from the center of the plume the concentration will drop from 1% to about 0.1% of C_o; at 10 m it will drop another 2 orders of magnitude. Considering that dispersion measured in the field is commonly orders of magnitude larger than that measured in the laboratory (Anderson, 1978), and that samples collected in the field may come from locations that are tens of meters from the source and not necessarily in the center of the plume, the chances of finding high concentrations from narrow fingers of DNAPL may be quite small. A more detailed discussion of what diameters may be considered "narrow" and how multiple fingers affect the contaminant plume is presented in Chapter 7.

4.4 Diffusion

4.4.1 Observations

After the flow was stopped for eight days, the mean velocity of the water was again adjusted to 100 cm/day. Samples from R2 were collected and analyzed at regular intervals in order to observe the extent to which the plume was affected by molecular diffusion during this time. The data collected within the first hour after flow was resumed is shown in Figure 4.12. For comparison, one of the 100 cm/day steady-state curves from Figure 4.8(d) has been included. Since the velocity prior to stopping the flow was also 100 cm/day, the

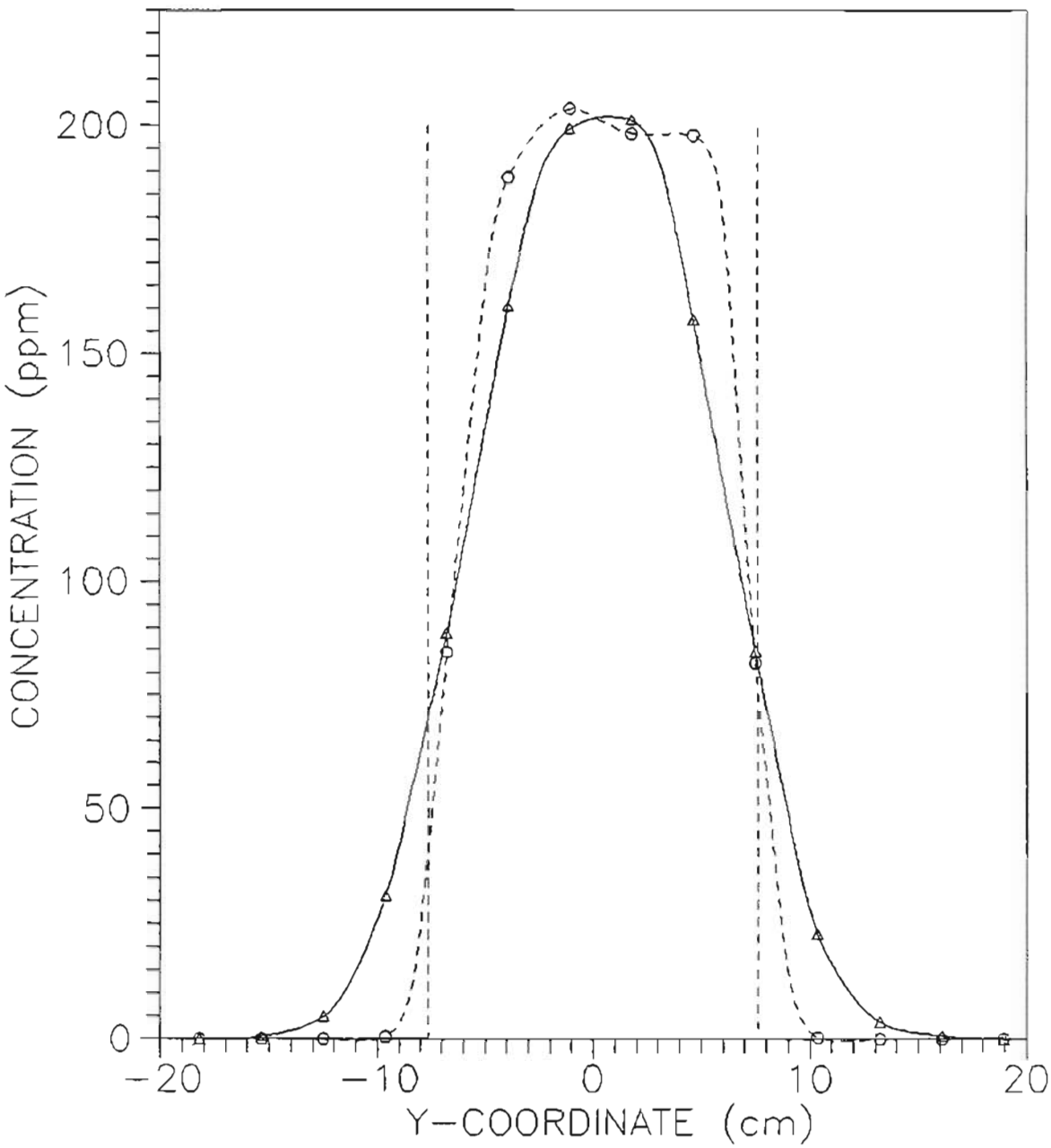

Figure 4.12: PCE concentrations measured across R2 within 1 hour after the resumption of 100 cm/day flow following 8 days with no flow. The dashed curve is a 100 cm/day steady-state plume.

increased spreading of the contaminant plume was due entirely to molecular diffusion.

The shape of the plume as measured at 4, 7 and 10 hours after the resumption of flow was almost identical to that found after the first hour. However, the results from samples collected at 12 hours showed the plume to be noticeably wider. The plume reached its maximum width after 14 hours. By 16 hours, it had nearly returned to its steady-state configuration. The results from the samples collected between 10 and 16 hours are shown in Figures 4.13(a)-(d).

The broadening that was observed in the plume between 12 and 16 hours after the resumption of flow was due to an increase in the mass of solute resulting from diffusion out of the source during the flow stoppage. This differed from the broadening that was observed in the early stages of the plume. In the early plume, which was relatively distant from the source during the flow stoppage, a constant mass of contaminant had spread out over time. Graphically, though the shape of the plume changed, the area under the curve remained the same. However, in the region surrounding the source, solute was able to continually diffuse from the residual DNAPL during the eight days that the flow was stopped. Therefore, not only did the plume broaden, but the area under the curve increased with time.

The data from the diffusion study was interpolated in order to estimate the location of the 50, 100 and 150 ppm concentration contours at different times in the experiment. This data is shown in Figure 4.14. It can be clearly seen in this graph that the widest

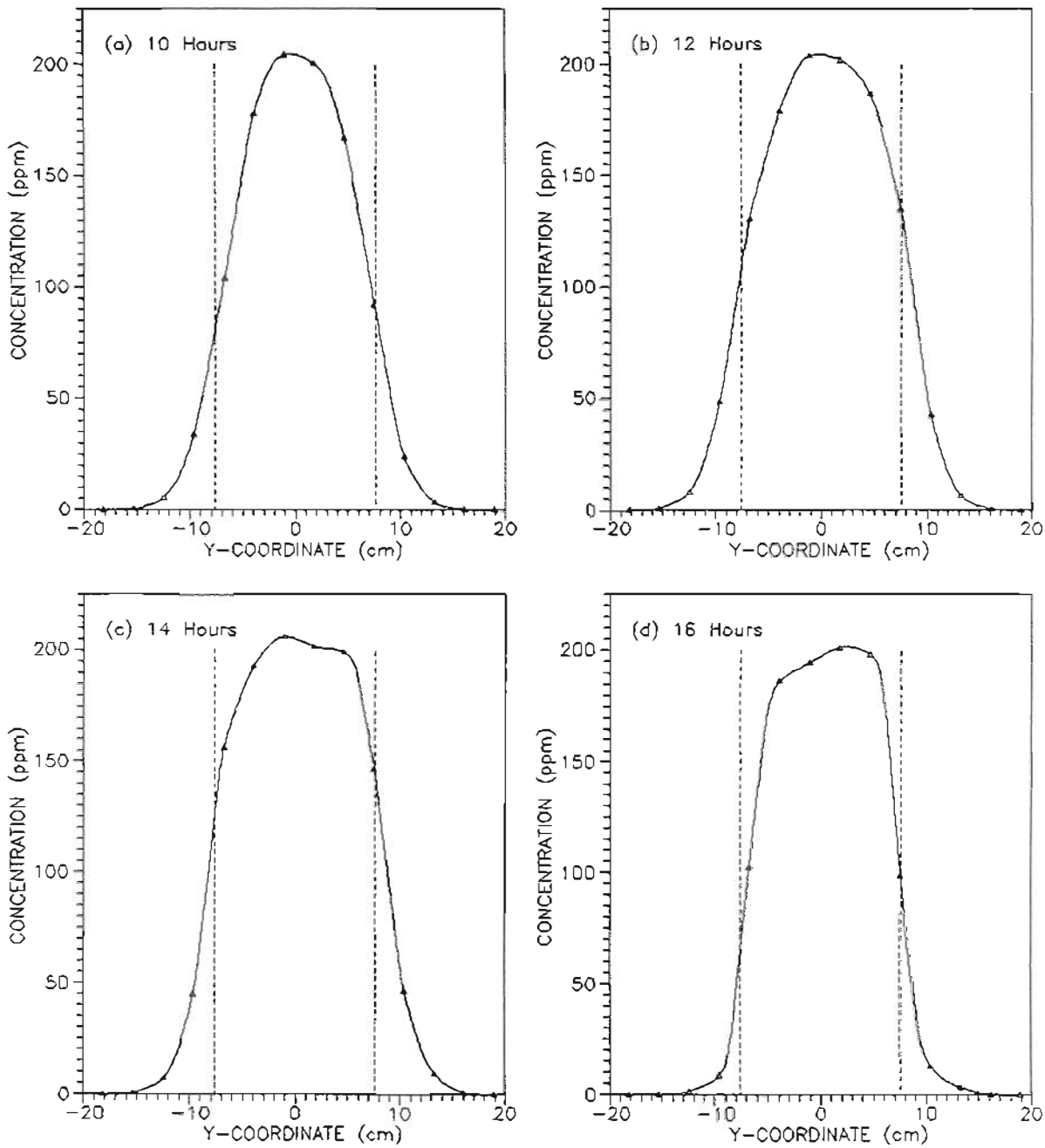

Figure 4.13: PCE concentrations measured across R2 between 10 and 16 hours after the resumption of 100 cm/day flow following 8 days with no flow.

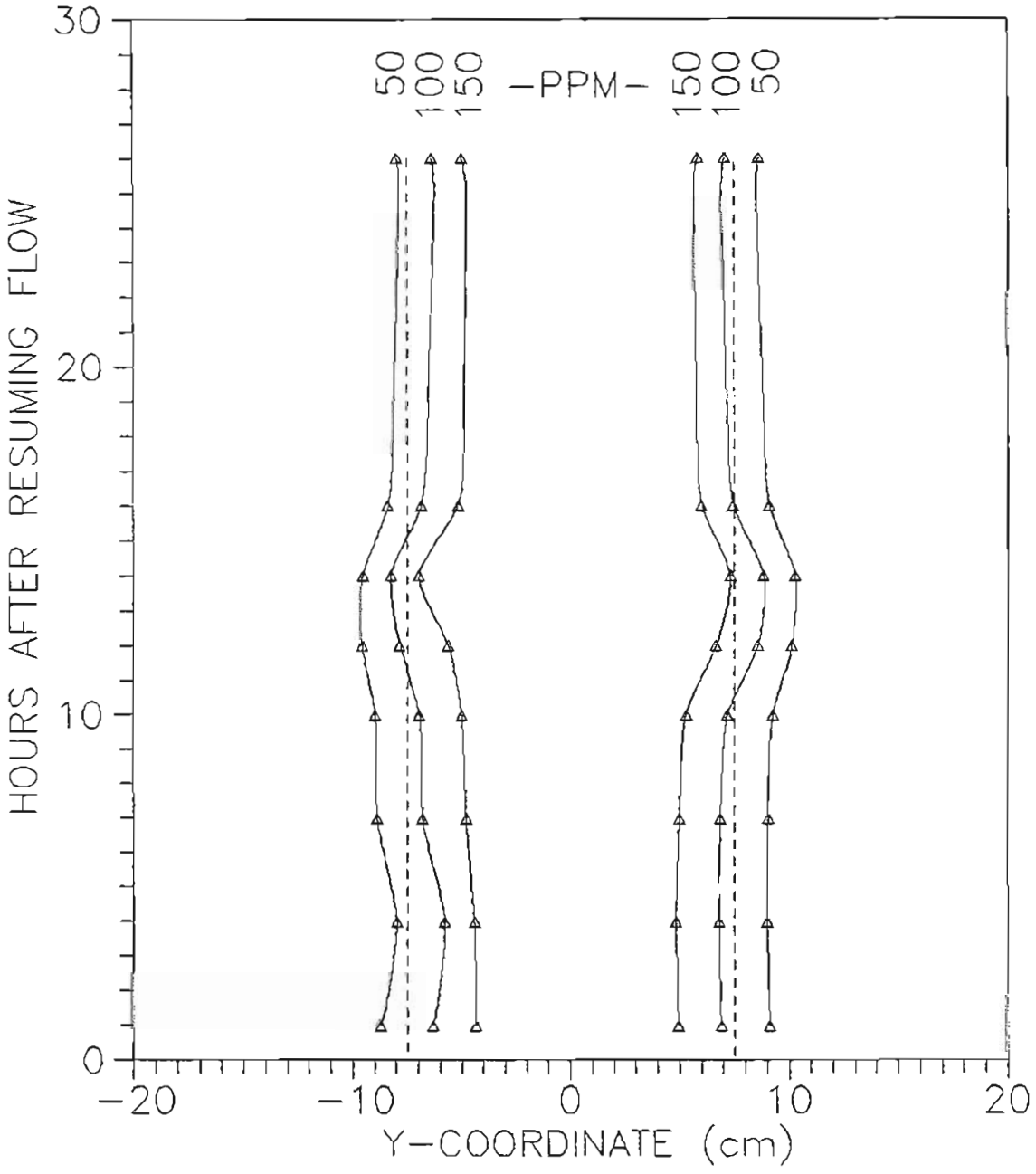

Figure 4.14: PCE concentration contours versus time following the resumption of 100 cm/day flow after 8 days with no flow.

portion of the contaminant plume arrived about 14 hours after flow was resumed. If it is assumed that this part of the plume had its origins in the widest part of the source, a distance of 47.5 cm from the sampling syringes, an estimated plume velocity of 81 cm/day is obtained. As with the breakthrough data discussed earlier, this velocity is also about 20% less than the value that had been calculated initially for the mean water velocity.

4.4.2 Models

Since the diffusion experiment was initiated on a plume that was at steady-state, the effects of longitudinal dispersion could be neglected (see Section 4.3.2). Due to the conditions of the experiment, the dispersion (D) of the plume shown in Figure 4.12 was separated into two components: (1) pure molecular diffusion (D^*) that occurred during the eight days that the flow was stopped, and (2) transverse dispersion (D_T) that occurred while the plume traveled a distance of 40 cm at 100 cm/day. Since the dispersion was not constant in this case, its variation had to be incorporated into the model used to simulate the data. This was done by considering D to be a function of time (Crank, 1975).

$$\frac{\partial C}{\partial t} = D(t) \frac{\partial^2 C}{\partial y^2} \qquad (4.15)$$

By substituting $dT = D(t)\, dt$, this equation becomes

$$\frac{\partial C}{\partial T} = \frac{\partial^2 C}{\partial y^2} \qquad (4.16)$$

Under the conditions of this experiment,

$$T = t_1 D^* + t_2 D_T \qquad (4.17)$$

where t_1 is the diffusion time and t_2 is the travel time.

After solving Equation 4.16 for T (the solution is analogous to Equation 4.13), Equation 4.17 was used along with the mean 100 cm/day value of D_T (Table 4.2) to solve for D^*. In this way, the molecular diffusion coefficient for PCE in the model aquifer was determined to be 4.3×10^{-6} cm^2/s. This compares favorably with an estimated value of 5.3×10^{-6} cm^2/s which was obtained by first using the method of Hayduk and Laudie (1974) to predict a value for the diffusion coefficient of PCE in water (D_o), and then correcting for diffusion in a porous medium by using the ratio of $D^*/D_o = 0.7$ given by de Marsily (1976) for sands.

The value of D^* calculated above was subsequently used along with Equations 4.2 and 4.3 to solve for values of dispersivity. These results are given in Table 4.3. The values of α_T are within the expected range for laboratory column studies and are 3-6 times smaller than the value of α_L. Although α_T is considered a constant, this data exhibits a trend of decreasing α_T with increasing velocity. Analysis of the data by means of an F-test shows that this trend is only moderately significant (10%).

Table 4.3: A summary of the diffusion and dispersion coefficients, and dispersivities calculated from the data collected in DE-1 for the advective-dispersive transport of PCE in Flintshot 2.8.

Stage of Experiment	Coefficient (cm^2/s)	Dispersivity (cm)
Breakthrough	(D_L)	(α_L)
	3.7×10^{-5}	0.12
Steady-state plume[a]	(D_T)	(α_T)
10-1	0.78×10^{-5}	0.036
10-2	0.79	0.037
30-1	1.44	0.037
30-2	1.03	0.022
60-1	1.41	0.018
60-2	1.87	0.027
100-1	2.28	0.020
100-2	2.68	0.024
No Flow	(D^*)	
	4.3×10^{-6}	

[a]The plume number indicates the nominal mean water velocity in cm/day and specifies whether it was the first steady-state at that velocity (1) or the second (2). Refer to Table 3.3 for the actual order in which the experiments were carried out.

4.5 Excavation of the Tank

During the excavation of the tank, the sand was removed in layers to examine a number of horizontal cross-sections. The first signs of the red dye showed up at a depth of 10 cm from the surface (8 cm above the water table) and appeared as a thin red line outlining the circular area that had been enclosed by the cylinder. This dye probably came off of the walls of the cylinder as it was pulled up and out of the sand. Below what had been the water table, the dye completely filled the circular area of each layer that was examined. No colorless areas were observed which the PCE might have bypassed. Nor were there any regions noticed in which the circular region of residual appeared distorted due to PCE mobilization after the removal of the cylinder. A lighter colored crescent-shaped area was consistently seen on the upgradient side of the residual zone. This was probably the region from which most of the dissolution occurred. The appearance of the residual zone is illustrated in Figure 4.15.

4.6 Conclusions

The results of DE-1 showed that the initial breakthrough of the dissolved PCE contaminant plume was rapid. During the first 34-56 hours of the experiment, the concentration increased to within 4% of the reported 20 ^{o}C aqueous solubility of this compound (200 ppm). Peak concentrations slowly continued to increase until they reached solubility levels at all of the velocities studied in this experiment. Heterogeneities resulting from layers formed during the filling of the

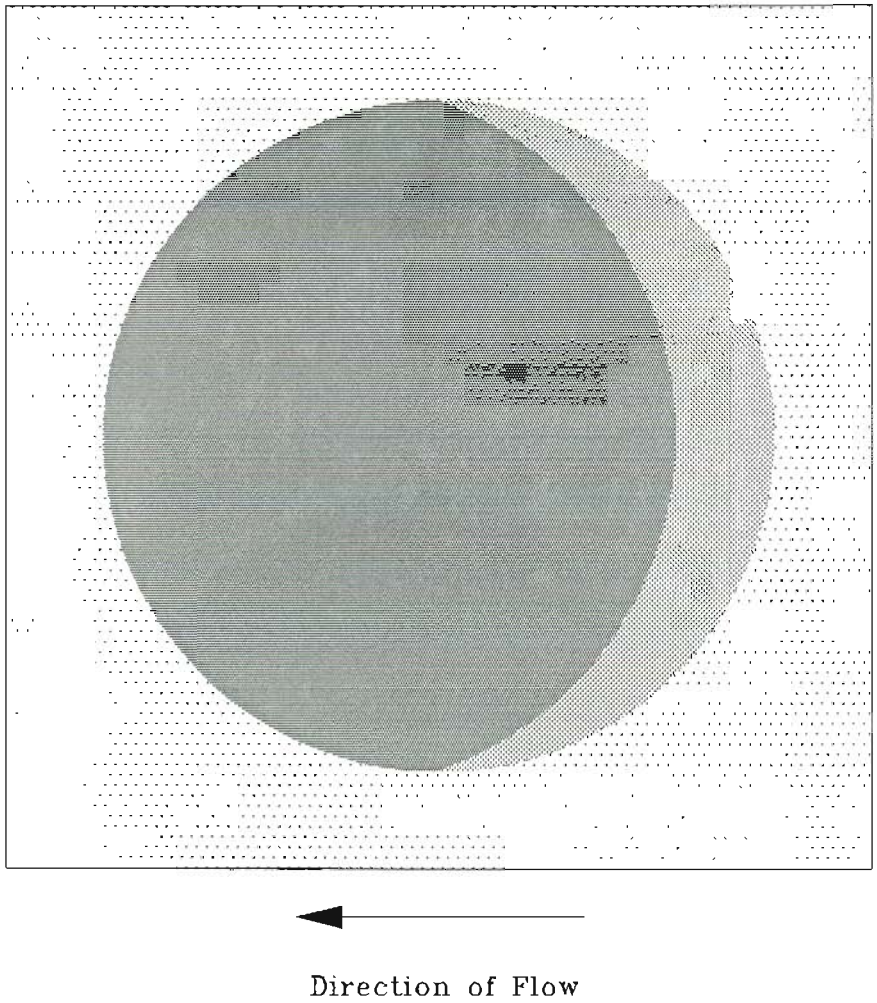

Figure 4.15: The zone of residual PCE as it appeared during the excavation of the tank following DE-1.

tank may have been responsible for the observed delay in the attainment of solubility level concentrations of PCE.

Both one and two-dimensional analytical solutions to the advection-dispersion equation were used to calculate values for the coefficients of longitudinal and transverse dispersion for the model aquifer. These values were small but within the range normally observed in laboratory column or tank studies. The contribution of diffusion to transverse dispersion was noticeable at velocities of 10 and 30 cm/day, but not at velocities of 60 or 100 cm/day. Since these velocities correspond to Peclet numbers of approximately 1-10, the decreasing effects of diffusion observed here agree with generally accepted contaminant transport theory.

The solubility level concentrations attained in this experiment are consistent with earlier work on contaminant source strength which indicates that in most groundwater flow regimes, mass transfer depends upon the solubility of the compound rather than the flow rate of the water. The high experimental concentrations agree with results of column studies but contrast with the low values observed in the field. Best-fit models of the steady-state contaminant plumes required an apparent source width equal to about 90% of the true width of the residual zone. This may have been due to a slight narrowing in the stream lines resulting from reduced permeability in the residual zone. If so, the effect may have been greater if the residual zone had contained a higher percentage of PCE. It is doubtful, however, that reduced permeability plays a major role in keeping field results

significantly lower than laboratory results. Since truly narrow sources, large values of dispersion, and increased distances from the source can all contribute to a rapid drop in concentrations downgradient from a zone of residual, these factors are more likely to contribute to low field results.

5. DISSOLUTION EXPERIMENTS #2 AND #3: RESULTS AND DISCUSSION

5.1 Dissolution Experiment #2

5.1.1 PCE Breakthrough

The first measurable PCE concentration in port R2-12 appeared 13 hours after the outer cylinder was pulled from the tank. This was earlier than in DE-1 because the cylinder was located closer to the end of the tank in DE-2 than in DE-1 (see Section 3.3.2). Except for its earlier arrival, the breakthrough was very similar to that observed in DE-1. Figure 5.1 compares the experimental data to a breakthrough curve generated with a 1-D analytical solution using the value of D_L obtained in DE-1. The fit appears to be quite reasonable. To obtain this curve, it was necessary to use a velocity of 25.4 cm/day. This was slightly higher than the velocity of 23.5 cm/day that was used to fit the data from DE-1 shown in Figure 4.11(a). However, it was still less than the initially calculated velocity of 30 cm/day that was used throughout DE-2. This continues the previously discussed trend of lower than expected velocities (see Section 4.2). CB was either not detected or only found at relatively low levels (<3 ppm) in the samples collected at this time.

As in DE-1, samples were periodically collected from the effluent

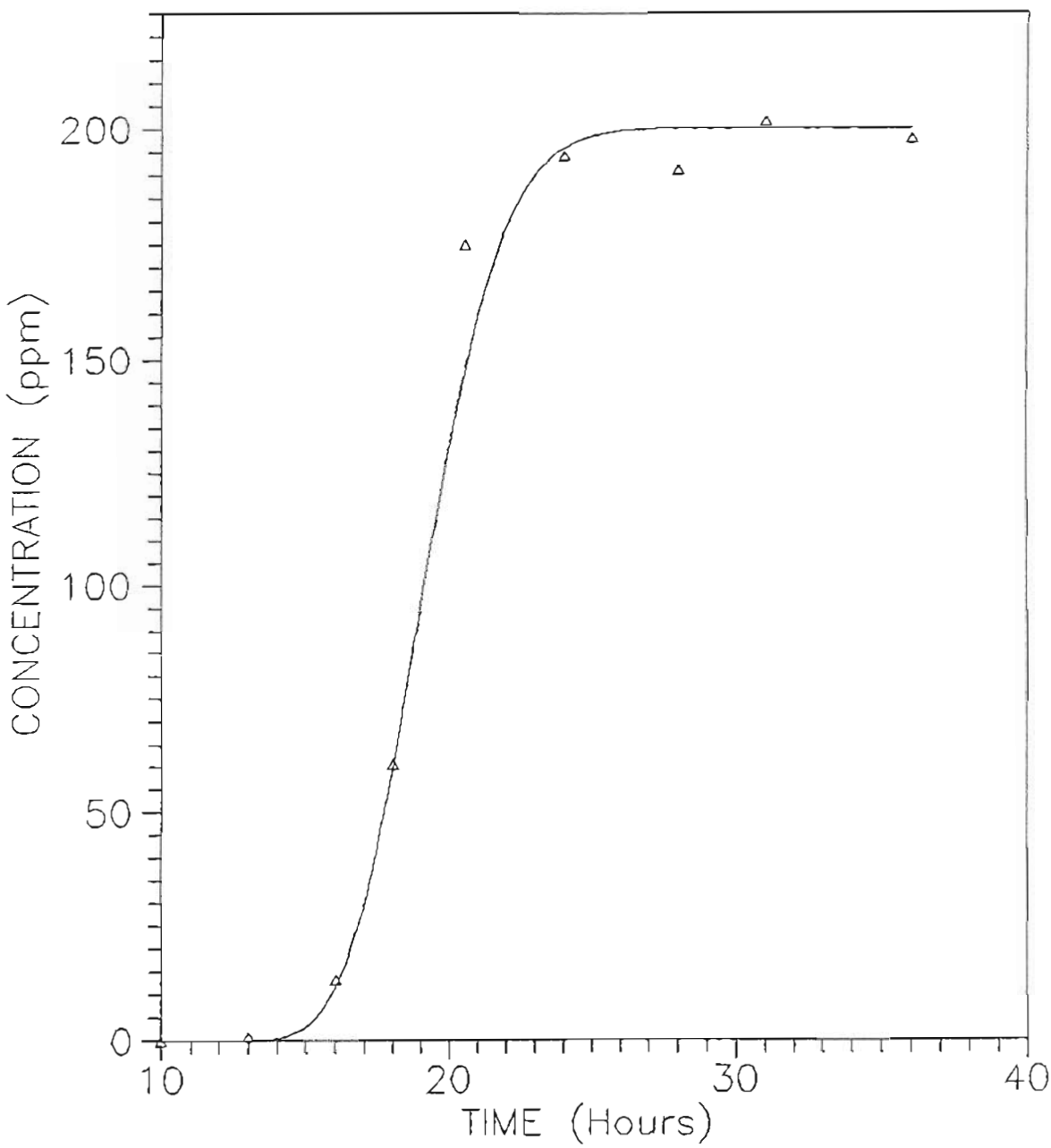

Figure 5.1: The breakthrough of PCE in DE-2 as measured at sampling port R2-12.

line to monitor overall mass transport from the tank. In DE-1, the first measurable amounts of PCE did not show up in the effluent until about 6 hours after it first appeared in samples from port R2-12. In DE-2, detectable amounts of PCE were already found in an effluent sample collected just prior to pulling the outer cylinder from the tank. This, of course, was due to the leak of PCE from the cylinder that was discussed earlier. However, the fact that the breakthrough of PCE at port R2-12 was well-behaved and predictable from the results of DE-1 indicates that the leak did not affect the contaminant plume in this portion of the model aquifer.

During the fourth day of the experiment, samples were collected from all of the ports in the path of the plume. The concentrations measured across rows R1-R3 are shown in Figure 5.2. The two pairs of dashed vertical lines represent the diameters of the cylinders used to prepare the residual zones. CB was not detected in any of the samples in R3 and only at relatively low levels (<2 ppm) in two of the samples in R2. However, in the center of R1, the concentration of CB was found to be almost 200 ppm. This was about 40% of the aqueous solubility of CB at 25 ^{o}C (488 ppm). The early appearance of CB in R1 indicates that the residual zone of PCE was probably not complete at this depth. The low levels of PCE found in this row corroborate this. The highest PCE concentrations measured in both R2 and R3 were found to be at solubility levels. The R3 plume was somewhat broader than the R2 plume. It does not seem likely that the concentrations at the elevation of R3 would have been affected by the PCE that escaped from

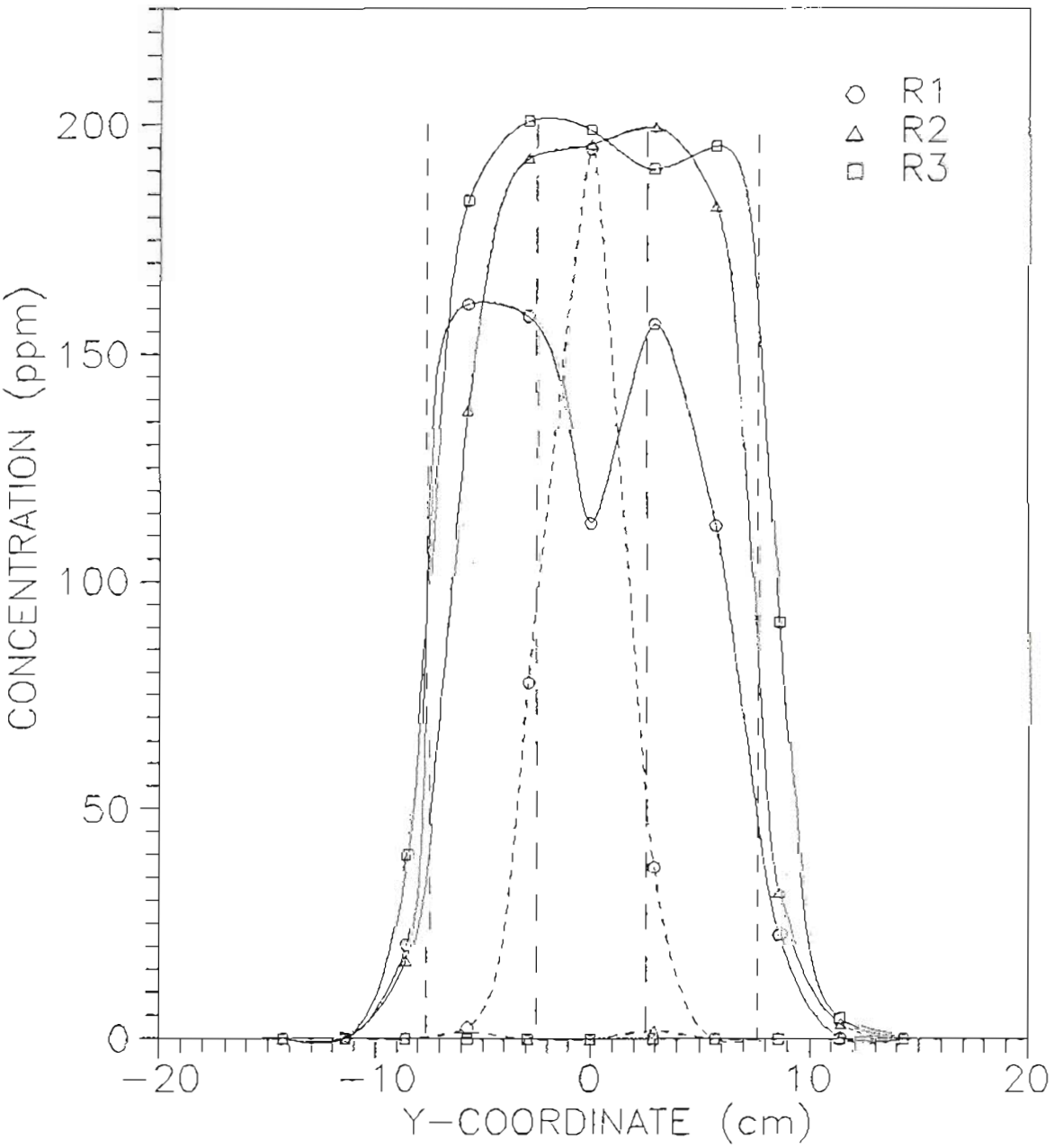

Figure 5.2: Concentrations of PCE (solid lines) and CB (dashed lines) measured across the contaminant plume 4 days after the start of DE-2.

the bottom of the cylinder. It is possible that some PCE flow occurred after the cylinder was removed and produced a slightly wider source near the bottom of the tank.

The R2 plume was very similar to the second 30 cm/day steady-state plume measured in DE-1. Figure 5.3 is a comparison of these two plumes. The y-coordinates of the corresponding data points in these two curves all differ by 1.8 cm. This was because careful positioning of the cylinder in DE-2 resulted in its center being right on the centerline of the tank. As mentioned in Section 4.1.1, the center of the cylinder in DE-1 was 1.8 cm off of the tank centerline. (Refer to Appendix B for information on sampling port coordinates.) Considering that the tank was completely excavated and repacked between experiments and that problems were encountered in the preparation of the PCE residual zone for DE-2, the reproducibility of the data was remarkably good. This indicated that, at least in this section of the aquifer, the PCE residual zone had been formed as planned. Since the CB residual zone was prepared without any problems, it was assumed that it was evenly distributed throughout the aquifer. Based on these early results, it was decided to focus the efforts of DE-2 on samples collected from R2. In this way, the plume could be sampled more frequently without necessitating the collection of an unmanageable number of samples. Also, since the residual zone appeared to be evenly distributed in this part of the tank, any changes observed in the plume could be attributed to normal transport and partitioning behavior rather than to the whims of a heterogeneous source.

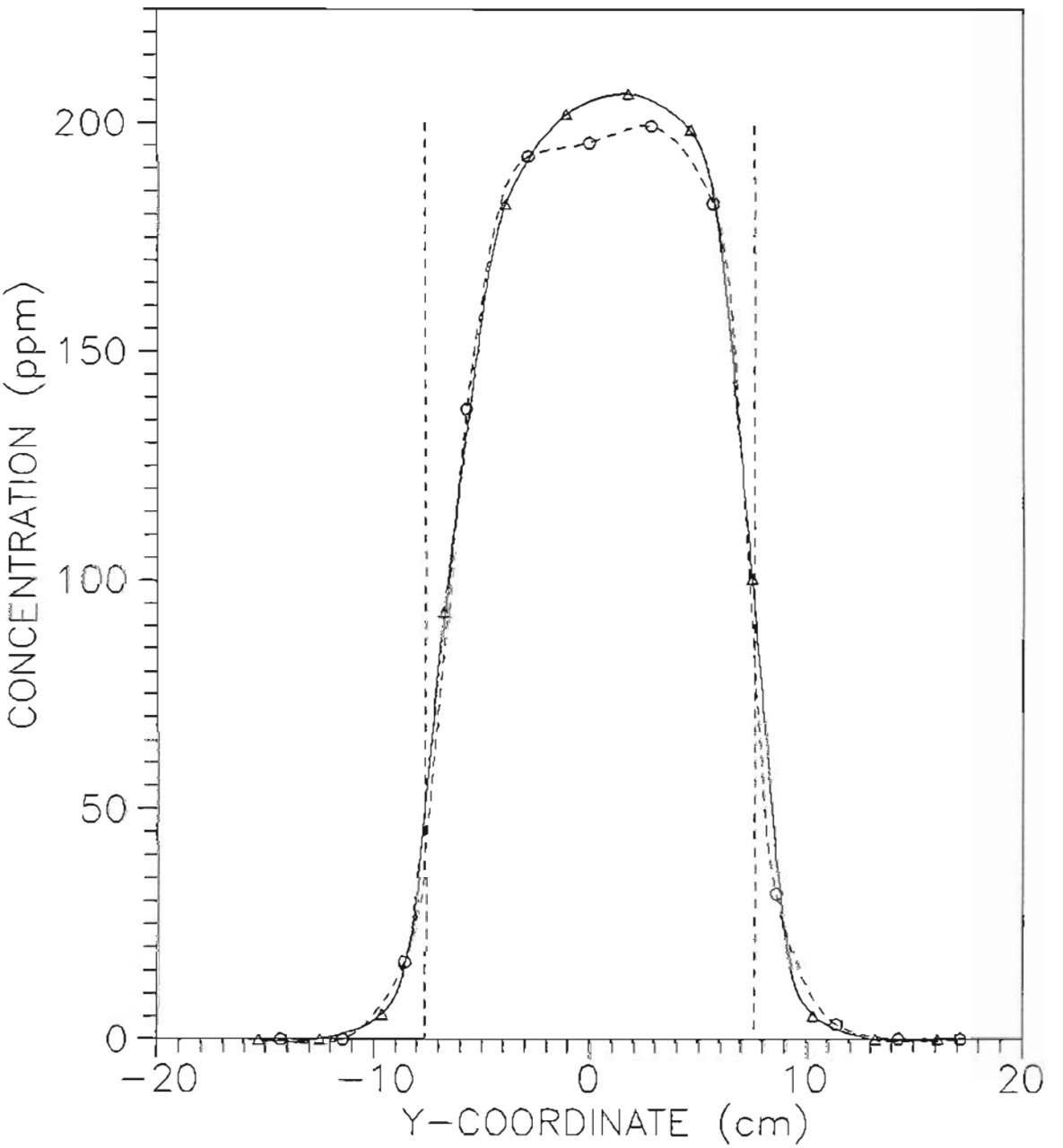

Figure 5.3: A comparison of PCE concentrations measured in R2 during DE-2 (solid line) to those measured in R2 at the same velocity during DE-1 (dashed line).

5.1.2 Interaction of the Two DNAPLs

The results of DE-1 have already shown that at typical groundwater velocities, contaminant levels in zones of residual saturation are controlled by the solubility of the compound rather than the velocity of the water. Under the conditions of DE-2 then, it was expected that when a given volume of water initially flowed down the center of the tank, it first encountered the residual PCE and quickly dissolved some of the contaminant. By the time that this volume of water reached the residual CB, it presumably already contained 200 ppm PCE. At this point, the situation became more complex. Since both PCE and CB are hydrophobic compounds, there was a strong tendency for the PCE that was dissolved in the water to partition into the droplets of residual CB as would be the case in a typical liquid-liquid extraction procedure. This affected the system in two ways. First, the concentration of PCE in the water was obviously reduced. Second, at that point the residual was no longer pure CB but a solution of CB and PCE. As more PCE was carried into this region, the mole fraction of CB in the residual continued to go down. Similarly, dissolved CB carried from the center of the source partitioned into the residual PCE encountered downgradient. Since the aqueous solubility of these compounds is controlled by their mole fractions and activity coefficients, the concentrations that were found in the contaminant plume changed as the composition of the residual changed.

To estimate the extent of the effect that the formation of mixed

residuals might have on the PCE and CB concentrations in DE-2, a computer model was used to simulate a steady-state plume that would result from such a mixed source. This was done by treating the residual zone as if it were actually three independent sources (Figure 5.4). The 5-cm section in the center of the PCE residual and containing all of the CB residual was treated as a source consisting of residual droplets of a solution of PCE and CB. The composition of the residual was arrived at by calculating what solution would be formed if all of the PCE and CB in this section of the source were mixed together. Taking into account the relative volumes of the PCE and CB zones and the saturations within each zone, a mole ratio for PCE to CB of 2:1 was calculated. Assuming ideal behavior, aqueous solubilities from this solution should be about 130 and 160 ppm for PCE and CB, respectively. The 5-cm sections on each side of the center were treated as sources of pure PCE. The concentration from each of these sources was therefore 200 ppm.

An analytical solution to the 2-D advection-dispersion equation (Equation 4.14) was used to calculate the concentrations that would be found in a steady-state plume at a distance of 20 cm from each of the 5-cm wide sources described above. The values of D_L and D_T that were obtained for the DE-1 data were used in the model. The principle of superposition was then applied to the three individual contaminant plumes to arrive at a final steady-state plume for DE-2. The results of this model are shown in Figure 5.5. The peak concentration of CB was 150 ppm; 30% of its pure solubility value. Because of the CB, the

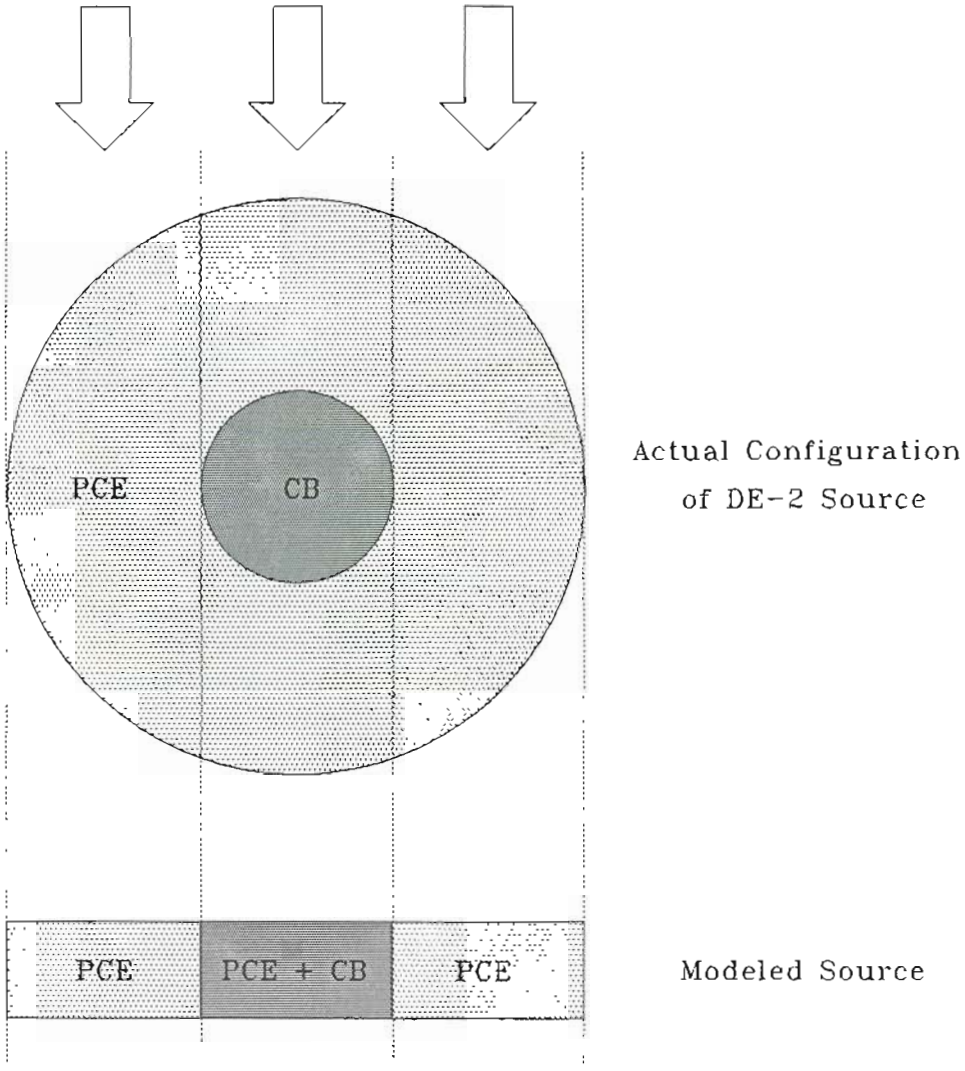

Figure 5.4: Comparison of the actual configuration of the source in DE-2 to that used in the computer simulation.

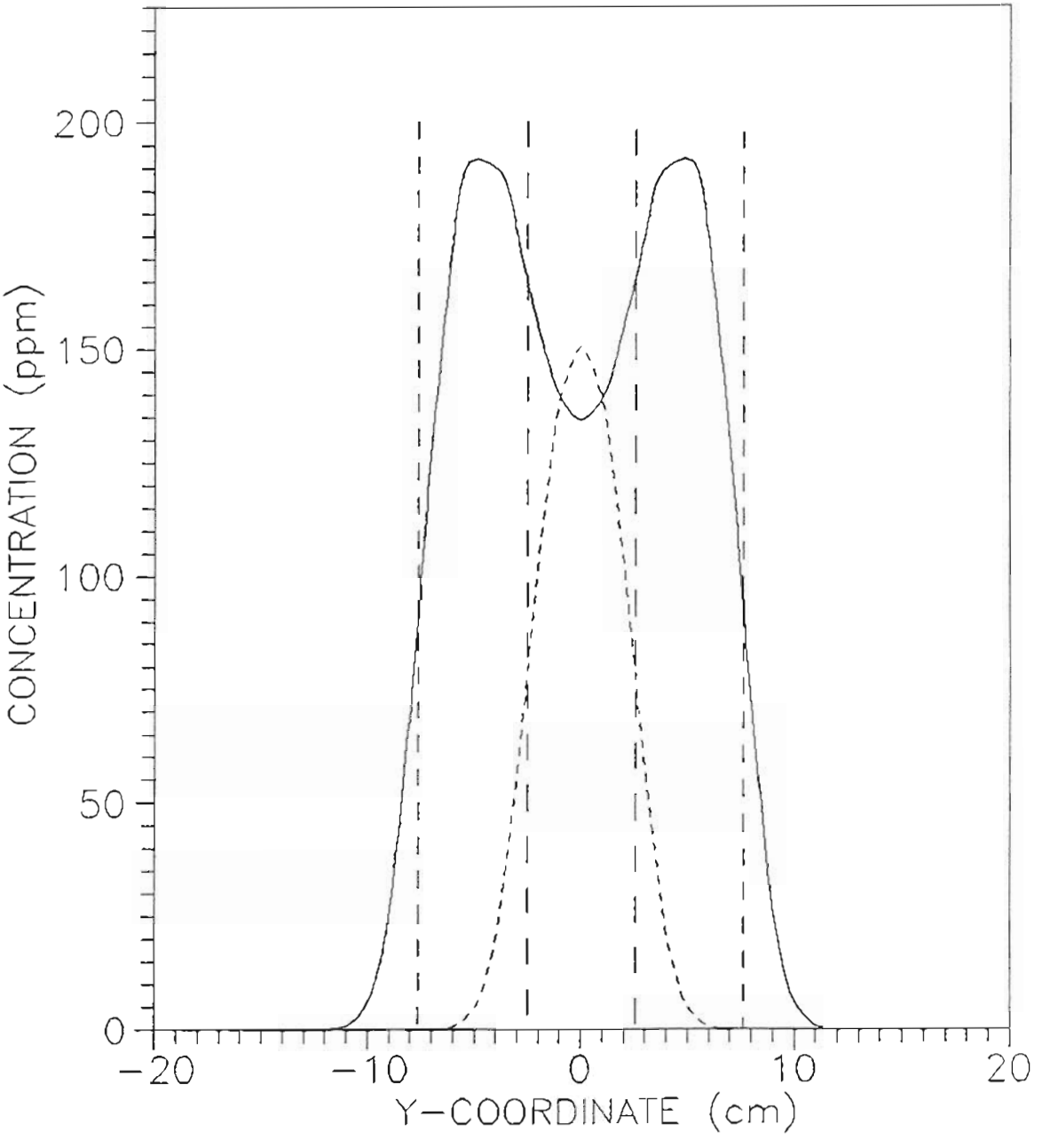

Figure 5.5: Model results for a steady-state plume calculated by assuming that the central one-third of the source was an ideal solution of PCE and CB. The solid line represents PCE and the dashed line represents CB.

concentration of PCE was reduced to 134 ppm in the center of the plume. However, since the PCE source was wider than the CB source, the PCE concentrations rose again on each side of the plume to 192 ppm before falling off to zero.

The "steady-state" plume discussed above is, of course, purely hypothetical. Even if the residual was initially a solution of PCE and CB, a true steady-state would never be reached. The composition of the residual would change continuously since the two compounds would dissolve out of it in a mole ratio that differed from what was initially present. (The only mixed residual capable of maintaining a constant composition under these conditions would be one made up of compounds having equal molar solubilities.) As the composition of the residual changed, so would the concentrations in the contaminant plume. Therefore, Figure 5.5 is only intended to illustrate the type of plume that may result in DE-2 from the partitioning of each of the dissolved contaminants into the residual of the other contaminant.

The actual evolution of the two contaminant plumes in this experiment is shown in Figures 5.6(a)-(d). These graphs clearly show the change from an initial PCE-only stage to a mixed PCE+CB stage. In spite of the fact that the model results shown in Figure 5.5 were based on a very simple representation of the conditions found in DE-2, they mimic the data shown in Figure 5.6(c) surprisingly well. The maximum CB concentration of 160 ppm that was measured 75 days into the experiment was only 10 ppm higher than the value calculated by the model. The inability to maintain a steady-state plume (due to the

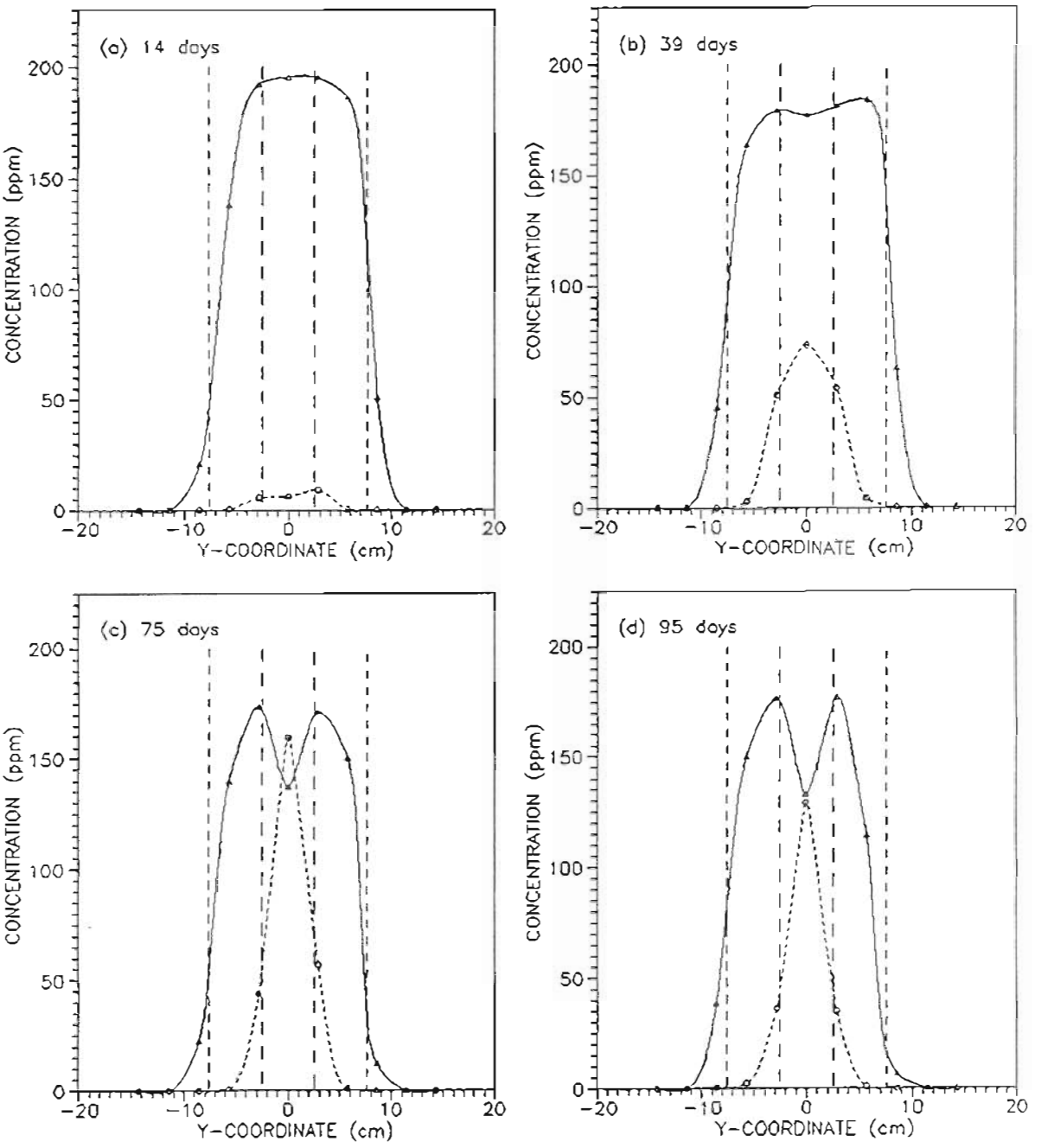

Figure 5.6: The evolution of the PCE (solid lines) and CB (dashed lines) contaminant plumes as measured across R2.

higher molar solubility of CB) is evidenced by the fact that the concentration of CB began to drop again after 75 days. At 95 days the concentration had dropped below 130 ppm.

The interaction of the two DNAPLs shown in DE-2 has significant implications for the investigation of contaminated aquifers. First of all, it serves as a reminder of how important it is to know as much as possible about the composition of the source of contamination. Whether a spilled DNAPL is pure PCE or only 10% PCE will obviously affect the eventual aqueous phase concentration of that compound. This information is necessary if reasonable predictions are to be made about the efficacy of a proposed remediation scheme or the level of contamination that might be expected at a downgradient compliance point. Unfortunately, source composition is not always easy to determine. Leaks from landfills are likely to consist of incredibly complex mixtures of compounds. Even leaks from underground storage tanks may contain a number of different liquids. Second, it raises a question about whether natural organic materials may affect the solubility of DNAPLs. A DNAPL passing through an organic-rich soil will probably dissolve humic materials from that soil. The presence of the humics in the immiscible phase should result in a decrease in the aqueous solubility of the components of the immiscible phase. Studies have been done on the effects of cosolvents such as methanol on the transport of hydrophobic compounds (Rao et al., 1983; Staples and Geiselmann, 1988). It may be just as important to investigate how cosolutes affect the solubility of these compounds.

5.2 A Comparison of Results from DE-2 and DE-3

As mentioned in Chapter 3, the delay in the breakthrough of CB in DE-2 was caused by two processes: (1) the reduction of the water velocity through the source due to a drop in the permeability caused by the presence of the residual, and (2) the partitioning of the dissolved contaminant into the droplets of residual PCE that were encountered downgradient. The evidence for the latter of these two factors has been discussed and illustrated in the previous section. The results of DE-1 have indicated that the first factor may only play a minor role. To confirm this, the column experiment described in Section 3.9 was designed to duplicate most of the conditions found in DE-2. Due to the nature of a column experiment, however, a delay in the breakthrough of CB from the column should only be attributable to partitioning. Comparison of the concentrations measured in the column experiment to those found in the center of the DE-2 plume should therefore be an indication of to what extent the results of DE-2 were affected by a reduction in the velocity of water through the residual.

The concentrations of PCE and CB as measured in samples collected from the center of the tank (port R2-12) are shown in Figure 5.7(a). The concentrations of these contaminants in samples collected from the column are shown in Figure 5.7(b). Both figures show a relatively rapid breakthrough of PCE leveling off at concentrations close to 200 ppm. The fact that 200 ppm concentrations of PCE were found in the column samples indicates that the method of collecting the samples

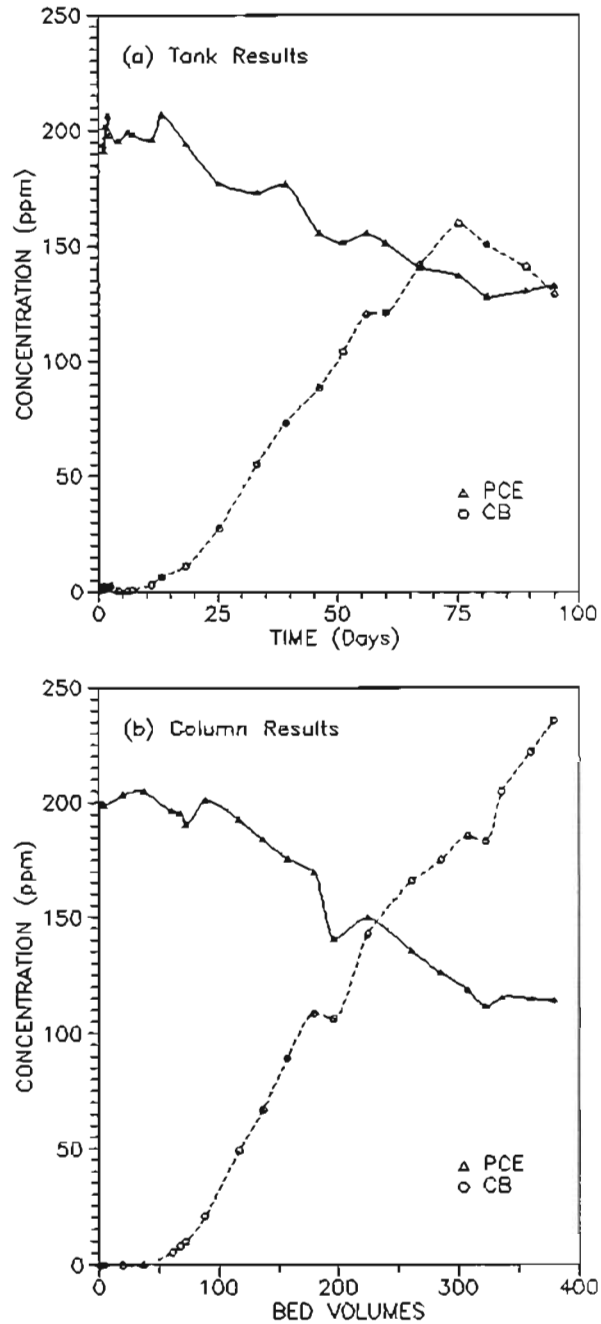

Figure 5.7: PCE and CB concentrations measured in samples collected from (a) port R2-12 of the tank during DE-2 and (b) the column.

directly in open vials did not cause a significant loss of this volatile component. Since CB is less volatile than PCE, the concentrations of this component should also have been essentially unaffected. The two figures clearly show a gradual decline in the PCE concentrations accompanied by a gradual increase in the CB concentrations. This resulted from the slowly changing composition of the residuals that was discussed in Section 5.2.

In order to make a more direct comparison of the two CB curves, the sample times for the tank experimental data were converted to bed volumes. To accomplish this, one bed volume was considered to be the time required for water traveling at the mean velocity to pass through the 5 cm thickness of the CB residual. The velocity calculated from the PCE breakthrough curve (Figure 5.1) was used to determine this time. To eliminate differences caused by unequal distances between the two CB residual zones and their respective sampling locations, the two sets of data had to be normalized to a common starting point. The tank data were normalized by subtracting the time required to travel the 25 cm distance from the downgradient end of the CB zone to the sampling syringe. The column data were normalized by subtracting the volume of water that was contained in the column below the CB residual zone. The equations below show how these factors were incorporated into the calculation of bed volumes.

$$\text{Bed Volumes (Tank)} = (\text{Time in days} - 0.98) \times 5.1 \qquad (5.1)$$

$$\text{Bed Volumes (Column)} = (\text{Effluent Volume} - 75)/35 \qquad (5.2)$$

The normalized CB results from the tank and column experiments are shown in Figure 5.8. Both plumes experienced a delay of about 50 bed volumes before the concentrations of CB became significant. This seems to indicate that the velocity of the water flowing through the residual zone in the tank was not significantly reduced by the presence of the residual. After about 75 bed volumes, the levels measured in the tank were always lower than the levels measured in the column. Analysis of the data from the nearly-linear central portion of the curves indicated that, on the average, the tank concentrations were only about 75% of the column concentrations. One of the contributing factors to the lower tank values was transverse dispersion. As discussed in Section 4.3.2, when the width of a contaminant source becomes narrower, the concentration in the center of the plume becomes more strongly affected by transverse dispersion. Although the PCE source was wide enough so that, at the distances used in these experiments, dispersion had no significant effect on the center of the plume, the CB source was not wide enough to escape the effect of dispersion. However, application of a 2-D model with the value of D_T obtained from the results of DE-1 indicates that transverse dispersion would only reduce the concentrations in the tank to 92% of what they would be without transverse dispersion. Clearly, factors other than dispersion were contributing to the differences in the two contaminant plumes.

In Section 3.4, two difficulties with the column experiment were mentioned. First, the DNAPL saturations had to be less than those in

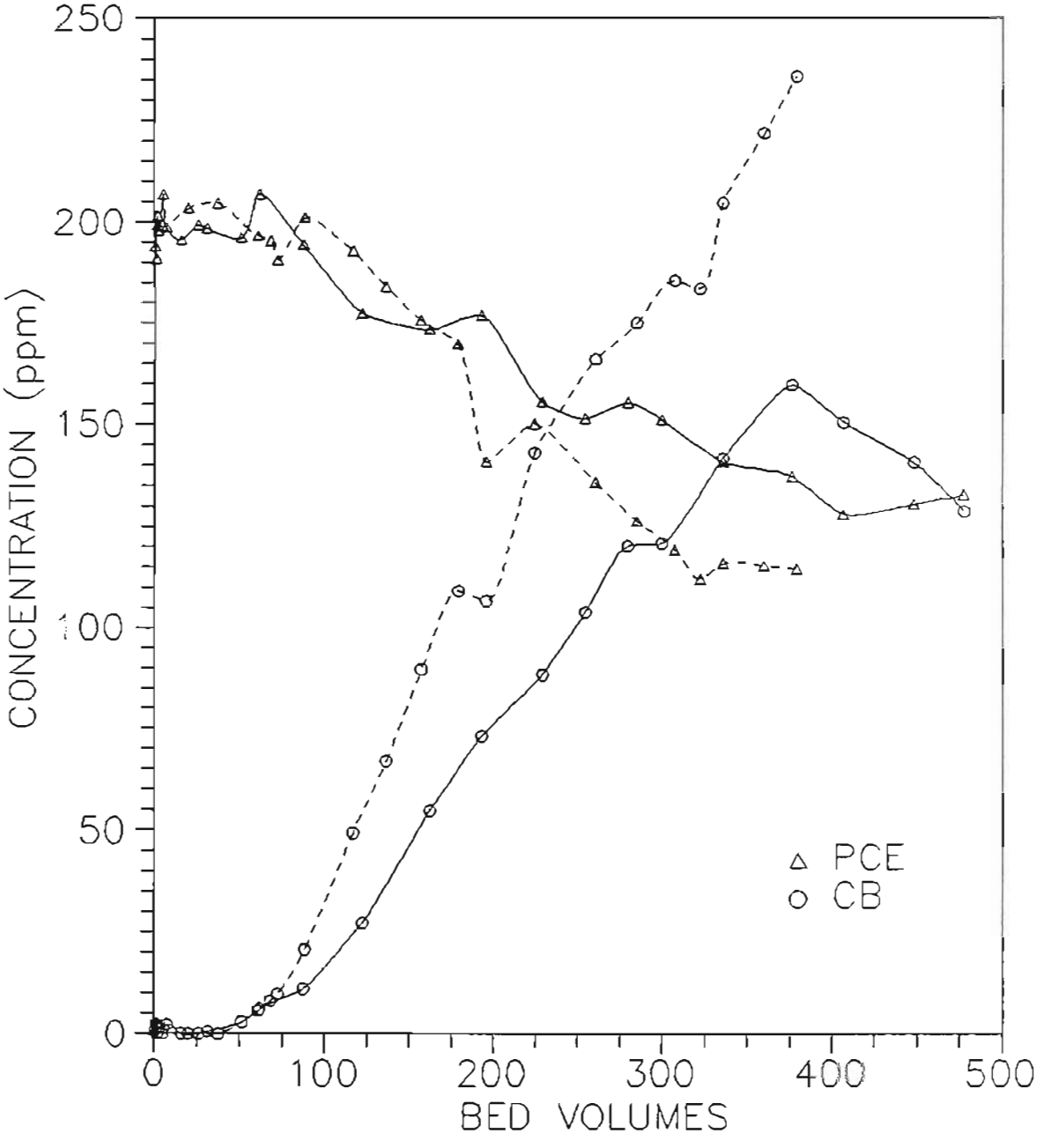

Figure 5.8: PCE and CB concentrations from both the tank (solid line) and the column (dashed line) plotted as a function of normalized bed volume.

the tank to avoid having the residuals become mobilized by the vertical water flow. Since this would have changed the composition of any mixed residuals that were formed, the solubilities of the compounds would also have been affected. Second, the column experiment had to be halted after 75 days due to a crack in the column. At that time, the CB concentration was still increasing. Since the PCE concentration in the column was beginning to level off, it was strongly suspected that the CB concentration would not have gone much higher. However, confirmation of that fact would have been useful. In order to investigate these matters, a computer model was written to simulate the conditions in the column. As in the real column, the model treated the steady-flow of water through three consecutive 5-cm long residual-containing sections. The first and third sections contained initial masses of PCE equal to a 10% saturation and the second section contained an initial mass of CB equal to the same saturation. As long as any PCE remained in the first section, water flowing into the second section was assumed to contain 200 ppm PCE. In order to account for the fact that the composition of the residual would be changing under the influence of the dissolved contaminant plume, the second and third sections were each divided into a number of subsections. Moving from one subsection to the next, the model readjusted the mole fractions of PCE and CB present based on the mass of contaminant entering from the previous subsection. Solute concentrations were then calculated from the mole fractions by assuming ideal equilibrium conditions. Concentrations

calculated in this manner for the final subsection were used for the "plume" emerging from the computer model.

Figure 5.9 compares the results obtained from the column experiment to the computer simulation using the model described above. The only adjustable parameter in the model was the number of subsections incorporated into the second and third residual-containing sections for purposes of making equilibrium-based calculations. The larger the number of subsections used, the faster that partitioning and dissolution equilibration were assumed to take place. The curve in Figure 5.10 was generated by dividing the second and third sections each into 5 subsections. This was equivalent to assuming that equilibrium was reached in a travel distance of 1 cm. Under the conditions of the experiment, this distance corresponded to a contact time of approximately 1 hour.

To illustrate the sensitivity of the model to the equilibration distance, Figure 5.10(a) compares the CB curve from Figure 5.9 to curves generated using different distances. Shorter distances (more rapid equilibration) had the effect of increasing the value of the peak concentration while also delaying its arrival. Conversely, longer distances resulted in a more elongated plume and reduced the value of its peak concentration. This is essentially what happens when the number of effective plates are decreased in a chromatography experiment. When the equilibration distance was set equal to the length of each section (5 cm), the curve lost the S-shape that is characteristic of a delayed breakthrough.

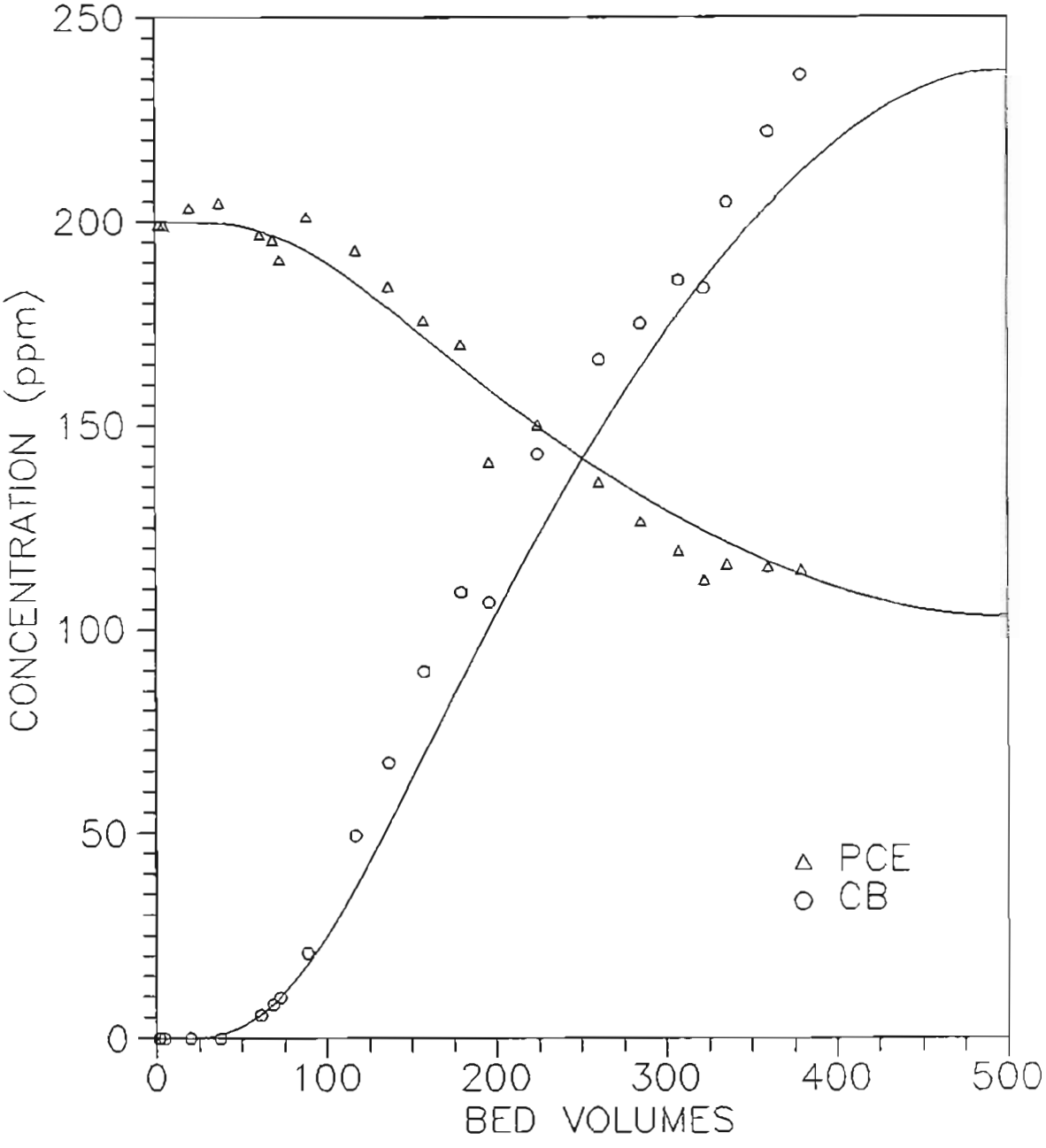

Figure 5.9: A comparison of computer model results to the data from the column experiment.

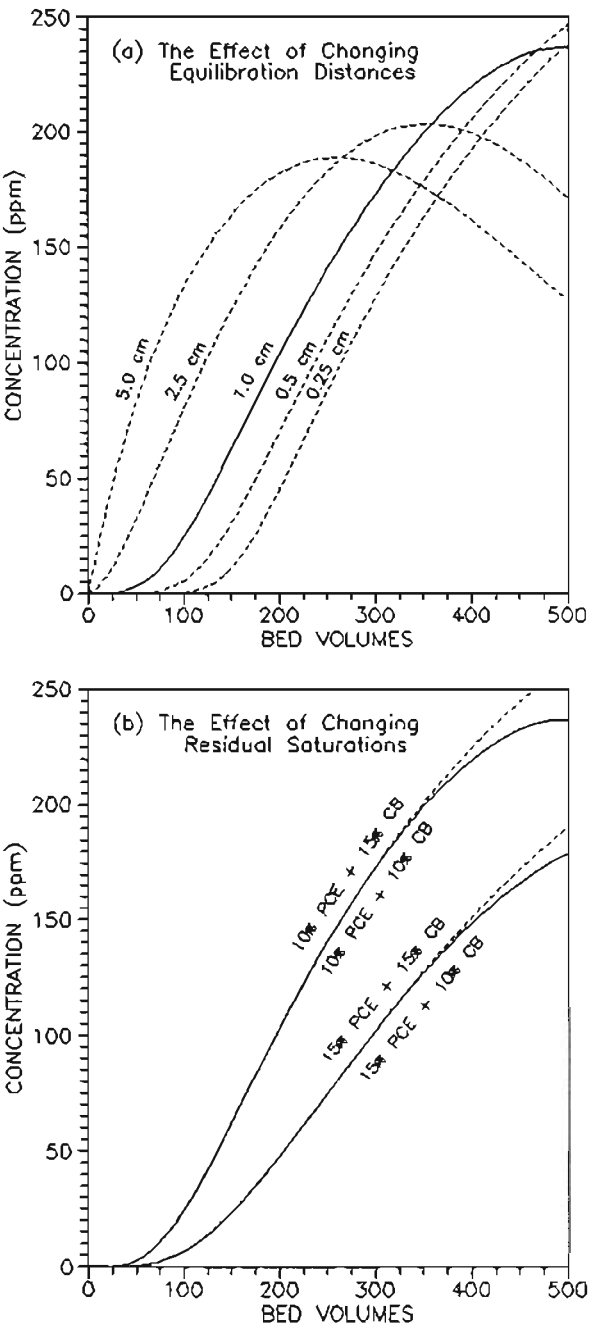

Figure 5.10: The effect of changing (a) the equilibration distance and (b) the residual saturations on the model results.

Figure 5.10(b) shows how the emergence of the CB plume would be affected by the relative saturation of the surrounding PCE residual. The four curves in this figure represent the possible combinations for systems having either 10% or 15% residuals of PCE and CB. Changing the saturation of PCE at a given saturation of CB had a greater effect on the CB contaminant plume than changing the saturation of CB at a given saturation of PCE. This resulted from the fact that the design of the experiment allowed the PCE to interfere with the dissolution of CB in two ways. First, PCE entering the CB residual zone partitioned into the CB and reduced its solubility. Second, the CB that was able to dissolve and move out of its residual zone encountered PCE residual downgradient, dissolved into it, and was further delayed.

Given the uncertainty in the saturation of the PCE residual in the tank, it is not possible to say for sure that a difference in the residual saturations was responsible for the differences observed in the tank and the column results. Considering that a higher PCE saturation was attained in DE-1 than was estimated in DE-2, and that the model results show that a higher PCE saturation will reduce the level of CB in the effluent, it seems likely the main reason for the difference may have been that the actual PCE saturation in the tank was higher than estimated. However, even if a higher PCE residual is assumed, the model does not predict the start of a rapid drop in the concentration of CB as early as was observed in the tank. This could have been due to a lower than expected CB saturation or the onset of biodegradation. The latter was thought to be more likely.

5.3 Conclusions

The results of DE-2 proved to be useful and informative in several respects. First, the data confirmed the observations that had been made about PCE in DE-1. The breakthrough was again rapid and concentrations equal to the solubility were easily attained. There is no doubt that similar conditions in a real aquifer would also result in the release of solubility level concentrations of contaminant. Second, the predictability of the DE-2 plume from the parameters measured in DE-1 verified the well-behaved nature of the model aquifer and its usefulness for studies of this kind. Finally, comparison of the CB data collected over a period of several months to data from a column experiment indicated that, at least at the residual saturations used in these studies, there was no significant reduction in the flow of water through the center of the residual zone. In spite of some difficulties and uncertainties in the formation of the PCE residual, the trend in the concentrations of CB could be easily explained.

For the case where a spilled DNAPL contains more than one compound, DE-2 demonstrated the importance of knowing the molar composition of the immiscible phase. This information is necessary to correctly predict the levels of contaminants that will be found in a plume downgradient from the source. It was possible to simulate the data from this experiment by means of a simple computer model. The algorithm for the model was based on the assumption that solute concentrations were controlled entirely by ideal equilibrium solution

behavior. Comparison of the model-generated data with the experimental results proved this to be a reasonable assumption. Model results were also useful in illustrating the trends that would be observed under conditions of varying saturations or equilibration distances. Although the model was not designed with the intention of calculating any specific physical or chemical parameters, results seemed to indicate that the time required to reach equilibrium for the dissolution and partitioning processes that controlled the solute concentrations in this system was on the order of an hour.

6. DNAPL FLOW EXPERIMENTS

6.1 Introduction

The data discussed in the previous chapters have clearly shown that residual DNAPLs in porous media are readily dissolved by groundwater flowing at typical velocities and attain concentrations equal to their solubilities. That being the case, other factors must be responsible for the fact that concentrations of contaminants found in the field are usually orders of magnitude lower than their solubilities. It has already been speculated that a possible cause may be the formation of narrow "fingers" of residual. These fingers form during immiscible fluid flow when a less dense, more viscous liquid is displaced by one that is more dense and less viscous (see Section 2.4.1). This is precisely the situation that occurs when a DNAPL penetrates the water table. Even though concentrations may be very high as a plume of contaminant emerges from a zone of residual, a narrow source and typical field dispersivities would soon dramatically reduce the contaminant levels. Only samples obtained from near the center of a plume not far downgradient from a source would contain high concentrations. Given the nature of field investigations, this type of sample would probably be very hard to find.

Several laboratory experiments were carried out in an attempt to

get a better understanding of immiscible fluid flow. The experiments were designed for the purposes of observing the qualitative nature of immiscible fluid flow, and for measuring the levels of residual saturation remaining after flow had stopped. The saturation values were of particular interest and importance because such data is almost nonexistent for CHCs. Since the residuals in the dissolution experiments were created in an artificial manner, the experiments in this chapter would provide an indication as to whether or not the previously used saturations were realistic. It was also hoped that fingers of DNAPL could be created and observed in a porous medium without resorting to the very high velocities or viscosity contrasts often employed in petroleum displacement studies. However, a thorough study of immiscible flow was outside the bounds of this research project.

6.2 Column Experiments

6.2.1 Experimental Procedure

The first DNAPL flow experiments were carried out in glass columns. The goals were to measure residual saturations in a saturated porous medium and to compare observations and results from two identical columns. Thirty cm long, 4.66 cm i.d. columns were used for this purpose. The bottom of each column was connected to a graduated glass tube fitted with a sidearm which was in turn connected via 1/4-inch tubing to a constant-head reservoir (Figure 6.1). This configuration was chosen to allow any DNAPL that passed through the

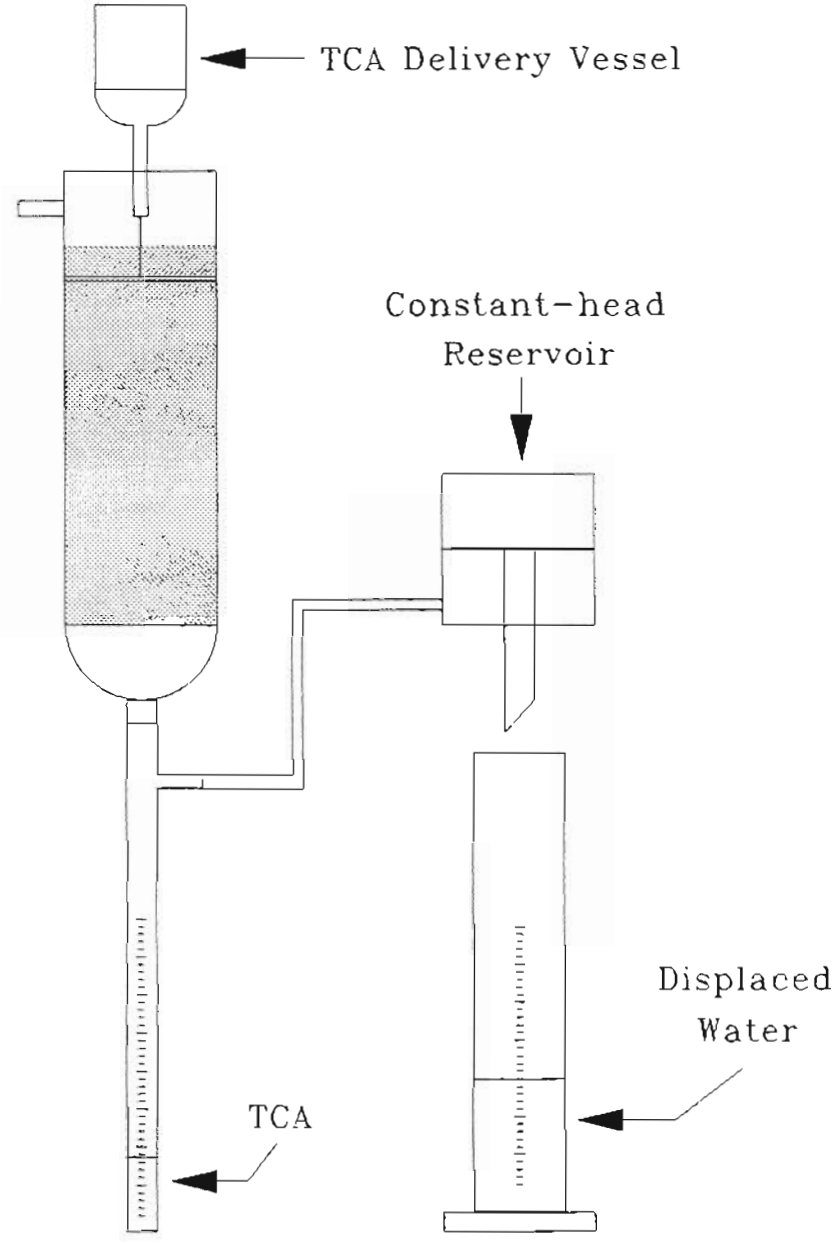

Figure 6.1: Column used to study 1,1,1-TCA flow and saturation in water-wet 35/80 mesh Borden sand.

columns to be collected and measured without interfering with the flow of water to and from the constant-head reservoir. Borden sand was used to fill the columns to a depth of 24 cm. Two pieces of 100 mesh wire screen were then placed on top of the sand in each column, and another 2 cm of sand was placed over the screens. The screens were added to create a narrow zone of higher permeability to ensure that the DNAPL would easily spread over the entire cross section of the column before penetrating the main body of sand. The columns were flushed overnight with deaerated water to remove residual air. After flushing, the water table was dropped to 20 cm below the surface of the sand. In spite of the drop in the water table, the sand in each column appeared nearly saturated with water due to capillary pressure.

The DNAPL used in these experiments was a solution of 1,1,1-TCA containing 0.1 g/L Oil Red EGN dye (Aldrich Chemical Co., Milwaukee, WI). The dye was added not only to aid in visually tracking the progress of the DNAPL movement, but also to provide a means of measuring the residual saturation of the DNAPL. The 1,1,1-TCA was slowly added to each column using a small glass reservoir (150 mL) which had a piece of glass tubing with a Luer hub attached to the bottom. A syringe needle was attached to the Luer hub and used to restrict the flow to 1-2 mL/min. The reservoir was positioned so that the needle penetrated the top 2 cm of sand and just touched the buried screens. When 1,1,1-TCA was introduced to the columns, it quickly spread through the screens and could be seen around the entire circumference. However, the 1,1,1-TCA was not able to immediately

penetrate the main body of sand and soon filled the top 2 cm and appeared on the surface. To allow sufficient time for the 1,1,1-TCA to penetrate the sand, it was added in 5-10 mL increments in intervals of 6-12 hours. Additions were continued until the red fluid emerged from the bottom of each column and began to collect in the graduated tubes. Water displaced from the columns by the infiltrating DNAPL was collected from the constant-head reservoir overflow tubes and the volume periodically measured.

The columns were then allowed to sit for several more days until 1,1,1-TCA drainage ceased. The total time from the initial 1,1,1-TCA addition until the columns were removed for analysis was 21 days. These experiments were performed in a cold room at 10 ^{o}C to reduce volatilization losses. Losses were further reduced by keeping the columns and the DNAPL reservoirs tightly covered with aluminum foil.

Before sliding the main plug of sand out of each column, the 2-cm deep layer on the top was dug out and the wire screens were removed. This top layer of sand, which appeared fairly dry, was discarded. The columns were then inverted and the wet sand slid out onto sheets of aluminum foil. Although there was some concern that inverting the columns would cause water and/or 1,1,1-TCA to flow back "up" the core of sand, since it did not take long to remove the sand and since the saturation analyses were only being done to obtain mean values for large sections of each core, this was not considered a serious flaw in the procedure. A metal spatula was used to slice the cores into 1-2 cm cross-sections. After observing the internal distribution of the

1,1,1-TCA, the sections of each core were placed into eight preweighed wide-mouth sample bottles and dried overnight at 105 ^{o}C. The bottles were then reweighed to determine the mass of each of the samples.

The mean DNAPL saturation for each section was calculated indirectly by spectrophotometrically determining the amount of dye remaining in each of the dried samples. This was accomplished as follows. A known volume of a 1:1 solution of dimethylsulfoxide and methanol (DM) was added to each of the sample bottles and the resulting mixture was stirred to dissolve the dye. After allowing the sand to settle, the absorbence of the Oil Red EGN dye in the DM was measured at 525 nm and a previously prepared standard working curve was used to convert absorbence to dye concentration. Since the initial concentration of dye in the 1,1,1-TCA was known, the volume of 1,1,1-TCA could be calculated from a simple dilution relationship.

$$V_{TCA} = \frac{([Dye] \text{ in DM})(V_{DM})}{([Dye] \text{ in TCA})} \qquad (6.1)$$

The volume of pore space in each section was calculated from the mass, porosity, and bulk density of the sand.

$$V_{pores} = M_s \, n/\rho_b \qquad (6.2)$$

The mean percent 1,1,1-TCA saturation for each section was then calculated from the ratio of these two volumes.

$$S_{TCA} = (V_{TCA}/V_{pores}) \times 100\% \qquad (6.3)$$

6.2.2 Results and Discussion

Since the columns used for the DNAPL saturation experiments were each packed with the same grade of sand, flushed with deaerated water and connected to constant-head reservoirs positioned at the same elevation, it was thought that the observations and results for the infiltration of 1,1,1-TCA into each of them would be reasonably similar. However, as can be seen in the summary of observations given in Table 6.1, differences began to show up as early as the second day. At that point it was already obvious that the infiltrating 1,1,1-TCA (as evidenced by the location of the red color) was becoming more evenly distributed in Column A than in Column B. This resulted in other noticeable differences between the columns. For one thing, the unevenly distributed 1,1,1-TCA in Column B was able to work its way more rapidly down one side of the column. It began to seep through the screen at the bottom on the fourth day. The 1,1,1-TCA in Column A did not make it to the bottom until the eighth day. Also, because the 1,1,1-TCA was more evenly spread out in Column A, more of it was immobilized as residual. Therefore, a much larger volume had to be added before the immiscible fluid reached the bottom (75 mL versus 45 mL).

In each of the columns, the apparent volume of 1,1,1-TCA that remained in the sand exceeded the volume of water that was displaced. Several factors could have contributed to this. First, in spite of an attempt to prevent it, the high vapor pressure of 1,1,1-TCA made some losses due to volatilization inevitable. Any 1,1,1-TCA that was lost

Table 6.1: A summary of the movement of 1,1,1-TCA through two identical 30-cm columns containing 35/80 mesh Borden sand. Each addition of 1,1,1-TCA is indicated as "+mL TCA" with the total given in parentheses. Volumes of water displaced from the sand and 1,1,1-TCA passing through the column are listed as totals up to the indicated day and time.

DAY	TIME	COLUMN A	COLUMN B
1	3:30 PM	+10 mL TCA (10).	+10 mL TCA (10).
	9:30 PM	+5 mL TCA (15).	+5 mL TCA (15).
2	9:00 AM	4 mL water. +10 mL TCA (25).	5 mL water. +10 mL TCA (25).
		[Red color visible in both columns at a distance of 10-12 cm from the surface.]	
	9:15 PM	7.5 mL water. +10 mL TCA (35).	8 mL water. +10 mL TCA (35).
		[TCA now visible 1/2-2/3 down the columns; color more evenly distributed in Column A.]	
3	10:45 AM	10 mL water. Color fairly even; 8 cm from bottom. +5 mL TCA (40).	12 mL water. Color quite uneven; 3 cm from bottom. +5 mL TCA (40).
	9:30 PM	Still 10 mL water. Color same as in AM. +5 mL TCA (45).	14 mL water. Color close to bottom. +5 mL TCA (45).
4	9:00 AM	11 mL water. TCA not yet out; Color 5 cm from bottom. +5 mL TCA (50).	15 mL water. TCA coming out; 0.3 mL TCA out. TCA additions stopped.
	5:00 PM	12 mL water. TCA not yet out. +5 mL TCA (55).	15 mL water. 1.0 mL TCA out.

(Continued on the next page)

(Table 6.1: Continued)

5	9:00 AM	13 mL water. TCA still not out. +5 mL TCA (60).	15 mL water. 1.2 mL TCA out.
6	Noon	+5 mL TCA (65)	-
7	9:00 AM	15 mL water. TCA still not out. +5 mL TCA (70)	15 mL water. 2.0 mL TCA out.
	5:30 PM	16 mL water. TCA still not out. +5 mL TCA (75).	15 mL water. 2.0 mL TCA out.
8	9:30 AM	17 mL water. TCA not yet out; but visible at bottom. TCA additions stopped.	15 mL water. 2.2 mL TCA out.
12	Noon	17 mL water. 2.6 mL TCA out.	15 mL water. 2.2 mL TCA out.
13	Noon	17 mL water. 2.9 mL TCA out.	15 mL water. 2.5 mL TCA out.
18	8:30 AM	17 mL water. 3.0 mL TCA out.	15 mL water. 2.6 mL TCA out.
22	9:00 AM	[No further change, so the columns were disconnected and the collection tubes removed from the bottoms. An additional 3.5 mL of TCA came out of each column during this step.]	
Final Volumes:		75 mL TCA added; 6.5 mL passed though. 17 mL water displaced.	45 mL TCA added; 6.1 mL passed through. 15 mL water displaced.

in this fashion before having a chance to penetrate the column and displace some water would have contributed to a volume difference. Since a larger volume of 1,1,1-TCA was added over a longer period of time to Column A, greater volatilization losses should have occurred there. Examination of the final volumes listed in Table 6.1 shows that the volume discrepancy was indeed much larger for Column A than for Column B. In fact, even though Column A received 30 mL more 1,1,1-TCA than Column B, the volume of water displaced from the two columns was almost identical. However, because of the high 1,1,1-TCA saturations found throughout Column A (discussed later in this section), it is doubtful that 1,1,1-TCA volatilization was the only factor contributing to the difference in measured volumes.

Although precautions were taken to reduce CHC volatilization from the columns, similar precautions were not taken to prevent evaporation of water from the constant-head reservoirs. If any evaporation from the reservoirs did occur, the volumes of water collected and measured during the 1,1,1-TCA infiltration would be less than the volumes that were actually displaced. However, losses due to evaporation from the two identical constant-head reservoirs should have been comparable. This may have contributed a small but equal amount to the volume discrepancy in each column.

Finally, despite having been flushed with deaerated water, the columns may not have been fully saturated prior to the addition of the 1,1,1-TCA. Enhanced permeability at the glass/sand interface could have contributed to more rapid removal of the visible air bubbles.

This would have given the columns the outward appearance of complete saturation even though residual air remained inside the columns. Small unnoticeable differences in the way that the columns were packed could also have created regions where residual air was more difficult to remove. Since there is no reason to assume that this unpredictable behavior would affect two columns to the same degree, this also may have contributed to the larger volume difference measured in Column A.

After removing the cores from the columns, inspection of the sand showed the distribution of 1,1,1-TCA to be consistent with the observations made during the infiltration step. The red dye appeared to be spread quite evenly throughout the Column A core whereas several cross-sections from the Column B core were noticeably free of dye on one side. Also, the sand from Column B generally looked wetter.

In both of the cores, the highest 1,1,1-TCA saturations were found at the top of the column (Table 6.2). This is certainly due, in part, to the fact that 1,1,1-TCA volatilization losses would have occurred near the surface leaving behind the nonvolatile dye. Because 1,1,1-TCA saturations were based on analysis of the dye, this excess dye would result in erroneously high values. However, since it is doubtful that significant volatilization losses would have occurred very far from the surface, saturations from the middle and bottom sections of the column are probably realistic. Not surprisingly, except for one location, all of the sections from Column A had higher 1,1,1-TCA saturations than the corresponding sections from Column B. That portion of Column B where the 1,1,1-TCA bypassed part of the core

Table 6.2: Mean percent saturation values for 1,1,1-TCA following the infiltration of this DNAPL into water-saturated 35/80 mesh Borden sand in 30-cm glass columns.

	Column A		Column B	
Section Number[a]	Length of Section (cm)	TCA Saturation (%)	Length of Section (cm)	TCA Saturation (%)
1	3.3	76	2.1	51
2	4.1	51	2.4	36
3	3.1	52	3.1	16
4	2.3	22	2.8	17
5	2.7	25	2.6	6
6	3.1	31	4.0	22
7	1.8	37	2.6	27
8	2.4	28	3.1	34

[a]The top two centimeters of sand were discarded from each column (see text). Section number 1 starts just below the discarded sand.

is easily noted by its significantly lower saturation. Most importantly, except for the high values near the top of both columns and the one low value in Column B, all of the 1,1,1-TCA saturations fall within the 15-40% range given by Wilson and Conrad (1984) for HCs. Therefore, this range of residual saturations also appears to be reasonable for CHCs in saturated porous media.

6.3 Narrow Box Experiments

6.3.1 Experimental Procedure

In order to better observe the progress of DNAPL infiltration into the saturated zone, several experiments were carried out in a tall, narrow box made from 1/4" thick plexiglas. The box was 88 cm high by 25 cm wide by 2.5 cm thick (internal dimensions). A frame of 1/2" aluminum rods attached to two ring stands was constructed to both hold the box and also prevent the front and back faces from bowing excessively when it was being packed with sand. A constant-head reservoir was connected via 1/4" tubing to inlets at the bottom of each side of the box (Figure 6.2). The box was packed with sand to a depth of 75 cm. No. 17 Silica sand was used for Flow Experiment #5 (FE-5) and F-80 sand was used for FE-6. After slowly filling the box from the bottom with water, the sand was flushed with deaerated water to remove residual air. When the sand was fully saturated with water, the flow of water was stopped and the constant-head reservoir was lowered to adjust the water table to a depth of 50 cm below the surface of the sand. The box was then allowed to drain resulting in

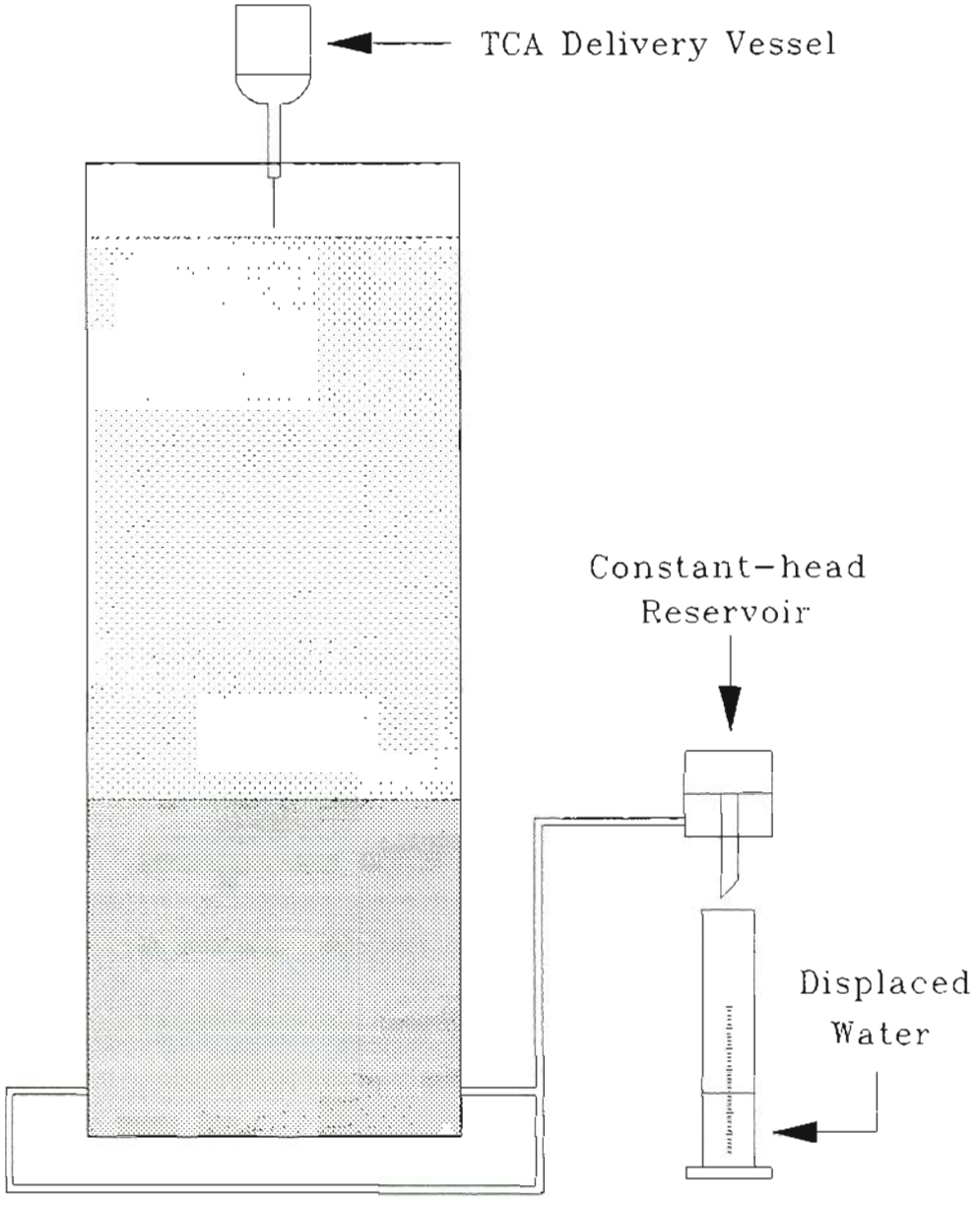

Figure 6.2: Plexiglas box used to observe the penetration of the water table by 1,1,1-TCA.

the formation of an unsaturated zone and a capillary fringe above the water table. In FE-5, the 50-cm depth of sand above the water table was divided roughly between a 20-22 cm vadose zone and a 28-30 cm saturated capillary fringe. Because the sand used in FE-6 was finer than that used in FE-5, the capillary fringe was higher. FE-6 had a 40-42 cm capillary fringe and a 8-10 cm vadose zone.

The DNAPL used in FE-5 and FE-6 was 1,1,1-TCA containing Oil Red EGN dye. As in the column experiments discussed above, the DNAPL was applied from a small reservoir through a piece of glass tubing with a syringe needle attached to control the flow rate at about 1 mL/minute. The DNAPL was applied to the surface only in the center of the box. The application rate was fast enough to ensure that the 1,1,1-TCA spread out to cover the full 2.5 cm thickness between the front and back walls of the box. It was slow enough, however, so that the infiltrating plume of DNAPL would not spread throughout the 25 cm width of the box and encounter the sides before reaching a reasonable depth. The water displaced from the box by the infiltrating DNAPL was collected and its volume measured periodically. These experiments were carried out in a cold room at 10 ^{o}C to reduce volatilization losses. The progress of each spill was recorded photographically.

6.3.2 Results and Discussion

In the early stages of FE-5, the 1,1,1-TCA flow rate was maintained at a little over 1 mL/minute. Later, however, the flow stopped as the needle apparently became clogged. Tapping on the

reservoir caused the flow to resume, albeit at a slower rate. This happened several times during the course of the experiment. Table 6.3 summarizes the addition of 90 mL of 1,1,1-TCA to the box. It also lists the volume of water that was displaced by the infiltrating DNAPL at various times during the course of this spill and includes observations about the progress of the plume.

When the 1,1,1-TCA was dripped onto the top of the sand, it was able to easily penetrate and move down through the vadose zone. Figure 6.3 shows the locations of the plume front at various times during this spill. Although the plume continued to broaden slightly during the early stages of the infiltration, its primary direction of movement was downward. After 30 minutes, 40 mL of 1,1,1-TCA had been added and the front of the plume was only about 1 cm from the capillary fringe. As the 1,1,1-TCA approached more closely, the saturated fringe began to collapse and the rate at which water was being displaced from the box increased. After 52 minutes, 45 mL of 1,1,1-TCA had been added. Although the front of the plume had advanced another 10 cm during that time, it was still separated from the capillary fringe by a couple of millimeters of obviously unsaturated sand. The movement of the fringe is also shown in Figure 6.3.

During the next 20 minutes, the DNAPL plume narrowed while it continued to push the top of the saturated zone down ahead of it. The collapse of the capillary fringe did not occur across the entire width of the box, however. Only that portion directly in front of the

Table 6.3: A summary of the movement of 1,1,1-TCA from the vadose zone into the saturated zone of a model aquifer consisting of No. 17 Silica sand packed in a plexiglas box (FE-5). Times marked with an asterisk correspond to the positions of the plume shown in Figure 6.3.

Elapsed Time (min)	Volume TCA In (mL)	Volume H_2O Out (mL)	Observations
5*	-	-	TCA has easily penetrated the surface.
10*	-	-	Plume has continued straight down.
20*	30	6	TCA has reached depth of 12-13 cm.
30*	40	17	TCA has approached within 1 cm of fringe.
52*	45	43	Top of capillary fringe has begun to collapse in front of advancing TCA.
72*	50	67	TCA has pushed into the saturated region of the capillary fringe.
90*	60	84	Plume shape has become more irregular.
105*	70	100	TCA has penetrated the water table.
110*	75	-	TCA has contacted one side of the box.
115*	80	-	Flow has continued down the side.
120*	85	115	TCA has reached the bottom of the box.
125	90	-	Addition of TCA has been halted.
150	90	135	Flow of displaced water has stopped.

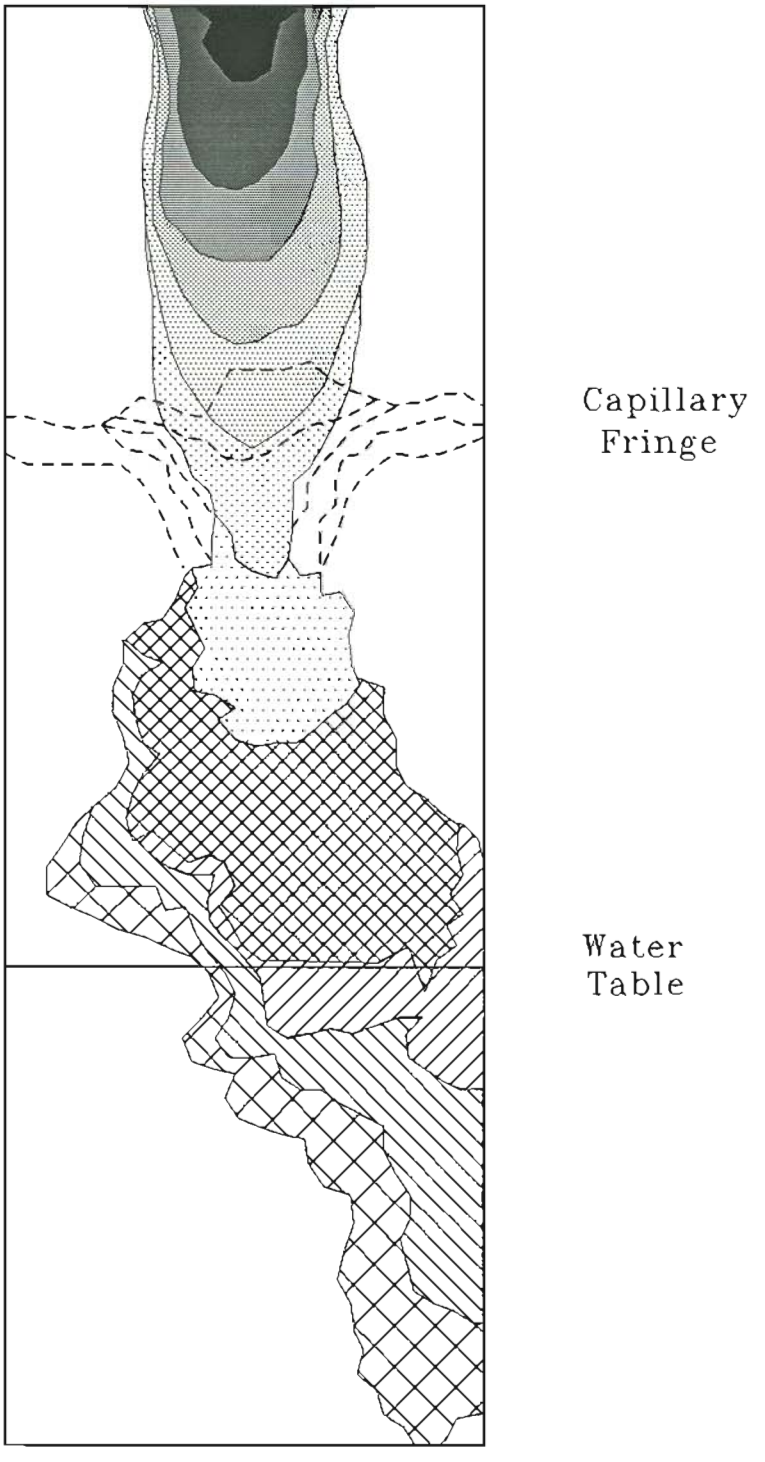

Figure 6.3: The movement of 1,1,1-TCA through No. 17 Silica sand (FE-5). The stages of the plume correspond to times listed in Table 6.3. The dashed lines mark the location of the capillary fringe.

advancing immiscible fluid moved significantly. Finally, after about 72 minutes, the fringe stopped collapsing and the 1,1,1-TCA penetrated water-saturated pores. At this point, the top of the capillary fringe had dropped down about 8-9 cm in the center of the tank and about 1 cm near the edges. As water continued to be displaced, the fringe did eventually drop another 1-2 cm near the sides of the box. But, it remained significantly higher there than in the center.

As the plume pushed its way into the water-saturated sand, it broadened and its shape became more irregular. Also, the flow no longer continued straight down the center of the box. After 105 minutes, the 1,1,1-TCA penetrated the water table. Shortly thereafter, it came into contact with the right side of the box. Infiltrating 1,1,1-TCA continued to flow down the right side, finally reaching the bottom after 2 hours. From this point on, of course, the 1,1,1-TCA was only able to spread out and fill the bottom of the box.

Water continued to flow from the box for another half hour. Eventually, a total of 135 mL of water was released from the box by the infiltration of 90 mL of 1,1,1-TCA. The volume of water collected was larger than the volume of 1,1,1-TCA that was added because two different mechanisms were involved in its release. Some of the water was physically displaced from the pores by the infiltrating DNAPL. Since part of the 1,1,1-TCA was immobilized as residual in the vadose zone, this process would only be responsible for a volume of water that was less than the volume of 1,1,1-TCA. The rest of the water was released from the sand by the collapsing capillary fringe.

As discussed in Section 2.2, the height to which a liquid can rise in a given porous medium is proportional to its interfacial tension. Since interfacial tensions between water and CHCs (γ_{wc}) are all significantly less than the interfacial tension between water and air (γ_{wa}), the introduction of a CHC will result in the reduction of the interfacial tension and the drainage of water from the capillary fringe. However, the extent to which the capillary fringe will change cannot be arrived at by a simple comparison of γ_{wc} and γ_{wa}. This is because the presence of a CHC also changes the system from one with two fluids to one with three fluids. Since CHCs are wetting fluids relative to air and nonwetting fluids relative to water, they will occupy regions of the pore spaces between air and water. The final water saturation will therefore be controlled by both the water-CHC and the CHC-air interfacial tensions.

It is interesting to note that the collapse of the capillary fringe started before the DNAPL actually made contact with the fully water-saturated pores. This probably occurred when vapors released from the advancing volatile liquid moved down under the influence of gravity, dissolved in the pore water, and reduced the interfacial tension. Since the relative vapor density at 20 ^{o}C for dry air saturated with 1,1,1-TCA to pure dry air is 1.47 (Schwille, 1988), the density driven flow of the vapors was to be expected. This is an important area for further research since contamination can reach the water table under these conditions even if the source remains immobilized in the vadose zone.

In FE-6, 1,1,1-TCA was also added to the center of the box at a rate of about 1 mL/minute. Although the flow occasionally slowed or stopped due to a clogged needle, tapping on the DNAPL reservoir started it again. Table 6.4 summarizes the addition of 50 mL of 1,1,1-TCA to the sand as well as the displacement of water from the box. Observations about the progress of the flow are also given. Figure 6.4 shows the locations of the plume front at various times during this spill.

In the early stages of FE-6, the plume began to narrow and move to the side as if deflected by the capillary fringe. However, it soon penetrated the fringe and immediately began to broaden. Since the capillary fringe was higher, it began to collapse and release increasing amounts of water from the tank earlier in the experiment. Due to the width of the plume, this collapse affected a much wider portion of the fringe. Although only 50 mL of 1,1,1-TCA was added to the box, a total of 134 mL of water was collected before DNAPL entered the lines leading to the constant-head reservoir and interfered with further displacement.

The most noticeable difference between the two flow experiments was the width of the plume. This was probably due to the fact that the finer sand had a lower permeability. Although the spill rate was the same for both of the experiments, the lower permeability in FE-6 would not allow as rapid of a downward penetration. The DNAPL, encountering relatively more resistance in front of it, had more of a tendency to flow to the sides. The broader plume was still about 7 cm

Table 6.4: A summary of the movement of 1,1,1-TCA from the vadose zone into the saturated zone of a model aquifer consisting of F-80 sand packed in a plexiglas box (FE-6). Times marked with an asterisk correspond to the positions of the plume shown in Figure 6.4.

Elapsed Time (min)	Volume TCA In (mL)	Volume H_2O Out (mL)	Observations
6	-	10	TCA has started to displace water.
9*	10	15	Plume has continued downward.
14*	-	-	Plume advance has slowed.
20*	20	33	TCA plume has been deflected slightly by the top of the capillary fringe.
30*	30	50	TCA has penetrated the capillary fringe causing it to collapse.
40*	-	-	The plume has started to broaden.
45*	-	-	Plume advance has speeded up.
50*	40	70	The plume has become quite broad.
55*	-	-	TCA has contacted both sides of the box.
70*	-	100	TCA has penetrated the water table.
82	50	108	Addition of TCA has been halted.
92*	50	118	Plume has advanced more rapidly down the sides of the box.
115	50	134	TCA has entered the constant-head reservoir lines.

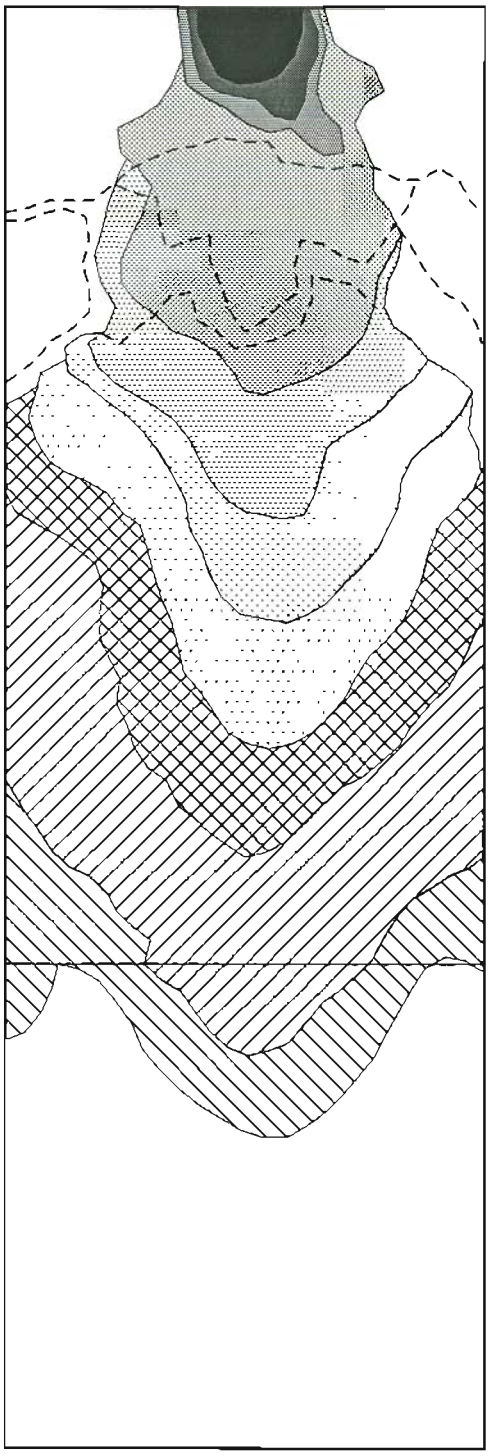

Figure 6.4: The movement of 1,1,1-TCA through F-80 sand (FE-6). The stages of the plume correspond to times listed in Table 6.4. The dashed lines mark the location of the capillary fringe.

above the water table when it reached the sides of the box. Interestingly enough, in spite of the fact that this plume was broader and had moved more slowly in the early stages than FE-5, its advance through the capillary fringe was actually faster.

Although the plume's more rapid advance seemed counterintuitive, an observation made later in the experiment may have accounted for it. For the first 70 minutes of this spill, the box had been positioned near a wall in order to facilitate photographing the plume. For this reason, all observations had been made from one side. After the plume had penetrated the water table, however, it was decided to turn the box around in order to see if the plume had also penetrated the water table in the back of the box. Surprisingly, although the sand pack was only 2.5 cm thick, the appearance of the plume from the back was totally different (Figure 6.5). At a depth of 15 cm, the plume had split in two and each half had flowed to one side leaving a DNAPL-free zone in the middle. The flow had then continued down, penetrating the water table on each side of the box. This was just the opposite of what had been observed from the front where a single plume had moved down through the center of the sand. During the next 20 minutes, while the plume continued to move down evenly in the front of the box, the halves of the plume in the back continued to broaden until they rejoined just above the water table. A roughly 15-cm high by 10-cm wide area in the center of the capillary fringe remained free of 1,1,1-TCA. Flow then continued primarily down the sides of the box into the saturated zone. Although completely surrounded, the 1,1,1-

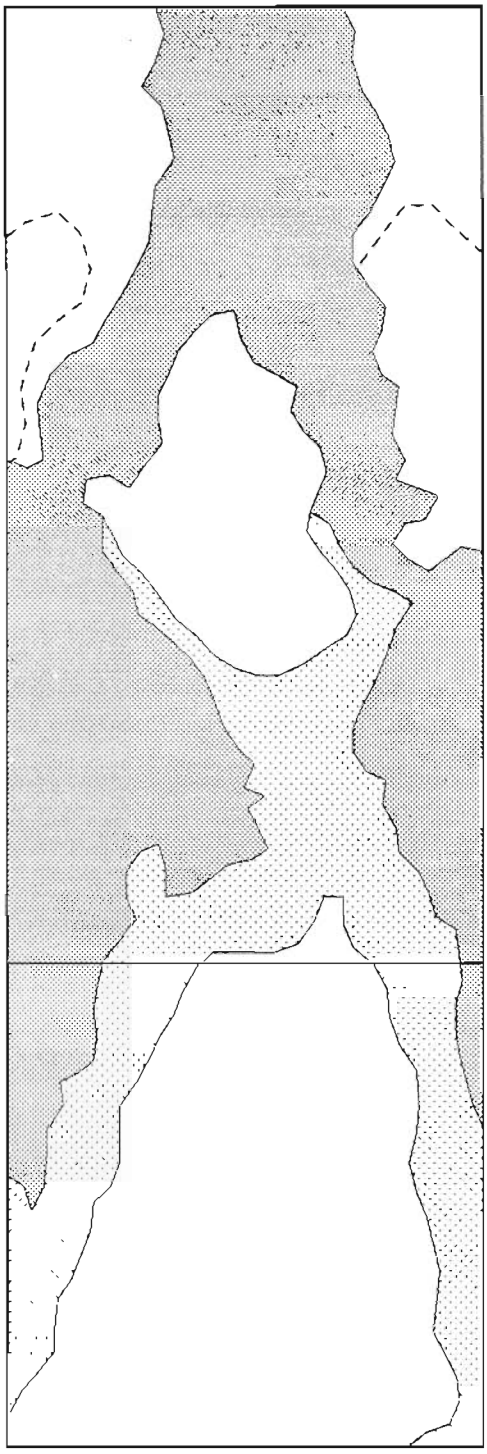

Figure 6.5: The location of the 1,1,1-TCA plume as seen from the back of the box in the latter stages of FE-6. The darker area marks the plume after 70 minutes; the lighter area marks the spreading that occurred between 70 and 90 minutes.

TCA-free area of the fringe was not infiltrated during the final stages of the spill. The rapid advance of the broad plume as seen from the front of the box was most likely due to the fact that the 1,1,1-TCA was not spreading throughout the full thickness of the sand. Rather, it was flowing preferentially in the region of the sand/wall interface.

Despite the seemingly incongruous results of FE-6, these observations are actually consistent with those from the column experiments and make an important point. When dealing with multiphase immiscible fluid flow in porous media, very minor differences in such factors as the way that the sand is packed, or the distribution of water or air in the pore spaces, can lead to large unpredictable differences in the flow and eventual distribution of DNAPLs. Also, in laboratory experiments, the walls of the apparatus may have an effect on the observed behavior. The magnitude of this effect is still a matter of debate. Schwille (1988) points out that for the sands used in his work, wall effects were either nonexistent or at most, only minimal. However, the sands used in FE-5 and FE-6 were finer than most of the sands used by Schwille. Therefore, wall effects may become more significant as the permeability of the sand decreases.

It is also important to note that many observations made during both FE-5 and FE-6 were consistent with and predictable from fluid flow theory. The 1,1,1-TCA was able to easily move through the vadose zone, but due to reduced relative permeability as the saturation of water increased, it had more difficulty pushing its way into and

moving through the capillary fringe. Lower permeability resulted in a broader plume, not only in the saturated zone versus the vadose zone, but also in a finer sand versus a coarser sand. Finally, due to a reduction in interfacial tension, the height of the capillary fringe changed noticeably in the presence of a CHC.

6.4 Small Tank Experiments

6.4.1 Experimental Procedure

Each of the sets of experiments discussed in the previous sections involved DNAPL flow that was confined by the walls of the experimental apparatus. Since it was unclear to what extent the behavior of the flow might have been affected by the walls, a set of experiments was designed in which a solution of DNAPL and red dye was poured into the center of a small sand-filled tank so that infiltration could occur without touching the walls. The tank used for these experiments was a 60 cm x 30 cm x 30 cm aquarium (Figure 6.6). Wire screens were mounted inside the tank about 2.5 cm from each end to create reservoirs used to provide horizontal flow of water through the sand. Both ends of the tank were connected by means of 1/4" tubing to constant-head reservoirs which were used to control both the water level in the tank and the flow rate through the sand. Sand (No. 17 Silica or Flintshot 2.8) was added to the tank by pouring in and leveling off about 1 L at a time. This produced a final sand pack made up of many thin horizontal layers. About 180 pounds of sand were required to fill the tank.

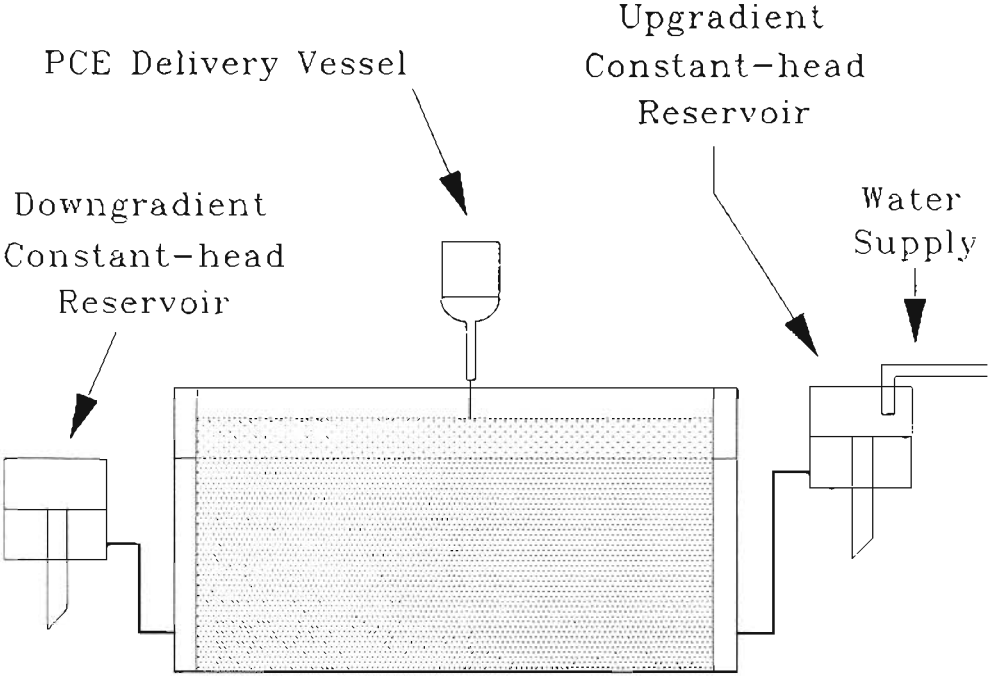

Figure 6.6: Small tank used to study the distribution and residual saturation of PCE in the vadose and saturated zones.

After packing the tank with sand, it was filled to the desired level with water in one of two ways. In some cases, the water level was first set at the top of the sand and the tank was flushed with deaerated water until small air bubbles were no longer visible on the inside of the glass. This usually required a specific discharge of at least 50 cm/day for a week to ten days. When the sand appeared to be fully saturated, the water table was dropped to the final desired level and the sand was allowed to drain for a week to establish a vadose zone and capillary fringe above the water table. This method produced a relatively broad drainage capillary fringe. In other cases the water table was set to the desired level at the beginning of the experiment and not changed. Flushing with deaerated water eventually produced a fully saturated zone below the water table. Water rose into the sand above the water table due to capillary action. Since saturation as a function of capillary pressure is subject to hysteresis, this method produced a much narrower imbibition capillary fringe. In both cases the flow of water was stopped before the DNAPL was added to the system.

Just prior to pouring the DNAPL into the tank, a 5-cm diameter by 1-cm deep depression was dug in the top of the sand to receive the DNAPL and prevent it from immediately spreading out across the surface. The top of the tank was then covered with a plexiglas sheet that was taped down to reduce volatilization losses during the course of the experiment. A small hole was drilled in the center of the plexiglas cover to accommodate the glass tube from the DNAPL reservoir

(described in section 6.2.1). Rapid spill rates were achieved by removing the rate-controlling syringe needle from the bottom of the tube.

The DNAPL used in this set of experiments was PCE containing 1 g/L of Oil Red EGN dye. This liquid was chosen over the previously-used 1,1,1-TCA because its greater density (1.62 g/cm^3 versus 1.34 g/cm^3) would facilitate penetration of the water table. During the course of the DNAPL infiltration, water displaced from the tank was collected and its volume was periodically measured. After allowing sufficient time for the DNAPL to penetrate the sand, the tank was carefully excavated and the three-dimensional movement of the non-aqueous phase identified by the distribution of the red color. In the latter stages of this procedure, the water table had to be dropped and kept below the working area to prevent water and PCE from flowing across the surface being excavated. Photographs were taken of the dye-distribution at a number of depths.

Samples were collected and analyzed for DNAPL saturation indirectly from the dye concentration. The procedure for this was similar to that described in Section 6.2.1 with two modifications. First, unlike the column experiments where entire sections of sand (some with dye and some dye-free) were analyzed for a mean saturation value, in these experiments an attempt was made to collect and analyze only samples of sand that contained dye. Second, the mass of each sample was measured both before and after drying in order to determine the total mass of liquid in each sample. After calculating the mass

of PCE, the mass of water was determined by difference. These modifications were made in order to obtain more realistic values of DNAPL residual saturations and to allow for comparison of DNAPL and water saturations.

6.4.2 Results and Discussion

A half dozen different spills were carried out in the small tank. This discussion will focus primarily on the results of three of these, FE-9, FE-10, and FE-11. A list of the dominant features of each of these experiments is given in Table 6.5. Briefly, FE-9 and FE-10 were the same except for the rate at which the PCE was added, and FE-10 and FE-11 were the same except for manner in which the capillary fringe was formed.

Because of the goal and the design of these experiments, the majority of the observations were made during the excavation of the tank following each spill. However, some differences were apparent even during the preliminary PCE addition and infiltration stages. The most notable difference had to do with the displacement of water from the tank during the addition of the DNAPL. In both FE-9 and FE-10, water began to be displaced from the tank almost immediately. In FE-9, in which PCE was added slowly, the water displacement rate was nearly twice the PCE addition rate. For example, after 1 hour, 20 mL of PCE had been added and 39 mL of water had been displaced. After 140 minutes the volumes of PCE and water were 45 mL and 93 mL, respectively. Although the water displacement rate in FE-10 could not

Table 6.5: A comparison of the similarities and differences between three spills carried out in the small sand tank.

	FE-9	FE-10	FE-11
Sand	Flintshot 2.8	Flintshot 2.8	Flintshot 2.8
Solvent Spill Rate	50 mL PCE Slow ~2.5 hrs	50 mL PCE Fast ~1 min	50 mL PCE Fast ~1 min
Cap. Fringe Thickness	Drainage ~18.5 cm	Drainage ~18.5 cm	Imbibition ~9.5 cm
Depth to Water Table	22.4 cm	22.2 cm	16.4 cm
Displaced Water	224 mL in 2 days	646 mL in 5 days	No water displaced
Visible PCE	Back of tank below water table; Bottom of tank	Bottom	Front and side near cap. fringe

keep up with the very rapid addition of PCE, it was still much faster than in FE-9. Within the first 8 minutes, 44 mL of water had been displaced. This volume increased to 86 mL within the first 30 minutes. The total volume of water displaced was 224 mL for FE-9 and 646 mL for FE-10. In FE-11, not only was there no immediate release of water from the tank, but no water at all was displaced during the five days between the addition of PCE and the excavation of the tank.

As discussed in Section 6.3.2, the enhanced water displacement resulted from the collapse of the capillary fringe. Considering the fact that a 1-cm thick layer of sand in the small tank would release about 500 mL of water when draining from a fully saturated state down to a residual saturation of 20%, the volumes displaced in FE-9 and FE-10 do not seem unusually large. Because FE-11 was carried out in an aquifer with an imbibition capillary fringe, it was expected that the volume of displaced water would be less than in the previous experiments. The fact that there was no water displaced at all was surprising at first. Observations made during the excavation of the tank (see below) yielded a possible explanation for this.

Prior to the excavation, the walls and the bottom of the tank were examined carefully for signs of PCE. In FE-9 and FE-10, PCE was readily visible on the bottom. In FE-9, a short, thin horizontal band of PCE was also visible from the back of the tank just below the water table. A similar band was visible from the front of the tank just below the top of the capillary fringe in FE-11. In neither case was the area of contact very large nor did the PCE appear to have moved

down along the glass after coming into contact with it. It was assumed, therefore, that the flow of DNAPL in these experiments was relatively unaffected by the walls of the tank. In FE-11, however, small droplets of PCE were seen seeping from the screen and flowing down into the water in the reservoir on one end of the tank. This was occurring just below the top of the capillary fringe. Although the loss did not appear significant, the volume of DNAPL that escaped from the sand in this manner was not known.

Careful excavation of the sand and examination of the dye showed that the DNAPL plume had a tendency to split apart and move around unpredictably in all of the three experiments. Figures 6.7, 6.8, and 6.9 each contain six drawings showing representative views of the distribution of PCE observed at various elevations above the water table in FE-9, FE-10, and FE-11, respectively. These drawings were made from photographs taken during the excavations. Each drawing covers a 25 x 30 cm area in the center of the tank. The circle shows the relative position of the 5-cm diameter depression on the surface into which the DNAPL was dispensed. The darker stippled areas represent those portions of a given layer which contained red dye. It should be noted that except for the very dry regions near the surface of the tank, the red color did not have the even appearance that is suggested by these drawings. Rather, a somewhat mottled appearance was more commonly encountered.

The distribution of PCE in FE-9 and FE-10 was very similar. At the surface, the DNAPL had spread out in a wide, nearly circular

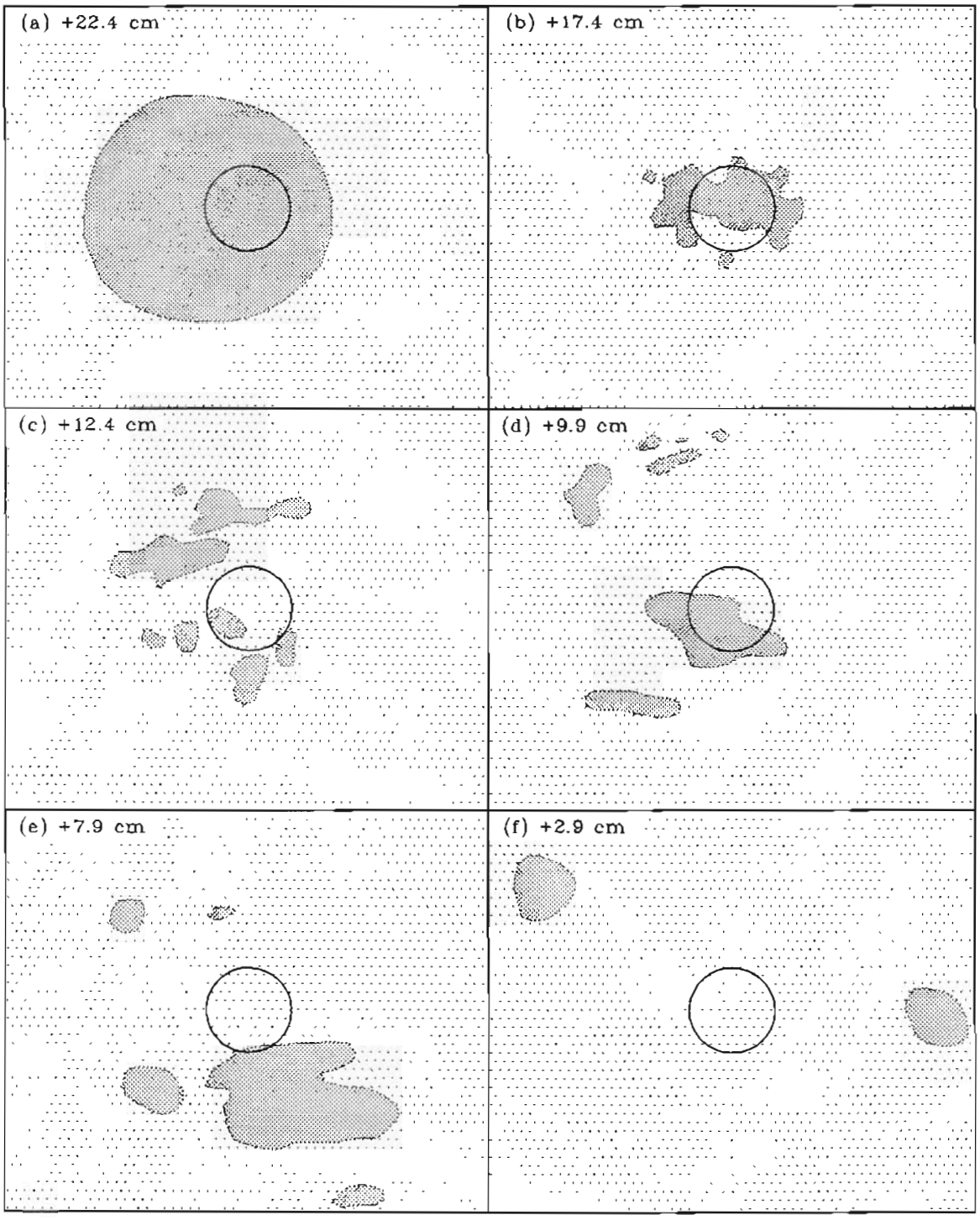

Figure 6.7: The distribution of PCE at various elevations above the water table during the excavation of the small tank following FE-9.

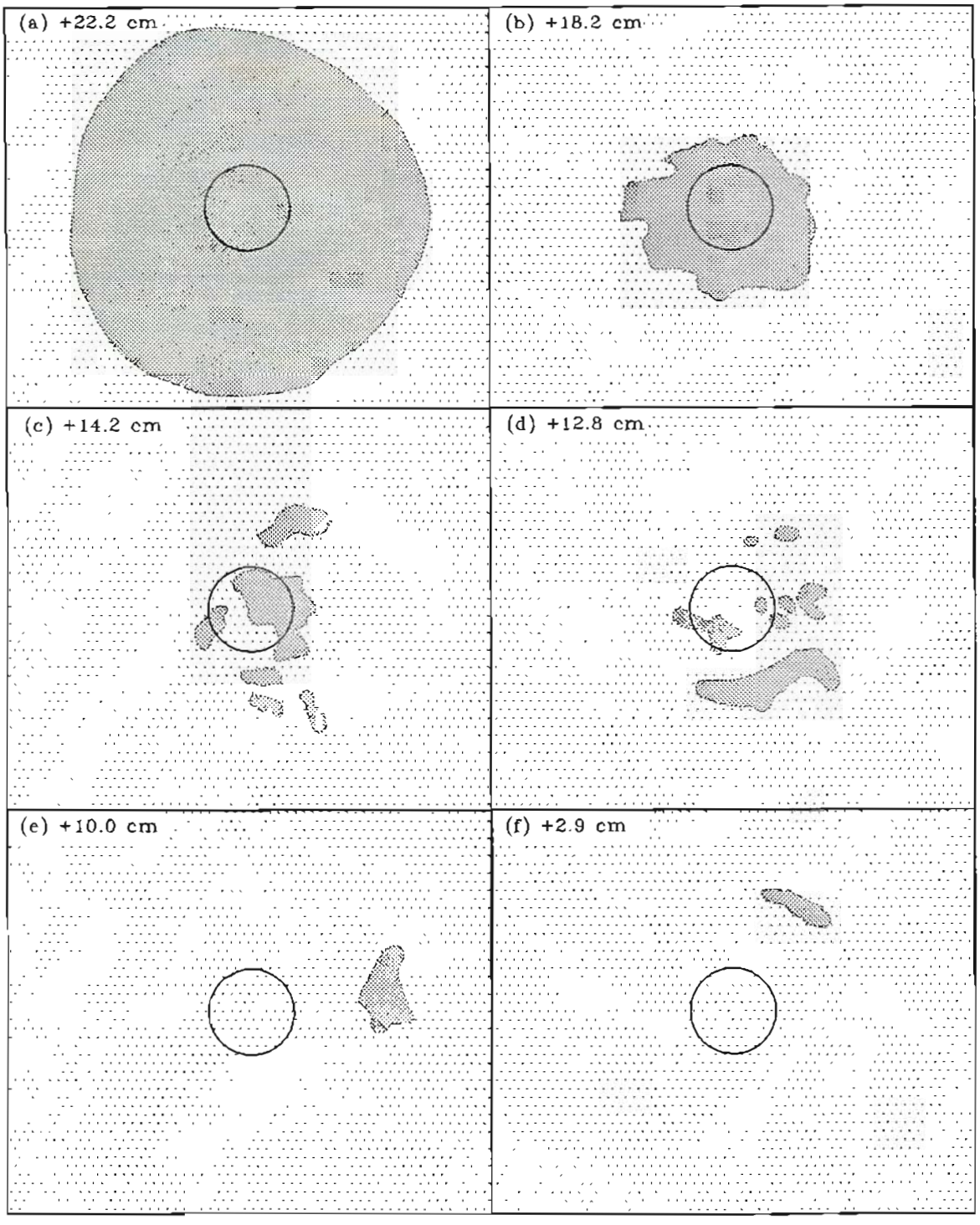

Figure 6.8: The distribution of PCE at various elevations above the water table during the excavation of the small tank following FE-10.

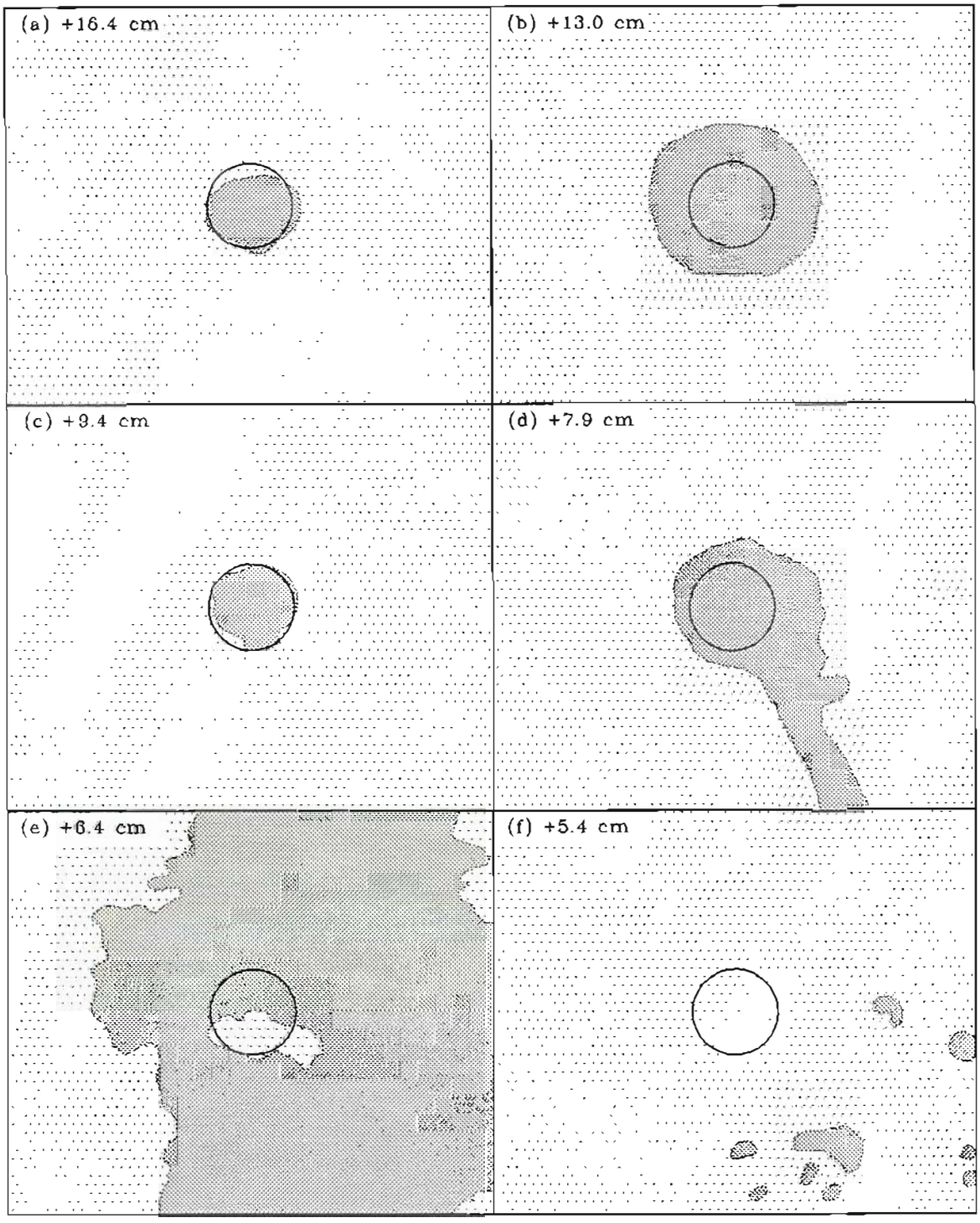

Figure 6.9: The distribution of PCE at various elevations above the water table during the excavation of the small tank following FE-11.

pattern which quickly narrowed within the first few centimeters. The more rapid spill appeared to form a broader plume in this region. Continuing down, each plume split into many small plumes, some of which began to move further from the center of the tank. It was not unusual to have plumes disappear from one location and reappear somewhere else within a depth of less than one centimeter. This seems to indicate that the generally downward migration of the PCE was actually a series of vertical and horizontal steps dictated by local heterogeneities as each small plume sought its own path of least resistance. In general, the plumes from FE-9 were more erratic and strayed further from the center of the tank than those from FE-10. This was probably due to the fact that the slower spill rate provided a smaller pressure head to the immiscible fluid and therefore made it subject to the effects of smaller permeability differences. PCE from FE-9 reached the bottom of the tank near the back left corner whereas in FE-10 it reached the bottom about midway between the center and the back.

The path followed by the PCE plume in FE-11 was very different from the two previous experiments. The plume did not spread out at the surface, but did begin to spread out within the top few centimeters. However, as the DNAPL reached the region where the sand was damp, the plume narrowed. By the time that it had encountered the top of the capillary fringe, the PCE had again spread out and covered about half of the area of the tank. It was at this elevation (+6.4 cm) that it contacted the glass at the front of the tank and also

began to seep through one of the screens. Within the next centimeter, the broad plume almost completely disappeared and only a few scattered small plumes remained (compare Figures 6.9(e) and (f)). After another one-half centimeter, all signs of these plumes had vanished; the PCE was unable to significantly penetrate the capillary fringe.

As mentioned earlier in this section, FE-11 also differed from the other two experiments in that no water was displaced from the constant-head reservoir when the PCE penetrated the sand. It was pointed out in Section 6.3.2 that water could be released from both physical displacement by the advancing DNAPL and from collapse of the capillary fringe. Since the PCE did not penetrate the saturated zone in FE-11, no water was physically displaced. The lack of a collapsing capillary fringe was probably due to the hysteretic nature of capillary pressure/saturation curves. Because of hysteresis, for any given value of capillary pressure a range of saturations are possible depending upon the wetting history of the system. The imbibition curve marks the low end of this range and the drainage curve marks the high end (Figure 6.10). If the water saturations in an air/water imbibition curve are less than or equal to those in a CHC/water drainage curve, then the addition of that CHC will not cause the imbibition capillary fringe to collapse. Since even after the capillary fringes in FE-9 and FE-10 had collapsed they were still higher than the imbibition fringe in FE-11, this seems to have been the case.

Results from the PCE-saturation analyses on samples collected

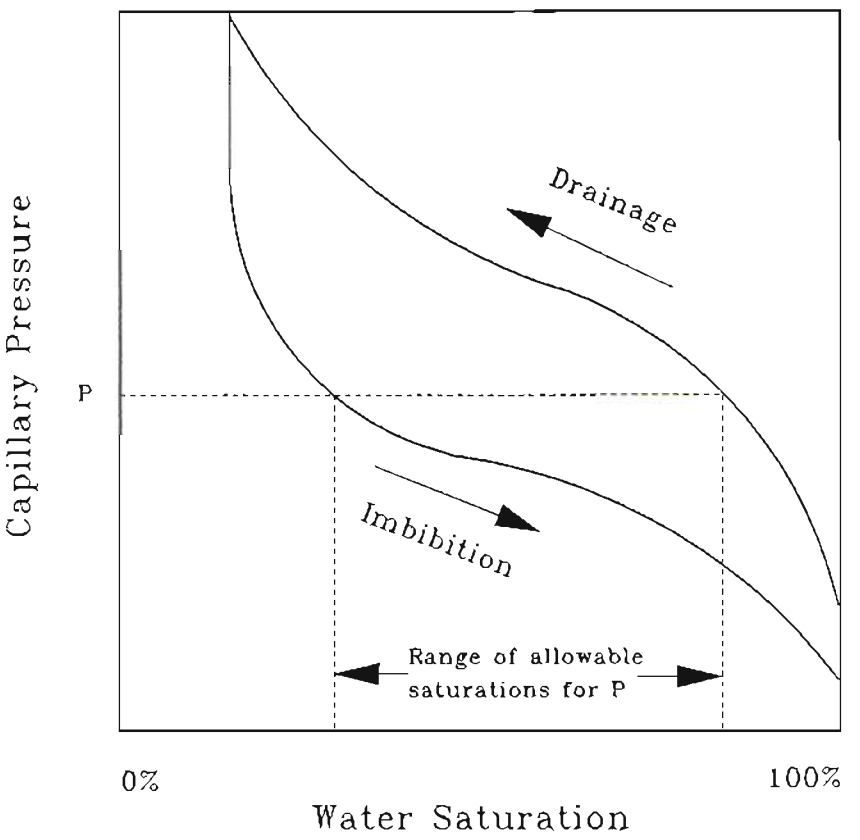

Figure 6.10: A capillary pressure-water saturation curve showing the range of water saturations possible for a given capillary pressure due to the hysteretic nature of the relationship.

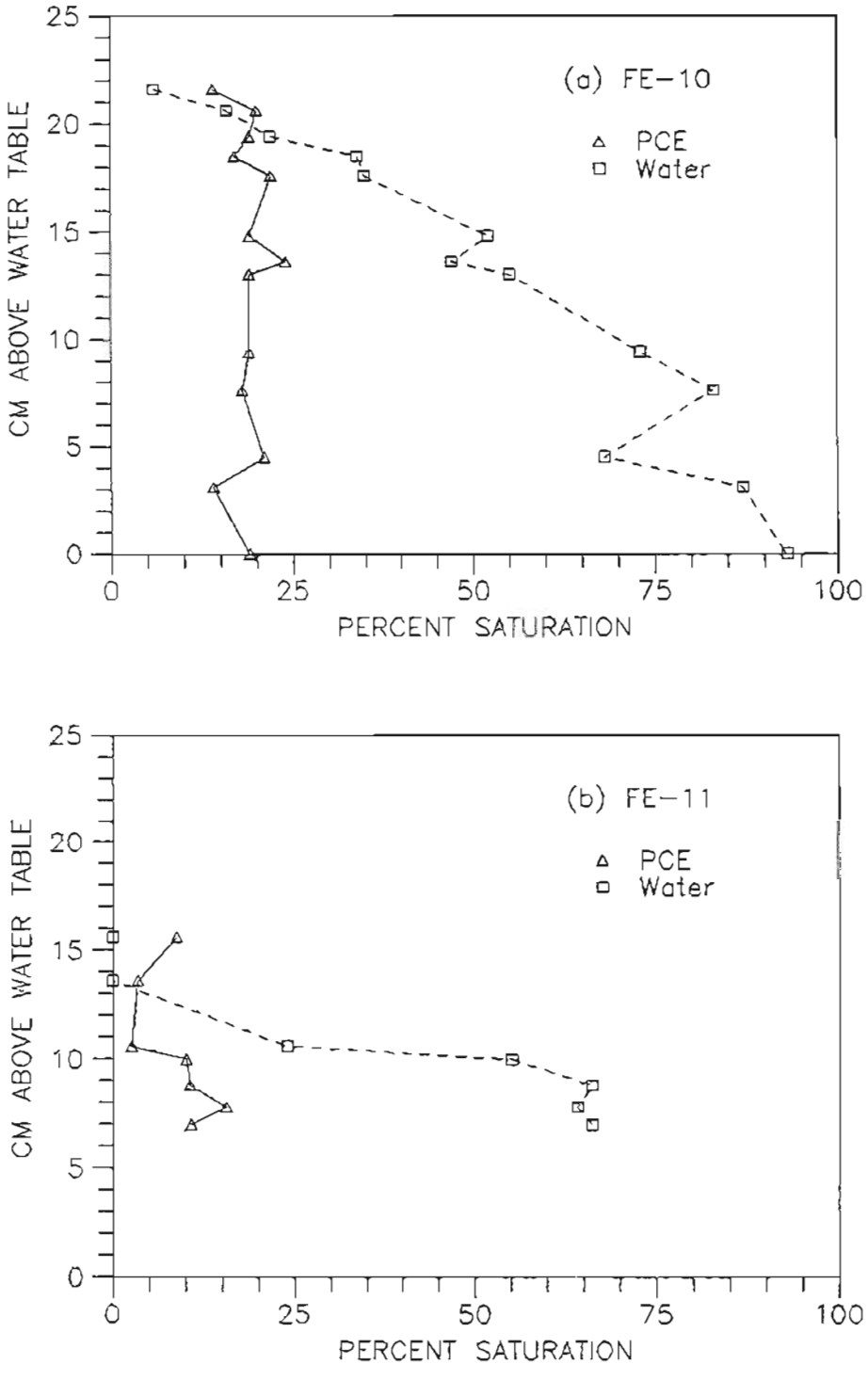

Figure 6.11: PCE and water saturations versus height above the water table following spills into model aquifers in which the capillary fringe resulted from (a) drainage, or (b) imbibition.

during the excavation of FE-10 and FE-11 are shown in Figures 6.11(a) and (b). Since the water table had to be lowered in the final stages of excavation, probably affecting the residual PCE saturations in this portion of the tank, values for FE-10 are only reported for samples collected above the original position of the water table. Surprisingly, all of the PCE saturations in FE-10 were about the same, between 15 and 20%. They remained the same even though the water saturation in the samples increased with depth from 5-90%. In FE-11, the results near the top of the tank fell below 10%. However, in the damp sand above the capillary fringe, these values increased to 15-20%. Because of the different preliminary procedures used, the sand at the top of the tank in FE-11 was the only totally dry sand in these experiments. Residual PCE saturations were apparently lower in dry sand than in damp sand. This trend differed from the one reported by Hoag and Marley (1986) for gasoline in sands. In their study, residual saturations of gasoline were less in initially water-wet sands than in the corresponding dry sands. The reason for this disagreement is not known. However, the DNAPL saturations measured in the wet sand in these two experiments were within the range reported by Wilson and Conrad (1984) for HCs.

Examination of Figures 6.11(a) and (b) also reveals a possible explanation for the inability of the PCE in FE-11 to penetrate the water table. Because of the narrower capillary fringe, the water saturation increased from 0-100% over a shorter distance in FE-11 than in FE-10. In any porous medium, as the saturation of water increases,

the permeability of the medium to a second fluid decreases. In both experiments, when the PCE encountered the zone of lower permeability, its forward motion would have slowed or stopped while pressure built up behind it from the influx of more PCE. As long as PCE was available, this build up would have continued. Eventually, either the pressure head would have become sufficient to overcome the capillary pressure barrier and the water table would have been penetrated, or the PCE would have begun to flow laterally. Because of the narrow fringe in FE-11, any PCE that built up behind the stalled infiltration front would have easily reached the region with very low water saturation. At that point, the spreading out of the PCE would have occurred rather easily.

6.5 Conclusions

The residual saturations measured for 1,1,1-TCA and PCE in these experiments agree with the range of values reported by Wilson and Conrad (1984) for HCs and by Schwille (1984) for CHCs. Residual saturations for 1,1,1-TCA in initially water-saturated sand were between 15-40%. These results were obtained by the traditional method of determining mean values for cross-sections of cores from column infiltration experiments. For PCE, residual saturations measured at a number of depths throughout the thickness of a saturated capillary fringe were between 15-25%. These values remained quite constant even though the water content of the samples increased with depth. The procedure used to obtain these data differed from previous experiments

in two important ways. First, the infiltration of PCE was allowed to take place in a tank which was large enough so that the progress of the immiscible fluid was not controlled by the walls of the tank. Second, the saturation measurements were made on small discrete samples which were collected during the excavation of the tank. When the samples were collected, only PCE containing sand was taken. The results, therefore, are probably a better indication of true residual saturations.

Observations made during the infiltration experiments bring out several important points. First, very minor differences in the characteristics of a porous medium can result in noticeable changes in the behavior of an infiltrating DNAPL. A slight reduction in the permeability due to changes in grain size or water saturation can cause a downward migrating DNAPL to flow laterally until it finds another more permeable spot through which to continue its downward progress. Under some circumstances, the fluid may continue to spread out and fail to penetrate the water table. It has already been mentioned that DNAPL infiltration fronts are inherently unstable. However, as Kueper and Frind (1988) point out, even for stable displacements, this kind of response to minor heterogeneities can result in widely scattered fingers of residual. Second, because the addition of a CHC causes a reduction in interfacial tension, the capillary fringe may collapse in front of an infiltrating DNAPL. Since permeability differences will affect the flow, this process may actually "funnel" the immiscible fluid into the capillary fringe and

aid in the eventual penetration of the water table. Finally, the walls of an experimental apparatus may have a definite effect on immiscible fluid flow. Although this effect may be minimal for coarse-grained materials, it probably becomes more important as grain size decreases. Experiments carried out in tanks like the one described in Section 6.4 can provide information about residual saturations and immiscible fluid flow without the possible interference of a wall effect.

7. MODEL STUDIES

7.1 Introduction

As mentioned in Chapter 1, in order to make the best possible predictions about a contaminant plume resulting from a DNAPL spill and aid in formulating the optimum plan for remedial action, it is vital to know the size, shape and strength of the source of contamination. Results of the dissolution experiments presented in this dissertation have provided much needed information about source strength. It has been shown that solubility-level concentrations of a DNAPL are readily reached in water flowing under typical hydraulic gradients through a region of residual DNAPL in a porous medium. The size of the observed contaminant plumes also indicated that, at least for the residual saturations used in these experiments, the flow of water was only minimally interfered with by the presence of the immiscible phase liquid.

In the DNAPL flow experiments, it was observed that even under nearly ideal conditions, the infiltration of a DNAPL into the saturated zone was very erratic and unpredictable. The immiscible fluid penetrated the water table as a number of scattered "fingers" rather than in one coherent plug. To date, however, field-scale experiments have not been conducted to expand on the results of these

studies. Therefore, the size, shape, and distribution of immiscible fingers in the saturated zone resulting from a large scale DNAPL spill is still subject to much speculation.

Although data from controlled field-scale experiments are not available, some information can be obtained from investigations of accidental DNAPL spills. Not surprisingly, these investigations have revealed a vast range of spill types and conditions. Release volumes have been estimated to be as low as 10 L at a TCE-contaminated site (Freeberg et al., 1987) to more than 20,000 L at a PCB and chlorobenzene-containing transformer oil spill site (Roberts et al., 1982). In some cases, samples collected in the field clearly show that the immiscible phase can not only easily penetrate the water table, but also flow along the surface of impermeable zones. For example, immiscible phase TCE and PCE have been found at a depth of 35 feet at the bottom of a 10 foot thick aquifer beneath an industrial site (Schmidtke et al., 1987). These DNAPLs were found in wells at this site over an irregularly shaped area that was roughly 2000 x 2000 feet. Unfortunately, descriptions of finger size and distribution are not available for known spill sites. In fact, at many spill sites, neither the volume nor the areal extent of the spill are well known and reported data may be limited to dissolved contaminant levels measured in groundwater monitoring wells.

Because of the obvious lack of information about immiscible fingers, the goal of the work presented in this chapter was to model initially-saturated contaminant plumes emanating from fingers of

residual PCE formed from a hypothetical spill. The model results were used to examine the possibility that the formation of fingers may be largely responsible for the fact that contaminant concentrations measured at spill sites are often only a few percent of their saturation values. To accomplish this, the size and distribution of the fingers were varied in an attempt to determine what conditions would be necessary to reduce contaminant concentrations to this level. Models were also used to investigate the contribution made to the contaminant plume by dissolution from horizontal pools of PCE. These pools may result when the infiltrating DNAPL spreads out on layers of lower permeability media within an aquifer or on the bottom of an aquifer.

7.2 Description of the Models

The models used in this chapter were analytical solutions to the three-dimensional advection-dispersion equation. They were adapted from equations by Sudicky (1988) for transport in an aquifer of finite thickness and infinite width. The use of analytical solutions required simplifying assumptions for the system being modeled. The main assumptions were that the source region had a regular shape and the aquifer was homogeneous and isotropic. These limitations were not considered a problem here, since the analytical solutions still allowed for an investigation of the effects on a contaminant plume of source finger size and spacing. More complicated sources such as multiple fingers or fingers and pools were handled by treating the

source as a number of individual simple sources, solving for the contribution from each part of the source separately, and using superposition to generate the final mathematical solution. Because of the limitations on the models, however, the results in this chapter should be considered "worst case" (i.e., highest concentration) scenarios. Heterogeneities likely to be found in real aquifers would probably only serve to make contaminant levels found in the field lower than what was predicted by these models.

Two computer models were used to generate the data presented in this chapter. Under the conditions described by the first model, clean water flowing through a parallelepiped residual zone was assumed to emerge with a contaminant concentration equal to the solubility of the DNAPL. For the purposes of this chapter, all residual zones modeled in this way will be referred to as "fingers" regardless of the dimensions of the zone. This model is illustrated in Figure 7.1. The analytical solution for this case as well as the definitions of the variables are also given in this figure. The computer program written for this model employed Gaussian quadrature for the solution of the integral expression. Since discussion will be limited to concentrations found in established plumes rather than in the breakthrough of new plumes, all of the calculations were made using times that were long enough to produce steady-state plumes within the range of distances being modeled. Mass balance calculations were also employed to provide information about the lifetimes of the fingers in the aquifer.

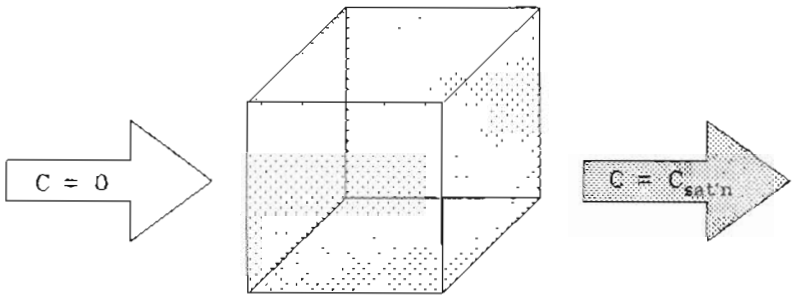

$$C(x,y,z,t) =$$

$$\frac{M_v}{4\,n\,L}\int_0^t \left[\operatorname{erfc}\left\{\frac{x - x_2 - vt'}{2\sqrt{D_x\,t'}}\right\} - \operatorname{erfc}\left\{\frac{x - x_1 - vt'}{2\sqrt{D_x\,t'}}\right\}\right]$$

$$\cdot\left[\operatorname{erfc}\left\{\frac{y - y_0}{2\sqrt{D_y\,t'}}\right\} - \operatorname{erfc}\left\{\frac{y + y_0}{2\sqrt{D_y\,t'}}\right\}\right] \cdot \left[\frac{z_2 - z_1}{L} +\right.$$

$$\left.\frac{2}{\pi}\sum_{k=1}^{\infty}\frac{1}{k}\cos\left(\frac{k\pi z}{L}\right)\left\{\sin\left(\frac{k\pi z_2}{L}\right) - \sin\left(\frac{k\pi z_1}{L}\right)\right\}\exp\left\{\frac{-k^2\pi^2 D_z\,t'}{L^2}\right\}\right]\,dt'$$

where ...

v = mean groundwater velocity
n = porosity
L = thickness of aquifer
M_v = volumetric mass transfer coefficient ($M/L^3\,T$)
x_1 = upstream x-coordinate of the source
x_2 = downstream x-coordinate of the source
y_0 = half-width of the source
z_1 = upper z-coordinate of the source (from top of aquifer)
z_2 = lower z-coordinate of the source (from top of aquifer)
D_x = coefficient of longitudinal dispersion
D_y = coefficient of transverse-horizontal dispersion
D_z = coefficient of transverse-vertical dispersion

Figure 7.1: Analytical solution to the three-dimensional advection-dispersion equation for solute transport from a zone of residual.

In order to generate an initial concentration equal to the solubility of the compound regardless of the size of the residual zone, the volumetric mass transfer coefficient (M_v) in Model 1 was calculated from the aqueous solubility (C_s) using the equation

$$M_v = C_s \, n \, \tilde{v} \, / \, (x_2 - x_1) \qquad (7.1)$$

where $(x_2 - x_1)$ was the dimension of the source in the direction of flow. The value of C_s was set equal to 200 ppm, the aqueous solubility of PCE at 20 ^{o}C.

In the situation described by the second model, contaminants were dissolved from a thin horizontal pool of DNAPL by water flowing over the pool. An illustration of this is given in Figure 7.2 along with the analytical solution for this case. In this model, the thickness of the pool was assumed to be insignificant relative to the thickness of the aquifer. Therefore, only one z-coordinate was necessary to define the depth of the pool. As in Model 1, Gaussian quadrature was employed for the solution of the integral expression and calculations were made only for steady-state plumes. Unlike the first model, however, it was not assumed that contaminant concentrations would necessarily reach solubility levels in the water flowing over a pool. This was because dissolution in Model 2 was restricted to the water/DNAPL pool interface where it is less efficient than dissolution from small droplets of residual which have a large surface area/volume ratio. Under these circumstances, mass transfer is strongly affected by the velocity of the water and the size of the pool.

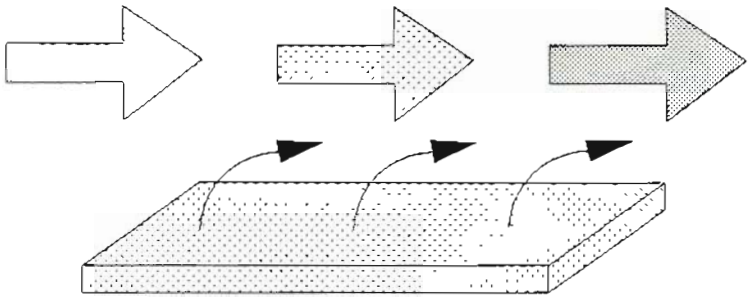

$$C(x,y,z,t) =$$

$$\frac{M_a}{4\,n\,L}\int_0^t \left[\operatorname{erfc}\left\{\frac{x - x_2 - vt'}{2\sqrt{D_x\,t'}}\right\} - \operatorname{erfc}\left\{\frac{x - x_1 - vt'}{2\sqrt{D_x\,t'}}\right\}\right]$$

$$\cdot \left[\operatorname{erfc}\left\{\frac{y - y_0}{2\sqrt{D_y\,t'}}\right\} - \operatorname{erfc}\left\{\frac{y + y_0}{2\sqrt{D_y\,t'}}\right\}\right]$$

$$\cdot \left[1 + 2\sum_{k=1}^{\infty}\cos\left(\frac{k\pi z}{L}\right)\cos\left(\frac{k\pi z_0}{L}\right)\exp\left\{\frac{-k^2\pi^2 D_z\,t'}{L^2}\right\}\right] dt'$$

where...

M_a = surface mass-transfer coefficient ($M/L^2\,T$)
z_0 = depth of horizontal pool from top of the aquifer

and all other variables are defined as in Figure 7.1.

Figure 7.2: Analytical solution to the three-dimensional advection-dispersion equation for solute transport from a thin pool of DNAPL.

Since data were not available for the surface mass-transfer coefficient (M_a) required for PCE in Model 2, a value was estimated from the data for TCE obtained by Schwille (1988) using a 150 cm long by 50 cm wide by 25 cm deep sand box. These data are listed in Table 7.1 along with similar data for 1,1,1-TCA. The values listed for both compounds are averages measured at each specified velocity. The experimental velocities were all higher than the 30 cm/day value modeled here. The data for TCE was considered more dependable since Schwille (1988) indicated that "substantial fluctuations" were observed in the 1,1,1-TCA data which were not observed in the TCE data. Extrapolation of the data resulted in an estimate for M_a of about 2 $g/m^2/day$.

Although Model 2 treats the value of M_a as a constant, the fact that the mass transfer is controlled by diffusion indicates that M_a is not a constant in a real system. Since diffusion is affected by concentration gradients, the rate should actually be larger on the upgradient end of the pool where clean water flows over the DNAPL than on the downgradient end where the overlying water already contains a certain amount of solute. However, given the lack of data on mass transfer from pools to flowing groundwater, using the average value given above was considered sufficient for estimates to be arrived at by the computer simulations in this chapter.

For the purposes of this study, all fingers and pools were assumed to have square cross-sections that were centered on the y-axis. In a real case, obviously, infiltration is likely to occur in

Table 7.1: Surface mass-transfer coefficients (M_a) for 1,1,1-TCA and TCE measured in a 150 cm long by 50 cm wide by 25 cm deep sand box (Schwille, 1988).

Compound	Experiment Number	Water Velocity (m/day)	M_a ($g/m^2/day$)
TCE	1	0.45	2.9
	6	0.9	4.3
	2	0.9	5.6
	3,4	1.8	9.3
	5	2.7	14.8
1,1,1-TCA	3	0.7	8.1
	1	2.0	12.8
	2	6.7	40.1

all directions around the origin of a spill. In the resulting mixed plume, however, slightly higher concentrations from fingers located downgradient from the origin will be offset by slightly lower concentrations from fingers located upgradient from the origin. Also, since the flow of water, and hence the predominant spread of contaminants was in the x-direction, small shifts of the plume in the x-direction do not make significant changes in the concentration at a given point. Therefore, confining the fingers and pools to the y-axis was not thought to be an overly restrictive simplifying assumption.

Retardation and biodegradation were not considered in the modeled contaminant plumes. Retardation would only increase the time required for the formation of the steady-state plume but would not affect the contaminant levels in that plume. Biodegradation, of course, would contribute to a further reduction in contaminant levels.

7.3 Hypothetical DNAPL Spills

For the model studies, groundwater contamination resulting from a hypothetical release of PCE was considered. It was assumed that the volume of PCE lost was sufficient to allow a total of 1000 L of the DNAPL to penetrate an aquifer that was 15 m thick. The porosity of the aquifer was 0.35 and the mean water velocity was 30 cm/day. The immobile PCE in the aquifer had a residual saturation of 15%. The source of all groundwater contamination was restricted to the DNAPL in the aquifer. Transport to or from the vadose zone was not considered. Preliminary simulations were conducted assuming that all 1000 L of PCE

entered the aquifer as a single finger. Subsequent simulations introduced a pool of DNAPL and then investigated contaminant plumes from multiple fingers or finger and pool combinations.

7.3.1 Single Fingers and Pools

7.3.1.1 Case A

For the initial set of model simulations, the 1000 L of PCE was considered to have entered the aquifer in a 5 m x 5 m area and to have penetrated as far as possible until it was immobilized at a residual saturation of 15%. The depth attainable under these conditions was only 0.76 m (Figure 7.3). For any given source, the parameters that control the shape of the resulting three-dimensional contaminant plume are the longitudinal dispersivity (α_x), the transverse horizontal dispersivity (α_y), and the transverse vertical dispersivity (α_z). (The relationship between the dispersivity and the coefficient of dispersion has been discussed in Section 4.2.2.) The steady-state concentration contours shown in Figure 7.4(a) were calculated using Model 1 with α_x = 1.0 m, α_y = 0.1 m and α_z = 0.01 m. These numbers are on the low end of the range of values for typical field scale dispersivities (Anderson, 1979) and should therefore provide a conservative estimate for the degree of spreading taking place in the contaminant plume for Case A.

Because the concentrations shown in Figure 7.4(a) are for a steady-state plume, they will not be affected by the magnitude of α_x. However, changes in α_y or α_z will result in changes in the plume. In

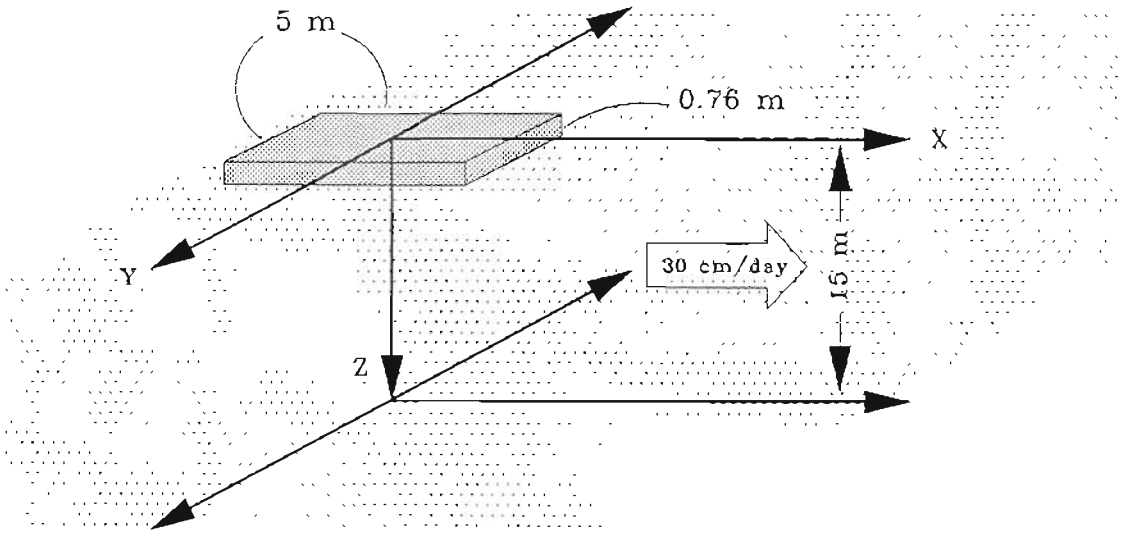

Figure 7.3: Sketch of the contaminant source for Case A. 1000 L of PCE at a residual saturation of 15% occupy a 5 m x 5 m x 0.76 m volume at the top of a 15 m deep aquifer.

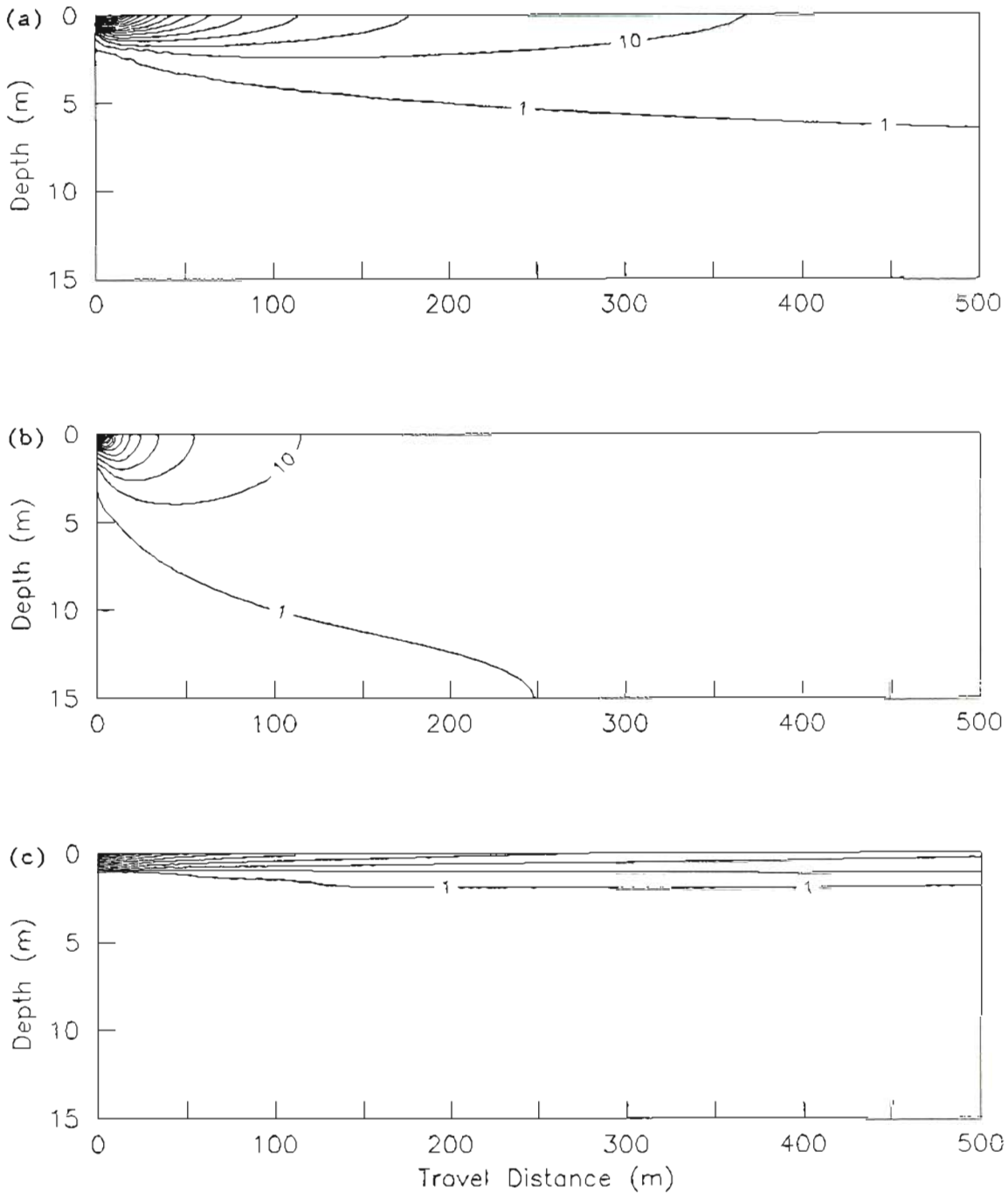

Figure 7.4: PCE concentrations (ppm) in the center of the plume (y = 0) for Case A showing the effect of changing the value of α_z. (a) α_z = 0.01 m, (b) α_z = 0.1 m, (c) α_z = 0 m. In all three plots α_x = 1.0 m and α_y = 0.1 m. Vertical exaggeration = 10x.

Figure 7.4(b), α_z was increased to 0.1 m. Because of the increased vertical spreading, the concentration in the center of the plume at a distance of 500 m dropped from 7.4 ppm to 2.4 ppm. On the other hand, Figure 7.4(c) shows the contaminant plume for Case A with $\alpha_z = 0$. Under these circumstances all of the spreading in the vertical direction can be attributed to the effects of molecular diffusion. The number used for the coefficient of molecular diffusion for PCE in this case was 4.3×10^{-6} cm^2/s (i.e, the value obtained in the diffusion experiment presented in Section 4.5). With $\alpha_z = 0$, the concentration in the center of the plume at 500 m increased to 38.2 ppm. These changes are further illustrated in Figures 7.5(a)-(c) which show cross-sections of the three plumes at x = 500 m.

Figures 7.6(a)-(c) illustrate the effect on the contaminant plume of changes in α_y. Figure 7.6(a) shows a plan view of the Case A plume at the surface of the aquifer with the same values of dispersivity as were used in Figures 7.4(a) and 7.5(a). Figure 7.6(b) shows the enhanced broadening that occurred when α_y was increased from 0.1 m to 1.0 m. Just as in the case of the tenfold increase in α_z discussed above, this change also caused the concentration in the center of the plume at a distance of 500 m to drop from 7.4 ppm to 2.4 ppm. Likewise, when α_y was reduced to 0 so that horizontal spreading was controlled solely by diffusion, the concentration at this point increased again, this time to 37.7 ppm.

Although contour plots such as those just discussed provide a good visual representation for the size and shape of plumes, an

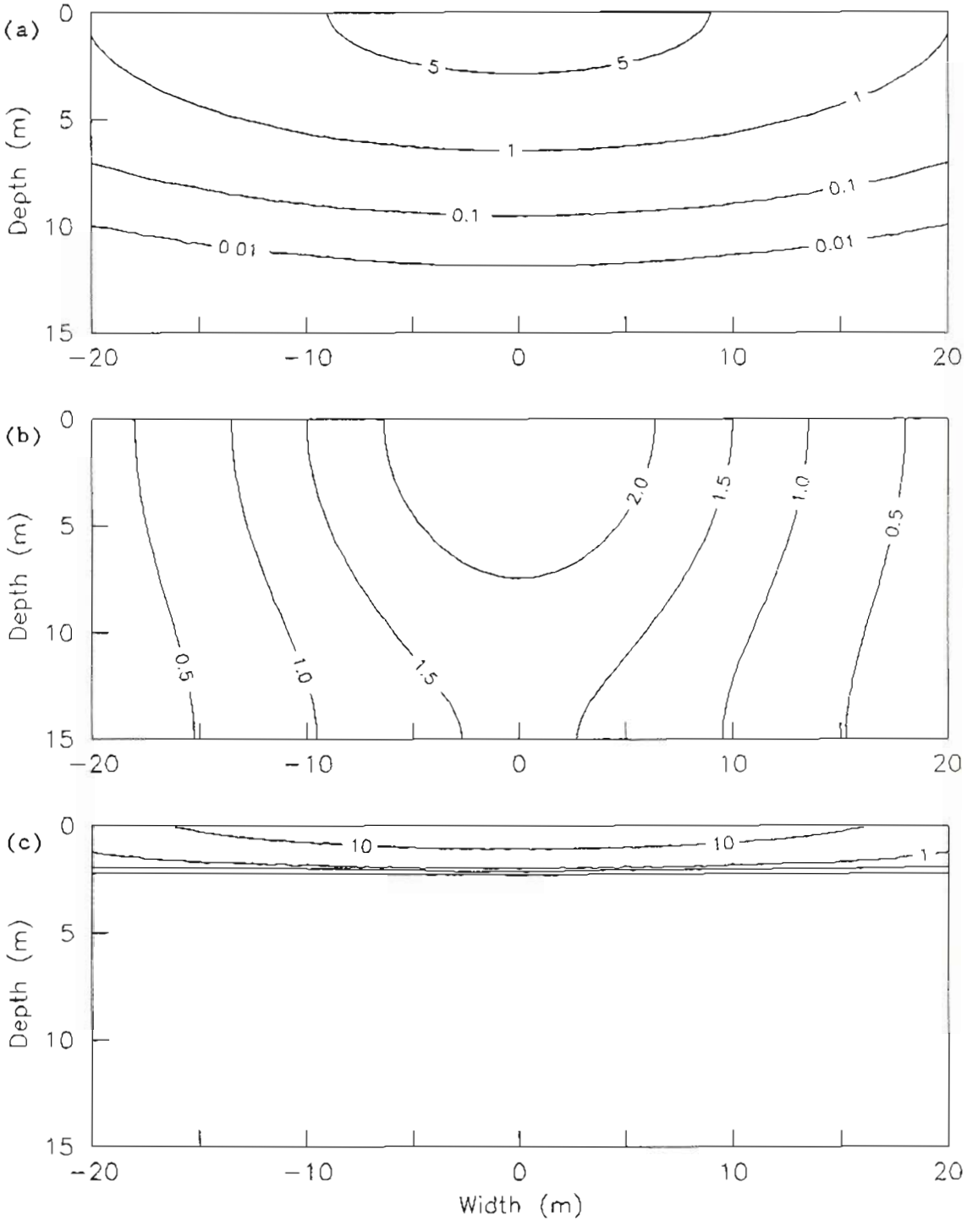

Figure 7.5: PCE concentrations (ppm) in the yz-plane across the plume at a distance of 500 m for Case A. Dispersivities are the same as in the corresponding plots in Figure 7.4.

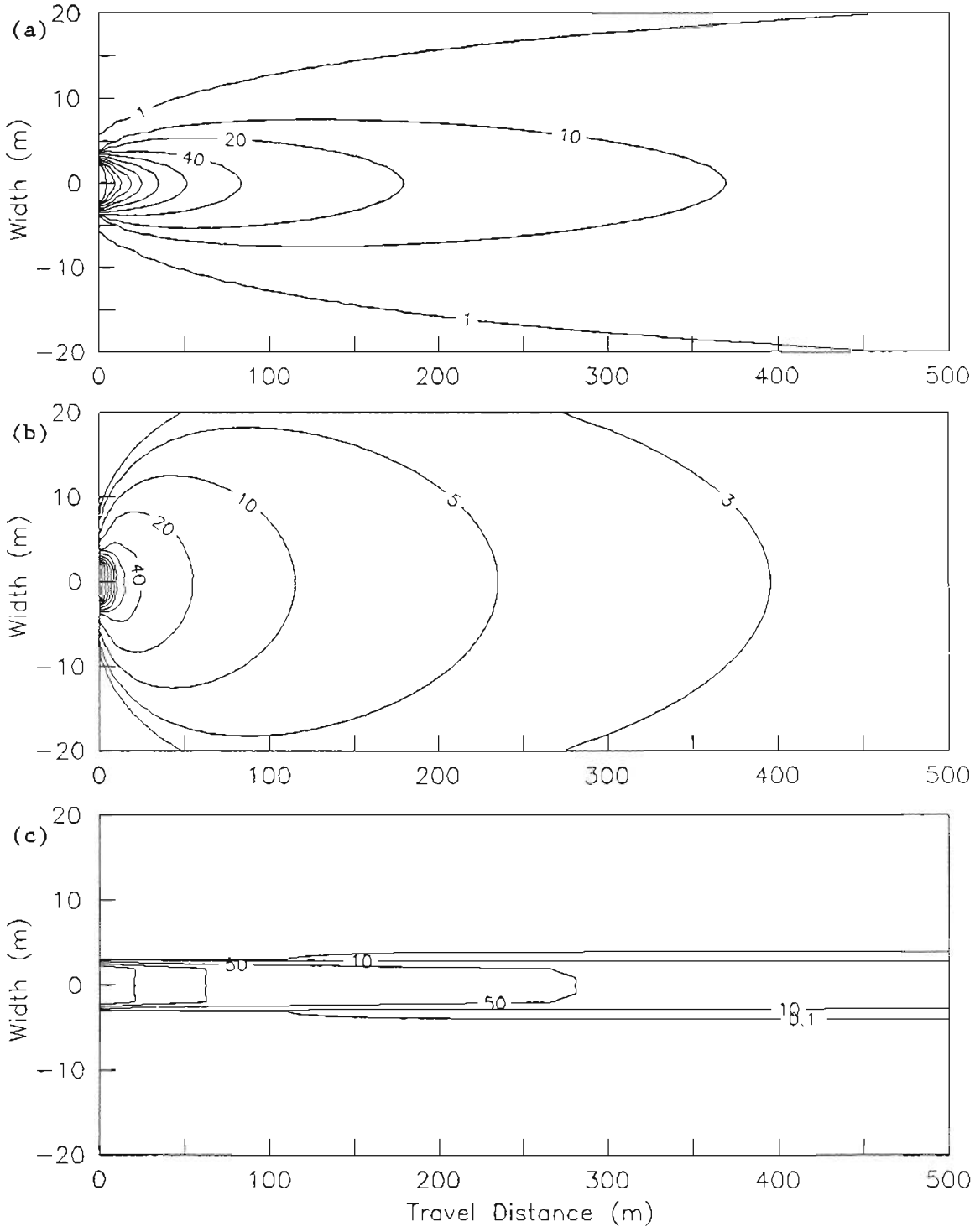

Figure 7.6: PCE concentrations (ppm) in the xy-plane at the surface of the aquifer for Case A showing the effect of changing the value of α_y. (a) α_y = 0.1 m, (b) α_y = 1.0 m, (c) α_y = 0 m. In all three plots α_x = 1.0 m and α_z = 0.01 m. Horizontal exaggeration = 5x.

important matter to be addressed is the level of contamination that may be encountered in sampling wells installed at a spill site. After all, a sample is not made up of water collected at a specific "point". Rather, it is a mixture of water that represents an average value over a volume that is determined by both the diameter and the screened interval of the well. For example, assume that six sampling wells were installed at the Case A spill site. The first three wells were located on the center of the plume at distances of 100 m, 250 m, and 500 m downgradient from the origin of the spill. The last three wells were located at the same distances but were offset 5 m from the center of the plume. Each well was assumed to have been constructed with three, 2-meter sampling intervals, one in the top 2 meters, one in the middle 2 meters, and one in the bottom 2 meters. The water sampled from each of the intervals was assumed to contain a contaminant concentration equal to the average value over that screened interval. Table 7.2 lists the concentrations that would be found in each of these eighteen sampling intervals. It is important to note from this data that for a source of this type, depth is the most critical factor controlling the level of contamination in that sample. Distance from the center of the plume also affects the solute concentration.

Further examination of the data reveals an interesting point. In water collected from the middle or lower level sampling intervals, the concentrations actually increase with increasing distance from the source. This is because these sampling intervals do not lie in the "shadow" of the source. Contaminants will reach any point in the

Table 7.2: Concentrations in hypothetical sampling wells located at the Case A spill site.

Well Location [(x,y) m]	Screened Interval (depth, m)	Concentration (ppm)
100, 0	0 - 2	25.2
	6.5 - 8.5	0.001
	13 - 15	0.0
250, 0	0 - 2	12.6
	6.5 - 8.5	0.12
	13 - 15	0.0
500, 0	0 - 2	6.9
	6.5 - 8.5	0.56
	13 - 15	0.001
100, 5	0 - 2	14.3
	6.5 - 8.5	0.001
	13 - 15	0.0
250, 5	0 - 2	9.9
	6.5 - 8.5	0.09
	13 - 15	0.0
500, 5	0 - 2	6.1
	6.5 - 8.5	0.50
	13 - 15	0.001

shadow of the source by means of advection. As the plume moves to greater distances, dispersion results in an increased loss of mass from this zone and concentrations drop off as expected. However, contaminants can only reach points outside the shadow of the source by means of dispersion. Since dispersion increases with travel distance, concentrations will initially increase with travel distance for points located at a given distance outside of the shadow of the source. Exactly how far downgradient this increase will continue depends upon the width of the source. It will not continue indefinitely, of course, since eventually the fixed amount of contaminant mass in a given cross-section of the plume will spread out sufficiently so that concentrations will decrease all across the plume. Although the increase in concentration with distance from the source is not a surprising result and is obvious from Figure 7.4(a), it is easy to imagine that a trend of increasing concentration with increasing distance from the source at a real field site might make one wonder about the reliability of the data or the location of the source.

Given sufficient information about the local hydrology and the location of the spill to allow reasonable positioning of sampling wells, the data for Case A indicate that it should not be difficult to obtain samples which contain relatively high (i.e., greater than 1% of C_s) concentrations of PCE. Obviously, the closer that the well is to both the source and the center of the plume, the higher the concentration will be in the samples. In some situations, conditions may not allow sampling wells to be placed close to the spill site.

For example, a building may be in the way or a landowner may not allow a well to be installed on his/her property. However, for the rest of the spill scenarios presented in this chapter, it will be assumed that the area of study will be within 100 m of the spill. As in Case A, data will be presented both as concentration contour plots and as mean values that might be obtained in typical sampling wells. In all cases, the dispersivities will remain α_x = 1.0 m, α_y = 0.1 m and α_z = 0.01 m.

7.3.1.2 Cases B and C

For the second simulation (Case B), the 1000 L of PCE was assumed to have formed a finger that penetrated all the way to the bottom of the aquifer, but did not spread out on the aquitard. With a 15% residual saturation, this resulted in a finger with a square cross-section that was 1.1 m on each side (Figure 7.7). Because the residual was spread throughout the thickness of the aquifer, the contaminant concentrations were not a function of depth (Figure 7.8(a)). Since the source was narrower than in Case A, the concentrations dropped off more rapidly than in the previous example (Figure 7.8(b)). The concentration in the center of the plume at 100 m was 19.5 ppm compared to 34.4 ppm in Case A.

The situation where a narrow finger made its way through the aquifer and then spread out to form a pool of DNAPL on the impermeable layer is illustrated in Case C (Figure 7.7). In this example, the finger was 20 cm square and the pool was 10 m square. Under these

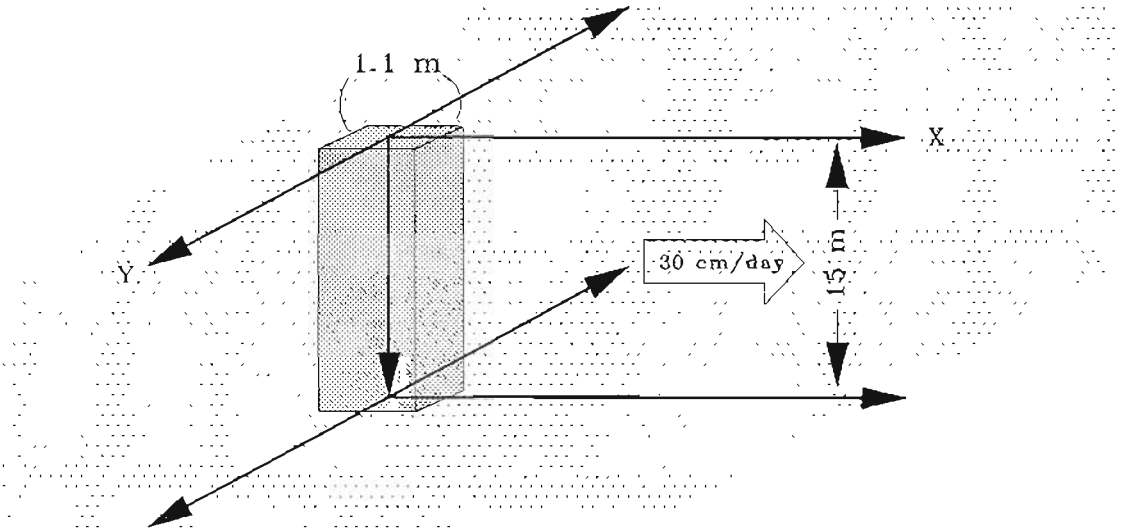

Case B

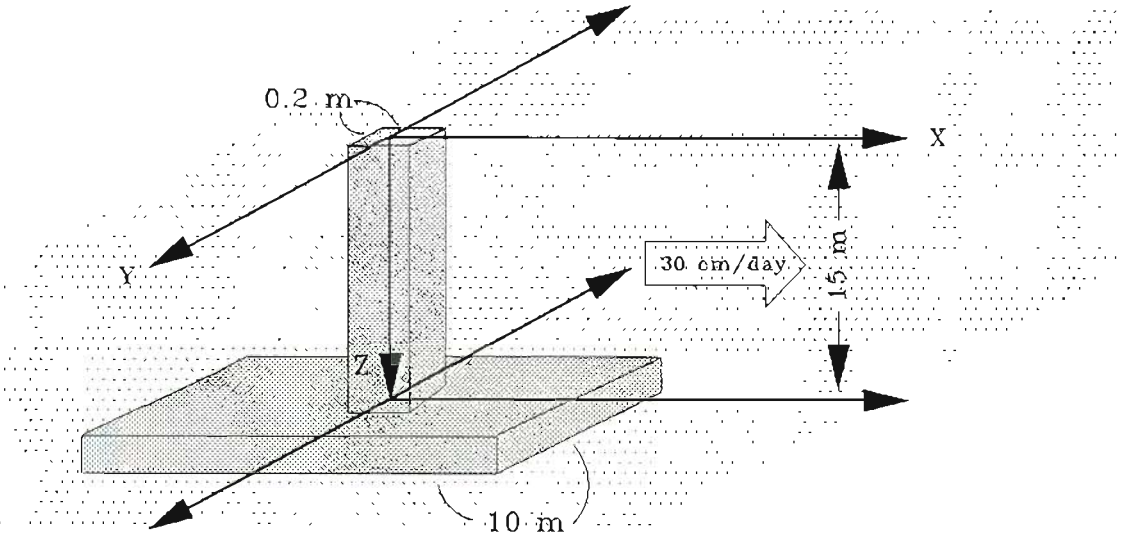

Case C

Figure 7.7: Sketch of the contaminant sources for Cases B and C.

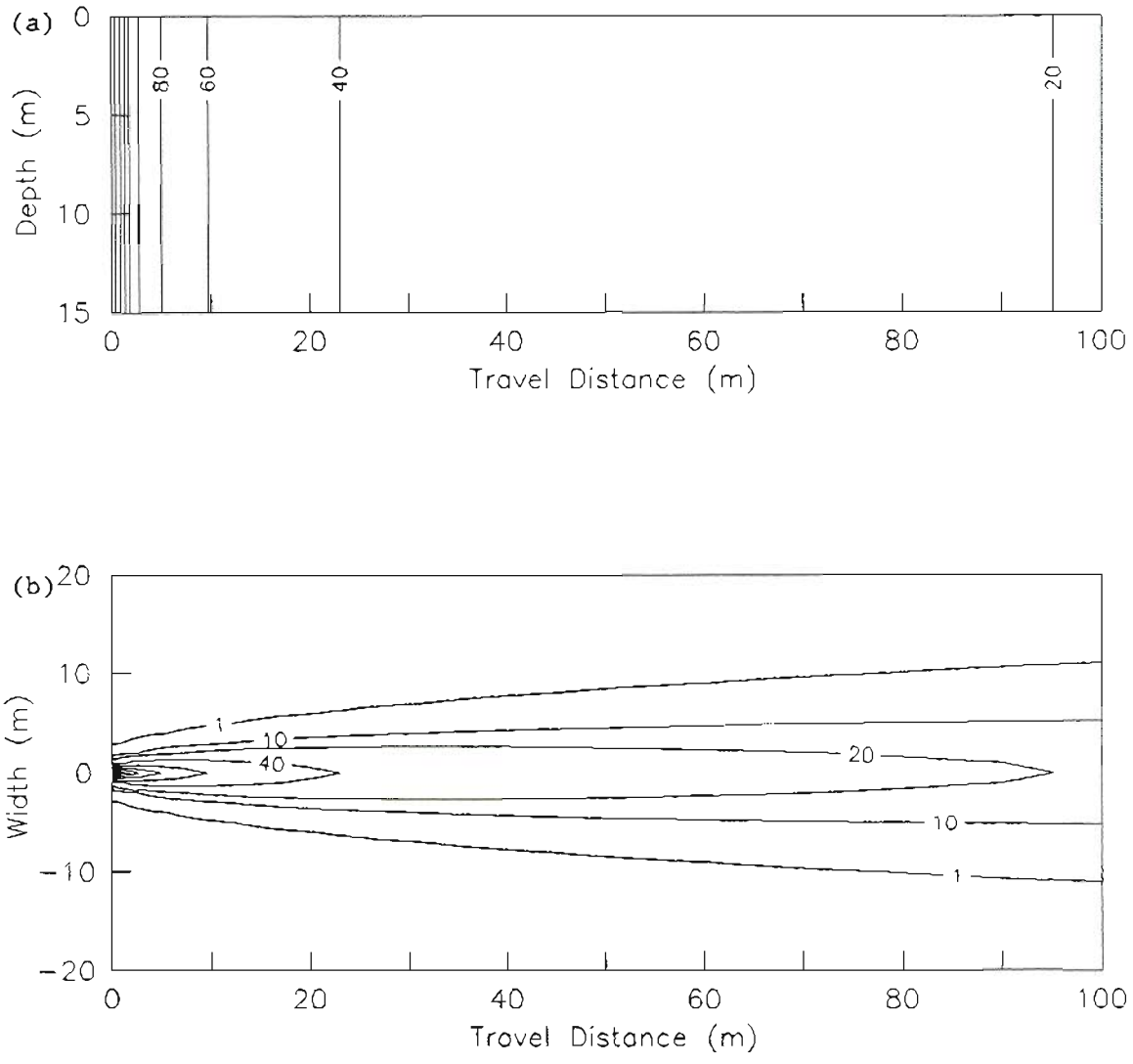

Figure 7.8: PCE concentrations (ppm) for Case B as viewed both (a) down the center of the plume and (b) across the plume.

circumstances, contaminant levels were low and constant with depth throughout the top two-thirds of the aquifer. Near the bottom, of course, concentrations rapidly increased due to the influence of dissolution from the pool (Figure 7.9).

Examination of the hypothetical sampling well data for Cases B and C (Table 7.3) reveals some similarities and some differences compared to the trends observed for Case A. As mentioned above, the concentrations for Case B were not a function of depth. However, values did decrease with travel distance along the center of the plume and increase with distance along a line 5 m from the center of the plume. The different source configuration for the Case C spill resulted in noticeable differences in the sampling well data. The influence of the pool resulted, of course, in significantly higher concentrations at the bottom of the aquifer. It also resulted in a reversal of the concentration trend found in the wells that were located 5 m from the center of the plume. In these wells contaminant levels increased with distance in the upper two sampling intervals, but then decreased with distance in the lower interval. This was due to that fact that the pool extended out to a distance of 5 m from the center of the spill. Therefore, the lowest sampling interval was still located within the shadow of the source whereas the upper two intervals were not.

In the investigation of groundwater contamination problems resulting from DNAPL spills, the number of sampling wells that are installed are certainly limited by financial considerations. It is

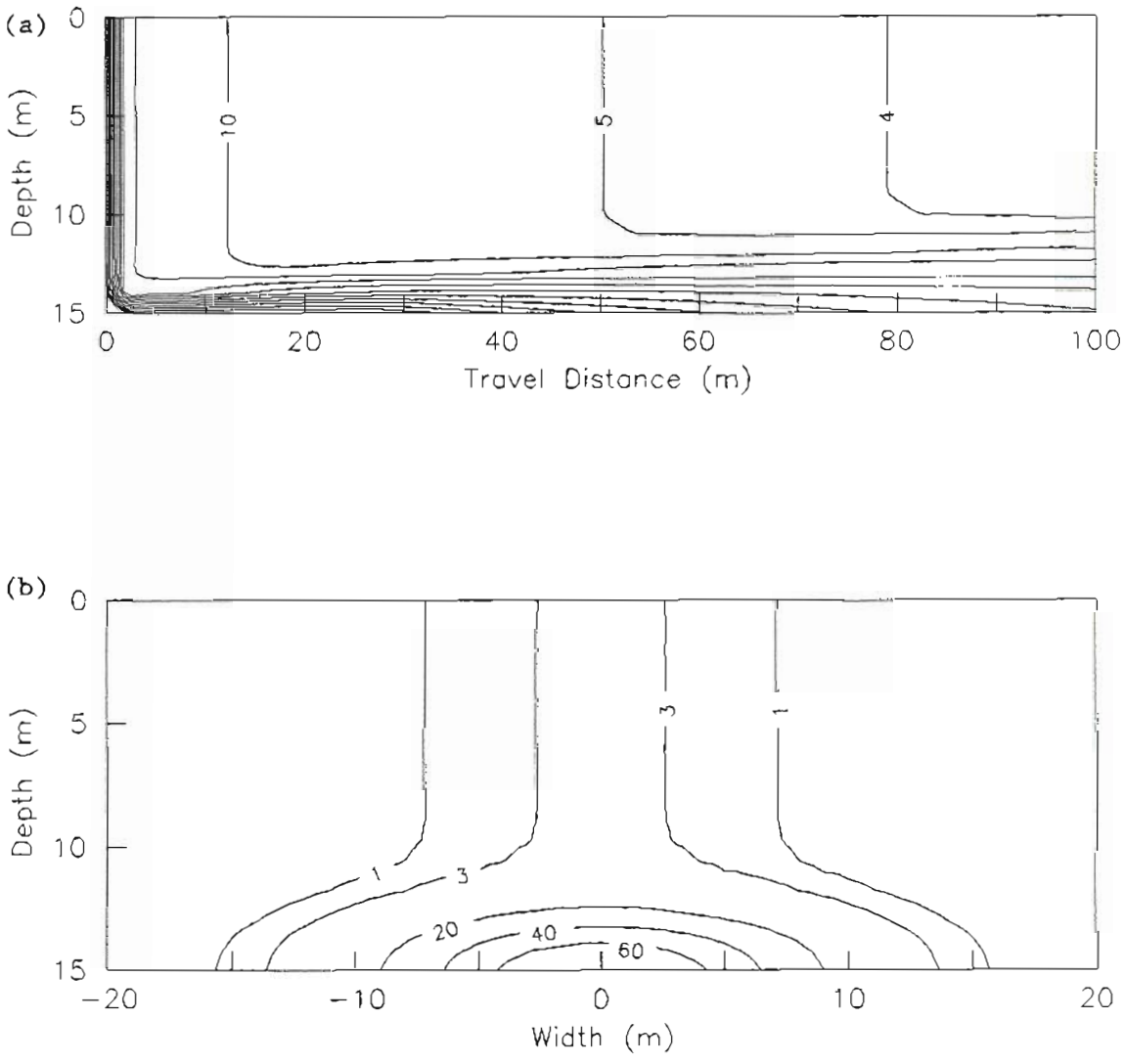

Figure 7.9: PCE concentrations (ppm) for Case C as viewed both (a) down the center of the plume and (b) perpendicular to the plume at a distance of 100 m.

Table 7.3: Concentrations in hypothetical sampling wells located at the Case B and Case C spill sites.

Well Location [(x,y) m]	Screened Interval (depth, m)	Concentration (ppm)	
		Case B	Case C
20, 0	0 - 2	42.8	7.9
	6.5 - 8.5	42.8	7.9
	13 - 15	42.8	98.0
50, 0	0 - 2	27.5	5.0
	6.5 - 8.5	27.5	5.0
	13 - 15	27.5	82.4
100, 0	0 - 2	19.5	3.6
	6.5 - 8.5	19.5	3.6
	13 - 15	19.5	59.7
20, 5	0 - 2	2.6	0.45
	6.5 - 8.5	2.6	0.45
	13 - 15	2.6	52.1
50, 5	0 - 2	8.0	1.4
	6.5 - 8.5	8.0	1.4
	13 - 15	8.0	45.2
100, 5	0 - 2	10.5	1.9
	6.5 - 8.5	10.5	1.9
	13 - 15	10.5	39.1

also true to say that this number is almost always less than that desired by those who are responsible for analyzing the data and planning the remedial action. However, the sampling well data for the hypothetical spills discussed above makes an important point about the strategy of spill investigations. That is, information gathered at several discrete depths within a given well by means of a true multilevel sampling device may be just as important as the information gathered from several wells. Indeed, vertical concentration profiles led Reinhard et al. (1984) to conclude that an accumulation of DNAPLs was located beneath a leachate plume originating in a sanitary landfill. In cases where significant differences exist in the transmissivity of adjacent water bearing zones, depth resolved wells have been shown to lead to improvements not only in the reliability of contaminant level data, but also in the hydrologic data (McIlvride and Rector, (1988)). Therefore, installation of depth-resolved sampling devices should certainly always be considered as a possible option for improving site investigation results.

7.3.1.3 Source Removal Times

The relatively high concentrations found in the contaminant plumes for Cases A, B, and C might lead one to conclude that the residual DNAPL would be rapidly removed by the groundwater. This is not the case, however. Although the concentrations may be very high relative to current drinking water standards (see Table 1.2), they are still low on an absolute scale. Since it is assumed that all water

flowing through a residual finger attains solubility-level concentrations of DNAPL, the removal time of a finger (t_f) can be calculated from the equation

$$t_f = M_f / n A_f \bar{v} C_s \quad (7.2)$$

where M_f is the total mass of residual DNAPL in the finger and A_f is the cross-sectional area of the finger perpendicular to the groundwater flow. The removal time of a pool of DNAPL (t_p) can be calculated from the equation

$$t_p = M_p / A_p M_a \quad (7.3)$$

where M_p is the mass of DNAPL in the pool, A_p is the surface area of the pool and M_a is the areal mass-transfer coefficient from the pool to the groundwater. Removal times calculated by these equations should only be considered lower limits since mass transfer may become less efficient in the latter stages of finger or pool dissolution. Sufficient experimental data on DNAPL dissolution is not available to indicate to what extent this may affect the times.

Because the residual zone in Case A had a small cross-sectional area perpendicular to the groundwater flow, the removal time calculated from Equation 7.2 was relatively long; in this case, 55.6 years. Since the area in Case B was over four times larger than in Case A, the estimated removal time of this finger was only 12.8 years. In Case C, the area of the finger was smaller, but so was the total mass of PCE in the finger. For Case C the finger removal time was

2.2 years. But, the most important characteristic of the Case C spill with regards to its removal time was the formation of the pool on the aquitard. Despite the large surface area of the pool, a surface mass-transfer coefficient of 2 $g/m^2/day$ resulted in a removal time of 21.5 years. It is apparent from these results that the relative distribution of a given spill volume between fingers and pools could have a significant impact on the removal time of the source in the aquifer.

7.3.2 Multiple Fingers and Pools

Since the evidence seems to indicate that there is a good chance that an infiltrating DNAPL will split into multiple fingers as it penetrates the saturated zone, the next set of simulations was designed to investigate contaminant plumes from sources consisting of multiple fingers. First, the effects on the plume of changing the distance between the fingers will be examined. Next, the diameter of the fingers will be changed. Finally, the plume resulting from a more complex source consisting of multiple fingers and pools will be discussed.

7.3.2.1 Case D

In the Case D simulation, it was assumed that five fingers of PCE penetrated the water table and made their way to the bottom of the aquifer. No pools were formed in this case. Since the volume was still taken to be 1000 L and the residual saturation was 15%, this

resulted in five fingers that were each 0.5 m square. One finger was located at the center of the spill (the z-axis) and two fingers were equally spaced along the y-axis on each side of the first finger. This was equivalent to taking the one large finger from the Case B spill, dividing it up into five equal-sized fingers and spreading those fingers out along the y-axis.

Since there is no data for the average distance between DNAPL fingers in saturated porous media, a reasonable first guess was based on other information. First of all, it seemed likely that fingers would penetrate the media where the immiscible fluid could take advantage of local regions of higher permeability. Second, in the analysis of the data from the detailed investigation of hydraulic conductivity variations at the Borden site, Sudicky (1986) found isotropic horizontal correlation lengths to be on the order of three meters. Therefore, for the Case D spill the assumption was made that the fingers were three meters apart.

Figures 7.10(a) and (b) show the steady-state contaminant plume that was modeled for the Case D source. Just as in Case B, since the fingers extended all the way to the bottom of the aquifer, contaminant concentrations remained constant with depth. Comparison of Figures 7.8(a) and 7.10(a) shows that even though both sources had the same volume of residual and extended throughout the thickness of the aquifer, the multiple finger source produced a more dispersed contaminant plume with a much smaller concentration gradient. For example, in the center of the Case B plume the concentration dropped from 42.8 ppm to

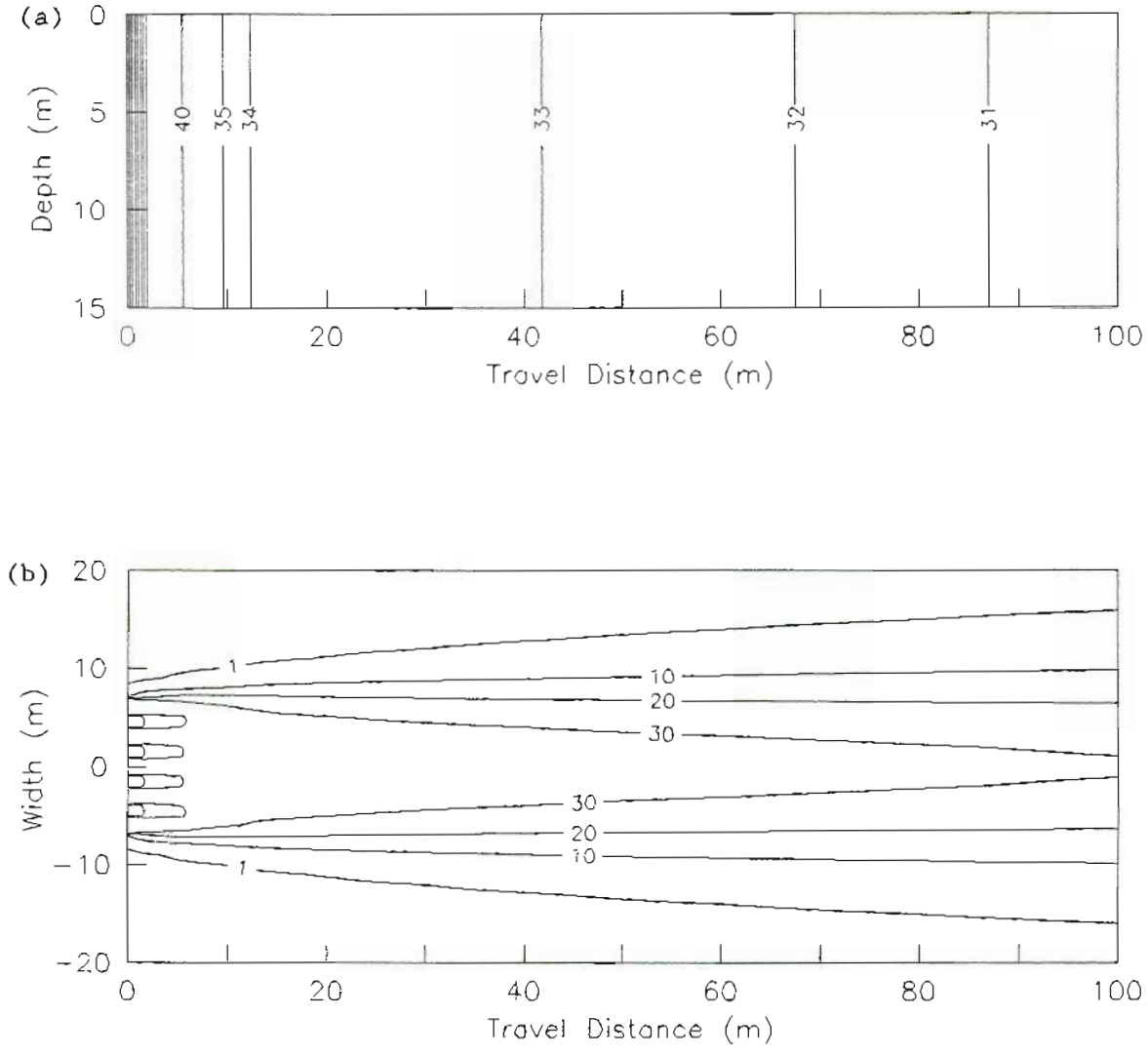

Figure 7.10: PCE concentrations (ppm) for Case D as viewed both (a) down the center of the plume and (b) across the plume.

19.5 ppm when moving from a distance of 20 m out to 100 m. In Case D, however, the concentration only changed from 33.4 ppm to 30.3 ppm. Although the source consisted of five discrete fingers of residual, Figure 7.10(b) shows that transverse horizontal dispersion was able to mix the individual plumes into what appeared to be one coherent plume within about the first 10 m. Because the five fingers in Case D presented a larger cross-sectional area to the groundwater flow, this source would be removed in a shorter time than the Case B source; 5.6 years compared to 12.8 years.

Since the concentrations for the Case D spill exceeded 30 ppm (15% of C_s) for the region within 100 m of the source, subsequent model simulations were performed to investigate how changes in finger spacing or finger size might further reduce the concentration to approximately 2 ppm (1% of C_s). To begin with, the effect on the contaminant plume of increasing the distance between fingers was studied. Figure 7.11(a) illustrates what happened to the Case D plume when the spacing was increased from 3 m to 6 m. Since the fingers were further apart, a longer travel distance was required before the individual plumes blended into one large plume. The 20 ppm contour shows up as five discrete plumes out to a distance of 20 m. Although the rate at which the PCE was released into the plume remained the same as before, the increased spacing reduced the concentration because the contaminants were essentially being mixed with larger volumes of clean water. The concentration in the center of the plume at a distance of 100 m was reduced from 30.3 ppm to 16.6 ppm. This

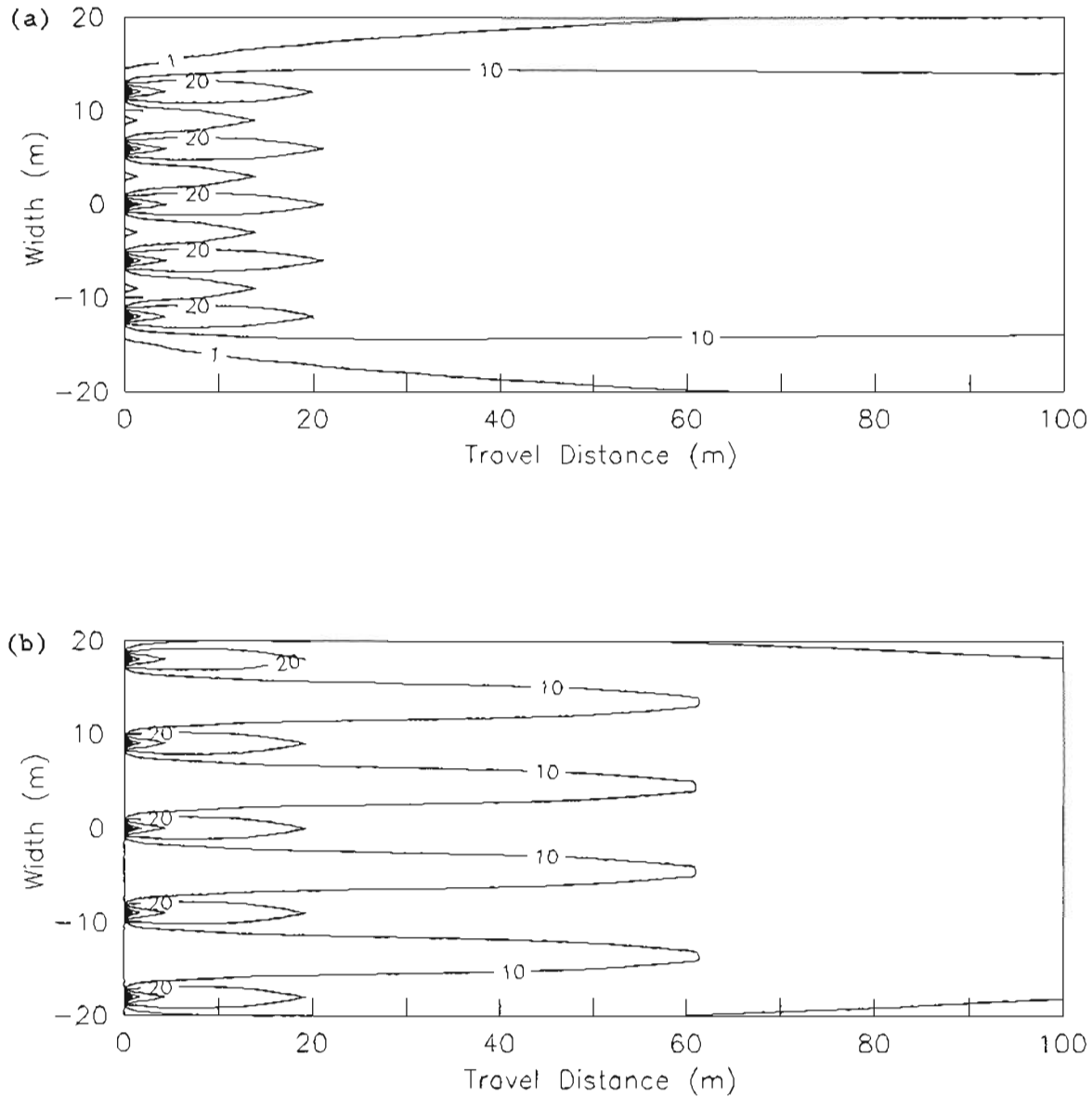

Figure 7.11: Contour plots showing the effect on the Case D spill of changing the distance between fingers from 3 m to (a) 6 m and (b) 9 m.

reduction clearly reflects the increased dilution resulting from a doubling in the amount of water for a given mass of solute.

In Figure 7.11(b), the individual contaminant plumes have become even more obvious when the finger spacing was further increased to 9 m. Under these conditions, even the 10 ppm contours remained separated out to a distance of over 60 m. Again, the effects of the increased spacing showed up as increased dilution in the mixed plume. In this case the concentration in the plume center at 100 m was only 11.3 ppm. Although it might seem unlikely that a spill would result in such widely scattered fingers, it is possible that DNAPL escaping from a leaking pipeline might move along the more permeable fill surrounding the pipe and eventually make its way down to an aquifer at a number of widely spaced points. If the groundwater flow was nearly perpendicular to the spacing, evidence for the widely spaced fingers might show up as a number of discrete areas of higher concentration. However, if the flow was fairly oblique, contaminants from widely spaced fingers may still quickly blend into one broad plume.

If the size of the fingers is reduced while maintaining a constant separation distance, the concentration of the contaminant plume will also be reduced due to the decrease in the mass released into a given amount of water. This is illustrated in Figures 7.12(a) and (b). In the computer simulations used to generate the data for each of these figures, the distance between the fingers was maintained at the 3 m value used in Case D. As previously seen in Figure 7.10(b), this spacing was close enough to allow the individual plumes

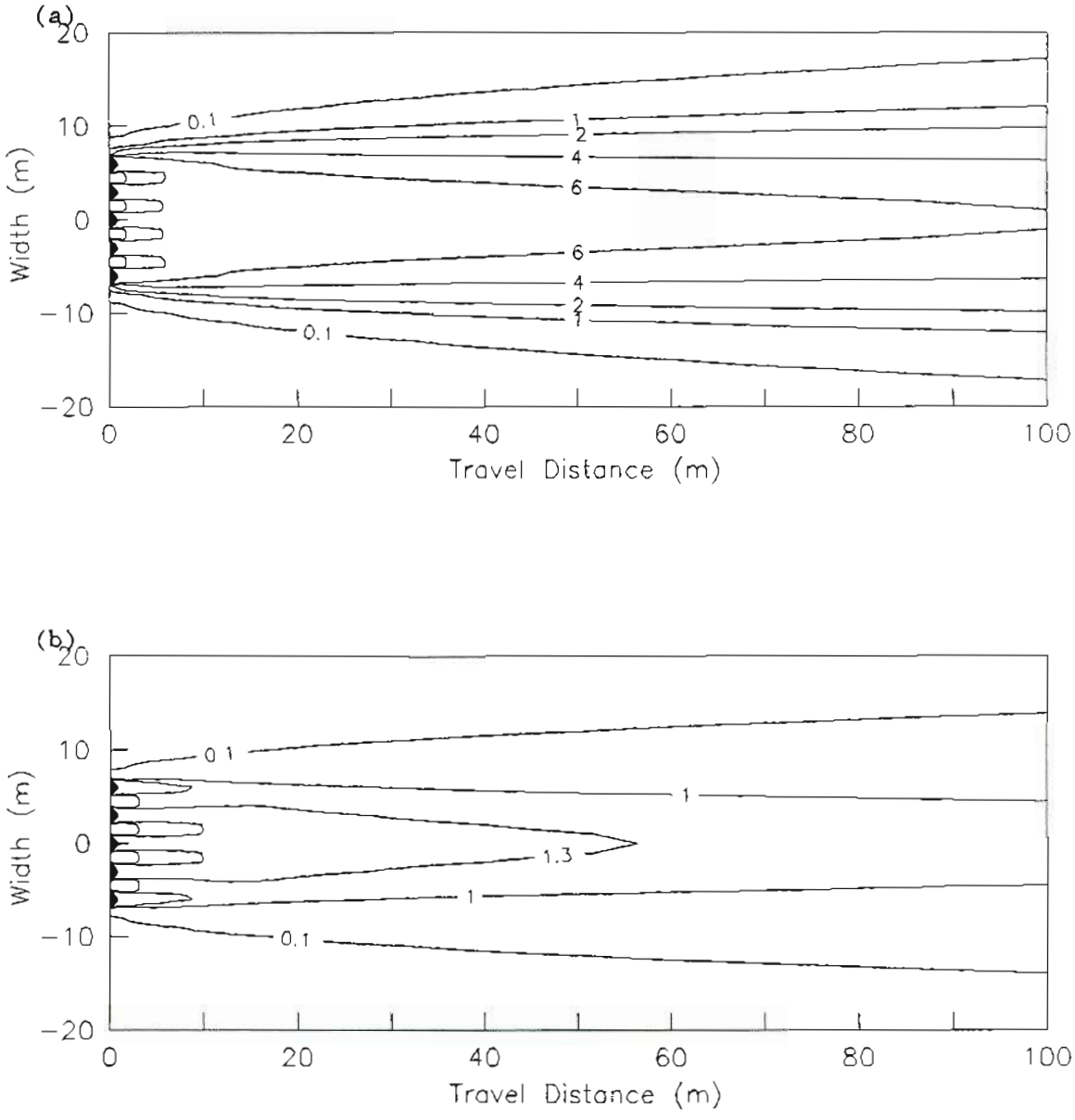

Figure 7.12: Contour plots showing the effect on the Case D spill of changing the size of the fingers from 50 cm to (a) 10 cm and (b) 2 cm.

to merge into one broad plume within about 10 m. For these model results, no attempt was made to allocate all 1000 L of the "spilled" PCE. The goal was simply to illustrate the effects on the plume of changing the diameter of the fingers.

In Figure 7.12(a), the diameter of the fingers was 10 cm, one-fifth the size of the fingers used in Case D. The fivefold reduction in contaminant mass was reflected in the concentration contours. The concentration in the center of the plume at 100 m was 6.1 ppm compared to 30.3 ppm previously obtained in Case D. Likewise, the further reduction in the diameter of the fingers to 2 cm (Figure 7.12(b)) resulted in another fivefold reduction in PCE concentrations. The 100 m plume center concentration was 1.2 ppm for fingers of this size.

The results discussed above serve to illustrate the fact that for solubility controlled dissolution from residual zones, simple mass balance considerations demand that the cross-sectional area of the fingers in the region of interest be no more than a few percent of the total area if the average plume concentration is also to be no more than a few percent of C_s. For the value of transverse horizontal dispersivity used in these model studies (0.1 m), a 3 m distance between fingers resulted in the formation of one broad contaminant plume within a distance of about 10 m from the source.

It is easy to produce a model plume that has a low concentration simply by using a source consisting of a number of small fingers. However, removal time considerations indicate that this is not likely to be the complete picture. The 10 cm fingers shown in Figure 7.12(a)

would be removed by the 30 cm/day flow in approximately 400 days. For the 2 cm fingers shown in Figure 7.12(b) the removal time would be reduced to only about 80 days. With an increase in the local groundwater velocity accompanying a pump-and-treat remediation scheme, removal of the source could be accomplished in a matter of weeks to months if the source consisted only of fingers with diameters in the range of 2-10 cm. For this reason, it seems likely that an established plume with relatively low concentrations would have to be indicative of a source which consists largely of pools where the mass-transfer is less efficient than it is from residual fingers. This is the type of source which will be discussed in Case E.

7.3.2.2 Case E

The Case E simulation represents a DNAPL spill that penetrated the water table in one location and then split into smaller fingers and spread out into a number of pools as it made its way to the bottom of the aquifer. The vertical lines in Figure 7.13 represent the location of the residual fingers in this simulation. The horizontal lines represent pools where the penetrating immiscible fluid encountered a zone of slightly lower permeability and spread out until it was able to again move downward. The initial finger was 10 cm in diameter and the diameters decreased with depth down to 2 cm near the bottom of the aquifer. As in the previous simulations, the fingers were assumed to have square horizontal cross-sections. The average diameter of the twelve pools was three meters. This corresponded with

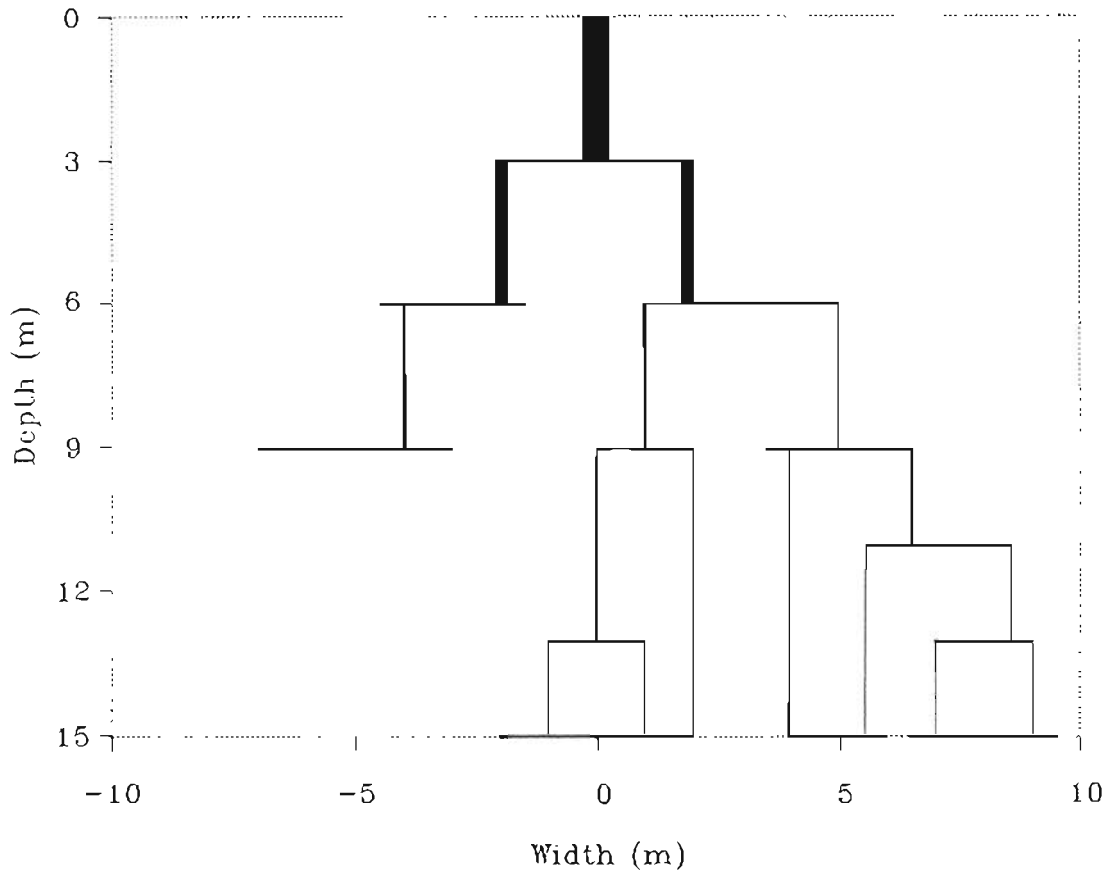

Figure 7.13: Diagram showing the relative location of the sixteen residual fingers and twelve pools of PCE that make up the contaminant source for Case E.

the previously mentioned horizontal correlation lengths calculated by Sudicky (1986) for the Borden site. Although Sudicky (1986) calculated vertical correlation lengths of 0.12 m, the use of a vertical spacing this small would have further complicated the picture by requiring a very large number of fingers and pools. This was not considered critical to this example since a large number of closely spaced small pools can be represented by a smaller number of larger, more widely spaced pools. Therefore, three meters was also used for the vertical spacing.

Figure 7.14(c) shows the PCE concentrations along the center of the steady-state contaminant plume for Case E. The relative contributions to the plume from the fingers and pools are illustrated in Figures 7.14(a) and 7.14(b), respectively. Comparison of Figures 7.14(b) and (c) demonstrate that the pools are indeed the predominant source of the contaminants. Even when all of the fingers have been depleted, the nature of the plume will not change significantly. As discussed in the previous section, this type of source should result in a contaminant plume that has a lower concentration and a longer lifetime than one consisting primarily of residual fingers.

Figure 7.15(c) shows a cross-section of the Case E plume at a distance of 100 m from the center of the spill. Concentrations range from a low of just over 3 ppm near the top of the aquifer to just over 22 ppm at the bottom of the aquifer. Higher concentrations resulting from a greater density of pools are clearly visible in the lower right hand side of the plume. The relative contributions to the plume from

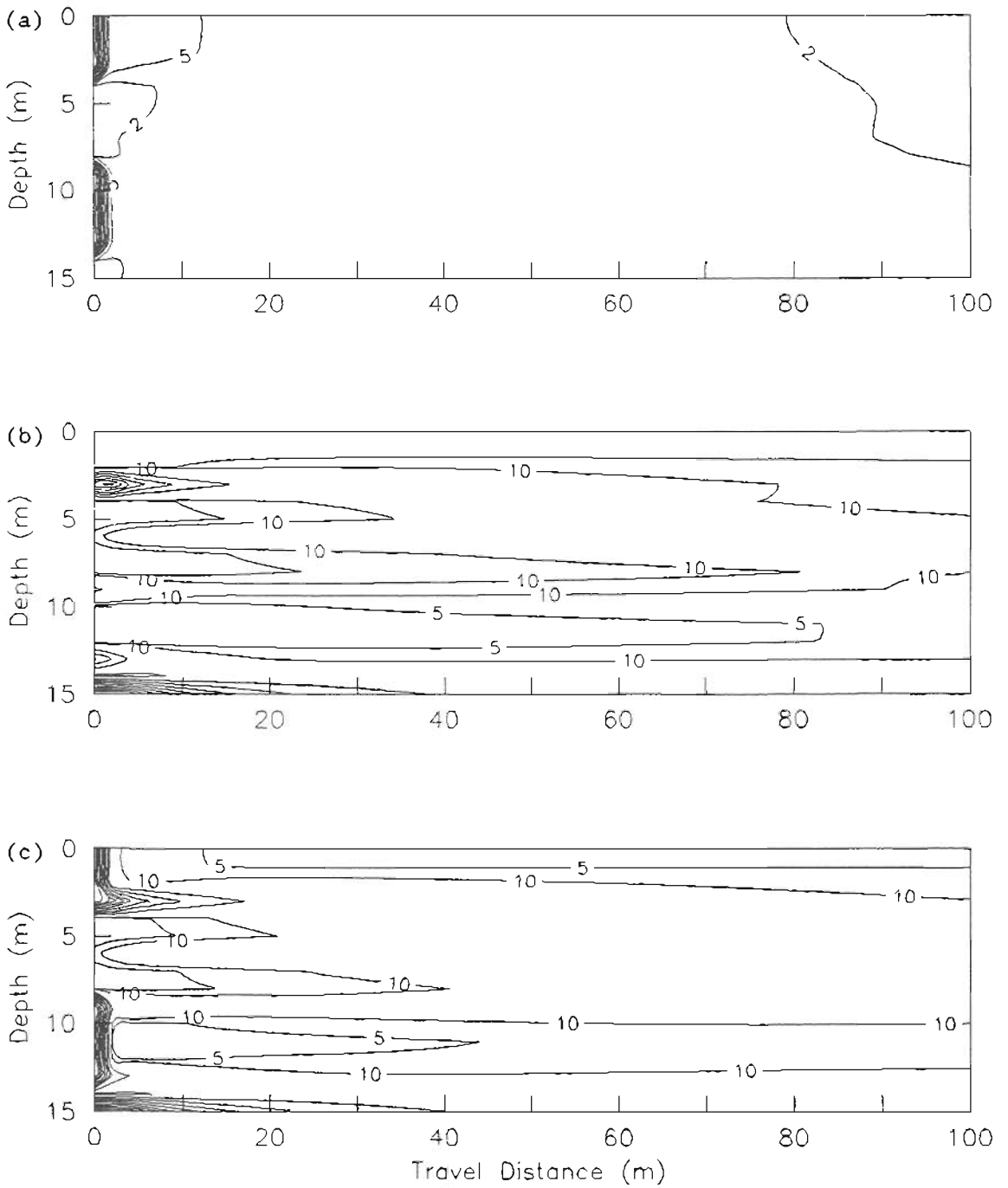

Figure 7.14: PCE concentrations (ppm) in the center of the plume (y = 0) for Case E. Concentrations shown are for contaminants emanating from (a) the sixteen fingers, (b) the twelve pools and (c) the total source.

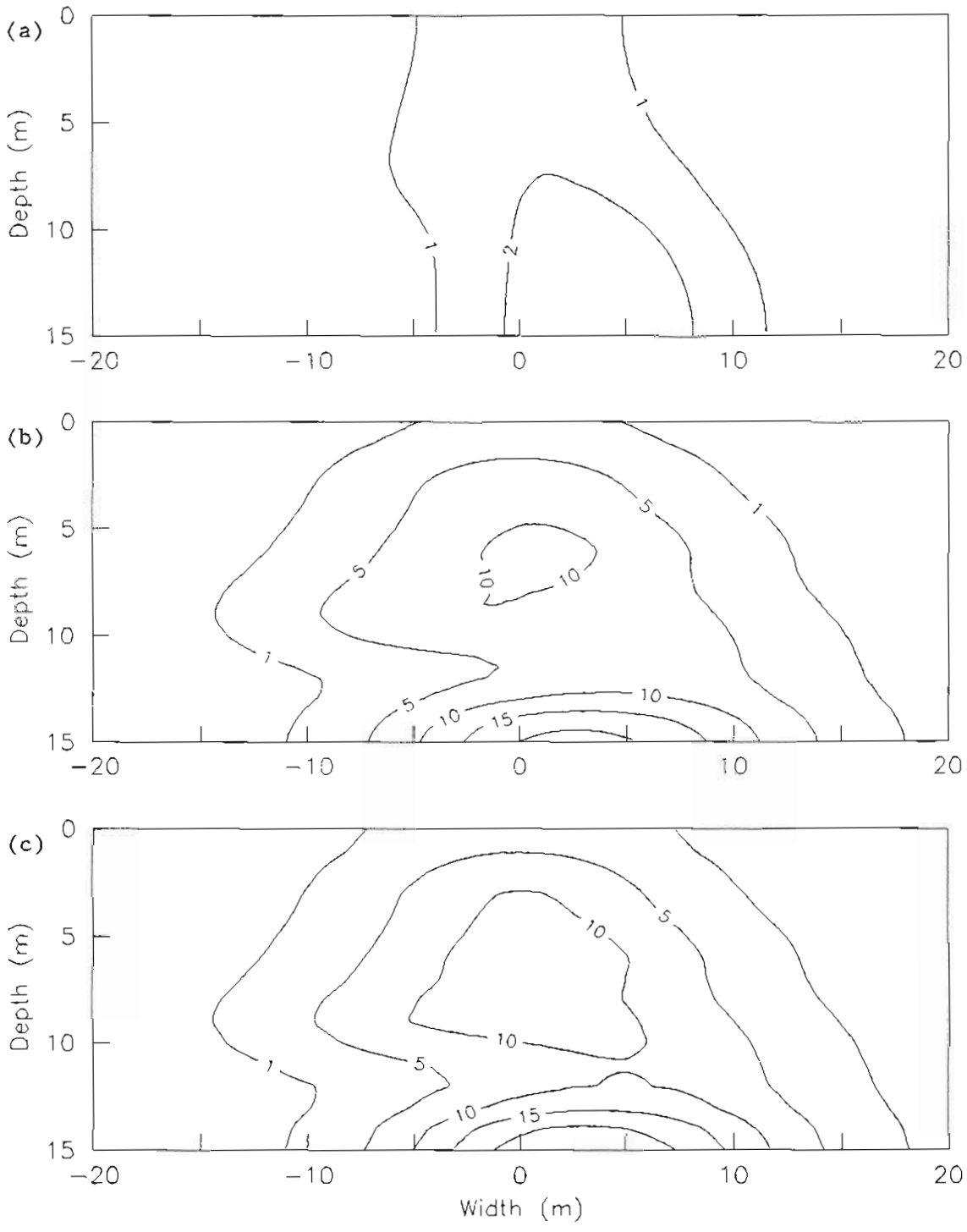

Figure 7.15: PCE concentrations (ppm) in the yz-plane across the plume at a distance of 100 m for Case E. Concentrations shown are for contaminants emanating from (a) the sixteen fingers, (b) the twelve pools and (c) the total source.

the fingers and pools are shown in Figures 7.15(a) and (b). This again demonstrates the predominant influence of the pools on the nature of the plume.

In Section 7.3, the surface mass-transfer coefficient was discussed and the point was made that even though the model treated this value as a constant, this would not be the case in reality due to the nature of diffusion. Because of this fact, the mean value per area measured over a small pool would probably be larger than the mean value per area measured over a large pool. Since the data used to estimate M_a was obtained in a 150 cm long tank, it was thought that the 2 g/m^2/day value could certainly be considered reliable for pools with lengths in the direction of flow on the order of 1 m. To test the effect of this limit on the contaminant plume, the Case E simulations were repeated with the length of each of the pools reduced to 1 m. The width of each of the pools was left unchanged. Therefore, the average width of the twelve pools remained 3 m.

The effect on the plume of the reduction in contaminant mass due to the reduction in pool length to 1 m is shown in Figure 7.16. Figure 7.16(a) illustrates the contaminant plume derived from just the pools. Figure 7.16(b) shows the complete plume derived from this plume in conjunction with the plume from the fingers previously shown in Figure 7.15(a). Although the change in the lengths of the pools reduced the amount of mass dissolving out of each pool from one-fourth to one-half of what it had been before, the pools still are the predominant contributors to the overall plume.

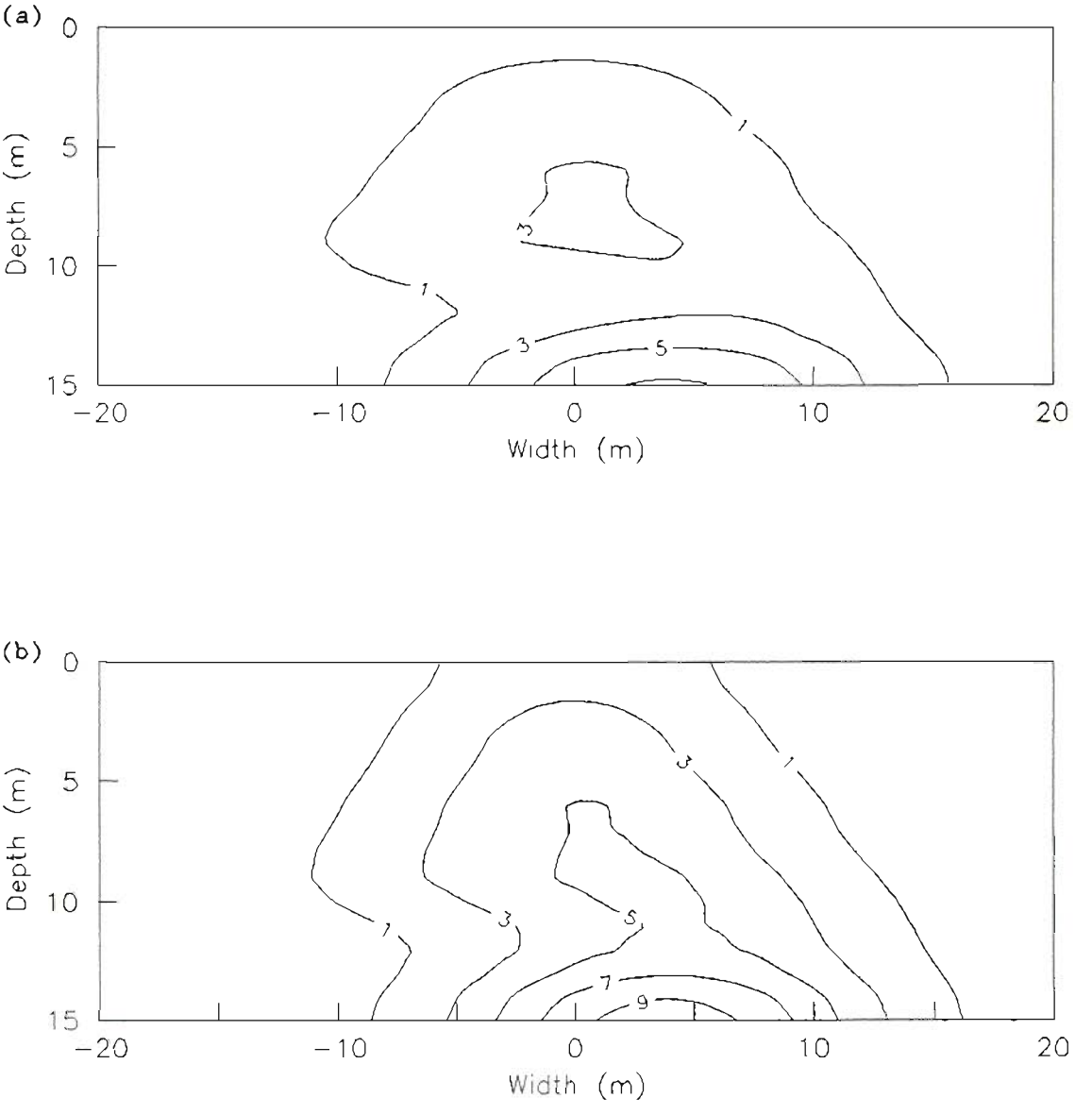

Figure 7.16: PCE concentrations (ppm) in the yz-plane for Case E when the length of each of the pools was reduced to 1 meter. Contours show contributions from (a) the twelve pools and (b) the total source.

7.4 Conclusions

Results of the model studies in this chapter have provided some insight into the nature of the sources of contamination in the saturated zone resulting from spills of DNAPLs. If the investigation of a DNAPL spill site reveals that the contaminant plume near the source has concentrations that are no more than a few percent of the solubility of the compound of interest, the source cannot consist of one large finger or even of a number of fingers larger than 10 cm in diameter spaced less than 3 m apart. To achieve concentrations that are on the order of a few percent of C_s, mass balance demands that the cross-sectional area of the fingers in the source region can be no more than a few percent of the total cross-sectional area of this region. However, small finger size also leads to the conclusion that the sources will be short lived. Since experience has shown that contaminant plumes are often not rapidly removed by pump-and-treat remediation schemes, it is apparent that a typical DNAPL spill in a saturated porous medium does not result in a source that consists predominantly of small fingers. Rather, the source is more likely to consist of a number of small scattered pools on the top of lower permeability layers from which mass transfer is less efficient. Therefore, the further study of mass transfer from stagnant pools of DNAPL into flowing groundwater should be considered an important area for future research.

8. SUMMARY AND CONCLUSIONS

Contamination of groundwater supplies from spills or leaks of DNAPLs is a matter of great concern. Field investigations have found contaminant concentrations that are many orders of magnitude larger than what is allowable for safe drinking water. However, these concentrations are still much lower than the solubility-level values that have been found in laboratory column studies. This research was undertaken to provide a thorough investigation of the dissolution and transport of selected DNAPLs by water flowing at typical hydraulic gradients and velocities in a model aquifer. It was hoped that this study would provide much needed information about the nature of contaminant plumes emanating from zones of residual DNAPL trapped below the water table. This information would either serve to confirm or refute the results of traditional column experiments.

To achieve the goals of this study, a model aquifer was constructed in a 75 cm wide by 100 cm long by 100 cm high tank. A cylindrical zone of residual DNAPL was created in the aquifer and the formation of the dissolved contaminant plume emanating from this zone was monitored at the downgradient end of the tank. Results have shown that the initial breakthrough of the dissolved contaminant plume was rapid. During the first 34-56 hours of dissolution experiment #1

(DE-1), the concentration of PCE increased to within 4% of its solubility (200 ppm). Maximum concentrations slowly continued to increase until they reached solubility levels at the 10-100 cm/day velocities studied in this project. Heterogeneities resulting from layers formed during the filling of the tank may have been responsible for the observed delay in the attainment of solubility level concentrations of PCE.

Both one and two-dimensional analytical solutions to the advection-dispersion equation were used to calculate values for the coefficients of longitudinal and transverse dispersion for the model aquifer. These values were small but within the range normally observed in laboratory column or tank studies. The contribution of diffusion to transverse dispersion was noticeable at velocities of 10 and 30 cm/day, but not at velocities of 60 or 100 cm/day. Since these velocities correspond to Peclet numbers of approximately 1-10, the decreasing effects of diffusion observed here agree with generally accepted contaminant transport theory.

The concentrations observed in this experiment are consistent with earlier work on contaminant source strength which indicates that in most groundwater flow regimes, mass transfer depends upon the solubility of the compound rather than the flow rate of the water. The high experimental concentrations agree with results of column studies but contrast with the lower values usually found in the field. Best-fit models of the steady-state contaminant plumes required a source width equal to about 90% of the width of the residual zone.

This may have been due to a slight narrowing in the stream lines resulting from reduced permeability in the residual zone. If so, the effect may have been greater if the residual zone had contained a higher percentage of PCE. It is doubtful, however, that reduced permeability plays a major role in keeping field results significantly lower than laboratory results.

A second large scale dissolution experiment (DE-2) was carried out in which residual zones of PCE and CB were both placed in the aquifer. Results for the breakthrough of the PCE contaminant plume confirmed the observations that had been made in DE-1. Breakthrough was again rapid and solubility level concentrations were easily attained. The predictability of the DE-2 plume from the parameters measured in DE-1 verified the well-behaved nature of the model aquifer and its usefulness for studies of this kind. Based on these results, it is clear that similar conditions in a real aquifer would also generate solubility level concentrations of contaminant.

Comparison of the CB data collected over a period of several months in DE-2 to data from a column experiment indicated that, at least at the residual saturations used in these studies, there was no significant reduction in the flow of water through the center of the residual zone. In spite of some difficulties and uncertainties in the formation of the PCE residual, the trend in the concentrations of CB could be easily explained. This further confirmed that reduced permeability in the residual zone does not play a major role in reducing contaminant concentrations.

A computer model was written to simulate the data from DE-2. This model assumed that solute concentrations were controlled entirely by ideal equilibrium solution behavior. Comparison of the model-generated data with the experimental results proved this to be a reasonable assumption. Model results were also useful in illustrating the trends that would be observed under conditions of varying saturations or equilibration distances. Although the model was not designed with the intention of calculating any specific physical or chemical parameters, results seemed to indicate that the time required to reach equilibrium for the dissolution and partitioning processes that controlled the solute concentrations in this system was on the order of an hour.

The results of DE-2 also serve to demonstrate that solubility level concentrations will only be obtained when the residual contains a pure compound. Although leaks from underground storage tanks may meet this requirement, leaks from landfill sites would not. Therefore, even under ideal conditions, solute concentrations from a landfill may start out at only a fraction of solubility levels due to the mixed nature of the source. Even initially pure residuals may pick up other organic material (natural or otherwise) and experience a reduction in solubility.

Small-scale DNAPL flow experiments were conducted to both observe the nature of DNAPL flow in porous media and measure the levels of residual saturation left by this flow. Saturations measured for 1,1,1-TCA and PCE agreed with the range of values reported by Wilson

and Conrad (1984) for HCs and by Schwille (1984) for CHCs. Residual saturations for 1,1,1-TCA in initially water-saturated sand were between 15-40%. For PCE, residual saturations measured at a number of depths throughout the thickness of a saturated capillary fringe were between 15-25%. These values remained quite constant even though the water content of the samples increased with depth.

Observations made during the infiltration experiments indicated that very minor differences in the characteristics of a porous medium can result in noticeable changes in the behavior of an infiltrating DNAPL. A slight reduction in the permeability due to changes in grain size or water saturation can cause a downward migrating DNAPL to flow laterally until it finds another more permeable spot through which to continue its downward progress. This kind of response to minor heterogeneities can result in the formation of both vertical fingers and horizontal pools of immiscible fluid below the water table.

Model studies were undertaken to investigate the relative importance of fingers and pools as a source of contaminant plumes. The size and distribution of fingers and pools were varied in a number of simulations in an attempt to produce contaminant plumes having concentrations on the order of a few percent of solubility. Results have shown that the combined demands of relatively low concentrations and long source life require a source that consists primarily of small pools rather than small fingers.

APPENDICES

Appendix A. PRODUCT DATA FOR OTTAWA SANDS

The following information was supplied by the Ottawa Industrial Sand Company, Ottawa, Illinois.

A.1 Flintshot Blasting Sands

Typical Size Analysis:	Average Mesh Size	Mode Millimeter Size
Flintshot 4.0	38 - 40	0.455 - 0.420
Flintshot 3.0	41 - 43	0.408 - 0.383
Flintshot 2.8	44 - 46	0.371 - 0.346
Flintshot 2.6	47 - 49	0.334 - 0.309
Flintshot 2.4	50 - 52	0.297 - 0.288

Typical Surface Profile (Anchor Pattern)*

	Flintshot 4.0	Flintshot 3.0	Flintshot 2.8	Flintshot 2.6	Flintshot 2.4
At 90 psi	3.0	2.8	2.7	2.6	2.4
At 60 psi	2.9	2.7	2.6	2.5	2.4

*mils of profile (0.001 inch) as measured by Proficorder Surface Measuring Instrument.

Surface Profile (Anchor Pattern) is the condition of the metal surface after blasting; its texture and relief, (the distance between the high and low points on the surface).

Typical Physical Properties:	
Mineral	Quartz
Color	White
Grain Shape	Rounded
Sphericity	0.8 - 0.9
Krumbein	0.8 - 0.9
Hardness (Moh)	7
Specific Gravity	2.65

Typical Chemical Analysis:		
SiO_2	(Silicon Dioxide)	99.808%
Fe_2O_3	(Iron Oxide)	0.016%
Al_2O_3	(Aluminum Oxide)	0.042%
TiO_2	(Titanium Dioxide)	0.014%
CaO	(Calcium Oxide)	<0.01%
MgO	(Magnesium Oxide)	<0.01%
LOI	(Loss-on-Ignition)	0.10%

A.2 No. 17 Silica

Physical Analysis

U.S Sieve No.	Millimeter Designation	Mean % on Sieve	Std. Dev.	Mean % Cumulative	Mean % Passing
30	0.595	-	-	-	100.0
40	0.420	8.1	3.9	8.1	91.9
50	0.297	44.5	7.3	52.6	47.4
70	0.210	28.8	4.9	81.4	18.6
100	0.149	12.7	4.3	94.1	5.9
140	0.105	4.4	2.3	98.5	1.5
200	0.074	1.1	0.5	99.6	0.4
270	0.053	0.2	0.2	99.8	0.2

	Mean
AFS Grain Fineness	49.9
Actual Surface Area (cm^2/gm)	102.0
Base Permeability	228.0
Theoretical Surface Area (cm^2/gm)	85.7
Coefficient of Area	1.19
Density (Uncompacted) (lb/ft^3)	90.8
Density (Compacted) (lb/ft^3)	95.9
Acid Demand (pH-4)	1.4

Chemical Analysis

SiO_2	99.806
Fe_2O_3	0.019
TiO_2	0.018
Al_2O_3	0.047
CaO	<0.01
MgO	<0.01
LOI	0.09

A.3 F-80

Physical Analysis

U.S Sieve No.	Millimeter Designation	Mean % on Sieve	Std. Dev.	Mean % Cumulative	Mean % Passing
30	0.595	-	-	-	100.0
40	0.420	0.2	0.2	0.2	99.8
50	0.297	2.0	0.9	2.2	97.8
70	0.210	22.9	3.8	25.1	74.9
100	0.149	38.7	3.1	63.9	36.1
140	0.105	26.4	2.6	90.3	9.7
200	0.074	8.1	2.0	98.4	1.6
270	0.053	1.7	4.2	100.1	0.0

	Mean
AFS Grain Fineness	80.5
Actual Surface Area (cm^2/gm)	175.7
Base Permeability	64.0
Theoretical Surface Area (cm^2/gm)	145.7
Coefficient of Area	1.22
Density (Uncompacted) (lb/ft^3)	88.3
Density (Compacted) (lb/ft^3)	93.0
Acid Demand (pH-4)	1.8

Chemical Analysis

SiO_2	99.692
Fe_2O_3	0.063
TiO_2	0.057
Al_2O_3	0.068
CaO	<0.01
MgO	<0.01
LOI	0.10

Appendix B. SAMPLING PORT COORDINATES

The coordinates used for graphs of experimental data and modeling results from DE-1 and DE-2 are given in this appendix. These numbers are in units of centimeters and are referenced to an origin located at the bottom of the tank on the downgradient edge of the cylinder. The x-axis was along the direction of flow. For a given experiment, therefore, all of the ports had the same x-coordinate. In DE-1, x = 40.0, and in DE-2, x = 20.0. The y-axis was oriented horizontally and the z-axis was oriented vertically. All of the ports in a given row, therefore, had the same z-coordinate and all of the ports in the column had the same y-coordinate. In DE-1, these were: R1, z = 59.4; R2, z = 39.6; R3, z = 19.8; and C, y = 1.8. The specific y-coordinates within the rows and z-coordinates within the column are listed below for DE-1. Because of a slight difference in the positioning of the cylinder from DE-1 to DE-2, the y-coordinates for DE-2 were all 1.8 cm less than those from DE-1.

Rows						Column			
Port	Y =	Port	Y =	Port	Y =	Port	Z =	Port	Z =
1	-29.6	9	-6.8	17	16.1	1	66.0	8	29.7
2	-26.8	10	-3.9	18	18.9	2	62.7	9	26.4
3	-23.9	11	-1.1	19	21.8	3	56.1	10	23.1
4	-21.1	12	1.8	20	24.7	4	52.8	11	16.5
5	-18.2	13	4.7	21	27.5	5	42.9	12	13.2
6	-15.3	14	7.5	22	30.4	6	36.3		
7	-12.5	15	10.4	23	33.2	7	33.0		
8	-9.6	16	13.2			8	29.7		

Appendix C. SELECTED EXPERIMENTAL DATA

This appendix contains the data used to generate the graphs of experimental results contained in Chapters 4 and 5. Concentrations are expressed in ppm. NQ means that a small peak was visible on the chromatogram but was too small for the software to quantify. ND means that no peak was detected.

C.1 Dissolution Experiment #1

C.1.1 Breakthrough Data

The initial breakthrough data was collected at a mean water velocity of 30 cm/day. The data listed below are for samples taken from the middle row of sampling ports (R2).

Time (hr)	Port							
	8	9	10	11	12	13	14	15
36	-	-	-	9.8	15.3	6.7	-	-
38	-	-	25.9	-	38.5	-	3.8	-
40	NQ	22.1	66.6	76.9	79.1	67.8	18.0	-
42	2.0	-	114.9	-	133.1	-	34.7	-
56	5.9	98.3	179.4	188.8	192.5	174.3	69.8	2.1

C.1.2 Initial Steady-State Plumes

30 cm/day

Port	Row or Column			
	R1	R2	R3	C
1	-	-	-	148.2
2	-	-	-	168.4
3	-	-	-	192.3
4	-	-	-	183.4
5	-	-	-	183.5
6	-	-	-	194.6
7	NQ	NQ	NQ	184.0
8	10.0	5.9	9.3	186.3
9	137.8	98.3	86.4	182.2
10	182.4	179.4	175.0	179.1
11	193.7	188.8	179.3	179.6
12	186.7	192.5	181.4	174.1
13	177.3	174.3	155.6	-
14	94.8	69.8	52.9	-
15	3.8	2.1	1.3	-
16	NQ	ND	NQ	-
17	ND	ND	NQ	-
18	-	-	-	-

60 cm/day

Port	Row or Column			
	R1	R2	R3	C
1	-	-	-	188.5
2	-	-	-	189.4
3	-	-	-	196.0
4	-	-	-	181.6
5	-	-	-	198.1
6	-	-	-	197.0
7	NQ	ND	NQ	186.0
8	1.1	1.5	3.6	184.2
9	77.9	88.4	96.0	201.2
10	187.6	194.6	189.2	186.1
11	193.6	197.4	188.7	189.5
12	188.1	201.0	190.0	186.4
13	162.4	195.8	164.1	-
14	45.6	64.1	48.8	-
15	0.3	0.4	0.1	-
16	NQ	NQ	NQ	-
17	-	-	-	-
18	-	-	-	-

100 cm/day

Port	Row or Column			
	R1	R2	R3	C
1	-	-	-	184.6
2	-	-	-	173.2
3	-	-	-	192.2
4	-	-	-	193.5
5	-	-	-	188.1
6	-	-	-	195.1
7	NQ	0.1	0.1	187.5
8	0.5	0.5	1.3	178.7
9	79.0	84.8	82.9	191.0
10	184.2	191.2	188.6	187.5
11	191.1	187.0	181.7	188.0
12	182.4	189.6	188.3	191.7
13	181.7	197.7	165.6	-
14	41.6	70.4	50.0	-
15	0.1	0.3	0.2	-
16	ND	0.2	0.2	-
17	-	-	-	-
18	-	-	-	-

10 cm/day

Port	Row or Column			
	R1	R2	R3	C
1	-	-	-	40.3
2	-	-	-	87.3
3	-	-	-	189.6
4	-	-	-	196.8
5	ND	NQ	NQ	189.4
6	ND	NQ	0.1	200.4
7	0.5	3.1	7.5	197.5
8	9.2	35.8	51.6	195.5
9	44.3	125.1	137.8	196.0
10	111.8	186.2	197.3	196.3
11	155.8	193.0	193.2	194.9
12	139.7	192.7	193.0	191.3
13	89.5	160.9	167.0	-
14	29.6	88.8	97.1	-
15	4.3	17.8	17.5	-
16	0.1	1.2	1.0	-
17	ND	ND	NQ	-
18	-	-	-	-

C.1.3 Replicate Steady-State Plumes

Samples for the replicate steady-state plumes were only collected from the middle row of sampling ports (R2).

Port	Mean Water Velocity (cm/day)			
	10	30	60	100
5	ND	-	-	-
6	ND	-	-	-
7	1.3	ND	ND	ND
8	21.8	5.5	1.6	0.5
9	96.3	93.0	88.2	84.6
10	172.7	181.9	183.6	188.6
11	198.1	201.8	201.2	203.6
12	195.6	206.4	202.4	198.2
13	176.6	198.3	190.1	197.8
14	108.4	100.2	82.9	82.2
15	27.4	5.3	1.3	0.4
16	2.4	ND	ND	ND
17	ND	-	-	-
18	ND	-	-	-

C.1.4 Diffusion Experiment

Samples for the experiment on the effects of molecular diffusion were only collected from R2.

Port	Hours After Resuming Flow						
	1	4	7	10	12	14	16
5	-	ND	ND	ND	ND	ND	ND
6	0.6	0.3	0.3	0.3	0.6	0.6	0.2
7	5.0	5.0	4.6	5.4	8.1	7.1	1.6
8	31.2	33.4	31.6	33.9	48.2	45.5	8.9
9	88.8	62.2	100.1	104.1	130.6	156.3	102.6
10	160.4	168.8	172.0	178.1	179.0	192.7	186.1
11	199.4	204.4	200.5	204.2	203.3	205.8	194.2
12	201.2	195.5	201.1	200.3	201.7	201.2	200.9
13	157.6	155.1	158.9	167.0	186.3	198.9	198.0
14	84.7	81.3	83.1	91.8	135.0	146.8	99.0
15	22.9	21.6	21.0	23.7	42.7	46.7	12.7
16	3.7	3.1	3.0	3.3	6.4	9.1	3.2
17	0.6	0.1	0.1	0.1	0.3	0.6	0.2
18	-	ND	ND	ND	ND	ND	ND

C.2 Dissolution Experiment #2

C.2.1 PCE data collected from sample ports in R2.

Days	Port								
	8	9	10	11	12	13	14	15	16
0.25	-	-	-	-	ND	-	-	-	-
0.42	-	-	-	-	ND	-	-	-	-
0.54	-	-	-	-	0.9	-	-	-	-
0.67	-	-	-	-	13.4	-	-	-	-
0.75	-	-	-	-	60.7	-	-	-	-
0.85	-	-	-	-	174.8	-	-	-	-
1.17	-	-	-	-	190.9	-	-	-	-
1.29	-	-	-	-	201.4	-	-	-	-
1.50	-	-	-	-	197.7	-	-	-	-
1.92	-	-	-	-	206.7	-	-	-	-
2.42	-	-	-	-	198.5	-	-	-	-
4.08	ND	16.9	137.3	192.4	195.5	199.2	182.1	31.6	3.3
6.08	-	-	-	-	199.2	-	-	-	-
7.14	-	-	-	-	198.4	-	-	-	-
11.06	ND	16.9	128.7	193.4	196.0	198.0	187.3	47.6	0.4
13.12	-	-	-	-	206.8	-	-	-	-
14.14	NQ	20.8	138.0	192.1	195.2	195.1	185.8	51.1	0.5
18.21	NQ	39.2	172.0	197.4	194.4	196.6	193.5	54.2	0.4
25.10	0.1	34.0	150.2	182.1	177.3	178.2	180.7	59.0	0.8
32.98	NQ	33.8	157.0	182.1	173.2	183.5	197.9	62.1	0.7
39.04	0.4	45.3	163.5	179.0	176.8	180.9	183.7	63.2	0.6
46.08	0.6	46.8	159.4	169.9	155.5	168.5	179.0	52.8	0.6
51.08	NQ	32.0	156.5	183.2	151.4	170.3	184.9	45.2	0.3
56.02	-	-	-	-	155.3	-	-	-	-
60.00	0.7	56.9	170.4	171.5	151.2	177.2	168.7	30.0	0.2
67.10	-	-	-	-	140.8	-	-	-	-
75.12	NQ	22.7	140.0	173.6	137.3	171.3	150.2	12.5	ND
81.08	-	-	-	-	128.0	-	-	-	-
89.21	-	-	-	-	130.4	-	-	-	-
95.00	0.2	38.5	150.0	176.4	132.8	177.0	114.4	6.8	ND
102.94	-	-	-	-	144.3	-	-	-	-

C.2.2 CB data collected from sample ports in R2.

Days	Port								
	8	9	10	11	12	13	14	15	16
0.25	-	-	-	-	ND	-	-	-	-
0.42	-	-	-	-	ND	-	-	-	-
0.54	-	-	-	-	ND	-	-	-	-
0.67	-	-	-	-	ND	-	-	-	-
0.75	-	-	-	-	ND	-	-	-	-
0.85	-	-	-	-	ND	-	-	-	-
1.17	-	-	-	-	2.3	-	-	-	-
1.29	-	-	-	-	1.7	-	-	-	-
1.50	-	-	-	-	1.4	-	-	-	-
1.92	-	-	-	-	1.4	-	-	-	-
2.42	-	-	-	-	2.3	-	-	-	-
4.08	ND	ND	1.4	ND	ND	1.7	ND	ND	ND
6.08	-	-	-	-	ND	-	-	-	-
7.14	-	-	-	-	0.6	-	-	-	-
11.06	ND	ND	ND	3.1	3.0	5.9	1.0	ND	ND
13.12	-	-	-	-	6.1	-	-	-	-
14.14	ND	ND	0.5	5.5	5.9	9.1	NQ	ND	ND
18.21	ND	ND	0.7	11.1	11.1	13.9	0.9	ND	ND
25.10	ND	ND	1.6	26.4	27.4	24.9	3.2	ND	ND
32.98	ND	ND	2.4	46.5	54.9	43.9	3.8	ND	ND
39.04	ND	ND	2.8	50.7	73.2	53.9	4.2	ND	ND
46.08	ND	ND	2.9	52.1	88.4	60.4	4.4	ND	ND
51.08	ND	ND	1.6	57.5	103.8	66.5	4.3	ND	ND
56.02	-	-	-	-	120.1	-	-	-	-
60.00	ND	1.3	3.2	55.6	120.8	69.6	3.6	ND	ND
67.10	-	-	-	-	141.6	-	-	-	-
75.12	ND	ND	0.7	44.2	159.6	57.0	1.1	ND	ND
81.08	-	-	-	-	150.5	-	-	-	-
89.21	-	-	-	-	140.7	-	-	-	-
95.00	ND	0.5	2.5	36.1	128.8	35.0	0.9	ND	ND
102.94	-	-	-	-	120.0	-	-	-	-

C.3 Dissolution Experiment #3

Volume (mL)	PCE	CB
6	2.7	ND
36	111.3	ND
126	199.1	ND
232	198.9	ND
770	203.3	ND
	212.5	ND
1382	205.4	ND
	203.9	ND
2208	198.8	5.6
	194.5	5.5
2458	195.4	8.2
	190.0	8.0
2613	190.5	9.8
3172	201.9	20.9
	200.2	20.8
4165	192.8	49.1
	192.9	49.7
4855	188.4	68.6
	179.5	65.5
5583	175.6	89.6
6353	171.3	108.8
	167.8	109.1
6927	141.5	108.8
	140.1	104.3
7929	148.8	142.1
	151.4	143.8
9205	138.0	169.9
	133.7	161.9
10054	126.7	175.6
	125.9	174.1
10841	117.6	182.5
	120.7	188.6
11359	111.9	183.5
	112.0	183.4
11833	115.3	201.3
	116.4	207.9
12685	114.9	221.7
	115.6	222.1
13347	113.2	231.4
	115.8	240.1

BIBLIOGRAPHY

Abelson, P. H., 1985, "Chemicals from Waste Dumps," Science, 229(4711):335.

Adamson, A. W., 1982, Physical Chemistry of Surfaces, 4th ed., Wiley and Sons, New York.

American Chemical Society, 1986, Environmental Science and Technology, 20(9):845.

American Chemical Society, 1987a, Environmental Science and Technology, 21(9):829.

American Chemical Society, 1987b, "EPA adopts drinking water standards," Chem. and Eng. News, 65(26):29.

Anderson, M. P., 1979, "Using Models to Simulate the Movement of Contaminants Through Groundwater Flow Systems," CRC Critical Reviews in Environmental Control, 9(2):97-156.

Bear, J., 1972, Dynamics of Fluids in Porous Media, American Elsevier, New York.

Bear, J., 1979, Hydraulics of Groundwater, McGraw-Hill, New York.

Bruch, J. C., and R. L. Street, 1967, "Two-Dimensional Dispersion," J. Sanit. Eng. Div., ASCE, 6:17-39.

Chuoke, R. L., P. van Meurs and C. van der Poel, 1959, "The Instability of Slow, Immiscible, Viscous Liquid-Liquid Displacements in Permeable Media," Trans. AIME, 216:188-194.

Conrad, S., E. Hagan and J. Wilson, 1987, "Why Are Residual Saturations of Organic Liquids Different Above and Below the Water Table?" Presented at the NWWA/API Conference on Petroleum Hydrocarbons and Organic Chemicals in Ground Water, Houston, TX.

Council on Environmental Quality, 1981, Contamination of Ground Water by Toxic Organic Chemicals, U.S. Government Printing Office, Washington, D.C.

Council on Environmental Quality, 1984, Environmental Quality: The Fifteenth Annual Report of the Council on Environmental Quality, U.S. Government Printing Office, Washington, D.C.

Crank, J., 1975, The Mathematics of Diffusion, Oxford University Press, New York.

Davies, O. L., and P. L. Goldsmith, eds., Statistical Methods in Research and Production, 4th Edition, Longman Inc., New York.

Dean, J. A., ed., 1973, Lange's Handbook of Chemistry, 11th Ed., McGraw-Hill, New York.

Driscoll, F. G, 1986, Groundwater and Wells, Johnson Division, St. Paul, MN.

de Marsily, G., 1986, Quantitative Hydrogeology: Groundwater Hydrology for Engineers, Academic Press, Orlando, FL.

Feenstra, S., and J. A. Cherry, 1988, "An Introduction to the Problem," in Dense Organic Solvents in Groundwater, J. A. Cherry and J. F. Pankow, eds., University of Waterloo Press (in progress).

Freeberg, K. M., P. B. Bedient and J. A. Connor, 1987, "Modeling of TCE Contamination and Recovery in a Shallow Sand Aquifer," Ground Water, 25(1):70-80.

Freeze, R. A., and J. A. Cherry, 1979, Groundwater, Prentice-Hall, Englewood Cliffs, NJ.

Fried, J. J., P. Muntzer and L. Zilliox, 1979, "Ground-Water Pollution by Transfer of Oil Hydrocarbons," Ground Water, 17(6):586-594.

Girifalco, L. A., and R. J. Good, 1957, "A Theory for the Estimation of Surface and Interfacial Energies. I. Derivation and Application to Interfacial Tension," J. Phys. Chem., 61:904-909.

Grane, F. E., and G. H. F. Gardner, 1961, "Measurements of Transverse Dispersion in Granular Media," J. Chem. and Eng. Data, 6(2):283-287.

Harleman, D. R. F., and R. R. Rumer, 1963, "Longitudinal and Lateral Dispersion in an Isotropic Porous Medium," J. Fluid Mech., 16: 385-394.

Hayduk, W., and H. Laudie, 1974, "Prediction of Diffusion Coefficients for Nonelectrolytes in Dilute Aqueous Solutions," AIChE Journal, 20(3):611-615.

Hoag, G. E., and M. C. Marley, 1986, "Gasoline Residual Saturation in Unsaturated Uniform Aquifer Materials," J. Environ. Eng. Div., ASCE, 112(3):586-604.

Homsy, G. M., 1987, "Viscous Fingering in Porous Media," Annual Review of Fluid Mechanics, 19:271-311.

Klute, A., 1965, "Laboratory Measurement of Hydraulic Conductivity of Saturated Soil," Methods of Soil Analysis, Part 1, C. A. Black, ed., American Society of Agronomy, Madison, WI, 210-221.

Klotz, D., K.-P. Seiler, H. Moser and F. Neumaier, 1980, "Dispersivity and Velocity Relationship from Laboratory and Field Experiments," J. Hydrology, 45:169-184.

Krill, R. M., and W. C. Sonzogni, 1986, "Chemical Monitoring of Wisconsin's Groundwater," Journal AWWA, 78(9):70-75.

Kueper, B. H., and E. O. Frind, 1988, "An Overview of Immiscible Fingering in Porous Media," J. Contam. Hydrol., 2:95-110.

Lehr, J., 1982, "How Much Ground Water Have We Really Polluted?" Groundwater Monitoring Review, 2(1):4-5.

Lin, C., G. F. Pinder and E. F. Wood, 1982, "Water and Trichloroethylene as Immiscible Fluids in Porous Media," Water Resources Program Report 83-WR-2, Water Resources Program, Princeton University, Princeton, NJ.

Mabey, W. R., J. H. Smith, R. T. Podoll, H. L. Johnson, T. Mill, T.-W. Chou, J. Gates, I. Waight Partridge, H. Jaber and D. Vandenberg, 1982, Aquatic Fate Process Data for Organic Priority Pollutants, Report No. 440/4-81-014, United States Environmental Protection Agency, Washington, D.C.

MacFarlane, D. S., J. A. Cherry, R. W. Gillham and E. A. Sudicky, 1983, "Migration of Contaminants in Groundwater at a Landfill: A Case Study," J. Hydrology, 63:1-29.

McIlvride, W. A., and B. M. Rector (1988), "Comparison of Short- and Long-Screen Monitoring Wells in Alluvial Sediments," Proceedings of the Second National Outdoor Action Conference on Aquifer Restoration, Ground Water Monitoring and Geophysical Methods, Water Well Journal Publishing Co., Dublin, OH.

Mixon, F. O., 1988, "Saturated and Capillary Fringe Ground-Water Behavior Near an Excavation," Ground Water, 26(2):148-155.

Munz, C., and P. V. Roberts, 1986, "Effects of Solute Concentration and Cosolvents on the Aqueous Activity Coefficient of Halogenated Hydrocarbons," Environmental Science and Technology, 20(8):830-836.

Ogata, A., and R. B. Banks, 1961, "A Solution of the Differential Equation of Longitudinal Dispersion in Porous Media," U. S. Geological Survey Professional Paper 411-I.

Pfankuch, H. O., 1963, "Contribution a l'etude des deplacements de fluides miscibles dans un milieu poreaux," Rev. Inst. Fr. Pet., 2(18):215-270.

Pfannkuch, H.-O., 1984, "Determination of the Contaminant Source Strength from Mass Exchange Processes at the Petroleum-Ground-Water Interface in Shallow Aquifer Systems," Proceedings of the NWWA/API Conference on Petroleum Hydrocarbons and Organic Chemicals in Ground Water, National Water Well Association, Worthington, OH, 111-129.

Press, W. H., B. P. Flannery, S. A. Teukolsky, and W. T. Vetterling, 1986, Numerical Recipes: The Art of Scientific Computing, Cambridge University Press, New York.

Pye, V. I., R. Patrick and J. Quarles, 1983, Groundwater Contamination in the United States, University of Pennsylvania Press, Philadelphia, PA.

Rao, P. S. C., A. G. Hornby and P. Nkedi-Kizza, 1983, "Influence of Solvent Mixtures on Sorption and Transport of Toxic Organic Compounds in the Subsurface Environment," paper presented at American Chemical Society Meeting, Washington, D. C.

Reinhard, M., N. L. Goodman and J. F. Barker, 1984, "Occurrence and Distribution of Organic Chemicals in Two Landfill Leachate Plumes," Environmental Science and Technology, 18(12):953-961.

Roberts, J. R., J. A. Cherry and F. W. Schwartz, 1982, "A Case Study of a Chemical Spill: Polychlorinated Biphenyls (PCBs) 1. History, Distribution, and Surface Translocation," Water Resources Research, 18(3):525-534.

Rose, D. A., and J. B. Passioura, 1971, "The Analysis of Experiments on Hydrodynamic Dispersion," Soil Science, 111(4):252-257.

Saffman, P. G., and G. Taylor, 1958, "The penetration of a fluid into a porous medium or Hele-Shaw cell containing a more viscous liquid", Proc. Royal Society London, A(245):312-329.

Scheidegger, A. E., 1960, "Growth of Instabilities on Displacement Fronts in Porous Media", The Physics of Fluids, 3(1):94-104.

Scheidegger, A. E., 1974, The Physics of Flow Through Porous Media, 3rd ed., University of Toronto Press, Toronto.

Schmidtke, K., E. McBean and F. Rovers, 1987, "Drawdown Impacts in Dense Non-aqueous Phase Liquids," Proceedings of the First National Outdoor Action Conference on Aquifer Restoration, Ground Water Monitoring and Geophysical Methods, National Water Well Association, Dublin, OH, 39-51.

Schwille, F., 1981, "Groundwater Pollution in Porous Media by Fluids Immiscible with Water," Sci. Total Environment, 21: 173-185.

Schwille, F., 1984, "Migration of Organic Fluids Immiscible with Water in the Unsaturated Zone," Pollutants in Porous Media: The Unsaturated Zone Between Soil Surface and Groundwater, B. Yaron, G. Dagon and J. Goldshmid, eds., Springer-Verlag, New York, 27-48.

Schwille, F., 1988, Dense Chlorinated Solvents in Porous and Fractured Media, translated by J. F. Pankow, Lewis Publishers, Inc., Chelsea, MI.

Staples, C. A., and S. J. Geiselmann, 1988, "Cosolvent Influences on Organic Solute Retardation Factors," Ground Water, 26(2):192-198.

Silliman, S. E., and E. S. Simpson, 1987, "Laboratory Evidence on the Scale Effect in Dispersion of Solutes in Porous Media," Water Resources Research, 23(8):1667-1673.

Sudicky, E. A., 1986, "A Natural Gradient Experiment on Solute Transport in a Sand Aquifer: Spatial Variability of Hydraulic Conductivity and Its Role in the Dispersion Process," Water Resources Research, 22(13):2069-2082.

Sudicky, E. A., 1988, University of Waterloo, Waterloo, Ontario, private communication.

van Dam, J., 1967, "The Migration of Hydrocarbons in a Water-Bearing Stratum", The Joint Problems of the Oil and Water Industries, The Institute of Petroleum, London, 55-96.

van der Waarden, M., A. L. A. M. Bridie and W. M. Groenewoud, 1971, "Transport of Mineral Oil Components to Groundwater - I: Model Experiments on the Transfer of Hydrocarbons from a Residual Oil Zone to Trickling Water," Water Research, 5:213-226.

Villaume, J. F., P. C. Lowe and D. F. Unites, 1983, "Recovery of Coal Gasification Wastes: An Innovative Approach," Proceedings of the Third National Symposium on Aquifer Restoration and Ground-Water Monitoring, National Water Well Association, Worthington, OH, 434-445.

Weast, R. C., ed., 1970, Handbook of Chemistry and Physics, 51st Ed., CRC Press, Cleveland, OH.

Wheatcraft, S. W., and F. Winterberg, 1985, "Steady State Flow Passing Through a Cylinder of Permeability Different From the Surrounding Medium," Water Resources Research, 21(12):1923-1929.

Wilson, J. L., and S. H. Conrad, 1984, "Is Physical Displacement of Residual Hydrocarbons a Realistic Possibility in Aquifer Restoration?" Proceedings of the NWWA/API Conference on Petroleum Hydrocarbons and Organic Chemicals in Ground Water, National Water Well Association, Worthington, OH, 274-298.

Yule, D. F., and W. R. Gardner, 1978, "Longitudinal and Transverse Dispersion Coefficients in Unsaturated Plainfield Sand," Water Resources Research, 14(4):582-588.

VITAE

The author was born in 1948 in Racine, Wisconsin. He spent his formative years on a hog farm, began his science education at Franksville Grade School, and eventually graduated from William Horlick High School in 1966.

After registering for the draft, the author enjoyed a summer in Europe and then began his college career at the University of Wisconsin-Racine Extension. Transferring to the University of Wisconsin-Madison in 1968, the author let his hair grow, continued his science education, and obtained his B.S. in Chemistry in 1970. After his student deferment expired, the author was invited to an Army Physical where he was told that he was too skinny to kill, and was sent home with a 1-Y classification. (Unfortunately, countless others were not as lucky.) Returning to the books, the author earned his M.S. in Chemistry in 1972.

After traveling and living in a tent for a year, the author worked at limited term jobs for the Wisconsin Department of Natural Resources and the University of Wisconsin Institute for Environmental Studies before finally settling into teaching College Chemistry. That job eventually took him to the University of Wisconsin-Parkside from 1977-1982.

Yielding to a desire for even higher education, the author moved to the Northwest in the fall of 1982. There he began working on his Ph.D. in Environmental Science and Engineering with Jim Pankow at the Oregon Graduate Center. Finally, after six years of playing in sand boxes, the author was granted his degree.

The author is currently employed in the Environmental Cleanup Division of the Oregon Department of Environmental Quality where he must continually deal with LUST (leaking underground storage tanks).

Lest the learned reader should think that all the author did was study, it should be added that the author married Kathy Leuker in 1971. The author is also blessed with two wonderful sons, Eric Michael, born in 1976, and Matthew Ryan, born in 1978. When all is said and done, the first five paragraphs of this Vitae can be thrown out as long as the last paragraph remains.